# INVESTIGATION OF POLYMORPHISM IN INOSITOL DERIVATIVES: SYNTHESIS, CRYSTALLOGRAPHIC STUDIES AND ANALYSIS OF INTERMOLECULAR INTERACTIONS

*A Thesis*

*Submitted to the University of Pune for the Degree of*

**Doctor of Philosophy**

*in*

**Chemistry**

*by*

K. Manoj

*Under the Guidance of*

**Dr. M. M. Bhadbhade and Dr. M. S. Shashidhar**

**Center for Materials Characterization and Division of Organic Chemistry, National Chemical Laboratory, Dr. Homi Bhabha Road, Pune, India- 411008.**

**April 2008**

*Dedicated to Mother Mary*

## CERTIFICATE

This is to certify that the work incorporated in the thesis entitled '**Investigation of Polymorphism in Inositol Derivatives: Synthesis, Crystallographic Studies and Analysis of Intermolecular Interactions**' submitted by **Mr. K. Manoj**, for the Degree of Doctor of Philosophy was carried out by him under our supervision at National Chemical Laboratory, Pune, India.


[**Dr. M. M. Bhadbhade**]
Research Supervisor
Center for Materials Characterization
National Chemical Laboratory
Pune-411008, India
Date:

[**Dr. M. S. Shashidhar**]
Research Co-supervisor
Organic Chemistry Division
National Chemical Laboratory
Pune-411008, India
Date:

## DECLARATION BY RESEARCH SCHOLAR

I hereby declare that the thesis entitled '**Investigation of Polymorphism in Inositol Derivatives: Synthesis, Crystallographic Studies and Analysis of Intermolecular Interactions**' submitted for the Degree of Doctor of Philosophy to the University of Pune, is the result of research work carried out by me under the supervision of **Dr. M. M. Bhadbhade** and **Dr. M. S. Shashidhar** at National Chemical Laboratory, Pune, India. The work is original and has not been submitted in part or full by me for any other degree or diploma to this or any other University.

[**K. Manoj**]

## Acknowledgements

*To my extreme delight, I would like to evince my heart felt gratitude to my research supervisor* ***Dr. M. M. Bhadbhade*** *for providing an incredible opportunity to pursue my career as a Ph. D. student and directing me to the fascinating area of polymorphism. My sincere thanks to him, for his invaluable advice, for his friendly nature, for his timely help and being a strong support both scientific and personal, on all difficult occasions during my stay in NCL.*

*I gratefully acknowledge* ***Dr. M. S. Shashidhar*** *my co-supervisor for his extensive scientific discussions, for his suggestions, for giving me complete freedom in research and constructive criticism which helped me a lot to focus my views in the proper perspective.*

*I wish to convey my sincere thanks to* ***Dr. R. G. Gonnade****, who supported me personally as well as scientifically on all stages of my research in NCL. He deserves a special mention, for helping me to learn the techniques of X-ray crystallography, for his valuable suggestions and guiding me as an elder brother.*

*I am very thankful to Dr. (Mrs.) V. G. Puranik, for her timely help, care, encouragement and maintaining a cheerful atmosphere in the X-ray lab. I would like to thank Dr. C. G. Suresh for his valuable help and suggestions during various stages of my research work. Also, I wish to express my gratitude to the 'Research Assessment Committee' members-Prof. Padhye, Dr. C. G. Suresh and Dr. N. N. Joshi, for their comments and suggestions in evaluating the progress of my research work.*

*I would like to thank Dr. Smitha Mule, Mr. Harikrishnan, Dr. S. D. Kulkarni and Dr. S. D. Pradhan for providing me TGA/DTA and DSC data and for the fruitful discussions. I also thank Central NMR, Elemental Analysis and FTIR and Library Facilities, NCL for providing me the respective data. I would like to thank Dr. Pedireddy, Mr. Marivel and Mr. Bhange for helping in carrying out X-ray powder analysis.*

*It is my pleasure to thank Prof. Gautam R. Desiraju, Department of Chemistry, Central University, Hyderabad, for fruitful scientific discussions and training on CSD statistical analysis. I owe special thanks to Dr. Malla Reddy, who has taken care, instructed and supported me during my stay in the Central University Campus, Hyderabad.*

*It is my great pleasure to thank Prof. T. N. Guru Row, Solid State and Structural Chemistry Unit, Indian Institute of Science, Bangalore for his valuable suggestions, discussions and for introducing me to the X-ray Charge Density Studies. Also the timely help from his students is greatly appreciated.*

*I also wish to thank Mr. Jovan Jose, University of Pune, for teaching me the basics of theoretical energy calculations. I would acknowledge Dr. Ganapathi, Central NMR Facility, NCL, for providing me the Gaussian'03 software.*

*I sincerely thank all the CMC staff for helping me during the course of my research work. Special thanks to Head of Center for Materials Characterization, Organic Chemistry Division and Physical Chemistry Division for providing lab infrastructure to complete my thesis in time. I express my sincere gratitude to Director, NCL for allowing me carry out research work in the prestigious and well equipped laboratory.*

*I would like to thank to all lab mates for their help, cooperation and a pleasant working atmosphere in the lab. I am very thankful to Ajish, Jovan and Sony for proof reading of this thesis. I have been fortunate to have a large number of good friends but I would like to confess that, it is not possible for me to acknowledge them individually. I sincerely thank all of them for their incessant moral support, kind cooperation, encouragement, help, respect, appreciation and for the scientific discussions.*

*The hospitality and homely atmosphere from the family members of Dr. M. M. Bhadbhade, Dr. M. S. Shashidhar, Dr. R. G. Gonnade and Dr. V. G. Puranik are sincerely acknowledged.*

*I take this opportunity to express my earnest respect to the science teachers of my school and graduation tutor Mr. Niaz Ahmed, for their way of teaching that build up my research career in science.*

*I would like to thank University Grant Commission-India for awarding Junior and Senior Research Fellowships.*

*Finally, I express my deepest sense of gratitude to my family members, for their endless support, encouragements, patience, care and love throughout my life.*

*10 April 2008, Pune* *K. Manoj*

# Contents

## Abstract

The thesis entitled ***'Investigation of Polymorphism in Inositol Derivatives: Synthesis, Crystallographic Studies and Analysis of Intermolecular Interactions'*** was motivated by the remarkable molecular association of **8**[Fig.1]; the diastereomers associated *via* C-H···O interactions leading to a very close packed lattice with no guest inclusion. However, bridging of diastereomers **8** *via* dipolar S=O···C=O short contacts with a slight change in their relative orientation created voids that included a number of guest molecules [Fig.1]. The nature and geometrical preferences of S=O···C=O contacts in the molecular association were first recognized by us.[1]

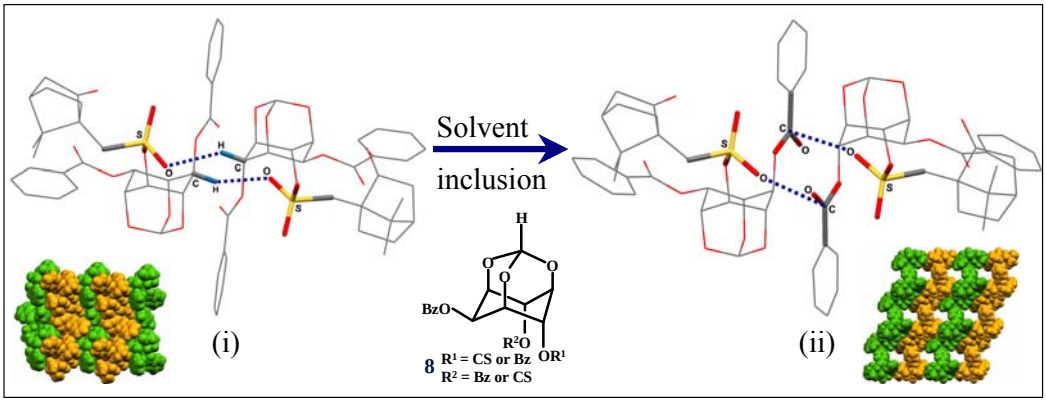


**Figure 1**: Dimeric association of **8** *via* (i) C-H···O interactions in solvent free form (ii) S=O···C=O short contacts in pseudopolymorphs. Inset shows the molecular organization in both the forms.

The present thesis describes the synthetic modifications of *myo*-inositol, structures of which were investigated for their molecular organizations *via* weak non-covalent interactions. To achieve this objective, compounds **8-23** were prepared [Chart 1], which do not have any conventional hydrogen bonding groups (–OH, –NH, –COOH, etc). Weak non-covalent interactions[2] are known to be involved in enzyme-substrate binding, ligand-receptor interactions, stabilization of protein conformations etc. Understanding of these interactions have importance in other areas such as crystal engineering,[3] host-guest complexes,[4] drug design[5] and controlling polymorphic modifications[6] in drugs, dyes and explosives. From this laboratory, we have already reported interesting cases of polymorphism, phase transitions among them[7] and pseudopolymorphic behavior[1] with varying guest specificities in several *myo*-inositol

derivatives. The work reported in this thesis, divided into seven chapters, covers interesting cases of polymorphism in *myo*-inositol derivatives, arising essentially due to weaker interactions.

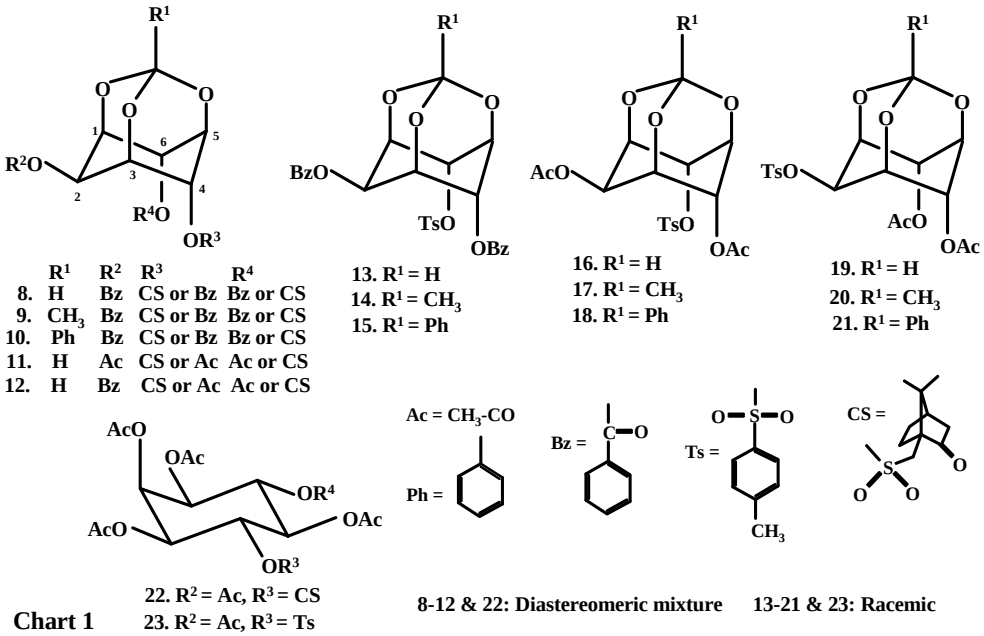


**Chart 1**

***Chapter 1*** reviews polymorphic behavior and various non-covalent interactions with special focus on dipolar interactions in molecular crystals. In the absence of any conventional hydrogen bonding, various other weak non-covalent interactions associate the molecules with different arrangements or conformations in the crystal lattice leading to the formation of polymorphs. Various dipolar interactions are reviewed, emphasizing its relevance in crystal engineering, molecular recognition and drug design. As mentioned, observation of molecular association *via* S=O···C=O contact has been pursued in the following chapters.

***Chapter 2*** discusses the role of dipolar interactions in the pseudopolymorphs and molecular organization of diastereomers in crystals of 2,4(6)-di-*O*-acyl-6(4)-*O*-camphorsulfonyl-*myo*-inositol 1,3,5-orthoesters (**8-12**). Diastereomers of **8** are associated *via* dipolar S=O···C=O contacts (perpendicular motif, Type-I), whereas crystal structures of **9** showed dipolar S=O···C=O intermolecular contacts with a

different geometry of interaction motif (sheared parallel, Type-II). The orthobenzoate derivative **10** did not show these dipolar interactions and exhibited extensive orientational disorder for the camphor moiety bearing sulfonyl group. Interestingly, diastereomers of **11** associated *via* well known dipolar C=O···C=O contacts[8] producing a helical molecular assembly in its crystal lattice, but **12** was obtained as amorphous solid.

***Chapter 3*** reports crystal structures of 2,4-di-*O*-benzoyl-6-*O*-tosyl *myo*-inositol orthoesters (**13**, **14** and **15**) that have the flexible tosyl group instead of the bulky chiral camphorsulfonyl group (**8**, **9** and **10** in *Chapter 2*). Among these, only the orthoacetate derivative **14** produced conformational[9] dimorphs concomitantly (plates and needle shaped) from dichloromethane-methanol mixture in monoclinic ($P2_1$: Form-I) and triclinic (*P-1*: Form-II) crystals. Tosyl groups in these dimorphs have different conformations [Fig. 2(ii)] due to the rotation around *O*-*S* bond (torsion angles 91º and 165º respectively). Interestingly, these two conformations are similar to those observed for **13** and **15** respectively *i.e.* the orientation of tosyl group in **13** with torsion angle 81º [Fig. 2(i)] is similar to Form-I crystals of **14** [blue colored in Fig. 2(ii)] and in **15** (torsion angle 161º) is similar to the Form-II of **14** [red colored in Fig. 2(ii), Fig. 2(iii)] to show the extent of similarity. However, Form-II crystals of **14** and orthobenzoate derivative **15** with extended conformations of tosyl group exhibits intramolecular S=O···C=O dipolar contacts and π···π interactions respectively.

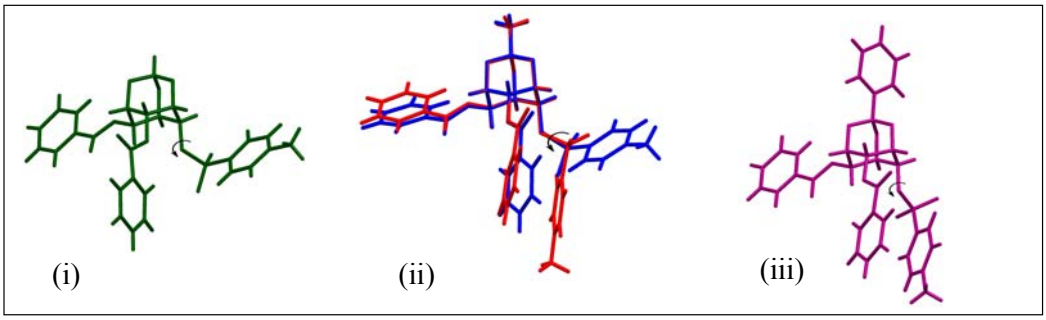


**Figure 2**: (i) Molecular conformation of **13**; (ii) Molecular overlap figure of dimorphs **14** [blue: Form-I, red: Form-II]; (iii) Molecular conformation of **15**.

***Chapter 4*** reports conformational dimorphs of both **16** and **17**. The polymorphs have different molecular orientations mainly because of the rotation of

tosyl group about the *O*-*S* bond; torsion angles in the monoclinic (Form-I: $P2_1/c$) and orthorhombic (Form-II: *Pbca*) crystals of **16** vary significantly (80º and 141º) [Fig. 3(i)], whereas triclinic (Form-I: *P-1*) and monoclinic (Form-II: $P2_1/c$) crystals of **17** showed very little difference in torsion angles (84º and 81º) [Fig. 3(iv)]. An interesting feature in all the conformational polymorphs is the formation of an isostructural string[10] (leaving out the orientation of tosyl group) linked *via* dipolar (ether)O···C=O contacts group [Fig. 3(ii), (iii), (v) and (vi)], which are further linked by other weak interactions to form different layers in their crystal lattice. It is noteworthy that in Form-II crystals of **16**, the tosyl group makes an intramolecular dipolar S=O···C=O contact, which could stabilize this conformation. Crystallization attempts of **18** from various solvents did not produce any crystals.

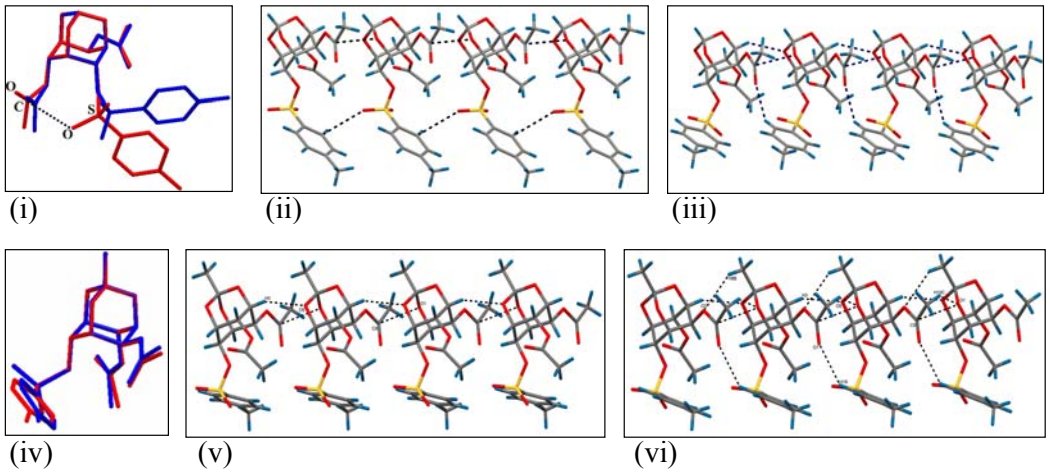


**Figure 3**: Molecular overlap figure of dimorphs (i) in **16** (iv) in **17** and isostructural molecular chains in (ii) orthorhombic form of **16** (iii) monoclinic form of **16** (v) monoclinic form of **17** (vi) triclinic form of **17**.

***Chapter 5*** discusses the polymorphic search of 2-*O*-tosyl 4,6-di-*O*-acetyl-*myo*-inositol orthoesters **19-21** [Chart 1]; which are positional isomers of **16-18** (*Chapter 4*). It is known that **14** exhibits conformational polymorphism; its analogues **19-21** were explored for the same properties. However, none of them exhibited conformational polymorphism, but **20** showed *solvatomorphism*.[11] Crystallization of **20** from most of the organic solvents gave moderately stable inclusion crystals. These isomorphous solvated crystals of **20** had very similar conformations and the host

architecture bridged *via* weak interactions creating voids (~ 8x7Å$^2$) that are occupied by the guest molecules [Fig. 4(i)]. It is interesting to note from the molecular overlap of **19**, **20** and **21** [Fig. 4(ii)] that significant conformational differences are again observed in the tosyl group orientation, which distinctly different for **20**. This has been shown to be a factor responsible for creating voids in the packing of molecules. Here again, centrosymmetric dipolar S=O···C=O interactions are observed only for molecular association in **21** [Fig. 4(iii)].

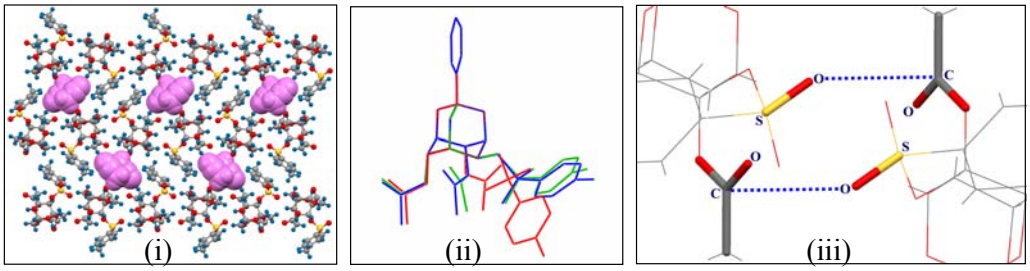


**Figure 4**: (i) Host-guest organization in inclusion crystals of **20**; (ii) Molecular overlap plot of **19** (green), **20** (red) and **21** (blue); (iii) Intermolecular S=O···C=O contacts in crystal of **21**.

After studying the orthoester bridged systems**,** ***Chapter 6*** reports simple inositol derivatives **22** and **23**. Only **22** produced crystals with the inclusion of solvents that yield three forms. The Form-I and Form-II crystals belong to the triclinic (space group *P1*), whereas the Form-III crystals are monoclinic $P2_1$. There are two solvent sites for the Form-II and Form-III crystals [Fig. 5(ii) and (iii)] but only one guest site is seen for Form-I [Fig. 5(i)]. An interesting feature in all the three forms of solvatomorphs of **22**, is well-conserved dimeric association of diastereomers *via* trifurcated C-H···O interactions between the sulfonyl oxygen and inositol ring H-atoms of the other diastereomer and *vice versa*. It is interesting to note that the host molecules are organized in two different crystalline forms, triclinic [Form-I, Fig. 5(i)] as well as monoclinic [Form-III, Fig. 5(iii)] with the same guest inclusion of dichloromethane, termed as *solvatopolymorphs*.[12] The detailed analysis of the host-host and host-guest arrangements and their interactions is discussed in this chapter. The crystallization experiments of various solvents and conditions of **23** always yielded monoclinic crystals.

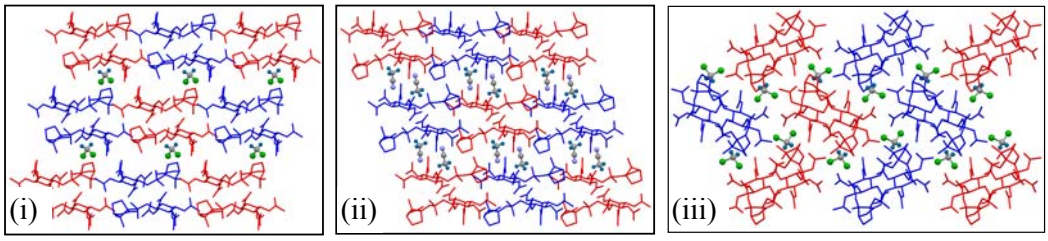


**Figure 5**: Different Host-guest packing in (i) Form-I, (ii) Form-II and (iii) Form-III crystals of **22**.

***Chapter 7*** reports statistical analysis carried out on weak bond dipolar interactions involving sulfonyl group with C$sp^2$ carbonyl carbon. We have classified the dipolar S=O···C=O interaction motif as Type-I, Type-II and Type-III [Fig. 6(i)] and its occurrence on statistical methods discussed in detail using Cambridge Structural Database (CSD). We have also explored the existence of dipolar S=O···C=O contacts (that bind the ligands to the receptor/protein) in the Protein Data Bank (PDB). It is noteworthy that S=O···C=O contacts were observed in the binding of N-tosyl-D-proline (ligand) to thymidylate synthase (an essential enzyme in pyrimidine metabolism) with therapeutic applications in cancer and infectious diseases [Fig. 6(ii)]. The studies/understanding of these weak interactions is of great interest because of many sulfa drugs which have S=O group, that could play a role in the ligand-receptor binding and also in the structure based drug design for potent drugs.

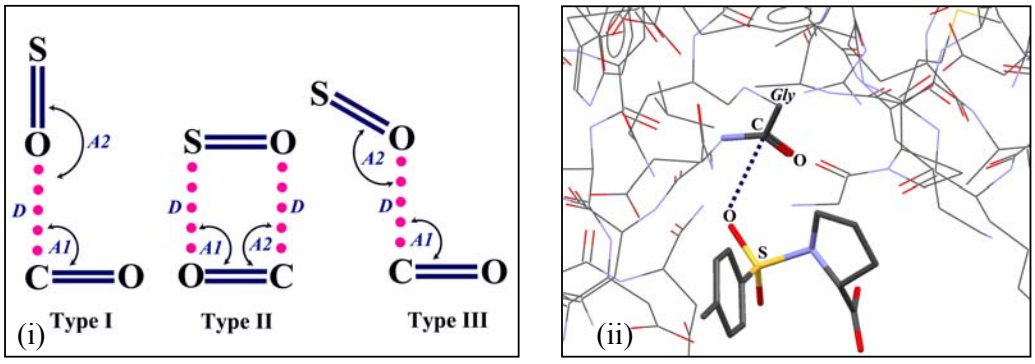


**Figure 6**: (i) Three possible interaction motif of S=O···C=O dipolar contacts; (ii) Protein crystal structure indicating the intermolecular S=O···C=O dipolar contacts [PDB code no.1F4E].

**References**


1. Manoj, K.; Gonnade, R. G.; Bhadbhade, M. M.; Shashidhar, M. S.; *Cryst. Growth Des*. **2006**, *6*, 1485.
2. (a) G. R. Desiraju; T. Steiner; *The Weak Hydrogen Bonds*: *In Structural Chemistry and Biology*, Oxford University Press: Oxford, New York, **1999**. (b) Munshi, P.; Guru Row, T. N.; *CrystEngComm*. **2005,** *7*, 608.
3. (a) Braga, D.; Grepioni, F.; *Acc. Chem. Res*. **2000**, *33*, 601. (b) Desiraju, G. R.; Crystal Engineering: *The Design of Organic Solids*, Amsterdam: Elsevier, **1989**.
4. Wang, Z.; Ch. Kravtsov, V.; Walsh, R. B.; Zaworotko, M. J.; *Cryst. Growth Des*. **2007**, *7*, 1154.
5. Olsen, J. A.; Banner, D. W.; Seiler, P.; Sander, U. O.; D'Arcy, A.; Stihle, M.; Műller, K.; Diedrich, F.; *Angew Chem. Int. Ed*. **2003**, *42*, 2507.
6. (a) Hilficker, R; *Polymorphism in Pharmaceutical Industry*, Wiley VCH: Weinheim, **2006**; (b) Bernstein, J; *Polymorphism in Molecular Crystals*, Oxford University Press: NewYork, **2002**. (c) Brittain, G. H; *Polymorphism in Pharmaceutical Solids*, Marcel Dekker: NewYork, **1999**.
7. (a) Gonnade, R. G.; Shashidhar, M. S.; Bhadbhade, M. M.; *Chem. Commun*. **2004**, 2530. (b) Gonnade, R. G.; Bhadbhade, M. M.; Shashidhar, M. S.; Sanki, A. K.; *Chem. Commun*. **2005**, 5870.
8. Allen, F. H.; Baalham, C. A.; Lommerse J. P. M.; Raithby, P. R.; *Acta Crystallogr*. **1998**, *B54*, 320.
9. Roy, S.; Banerjee, R.; Nangia, A.; Kruger, G. J.; *Chem. Eur. J*. **2006**, *12*, 3777.
10. Kálmán, A.; *Acta Cryst*. **2005**, *B61*, 536.
11. Chopra, D.; Guru Row, T. N.; *Cryst. Growth Des*. **2006**, *6*, 1267.
12. Ibragimov, B T; *CrystEngComm*. **2007**, *9*, 111.

## General Remarks

1. All the solvents used were purified using the known literature procedures.
2. Petroleum ether used in the experiments was of 60-80 °C boiling range, unless otherwise mentioned.
3. Column chromatographic separations were carried out by gradient elution using silica gel (230-400 mesh) with ethyl acetate-light petroleum ether mixture.
4. All the melting points reported were recorded using an electro-thermal melting point apparatus or with Buchi Melting Point apparatus B-540.
5. IR spectra were recorded on Shimadzu FTIR instrument in chloroform solution.
6. NMR spectra were recorded on Bruker ACF-200 and AV-200 spectrometers. Chemical shifts (δ) reported are referred to internal reference Tetramethylsilane. The following abbreviations were used: s = singlet, 2s = two singlet, d = doublet, 2d = two doublet, t = triplet, q = quartet, m = multiplet.
7. Micro analytical data were obtained using a Carlo-Erba CHNS-O EA 1108 Elemental Analyzer. Elemental analyses observed for all the newly synthesized compounds were within the limits of accuracy (0.4 %).
8. The hot stage microscopy (HSM) studies were carried out on a Leica polarizing microscope equipped with a heating stage P35.

# Chapter 1

## Exploring Polymorphism *via* Weak Non-Covalent Interactions in Molecular Crystals

# Chapter 1

## 1.1. Introduction

Polymorphism, the ability of a compound to exist in more than one crystal form or modifications, has gained paramount importance in many areas of science as well as in industries.[1-3] Mc Crone defines polymorph as '*a solid crystalline phase of a given compound resulting from the possibility of at least two different arrangements of the molecules of that compound in the solid state*'.[4] Polymorphs have the same chemical composition but different physical properties due to their different molecular arrangements in the crystal lattice as a result of differences in non-bonded intermolecular interactions such as hydrogen bonding, van der Waals, electrostatic, π···π stacking interactions. Research involving polymorphism is becoming increasingly important in pharmaceutical solids, dyes, pigments, explosives and specialty chemicals because of the required consistency in physical and chemical properties that can be achieved by restricting the formation of undesired solid form/polymorphs.[5] However, the number of polymorphic modifications that can exist or its prediction seems to be a difficult problem because of the complexity of intermolecular interactions.[6] Thus, the statement "*every compound has different polymorphic forms and the number of forms known for a given compound is proportional to the time and energy spent in research on that compound*" made by Mc Crone in 1969 still appears to be significant.[7]

The investigation of polymorph formation and its control is crucial for the design of solids with desired properties.[8] This is of utmost importance because of the problems encountered with molecular solids ranging from unexpected appearance or

disappearance of a particular polymorph, inability to reproduce known polymorphs and conversion of one polymorph to another during processing or storage of solids (especially in pharmaceutical industries). A well known example is that of ritonavir, a peptidomimetic drug for the treatment of HIV-1 infection[9] recalled in 1998 by Abbot Laboratories. Investigations revealed that the appearance of a new orthorhombic needle shaped polymorph (of ritonavir had slower dissolution) during processing compromised the oral bioavailability [Fig. 1.1] of the drug.[10] After controlling the undesired form, the reformulated ritonavir tablet was restored in the market in 1999.[11] Therefore, pharma industries employ high throughput screening to generate a number of polymorphs of a drug or drug intermediate and attempt to understand the processes involving the identification, characterization and their interrelationships, which can be exploited for the selection of a suitable form as drug candidate.[12]

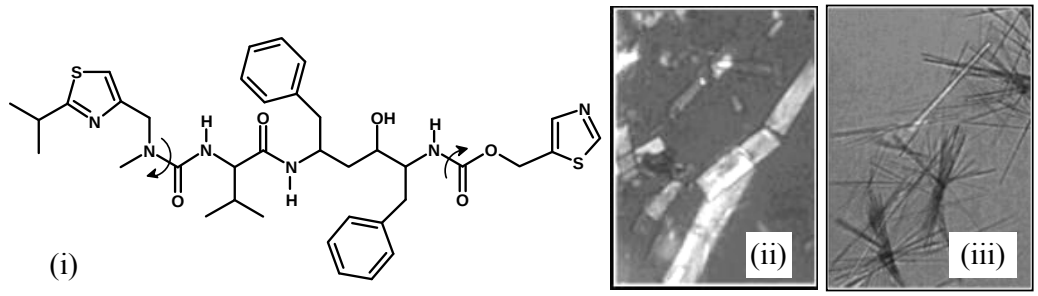


**Figure 1.1**: (i) Structure of ritonavir; (ii) Form I [Monoclinic, $P2_1$]; (iii) Form II [orthorhombic, $P2_12_12_1$] crystals with different molecular conformations.

Approximately one third of organic compounds and about 80 % of the marketed pharmaceutical solids exhibit polymorphism under experimentally accessible conditions.[13-15] Our quick search showed that the entries in the Cambridge Structural Database[16] reports 8051 structures that qualify the word '*polymorph*' in '*organic*' molecules. With the potentially high financial gain of patent protection, pharmaceutical companies are now increasingly focusing on new intellectual property rights on polymorphic forms that allow them to be the first in the market, keeping

ahead of other companies. However, the use of the term *New Polymorph* should proceed with the careful check of crystallographic data having significantly good accuracy and precision, to avoid controversial debate.[17,18] In addition, the crystalline forms that are not fully characterized, contain disorder or have modulated conformations due to the effect of temperature and pressure are also under scrutiny to include them as 'true polymorphs.'[19]

The main objective in the study of polymorphism is to understand the effect of various parameters of crystallization experiment in controlling the 'nucleation' to obtain a desired polymorph.[20] Gay Lussac observed in 19$^{th}$ century that during crystallization, an unstable form was obtained first that subsequently transformed into second stable form. This statement was then explained thermodynamically by Ostwald, known as "*Ostwald's step rule*" which states that, "*In all process, it is not the most stable state with the lowest amount of free energy that is initially formed, but the least stable state lying in the free energy to the original state.*"[21] The practical inference of this rule indicates that it should be possible to isolate the different polymorphs of a given compound at different stages of supersaturation or supercooling. However, the crystallization of a compound is still a poorly understood process; although it is known to be a multi step process governed by a combination of thermodynamic and kinetic factors, like most chemical reactions.[22] Depending on the conditions, the crystallization of a polymorph from a solution may be under kinetic or thermodynamic control. The effect of solvent, an important kinetic factor influencing nucleation, continues to be the subject of investigations.[23] In a crystallization process, two or more domains overlap forcing the polymorphs to crystallize simultaneously in the same crystallization flask resulting in *concomitant polymorphs*.[24] The energetically equivalent structures of concomitant polymorphs provide excellent input for the validation of lattice energy programs and crystal structure prediction programs.[25]

## 1.2. Types of polymorphism

We have classified polymorphism broadly into five categories - *packing polymorphism*, *conformational polymorphism*, *pseudopolymorphism*, *solvatomorphism* and *solvatopolymorphism*. However, the terminology used to refer to crystals that contain solvents is not consistent and often confusing. This is reflected in the recent debate on the term pseudopolymorphism.[26] Various other terms such as inclusion crystals, solid adducts, molecular complex, solvates, clathrates, channel compounds, host-guest systems, etc. have been used in the literature to address specific phenomenon of these crystals. A brief description of five categories of polymorphism is given below.

### *1.2.1. Packing Polymorphism*

Packing Polymorphism generally occurs in relatively rigid molecules. In packing polymorphs, the molecules are arranged differently in the crystal lattice resulting from different kinds of intermolecular interactions.[27] For example, paracetamol [4-hydroxyacetanilide, Fig. 1.2(i)] exists in monoclinic ($P2_1/n$) and orthorhombic (*Pbca*) forms.[28] In both the forms, the conformation of individual molecules remains the same [Fig. 1.2(ii)]; but molecules are differently packed in crystal *via* different hydrogen bonding interactions [Fig. 1.2(iii) and (iv)].

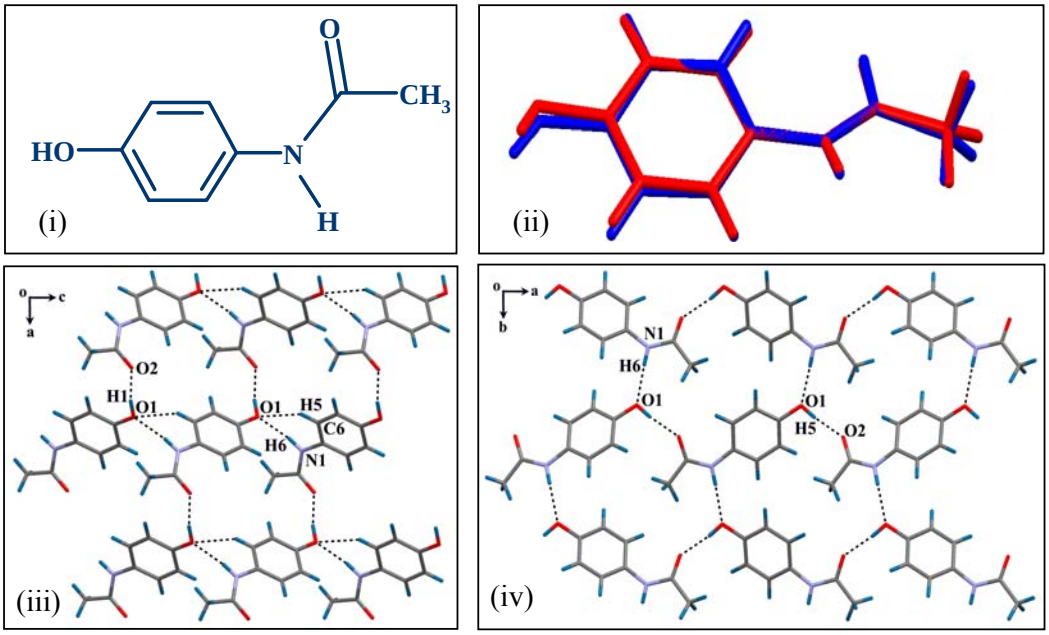


**Figure 1.2**: (i) Structure of paracetamol; (ii) molecular overlap plot in monoclinic [red] and orthorhombic [blue] forms; (iii) packing of molecules viewed down b-axis in the monoclinic form; (iv) molecular packing viewed down c- axis in the orthorhombic form.

### *1.2.2. Conformational Polymorphism*

The existence of two or more polymorphs of a substance in which the conformation of individual molecules differs significantly, are said to be conformational polymorphs.[29] This phenomenon generally occurs with flexile molecules, which can adopt different orientations in the crystal lattice. In conformational polymorphs, the changes occur at molecular level due to the involvement of intra- and intermolecular interactions. For example, sulfapyridine [Fig. 1.3(i)], used as an antibacterial drug in the treatment of pneumonia, exhibited polymorphic modifications with orthorhombic (*Pbca*) and monoclinic forms ($P2_1/c$ as well as *C2/c*) with different molecular conformations [Fig. 1.3(ii)-(v)].[30] Conformational polymorphism of tosylated *myo*-inositol derivatives is discussed in *Chapters 3* and *4* of this thesis.

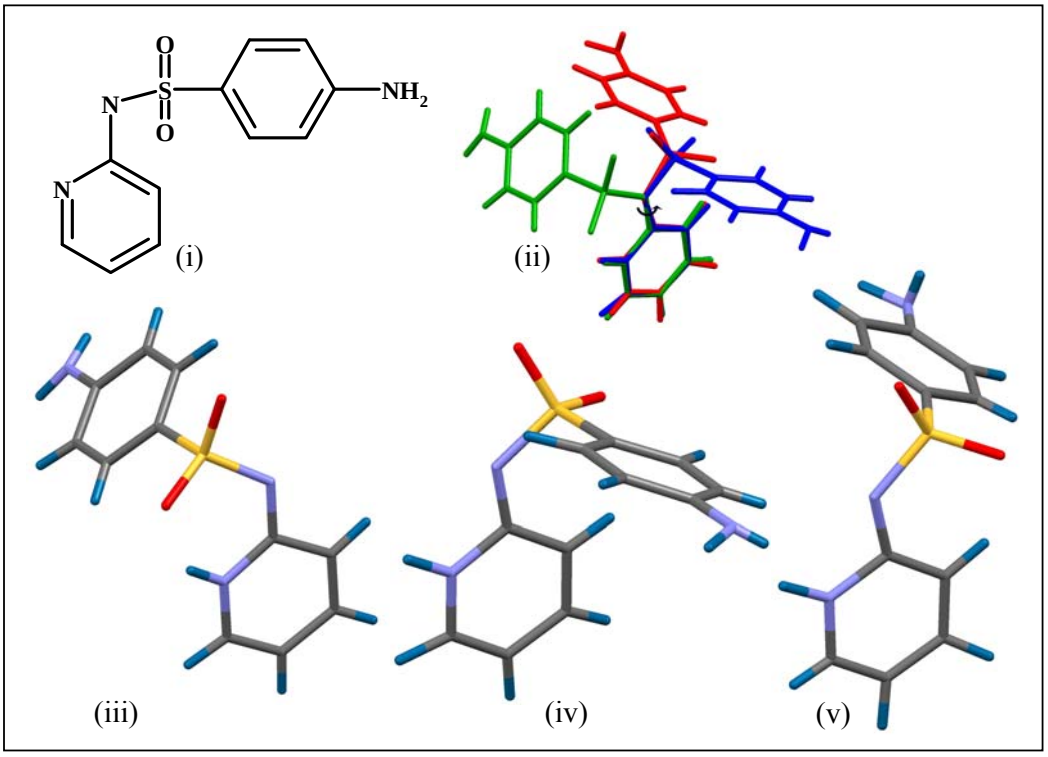


**Figure 1.3**: (i) Structure of sulfapyridine; (ii) Molecular overlap plot of orthorhombic [red: *Pbca*] and monoclinic forms [blue: *P21/c*, Green: *C2/c*]; Molecular conformations in (iii) monoclinic, *C2/c*; (iv) monoclinic, $P2_1/c$; (v) orthorhombic, *Pbca* crystals.

### *1.2.3. Pseudopolymorphism*

This term has been generally used to describe solvated crystals in pharmaceutical sciences and the term has become familiar with chemists also. Pseudopolymorphs are different crystal forms of a compound that exhibits inclusion of solvents as well as a solvent free form; in other words, it is the polymorphic modification of host molecule other than the included solvents.[2,19] Therefore, pseudopolymorphs have different molecular organization of host molecules in their crystals. Pseudopolymorphic behavior of inositol derivatives is described in *Chapter2*.

### *1.2.4. Solvatomorphism*

Crystalline substances with solvent molecules incorporated in their crystal lattice *via* non-covalent intermolecular interactions are termed as solvatomorphs.[3,31] Solvatomorphs may be obtained from different solvents and/or with their different stoichiometric ratios. Examples of solvatomorphs of *myo*-inositol derivative are presented in *Chapter 5*.

### *1.2.5. Solvatopolymorphism*

Solvatopolymorphism is referred to the phenomenon of existence of different crystal modifications of the same constituents (host and guest), in the same or different stoichiometric ratios.[32] Thus, solvatopolymorphism is a special category of solvatomorphism. Solvatopolymorphs are different crystal modifications of the same solvate whereas; solvatomorphs are crystal forms containing different solvents. *Chapter 6* presents an interesting case of solvatopolymorphism of a *myo*-inositol derivative.

## 1.3. Polymorphism in *myo*-Inositol

Inositols are cyclohexane-hexols; there are nine known stereoisomers [Chart 1.1]; out of which four isomers (*myo*-, *neo*-, *chiro*-, and *scyllo*-Inositol) have been recognized to occur in nature while the others (*cis*-, *epi*-, *allo*-, and *muco*-Inositol) are unnatural synthetic isomers.[33] *myo*-Inositol being the most abundant, occurs widely in nature in both free and combined forms. *myo*-Inositol has five equatorial hydroxyl groups and one axial hydroxyl group. There is a plane of symmetry passing through *C2* and *C5* atoms [Chart 1.2]. The carbon atom at the axial position is labeled as *C2* and the other ring carbon atoms are numbered *C1* to *C6* starting from *C1* atom and proceeding around the ring either in clockwise or anticlockwise fashion. According to convention, an anti-clockwise numbering in unsymmetrically substituted *myo*-inositol leads to the D-configuration and the clockwise numbering leads to L-configuration.[34]

However, International Union of Biochemistry (IUB) nomenclature allows all biologically relevant compounds to be denoted as the D-isomer.[35] Although *myo*-inositol has the *meso* configuration, many optically active derivatives of *myo*-inositol occur in nature.

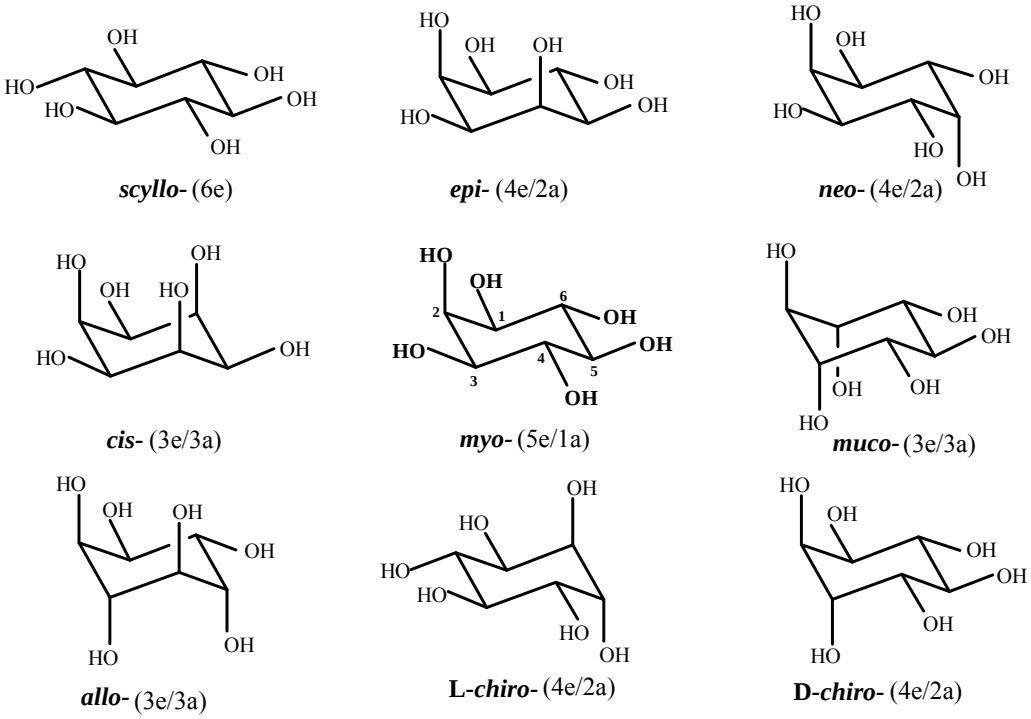


**Chart 1.1**

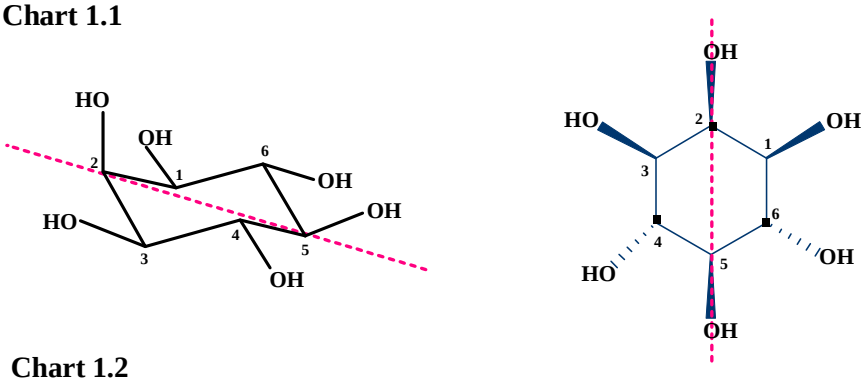

**Chart 1.2**

Chemistry and biology of *myo*-inositol derivatives has been investigated extensively in the recent past due to the involvement of phosphoinositols in cellular signal transduction mechanisms[36] and anchoring of certain proteins to cell membranes.[37] These developments in biology and their consequences in medicine have necessitated simpler methods for the synthesis of various inositol derivatives.[38]

The key intermediate for the synthesis of the biologically important derivatives of inositols are the hydroxyl group protected derivatives (having the free hydroxyl derivatives at the desired position) that allow further modification or derivatization of *myo*-inositol to yield biologically important natural or unnatural products. Sureshan *et al*. reviewed the various regioselective reactions of hydroxyl group in *myo*-inositol.[39] Orthoesters of the *myo*-inositol obtained by the simultaneous protection of the three C1, C3 and C5 substituted hydroxyl groups of **1** [Scheme 1.1] are important intermediates for the preparation of biologically important phosphoinositols and their derivatives, glycosyl inositols and cyclitol based metal complexing agents.[40] Due to the centro-symmetry of *myo*-inositol orthoformate (**2**), substitution at *C4* (or *C6*) position resulted in the formation of racemates or diastereomeric mixture (if the substituting group is chiral).

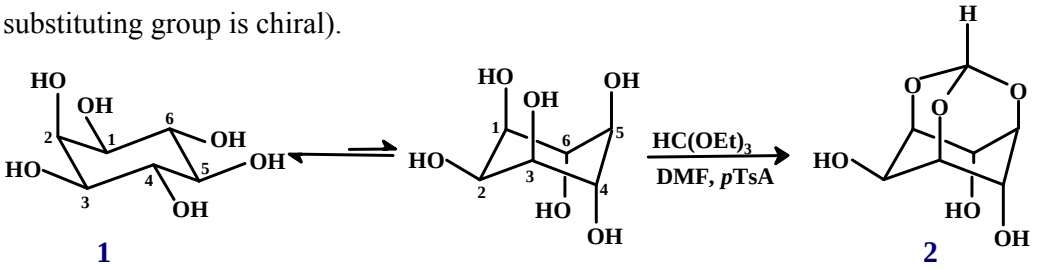


**1** **2**

**Scheme 1.1**

Although a large number of *myo*-inositol derivatives were explored for their synthetic utility and biological activities, very few are examined for solid state properties. The crystal structure (monoclinic form, space group $P2_1/c$) of *myo*-inositol was first determined by Rabinovich and Kraut in 1964.[41] However, its orthorhombic polymorph (space group, $Pna2_1$) was investigated recently.[42] An exciting case of jumping crystals of racemic 3,4-di-*O*-acetyl-1,2,5,6-tetra-*O*-benzyl-*myo*-inositol upon heating and their thermal phase transformation into polymorphs was well characterized by Steiner *et al*. in 1993.[43] We have investigated interesting cases of solid state reactions (as acyl migrations) for the crystalline forms of various *myo*-inositols.[44-46] Recently, Simperler *et al*. correlated the melting points of various

isomers of inositol with their hydrogen bonding patterns.[47] Day *et al*. used combined methods of single-crystal structure solution, structure solution from powder diffraction data and lattice energy search for the structural elucidation of possible polymorphs of *scyllo*-inositol.[48]

Our group has been engaged in the synthesis and solid-state structural studies of various protected inositol derivatives for the last two decades.[39,44-46,49-53] We initiated exploring polymorphic behavior after the serendipitous discovery of selective encapsulation of dihalomethanes by racemic 1,2,3,5,6-penta-*O*-benzoyl-4-*O*-tosyl-*myo*-inositol, which showed a significant role of 'halogen bonding' interactions in the inclusion crystal formation.[49] Gonnade *et al*. investigated a fascinating polymorph conversion of hexa-*O*-benzoyl *myo*-inositol, in which the metastable chiral polymorph formed under kinetic conditions, slowly transformed to an achiral form upon standing in the mother liquor.[50] They also reported a few more cases of transformations amongst polymorphs of *myo*-inositol derivatives; (i) concomitant polymorphs and their thermal phase transformation due to the interplay of halogen bonding interactions;[51,52] (ii) solvent dependent dimorphs of *myo*-inositol orthobenzoate with isostructural molecular layers linked *via* different weak interactions.[53] These observations indicated the interplay of various weak intermolecular interactions during nucleation for a given crystallization condition. The role of weak dipolar interactions in the molecular association in *myo*-inositol derivatives were recognized,[54] pursued further by our group and is one of the main motives in undertaking the work reported in this thesis.

### 1.4. Non-covalent Interactions in Molecular Crystals

Non-covalent interactions play an essential role in the molecular aggregation to form crystals.[55] The study of these interactions is of great current interest because of their involvement in various biological processes such as self-assembly of DNA,

conformational stabilization of proteins, enzyme-substrate complexes, ligand-receptor recognition etc.[56] In depth knowledge of these weak interactions is highly desirable to design new drugs 'rationally' that have better affinity/selectivity to their receptor proteins.[57] The non-covalent interactions can contribute to stabilization energies of a maximum of ~ 10 kcal/mol and are considerably weaker than conventional covalent bonds.[58] Therefore, to recognize and describe these weak interactions, it is essential to apply the most accurate experimental methods and quantum mechanical calculations and is one of the most challenging tasks of contemporary science.[59] Single crystal structure analysis by X-ray/neutron diffraction is the most appropriate technique that provide accurate information on the intermolecular interactions in the solid state.

The formation of a crystal involves overall optimization of attractive and repulsive intermolecular interactions between the molecules that leads to the periodic three dimensional arrangements in the crystal lattice. However, the various intermolecular interactions that govern the process of crystallization remains intractable even for small organic molecules because of the complexity with which molecules interact with each other.[60] Moreover, the mechanisms that drive the nucleation of polymorphs still remain at immature stage making the prediction of polymorphs a formidable challenge.[61]

Charge density analysis has gained immense importance in recent years, because it allows one to observe and quantify the intermolecular interactions beyond distance-angle geometry criteria.[62] The non-covalent interactions in molecular crystals can typically be divided into strong, moderate and weak interactions,[56] although the demarcation between them is not sharp. The strength of various interactions were systematically reviewed by Munshi *et al*. using X-ray charge density analysis of coumarin derivatives as model systems.[63] They characterized the interactions (15 types) of varying strengths. The exponential dependence of electron density, (ρb) on interaction length, (*R*ij) is shown in Figure 1.4.

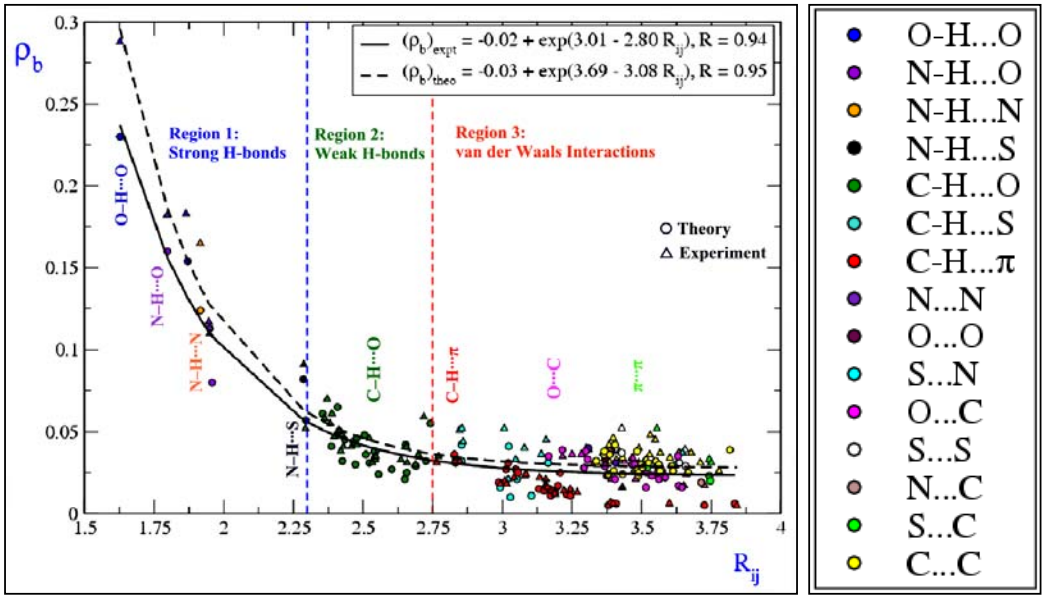


**Figure 1.4**: Exponential dependence of electron density, ρb (**r**) [eÅ$^{-3}$] on interaction length, *R*ij [Å] of 15 types of interactions and 114 data points, the circles and triangles represent experimental and theoretical values respectively and the solid and broken black lines represent the corresponding fittings.[63] The inset gives the details of the fitting models along with correlation coefficients R and the color code for each type of interactions. The interactions, categorized are marked accordingly.

Based on the values of *R*ij, in the range of 1.6 to 3.8 Å and the corresponding values of ρb, lie between 0.3 to 0.005 eÅ$^{-3}$, they separated the range of interactions from hydrogen bonds to van der Waals interactions into three categories. The hydrogen bonds such as, O-H···O, N-H···O, N-H···N and N-H···S fall in the region of strong hydrogen bonds (*R*ij < 2.3 Å, ρb > 0.08 eÅ$^{-3}$), *region 1*. The C-H···O interactions reside in the weak hydrogen bond region (2.3 Å < *R*ij < 2.75 Å, 0.07 eÅ$^{-3}$ > ρb > 0.02 eÅ$^{-3}$), *region 2*. The interactions like, C-H···π, C-H···S and π···π (O···C, N···N, C···C, O···O, S···S, S···C, S···N and N···C) are among the weakest types of interactions and belong to the van der Waals interaction region (*R*ij > 2.75 Å, ρb < 0.05 eÅ$^{-3}$), *region 3*. However, the borders between the categories are not clear cut

and some interactions are difficult to classify. Among non-covalent interactions, *hydrogen bonding* is the most exclusively studied and recognized as strong, specific and highly directional intermolecular interactions.[56] This has emerged as the most important organizing principle not only for the crystal engineering but also for structure of biologically important molecules[64] and supramolecular chemistry.[65] The significance of other weak hydrogen bonding interactions such as C-H···O,[56] C-H···N,[66] C-H···F,[67] C-H···π,[68,69] C-H···X (X = Cl, Br, I),[70] in the molecular packing arrangement were characterized earlier. Although the van der Waals (dipole-dipole, dipole-induced dipole and dispersion) interactions such as π···π,[71] halogen-halogen interactions[72] etc. contribute less energies among the other intermolecular interactions, they play a decisive role in molecular aggregation in the absence of other stronger interactions.

### *1.4.1. Analysis of Weak Interactions using CSD and PDB*

There may be many intermolecular interactions in a crystal structure; it is not possible that all the measured interactions have the expected geometries for stable interactions.[73] Therefore, it is necessary to analyze experimentally observed interactions on a statistical basis, taking results from a large number of crystal structure determinations.[74] The establishment of databases like Crystallographic Structural Database (CSD),[16] Inorganic Crystal Structure Database (ICSD),[75] Protein Data Bank (PDB),[76] etc. provide an opportunity to analyze the nature of weak interactions. The first systematic analysis was carried out by Dunitz *et al*. to study the orientational preferences of non-covalent contacts around the divalent sulfur by electrophiles and nucleophiles.[77]

The Crystallographic Structural Database (CSD) is a wealth of structural information from which one can retrieve intermolecular interactions in organic/organometallic compounds within an environment surrounding a specific

functional group.[74,78] The number of crystal structures stored in the CSD[16] is now sufficiently large to allow systematic survey of various weak interactions. Similarly a large number of protein crystal structures (~ 49,000 in 2007) in the PDB[76] can provide insights into the three dimensional arrangement of macromolecules and play a very significant role in molecular biology, medicine and drug discovery. This structural information is useful in understanding the orientational preferences for a selected functional group and the possible binding area of the ligand or receptor.[79,80] It is noteworthy that the geometrical analysis of functional group interactions in the enzyme-ligand complexes reported by Tintelnot and Andrews were in a good agreement with the same deduced from the statistical studies of small molecules.[81] Another remarkable study on the preferred interaction geometries of several functional groups found in the protein sequences were carried out by Klebe[82] using CSD. Interestingly, a similar search on the same groups found in the ligand-protein complexes (restricted to most precise data in the PDB) also showed identical distribution of geometries as observed from CSD. These geometrical restraints can be translated into rules, which may serve as guidelines in drug design and are introduced in programs [*SYBYL*[83] and *LUDI*[84]] as the 'composite crystal field environments'. Also, Taylor *et al*. highlighted the importance of crystallographic data for suggesting isotropic replacements in modeling protein-ligand interactions and constructed composite crystal environments for carbonyl and nitro groups.[85]

The weaker the interaction, the more relevant is the database analysis approach towards their understanding.[75] In the absence of any conventional hydrogen bonding, various other weak non-covalent interactions (which are energetically equivalent) can associate the molecules with different arrangements or conformations in the crystal lattice leading to the formation of polymorphs. Since this thesis reports the importance of weak non-covalent interactions with a special focus on the dipolar

contacts in the polymorphic modifications, conformational changes and solvent inclusions, an account of dipolar interactions is given below.

### *1.4.2. Dipole-Dipole Interactions in Organic Crystals*

When molecules pack in the crystalline state so that the (free) energy of the total arrangement is minimized, functional groups on these molecules are probably packed in a preferential manner that accommodates their interaction requirements. There may be many intermolecular interactions around one molecule in a crystal and some of the geometries may be distorted as the system compromises various possible interactions in order to minimize the total energy of the entire crystal. However, evaluating various weak interactions both qualitatively and quantitatively is one of the challenging tasks especially for dipolar-dipolar interactions.[86] To understand the difficulties, one should distinguish between different types of dipoles. In the case of molecular dipoles, there is a clear consensus in the literature. But, it is well established that such molecular dipoles do not play a decisive role in crystal packing.[87] However, for other types of dipoles, the situation is more complicated. One such area is the bond dipole-bond dipole interaction (A bond dipole is a dipole moment associated with a given bond) and the dipolar contacts of this type are investigated in the present thesis.[88]

Bond dipoles result from the assymmetric distribution of electrons in a covalent bond. The more electronegative atom is surrounded by electron density in excess that is required to balance its nuclear charge and therefore bears a partial negative charge ($\delta^-$). The less electronegative atom, lacking sufficient electron density to balance the nuclear charge, bears a positive charge ($\delta^+$). The attractive force between these dipoles result in bond dipolar interactions and their energy is directly proportional to the polarizabilty of the bond [Fig 1.5]. The strength of these interactions depends on the distance and the relative orientation of the dipoles.[89]


**Figure 1.5**: Schematic representation of bond dipole-dipole interactions.

Bolton first recognized the dipolar carbonyl-carbonyl interaction in the organic molecular crystals in 1963.[90] However, Davies and Blum had first observed these dipolar interactions in the crystals of parabanic acid in 1953.[91] Later, Bolton examined the crystal structure of alloxan, which showed interesting molecular association *via* dipolar C=O···C=O contacts instead of conventional hydrogen bonding (N–H···O) interactions.[92] In the structural studies of quinonoid compounds, Bernstein *et al*. concluded that interactions of carbonyl group possible either *via* C–H···O(=C) or C=O···C=O contacts.[93] Burgi *et al*. correlated the nucleophilic approach of oxygen to the carbonyl centre in the chemical reaction pathways using crystal structure data of short O···C=O contacts.[94] In contrast, Gavezzotti studied carbonyl and nitrile bond dipoles in the Cambridge Structural Database (CSD) and concluded that even for such strong dipoles, the electrostatic packing energy is often negligible.[95] On the other hand, Allen *et al*. described the nature of geometries and energies of carbonyl-carbonyl interactions and inferred that these interactions are important in crystal packing.[96] Recently, Lee *et al*. reexamined the dipolar interactions of C≡N, C=O and C–F and explained the contradiction between Gavezzotti and Allen's results.[88] The former implicitly considered the distance dependence law, while the latter was more concerned with orientational effects.

Allen *et al*. used a combination of systematic database analysis and high level *ab initio* molecular orbital calculations to provide a significant insight into the nature of non-covalent C=O···C=O interactions.[96] They classified the dipolar interactions into three types; perpendicular (Type-I), anti-parallel (Type-II) and sheared parallel

(Type-III) motifs as shown in chart 1.3. The results obtained from the *ab initio* calculations of these interaction motifs using intermolecular perturbation theory (IMPT at 6-31G** level), indicated an attractive energy contribution that are comparable to medium strength hydrogen bonds. Later, Diederich *et al*. analyzed other halogenated dipolar interactions, C–F···C=O, C–Cl···C=O, C–Br···C=O and C–I···C=O and investigated the affinity of ligand to the thrombin active site *via* C–F···C=O contacts.[97] Wolf investigated an interesting case of polymorphic transformation of sulfone fungicide in which the metastable pale yellow color crystals (orthorhombic form) transformed to colorless monoclinic crystals in the presence of sun light.[98] The structural studies indicated that the metastable form possessed short dipolar S=O···C=O and C=O···S=O intramolecular interaction whereas the monoclinic form with longer geometries of these contacts.[99]

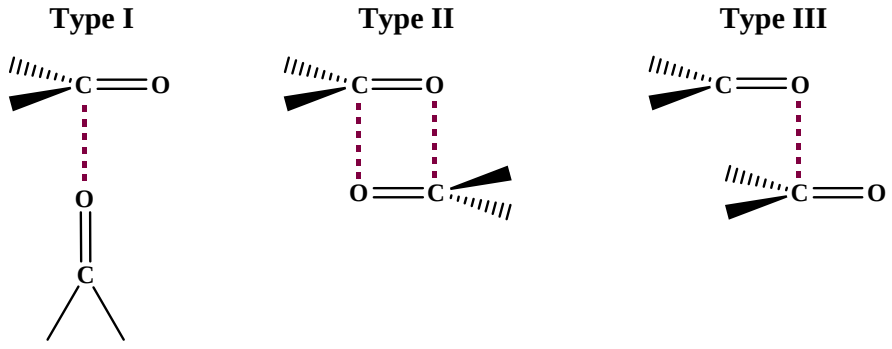


**Chart 1.3**

### *1.4.3. Applications of Dipole-Dipole Interactions*

The significance of weak interactions is recognized in all the branches of chemistry. The studies of non-covalent interactions are of profound importance in crystal engineering,[100] host-guest complexes,[101] drug design[57,79] as well as controlling polymorphic modifications in drugs,[1,3] dyes[102] and explosives.[103] The understanding of intermolecular interactions in the context of crystal packing can be useful for the designing of new solids with desired properties.[100] There are many reports of variation in color, mechanical properties and solubilities of polymorphs in the literature due to

the interplay of weak interactions.[104] The quantitative analysis of these interactions can be exploited for understanding structure-property correlations, reaction mechanisms and solid state reactivities.[105]

Although dipolar C=O···C=O contacts were observed earlier,[90] its importance in various fields is being recognized only recently. The changes in the interaction motif of carbonyl-carbonyl interactions were found to be responsible for the unusual thermodynamic properties of acetone, which had remained a mystery since 1929.[106] Maccallum *et al*. demonstrated the importance of C=O···C=O contacts in stabilizing the α-helices, β-sheets and the right-hand twist often observed in β-strands.[107] In depth knowledge of dipolar interactions can be effectively exploited in medicinal chemistry for the enhanced binding and/or selectivity in lead optimization and thereby design novel drug candidates (Structure Based Drug Design). For example, Diederich *et al*. investigated the enhanced activity of fluorinated thrombin inhibitors *via* dipolar C–F···C=O interactions in the active site [Fig 1.6(i)].[97] Such dipolar interactions were also involved in the binding of trifluoroacetyl dipeptide anilide inhibitor to porcine pancreatic eleastase enzyme [Fig 1.6(ii)].[108]

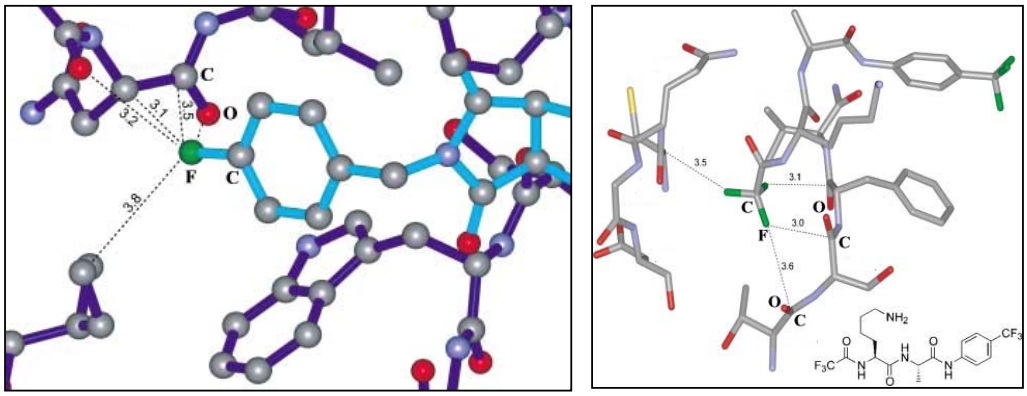


**Figure 1.6**: (i) Binding mode of the fluorinated inhibitor in the D pocket of thrombin [PDB code 1OYT]; (ii) C–F···C=O interactions in the crystal structure of the complex between porcine pancreatic elastase and and an inhibitor of the trifluoroacetyl peptide class at 2.50 Å resolution [PDB code 2EST].

## 1.5. Scope of the Present Studies

The work reported in this thesis was planned with the objective of exploring the polymorphic behavior of *myo*-inositol derivatives, as these compounds exhibited fascinating structural phenomena.[49-53] The structures of all the molecules reported in this thesis were so chosen that they do not bear functional groups capable of forming conventional hydrogen bonds. It was speculated that this would offer possibilities of observing interplay of different weaker interactions in the polymorphic modifications of inositol derivatives. The research work initiated with the structural studies of **8** [Chart 1.4], showed rather unexpected short contacts between S=O and C=O that associated the diastereomers of **8** (*Chapter 2*). This is considered as bond dipolar interaction between S=O and C=O, similar to C=O···C=O and C-F···C=O interactions described earlier. The CSD survey showed that these contacts indeed existed in a large number of crystal structures but were not recognized.[54] It was thought worthwhile to pursue the manifestation of this S=O···C=O dipolar interactions in molecules that contain these groups in different environments. Thus, synthetic modifications of *myo*-inositol (**1**) were carried out, structures of which were investigated for their molecular association with a special focus on dipolar contacts. Accordingly, compounds **9-23** containing S=O and C=O groups were prepared [Chart 1.4]. These studies on non-covalent interactions can have potential implications in understanding the receptor-ligand binding and designing lead compounds in *Structure Based Drug Design* approach. In this context, dipolar S=O···C=O interactions are thought to be relevant because of the presence of this moiety in sulfa drugs.

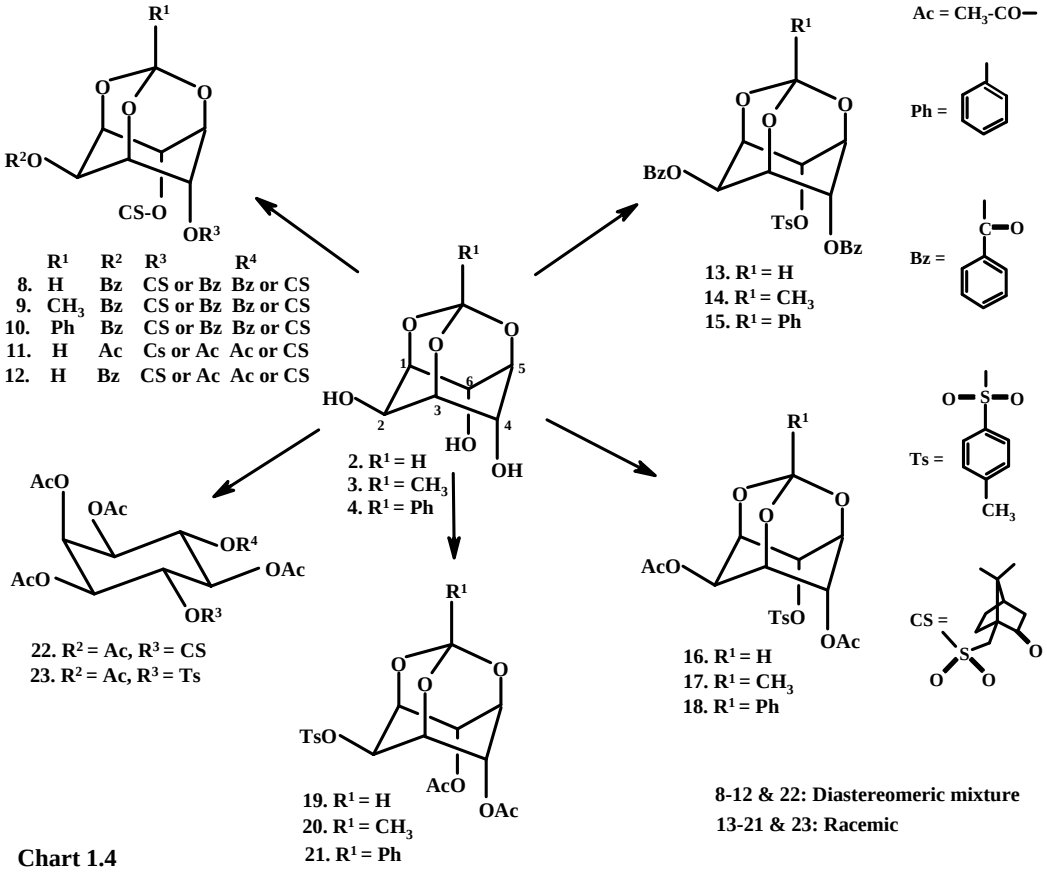
R1
R2O
CS-O
OR3
R1 R2 R3 R4
8. H Bz CS or Bz Bz or CS
9. CH3 Bz CS or Bz Bz or CS
10. Ph Bz CS or Bz Bz or CS
11. H Ac Cs or Ac Ac or CS
12. H Bz CS or Ac Ac or CS
HO
HO
OH
2. R1 = H
3. R1 = CH3
4. R1 = Ph
BzO
TsO
OBz
13. R1 = H
14. R1 = CH3
15. R1 = Ph
Ac = CH3-CO
Ph =
Bz =
C
O
O
S
O
Ts =
CH3
CS =
AcO
OAc
OR4
OAc
AcO
OR3
22. R2 = Ac, R3 = CS
23. R2 = Ac, R3 = Ts
TsO
AcO
OAc
19. R1 = H
20. R1 = CH3
21. R1 = Ph
AcO
TsO
OAc
16. R1 = H
17. R1 = CH3
18. R1 = Ph
8-12 & 22: Diastereomeric mixture
13-21 & 23: Racemic

**Chart 1.4**

# Chapter 2

## Recognition of S═O···C═O Dipolar Interactions in Diastereomeric Association: Pseudo-polymorphism in 2,4(6)-di-*O*-Benzoyl-6(4)-*O*-[(1*S*)-10-Camphorsulfonyl]-*myo*-Inositol-1,3,5-Orthoformate

# Chapter 2

## 2.1. Introduction

The role of solvents in crystallization and crystal growth is not completely understood because of the complex nature of non-bonded interactions between the host and solvent molecules.[109] Normally, during the formation of crystals of a single compound, solute-solvent interactions are replaced by solute-solute interactions. However, when non-covalent interactions between the solute and the solvent molecule are comparable or more favorable than solute-solute interactions, solvated crystals are formed. The affinity of a host molecule for a given guest depends on the nature of host, guest and the medium of crystallization under defined conditions of temperature, pressure and their concentration, apart from steric requirements of host and guest molecules. An insight into inclusion behavior has applications in pharmaceutical and chemical industries for the purification and resolution of drugs, trapping and storage of toxic materials, matrices for slow drug release, controlling pseudo polymorphic behavior etc.[110]

This chapter reports the diastereomeric association *via* dipolar interactions that led to synthesize various *myo*-inositol derivatives. Different molecular organization that involves the interplay of C–H···O and dipolar S=O···C=O short contacts is observed in pseudopolymorphs of **8** [Scheme 2.1]. Molecular packing in their crystal lattices is modulated depending upon the solvent and the nature of weak association between the molecules. Therefore, related *myo*-inositol derivatives [Scheme 2.1] were prepared to explore for their polymorphic behavior *via* weak interactions.

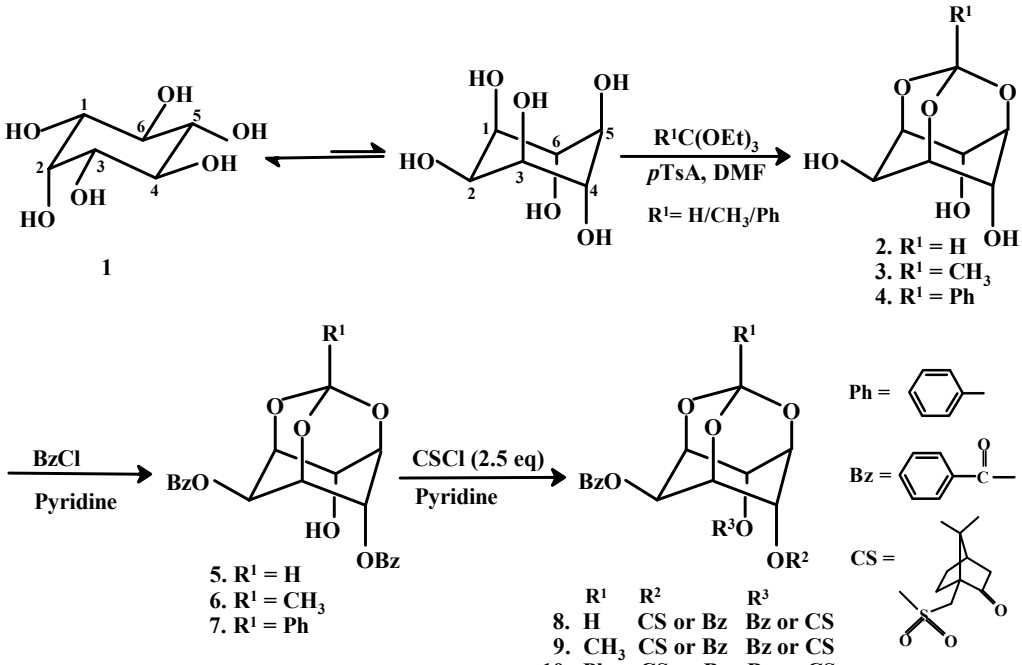


**Scheme 2.1**

## 2.2. Experimental Section

### *2.2.1. Synthesis*

*2.2.1.1. Preparation of 2,4(6)-di-O-benzoyl-6(4)-O-[(1S)-10-camphorsulfonyl]-myo-inositol 1,3,5-orthoformate* (**8**, *mixture of diastereomers*)

A mixture of racemic 2,4-di-*O*-benzoyl *myo*-inositol 1,3,5 orthoformate (0.398 g, 1 mmol), camphorsulfonyl chloride (0.750 g, 3 mmol) and pyridine (10 mL) was stirred at room temperature for 72 h. The solvents were evaporated from the reaction mixture under reduced pressure and the gummy residue was dissolved in chloroform, washed with dilute hydrochloric acid, dilute sodium bicarbonate solution, water and finally with brine. The organic layer was dried over anhydrous sodium sulphate, solvents were evaporated under reduced pressure and the product finally purified by column chromatography using ethyl acetate-light petroleum mixture as eluent (0.604 g, 99 %).[111]

Data for **8**:

**M.P.**: 159-160 °C

**IR** ($CHCl_3$)**ν**: 1717, 1734 $cm^{-1}$

**$^1$H NMR** ($CDCl_3$, 200 MHz): **δ** 0.75-0.81 (2s, 3H, Me), 0.95-1.00 (2s, 3H, Me), 1.24-1.32 (m, 1H), 1.63-1.69 (m, 1H), 1.84-1.98 (m, 3H), 2.04-2.11 (m, 2H), 2.85-2.98 (2d, 1H), 3.50-3.60 (2d, 1H), 4.60-4.80 (m, 2H, Ins H), 4.80-4.90 (m, 1H, Ins H), 5.50-5.65 (m, 2H, Ins H), 5.70 (d, *J* = 1.0 Hz, 1H, Ins H), 5.86-5.90 (m, 1H, $O_3CH$), 7.40-7.65 (m, 6H, ArH), 8.10-8.20 (m, 4H, ArH) ppm.

**$^{13}$C NMR** (50 MHz, $CDCl_3$): **δ** 19.5, 24.9, 26.8, 26.9, 42.3, 42.7, 48.1, 48.3, 57.9, 63.3, 67.4, 67.6, 69.2, 69.5, 69.9, 72.4, 72.6, 76.6, 93.4, 96.4, 103.1, 128.6, 128.7, 128.9, 129.4, 130.0, 130.1, 133.6, 133.8, 165.0, 165.1, 165.9, 187.5, 213.8, 213.9 ppm.

**Anal. Calcd for $C_{31}H_{32}O_{11}S$**: C, 60.77; H, 5.26. Found: C, 60.56; H, 5.21 %.

*2.2.1.2. Preparation of 2,4(6)-di-O-benzoyl-6(4)-O-[(1S)-10-camphorsulfonyl]-myo-inositol 1,3,5-orthoacetate* (**9**, *mixture of diastereomers*)

A mixture of pyridine (10 mL), racemic 2,4-di-*O*-benzoyl *myo*-inositol 1,3,5-orthoacetate (0.412 g, 1 mmol) and camphorsulfonyl chloride (0.750 g, 3 mmol) were stirred at room temperature for 24 h. Pyridine was evaporated under reduced pressure and the residue obtained was worked up with chloroform. The crude **9** was purified (0.451 g, 72 %) by column chromatography over silica (eluent: ethyl acetate-petroleum ether 1:9).[112]

Data for **9**:

**M.P.**: 153-154 °C

**IR** ($CHCl_3$)**ν**: 1718, 1733 $cm^{-1}$

**$^1$H NMR** ($CDCl_3$, 200 MHz): **δ** 0.71-0.77 (2s, 3H, Me), 0.92-1.02 (2s, 3H, Me), 1.43 (s, 1H), 1.62 (s, 3H, $O_3CMe$), 1.64-1.73 (m, 1H), 1.88-2.10 (m, 3H), 2.26-2.42 (m,

2H), 2.81-2.98 (m, 1H), 3.46-3.59 (2d, 1H), 4.61-4.76 (m, 2H, Ins H), 4.76-4.83 (m, 1H, Ins H), 5.47-5.59 (m, 2H, Ins H), 5.78-5.86 (m, 1H, Ins H), 7.43-7.63 (m, 6H, ArH), 8.10-8.18 (m, 4H, ArH) ppm.

**$^{13}$C NMR** ($CDCl_3$, 50 MHz): **δ** 19.4, 19.5, 23.9, 24.7, 26.7, 26.8, 42.2, 42.6, 47.9, 48.0, 48.1, 57.7, 57.8, 62.3, 67.3, 67.4, 67.5, 69.8, 70.0, 70.3, 72.4, 72.6, 109.2, 128.4, 128.6, 128.8, 129.3, 129.9, 130.0, 133.5, 133.6, 165.1, 165.9, 213.9 ppm.

**Anal. Calcd for $C_{32}H_{34}O_{11}S$**: C, 61.33; H, 5.47. Found: C, 61.49; H, 5.42 %.

*2.2.1.3. Preparation of 2,4(6)-di-O-benzoyl-6(4)-O-[(1S)-10-camphorsulfonyl]-myo-inositol-1,3,5-orthobenzoate* (**10**, *mixture of diastereomers*)

A mixture of racemic 2,4-di-*O*-benzoyl-*myo*-inositol 1,3,5-orthobenzoate[46] (0.237 g, 0.5 mmol) and camphorsulfonyl chloride (0.375 g, 1.5 mmol) in pyridine (8 mL) were stirred at room temperature for 48 h. Pyridine was evaporated under reduced pressure and the residue obtained was worked up with chloroform. The crude **10** was purified (0.253 g, 74 %) by column chromatography over silica (eluent: ethyl acetate-petroleum ether 1:9).

Data for **10**:

**M.P.**: 159-160 °C

**IR** ($CHCl_3$)**ν**: 1712, 1735 $cm^{-1}$

**$^{1}$H NMR** ($CDCl_3$, 200 MHz): **δ** 0.69-0.80 (2s, 3H, Me), 0.91-1.05 (2s, 3H, Me), 1.09-1.25 (m, 1H), 1.40-1.77 (m, 1H), 1.82-2.13 (m, 3H), 2.18-2.44 (m, 2H), 2.83-3.03 (m, 1H), 3.50-3.63 (2d, 1H), 4.81-5.05 (m, 3H, Ins H), 5.61-5.73 (m, 2H, Ins H), 5.95-6.03 (m, 1H, Ins H), 7.39-7.65 (m, 9H, ArH), 7.69-7.77 (m, 2H, ArH), 8.11-8.20 (m, 4H, ArH) ppm.

**$^{13}$C NMR** ($CDCl_3$, 50 MHz): **δ** 19.7, 25.0, 27.0, 27.1, 42.6, 42.9, 48.3, 48.5, 58.1, 62.7, 67.7, 67.8, 68.4, 68.6, 70.9, 71.1, 71.4, 72.7, 72.9, 108.2, 125.7, 128.4, 128.8,

129.0, 129.6, 130.3, 130.4, 133.8, 134.0, 136.3, 165.3, 165.4, 166.2, 214.1, 214.2 ppm.

**Anal. Calcd for $C_{37}H_{36}O_{11}S$**: C, 64.52; H, 5.27. Found: C, 64.50; H, 5.37 %.

*2.2.1.4. Preparation of 2,4(6)-di-O-acetyl-6(4)-O-[(1S)-10-camphorsulfonyl]-myo-inositol 1,3,5-orthoformate* (**11**, *mixture of diastereomers*)

The dibenzoate **8** (0.612 g, 1 mmol) was heated with *tert*butylamine (5 mL) in methanol (8 mL) under reflux for 8 h. The residue obtained after removal of volatile liquids was dissolved in pyridine (4 mL), a solution of acetic anhydride (0.3 mL, 3 mmol) in pyridine (4 mL) was added drop wise at 0 °C, and then the mixture stirred for 24 h. Pyridine was evaporated under reduced pressure and the residue obtained was worked up with chloroform. The crude **11** was purified by column chromatography over silica (eluent: ethyl acetate-petroleum ether 1:9) to obtain **11** (0.464 g, 95 %) as white solid.

Data for **11**:

**M. P.**: 152-153 °C

**IR** ($CHCl_3$)**ν**: 1736, 1749 $cm^{-1}$

**$^1$H NMR** ($CDCl_3$, 200 MHz): **δ** 0.84-0.94 (2s, 3H, Me), 1.06-1.14 (2s, 3H, Me), 1.45-1.84 (m, 3H), 1.92-2.02 (m, 2H), 2.14 (s, 3H, MeCO), 2.22 (s, 3H, MeCO), 2.30-2.55 (m, 2H), 2.98-3.16 (m, 1H), 3.58-3.73 (2d, 1H), 4.29-4.39 (m, 1H, Ins H), 4.46-4.54 (m, 1H, Ins H), 4.66-4.78 (m, 1H, Ins H), 5.13-5.23 (m, 1H, Ins H), 5.37-5.47 (m, 1H, Ins H), 5.48-5.57 (m, 1H, Ins H), 5.59 (d, $J$ = 1.0 Hz, 1H, $O_3C$) ppm.

**$^{13}$C NMR** (50 MHz, $CDCl_3$): **δ** 19.5, 19.5, 20.7, 20.9, 24.5, 25.2, 26.7, 26.8, 42.3, 42.3, 42.5, 42.8, 47.8, 48.0, 48.3, 57.8, 58.0, 62.5, 62.6, 66.8, 66.9, 67.1, 67.2, 68.8, 68.9, 68.9, 69.1, 72.3, 72.7, 102.7, 169.5, 170.2, 214.0, 214.4 ppm.

**Anal. Calcd for $C_{21}H_{28}O_{11}S$** : C, 51.64; H, 5.74. Found: C, 51.23; H, 5.97 %.

*2.2.1.5. Preparation of 2-O-benzoyl-4(6)-O-acetyl-6(4)-O-[(1S)-10-camphorsulfonyl-myo-inositol 1,3,5-orthoformate* (**12**, *mixture of diastereomers*)

The dibenzoate **8** (0.612 g, 1 mmol) was heated with *tert*butylamine (5 mL) in methanol (8 mL) under reflux for 8 h. The residue obtained after removal of volatile liquids was dissolved in pyridine (4 mL), a solution of benzoyl chloride (0.12 mL, 1.01 mmol) in pyridine (2 mL) was added drop wise at 0 °C, and the mixture stirred at room temperature for 8 h. Then a solution of acetic anhydride (0.2 mL, 2 mmol) in pyridine (2 mL) was added to the reaction mixture and continued stirring for 12 h. The solvents were evaporated from the reaction mixture under reduced pressure and the gummy residue obtained worked up with ethyl acetate and finally purified by column chromatography to obtain **12** (0.508 g, 92 %) as gum.

Data for **12**:

**M.P.**: 56-58 °C

**IR** ($CHCl_3$)**ν**: 1724, 1747 $cm^{-1}$ (C=O)

**$^1$H NMR** (200 MHz, $CDCl_3$): **δ** 0.88, 0.92 (2s, 3H, Me), 1.11, 1.12 (2s, 3H, Me), 1.40-2.25 (m, 5H), 2.17 (s, 3H, MeCO), 2.32-2.50 (m, 2H), 3.02-3.17 (2d, 1H), 3.63-3.75 (2d, 1H), 4.44-4.52 (m, 1H, Ins H), 4.59-4.69 (m, 1H, Ins H), 4.72-4.82 (m, 1H, Ins H), 5.38-5.50 (m, 2H, Ins H), 5.56-5.62 (m, 1H, Ins H), 5.64 (d, *J* = 1.0 Hz, 1H, $O_3C$), 7.36-7.66 (m, 3H, ArH), 8.11-8.18 (m, 2H, ArH) ppm.

**$^{13}$C NMR** ($CDCl_3$, 50 MHz) **δ**: 19.6, 20.7, 24.6, 25.2, 26.8, 26.9, 42.3, 42.4, 42.6, 42.8, 48.0, 48.1, 48.2, 48.5, 57.9, 58.0, 63.1, 67.1, 67.2, 67.3, 69.0, 69.1, 69.3, 72.5, 72.9, 102.9, 128.5, 129.3, 129.9, 133.5, 165.9, 169.6, 214.0, 214.4 ppm.

**Anal. Calcd for $C_{26}H_{30}O_{11}S$**: C, 56.72; H, 5.49; Found: C, 57.00; H, 5.40 %.

### *2.2.2. Crystallization*

All the crystallization experiments were carried out under identical conditions, by dissolving the diastereomeric mixture completely in the required solvent or

mixture of solvents (1:1) followed by the addition of light petroleum ether (bp 40-60 $^0$C) drop-wise till turbidity appeared. The clear solution obtained after vigorous shaking or warming, was allowed to stand for 1-5 days at room temperature to obtain colorless crystals for **8** and **11**. Crystals of **9** and **10** were obtained from a solution of dichloromethane-methanol (4:1) mixture by slow evaporation in a closed container at room temperature. Crystallization attempts from various solvents failed to produce crystals for **12**, resulting in a gummy product.

### *2.2.3. Crystallographic Details*

X-ray intensity data for solvates of **8** and solvent free crystals of **9**-**11** were collected on a Bruker SMART APEX CCD diffractometer in omega and phi scan mode, $\lambda_{MoK\alpha}$ = 0.71073 Å. Due to moderate stability (~ 2-6 days) of solvated crystals of **8**, X-ray intensities were measured at low temperature (133 K) using OXFORD LN2 cryosystem. All the intensities were corrected for Lorentzian, polarisation and absorption effects using Bruker's *SAINT* and *SADABS* programs.[113] The crystal structures were solved by Direct methods using program *SHELXS-97*; the full-matrix least squares refinements on $F^2$ were carried out by applying geometrical constraints especially for the guests having lower occupancies and disorder in the crystal lattice using *SHELXL-97*.[114] Planar guests like benzene (**8·BZ**) and pyridine (**8·PY**) exhibit statistical disorder about crystallographic 2-fold axis, that is modeled using DFIX and FLAT options whereas the disorders of dioxane (**8·DX**) and THF (**8·THF**) molecules were modeled using the DFIX and DANG options in *SHELXL-97* during refinement. Hydrogen atoms were included in the refinement as per the riding model. All the space groups are non-centrosymmetric (chiral) because of the presence of the camphor moiety and flack parameters could be refined in the least-squares due to the presence of a heavy atom (sulphur). Table 2.1 summarizes the crystallographic data for pseudopolymorphs of **8** and **9**-**11**.

**Table 2.1**: Summary of crystallographic data for **9-11** and pseudopolymorphs of **8**.

| Crystal data | **8** | **8·DX** | **8.DXTHF** | **8.BZ** |
|---|---|---|---|---|
| Chemical Formula | $C_{31}H_{32}O_{11}S$ | $C_{31}H_{32}O_{11}S$ 1.38($C_4H_8O_2$) | $C_{31}H_{32}O_{11}S$ 1.0($C_4H_8O_2$) 0.25($C_4H_8O$) | $C_{31}H_{32}O_{11}S$ 0.75($C_6H_6$) |
| $M_r$ | 612.63 | 733.77 | 718.76 | 669.70 |
| Temperature/K | 298(2) | 133(2) | 133(2) | 133(2) |
| Morphology | Plate | Plate | Plate | Plate |
| Colour | Colorless | Colorless | Colorless | Colorless |
| Crystal size (mm) | 0.57 x 0.40 x 0.22 | 0.37 x 0.35 x 0.13 | 0.38 x 0.33 x 0.17 | 0.51 x 0.25 x 0.19 |
| Crystal system | Monoclinic | Monoclinic | Monoclinic | Monoclinic |
| Space group | *P2₁* | *P2₁* | *P2₁* | *C2* |
| *a* (Å) | 14.115(3) | 15.937(4) | 15.966(3) | 31.182(4) |
| *b* (Å) | 11.592(3) | 11.054(3) | 11.068(3) | 11.2219(13) |
| *c* (Å) | 17.743(4) | 22.206(6) | 22.264(5) | 22.715(3) |
| $\alpha$ (°) | 90 | 90 | 90 | 90 |
| $\beta$ (°) | 92.529(4) | 108.432(4) | 108.676(4) | 109.948(2) |
| $\gamma$ (°) | 90 | 90 | 90 | 90 |
| *V* (Å$^3$) | 2900.2(11) | 3711.3(16) | 3727.0(14) | 7471.8(15) |
| *Z*, $D_x$ (Mg m$^{-3}$) | 4, 1.403 | 4, 1.313 | 4, 1.281 | 8, 1.191 |
| $\mu$ (mm$^{-1}$) | 0.175 | 0.154 | 0.151 | 0.143 |
| *F(000)* | 1288 | 1552 | 1520 | 2912 |
| $T_{min}$ , $T_{max}$ | 0.907, 0.963 | 0.945, 0.980 | 0.945, 0.975 | 0.931, 0.974 |
| $\theta_{max}$ (°) | 26.0 | 25.0 | 25.0 | 25.0 |
| *h* (min, max) | (-17, 17) | (-18, 18) | (-18, 18) | (-36, 36) |
| *k* (min, max) | (-14, 14) | (-13, 13) | (-7, 13) | (-13, 13) |
| *l* (min, max) | (-21, 21) | (-26, 26) | (-22, 26) | (-27, 27) |
| No. of refl$^n$ collected | 22352 | 35635 | 23847 | 36183 |
| No. of unique refl$^n$ | 11213 | 12908 | 9623 | 13103 |
| No. of observed refl$^n$ | 10237 | 9889 | 7016 | 8587 |
| No. of parameters | 779 | 875 | 982 | 900 |
| $R_{int}$ | 0.026 | 0.046 | 0.059 | 0.026 |
| $R_1$_obs, $R_1$_all | 0.048, 0.053 | 0.091, 0.115 | 0.070, 0.099 | 0.067, 0.091 |
| $wR_2$_obs, $wR_2$_all | 0.123, 0.127 | 0.247, 0.269 | 0.177, 0.197 | 0.173, 0.185 |
| GoF | 1.02 | 1.02 | 1.05 | 0.94 |
| $\Delta\rho_{max}$, $\Delta\rho_{min}$ (e Å$^{-3}$) | 0.37, –0.23 | 1.74, –0.48 | 0.61, –0.35 | 0.67, –0.26 |
| Flack parameter | -0.05(6) | –0.21(16) | 0.08(16) | 0.08(10) |

**Table 2.1**: Continued.

| Crystal data | **8·DCM** | **8·HX** | **8·PY** | **8·THF** |
|---|---|---|---|---|
| Chemical Formula | $C_{31}H_{32}O_{11}S$ 1.38($CH_2Cl_2$) | $C_{31}H_{32}O_{11}S$ 0.25($C_6H_{10}O$) 0.75($C_6H_{12}$) | $C_{31}H_{32}O_{11}S$ 1.63($C_5H_5N$) 0.38($H_2O$) | $C_{31}H_{32}O_{11}S$ 1.33($C_4H_8O$) |
| $M_r$ | 729.40 | 678.74 | 728.02 | 685.21 |
| Temperature/K | 133(2) | 133(2) | 133(2) | 133(2) |
| Morphology | Needle | Needle | Plate | Needle |
| Colour | Colorless | Colorless | Colorless | Colorless |
| Crystal size (mm) | 0.71 x 0.21 x 0.14 | 0.73 x 0.18 x 0.05 | 0.65 x 0.62 x 0.31 | 0.38 x 0.16 x 0.12 |
| Crystal system | Monoclinic | Monoclinic | Monoclinic | Monoclinic |
| Space group | *C2* | *C2* | *C2* | *C2* |
| *a* (Å) | 30.561(17) | 31.047(6) | 30.623(9) | 30.675(6) |
| *b* (Å) | 10.925(6) | 11.2665(18) | 11.129(4) | 11.218(2) |
| *c* (Å) | 22.255(12) | 22.631(4) | 22.529(7) | 22.323(5) |
| $\alpha$ (°) | 90 | 90 | 90 | 90 |
| $\beta$ (°) | 114.922(10) | 109.880(4) | 111.050(5) | 113.729 (6) |
| $\gamma$ (°) | 90 | 90 | 90 | 90 |
| *V* (Å$^3$) | 6739(6) | 7444(2) | 7165(4) | 7032(2) |
| *Z*, $D_x$ (Mg m$^{-3}$) | 8, 1.438 | 8, 1.211 | 8, 1.350 | 8, 1.294 |
| $\mu$ (mm$^{-1}$) | 0.353 | 0.145 | 0.155 | 0.154 |
| *F(000)* | 2996 | 2972 | 3066 | 2888 |
| $T_{min}$ , $T_{max}$ | 0.777, 0.950 | 0.901, 0.993 | 0.906, 0.954 | 0.944, 0.982 |
| $\theta_{max}$ (°) | 25.0 | 25.0 | 25.0 | 25.0 |
| *h* (min, max) | (-36, 36) | (-36, 36) | (-36, 34) | (-36, 36) |
| *k* (min, max) | (-12, 12) | (-13, 12) | (-13, 13) | (-13, 13) |
| *l* (min, max) | (-26, 25) | (-26, 26) | (-26, 26) | (-26, 26) |
| No. of refl$^n$ collected | 24219 | 26352 | 25788 | 33911 |
| No. of unique refl$^n$ | 11278 | 11718 | 12508 | 12365 |
| No. of observed refl$^n$ | 8132 | 10023 | 11721 | 11604 |
| No. of parameters | 861 | 951 | 929 | 954 |
| $R_{int}$ | 0.071 | 0.030 | 0.018 | 0.035 |
| $R_1$_obs, $R_1$_all | 0.091, 0.125 | 0.071, 0.082 | 0.050, 0.532 | 0.061, 0.063 |
| $wR_2$_obs, $wR_2$_all | 0.199, 0.219 | 0.197, 0.209 | 0.145, 0.149 | 0.169, 0.172 |
| GoF | 1.07 | 1.05 | 1.05 | 1.08 |
| $\Delta\rho_{max}$, $\Delta\rho_{min}$ (e Å$^{-3}$) | 0.98, –0.49 | 0.86, –0.30 | 0.93, –0.60 | 1.00, –0.28 |
| Flack parameter | 0.09(10) | –0.1(4) | 0.02(8) | -0.01(8) |

**Table 2.1**: Continued.

| Crystal data | **8·PYDX** | **9** | **10** | **11** |
|---|---|---|---|---|
| Chemical Formula | $C_{31}H_{32}O_{11}S$ 0.88($C_5H_5N$) 0.38($C_4H_8O_2$) | $C_{32}H_{34}O_{11}S$ | $C_{37}H_{36}O_{11}S$ | $C_{21}H_{28}O_{11}S$ |
| $M_r$ | 691.71 | 626.65 | 688.72 | 488.49 |
| Temperature/K | 133(2) | 298(2) | 133(2) | 298(2) |
| Morphology | Plate | Block | Plate | Needle |
| Colour | Colorless | Colorless | Colorless | Colorless |
| Crystal size (mm) | 0.59 x 0.29 x 0.18 | 0.68 × 0.25 × 0.14 | 0.45 × 0.23 × 0.20 | 0.74 × 0.15 × 0.13 |
| Crystal system | Monoclinic | Triclinic | Monoclinic | Monoclinic |
| Space group | *C2* | *P1* | $P2_1$ | $P2_1$ |
| *a* (Å) | 30.896(3) | 11.5241(16) | 11.474(2) | 13.429(3) |
| *b* (Å) | 10.9667(11) | 11.6958(16) | 21.557(3) | 11.321(3) |
| *c* (Å) | 22.408(2) | 12.453(2) | 14.111(2) | 14.888(4) |
| $\alpha$ (°) | 90 | 80.499(3) | 90 | 90 |
| $\beta$ (°) | 111.469(2) | 62.449(2) | 98.894(4) | 97.732(4) |
| $\gamma$ (°) | 90 | 75.937(2) | 90 | 90 |
| *V* (Å$^3$) | 7065.8(12) | 1440.8(4) | 3448.4(10) | 2242.8(10) |
| *Z*, $D_x$ (Mg m$^{-3}$) | 8, 1.300 | 2, 1.444 | 4, 1.327 | 4, 1.447 |
| $\mu$ (mm$^{-1}$) | 0.153 | 0.177 | 0.155 | 0.205 |
| *F(000)* | 2907 | 660 | 1448 | 1032 |
| $T_{min}$ , $T_{max}$ | 0.915, 0.973 | 0.976, 0.889 | 0.934, 0.970 | 0.863, 0.974 |
| $\theta_{max}$ (°) | 25.0 | 25.0 | 25.0 | 25.0 |
| *h* (min, max) | (-35, 36) | (-13, 13) | (-10, 12) | (-15, 15) |
| *k* (min, max) | (-13, 10) | (-13, 13) | (-23, 23) | (-12, 13) |
| *l* (min, max) | (-26, 14) | (-14, 13) | (-15, 15) | (-17, 17) |
| No. of refl$^n$ collected | 14077 | 9388 | 14680 | 16192 |
| No. of unique refl$^n$ | 9421 | 7596 | 8771 | 7660 |
| No. of observed refl$^n$ | 7094 | 7284 | 3660 | 6509 |
| No. of parameters | 923 | 799 | 325 | 603 |
| $R_{int}$ | 0.026 | 0.039 | 0.059 | 0.032 |
| $R_1$_obs, $R_1$_all | 0.078, 0.100 | 0.052, 0.054 | 0.189, 0.304 | 0.048, 0.059 |
| $wR_2$_obs, $wR_2$_all | 0.213, 0.234 | 0.134, 0.136 | 0.426, 0.495 | 0.111, 0.116 |
| GoF | 1.04 | 1.09 | 1.35 | 1.01 |
| $\Delta\rho_{max}$, $\Delta\rho_{min}$ (e Å$^{-3}$) | 1.17, –0.38 | 0.54, –0.29 | 1.11, –0.42 | 0.46, –0.18 |
| Flack parameter | 0.00(15) | 0.00(8) | 0.07(5) | –0.05(7) |

The crystal structure of **10** exhibited a very high degree of orientational disorder, for the camphor moiety. The disorder became evident during the structure solution itself, having very low peak heights and some missing atoms belonging to this group. The alternate orientations for the camphor were difficult to resolve individually, only the major site is included in the refinement. Geometrical (DFIX and FLAT) and anisotropic displacement constraints (DELU and SIMU) were applied to camphor and phenyl rings in the least-squares refinement procedure. All the atoms are kept isotropic, as the refinement was not stable for the anisotropic treatment for the disordered non-H atoms.

### *2.2.4. Thermal Analysis (DTA/TGA)*

The Differential Thermal Analysis (DTA) and Thermo-Gravimetric Analysis (TGA) of all the inclusion crystals of **8** were analyzed using a Seiko DTA/TG 320 instrument. About 3-6 mg of the crystalline sample was placed in an aluminium pan and heated from 40 to 200 $^{\circ}$C at a rate of 10 $^{\circ}$C/minute. An empty pan was used as the reference and dry nitrogen was used for purging (50 mL/min).

## 2.3. Results and Discussion

### *2.3.1. Crystallization of* 8

Crystallization of **8** from different solvents showed clear preferences in crystal growth behavior. Suitable crystals (for Single Crystal X-ray studies) were not obtained from acetone, methanol, cyclohexane, nitromethane, trimethyl amine and diiodomethane; whereas crystallization from chloroform, ethyl acetate, dibromomethane and dimethylformamide gave good crystals (**8**) without inclusion of any of these solvents. However, when benzene, dichloromethane (DCM), cyclohexanone, pyridine, dioxane and tetrahydrofuran (THF) were used for

crystallization, the crystals of **8·BZ**, **8·DCM**, **8·HX**, **8·PY**, **8·DX** and **8·THF** were obtained that included the respective solvent molecules as guests in their crystal lattice. The guest selectivities among these were further investigated using 1:1 mixture of solvents for crystallization of **8**. Crystallization from DCM-benzene, DCM-THF, DCM-dioxane, DCM-pyridine (1:1) and DCM-THF-dioxane (1:1:1) mixtures resulted in the inclusion of the guest solvent other than DCM. Crystallization of **8** from a 1:1 mixture of pyridine and dioxane showed a preferred inclusion of pyridine (**8·PYDX**) whereas from dioxane-THF (1:1) mixture, the host molecules favored inclusion of dioxane over THF (**8·DXTHF**). All the solvated crystals were transparent and stable in open atmosphere for ~ 2-6 days and disintegrated slowly into powder form after this period. The crystals of **8** obtained from different solvents could be categorized into three forms. Form-I (without any solvent inclusion, **8**) having the monoclinic space group $P2_1$; Form-II (**8·DX**, **8·DXTHF**) belonging to the same space group as Form-I; and Form-III (**8·BZ**, **8·DCM**, **8·HX**, **8·PY**, **8·DX** and **8·PYDX**) crystals with majority of the solvents belonging to the monoclinic space group *C2*.

### *2.3.2. Thermal analysis of* **8**

The DTA/TGA curves for Forms I, II and III crystals are shown in figure 2.1. The crystals of the solvent free Form-I [Fig. 2.1(i)] showed only a single sharp melting endotherm at ~ 159.0 °C, whereas solvates showed an extra endotherm before the final melting curve of the crystals, indicating the possible structural phase transformation due to the escape of the guest solvent. Thermogravimetric analyses of all the solvates showed a continuous weight loss (11-23 %), in the temperature range 55-120 °C due to the release of included solvents from the crystal lattice. However, the final melting endotherm in the range 147-160 °C was the same for all the crystals matching with the melting of the solvent free crystal.

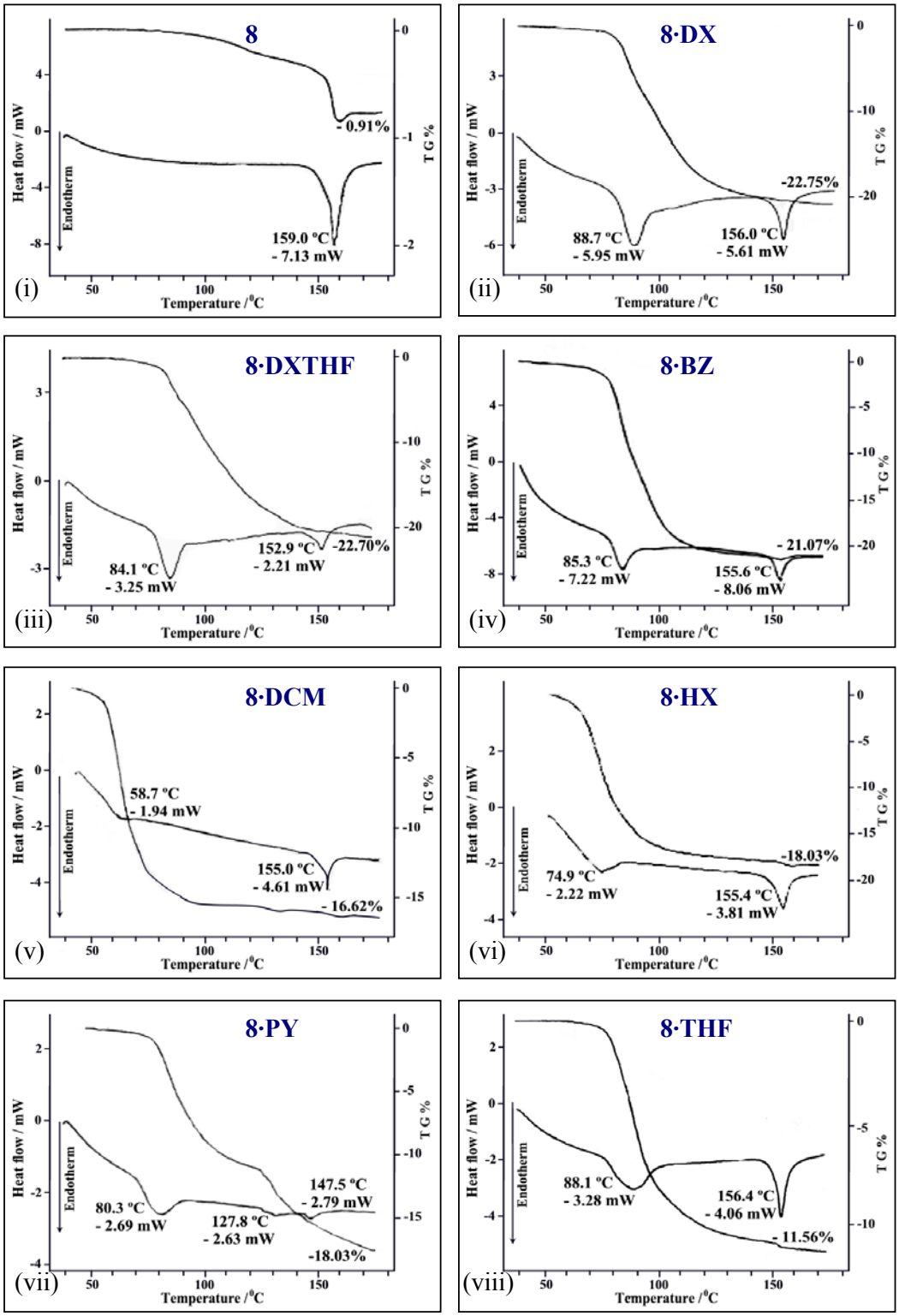


**Figure 2.1**: DTA/TGA curves of (i) Form-I, (ii)-(iii) Form-II and (iv-ix) Form-III crystals of **8**.

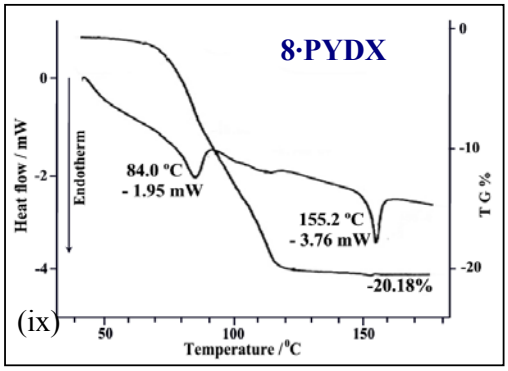


**Figure 2.1**: Continued.

### *2.3.3. Host-host interactions in* **8**

A common feature in all the three crystal forms was the molecular association between the diastereomers of **8**. In the absence of any conventional strong hydrogen bonding interactions, the bridging of **8** occurred *via* two pseudo-centrosymmetric C–H···O interactions (C6–H6···O9' and C4'–H4'···O9) in Form-I and *via* dipolar S═O···C═O interactions (S1'═O9'···C15 and S1═O9···C15') in Forms II and III [Fig. 2.2]. In all the pseudopolymorphs, the oxygen atom O9 (O9') of the -$SO_2$ group from one diastereomer approaches the C$sp^2$ atom C15' (C15) of the benzoate group of the other diastereomer almost perpendicularly and the O···C distances are significantly shorter (2.899-3.114 Å) than the sum of the van der Waals radii of O and C atoms (3.22 Å) [Table 2.2]. It was thought worthwhile to examine the occurrence of these short contacts in the other related structures available in the Cambridge Crystallographic Database (CSD). The statistical survey of CSD indeed clearly signified the existence of S═O···C═O interaction [*details are given in Chapter 7*]. However, the role of these dipolar contacts in the molecular association was first pointed out by us.[55] In fact these contacts can be categorized under bond dipole-dipole interactions, such as C=O···C=O and C–F···C=O suggested to play a role in folding of proteins[107] and improved binding of the fluorinated drug to receptors[97] respectively. As reported in the literature (C=O···C=O),[96] these dipolar interactions could contribute

attractive stabilization energies, which are comparable in strength to that of weak C–H···O interactions.

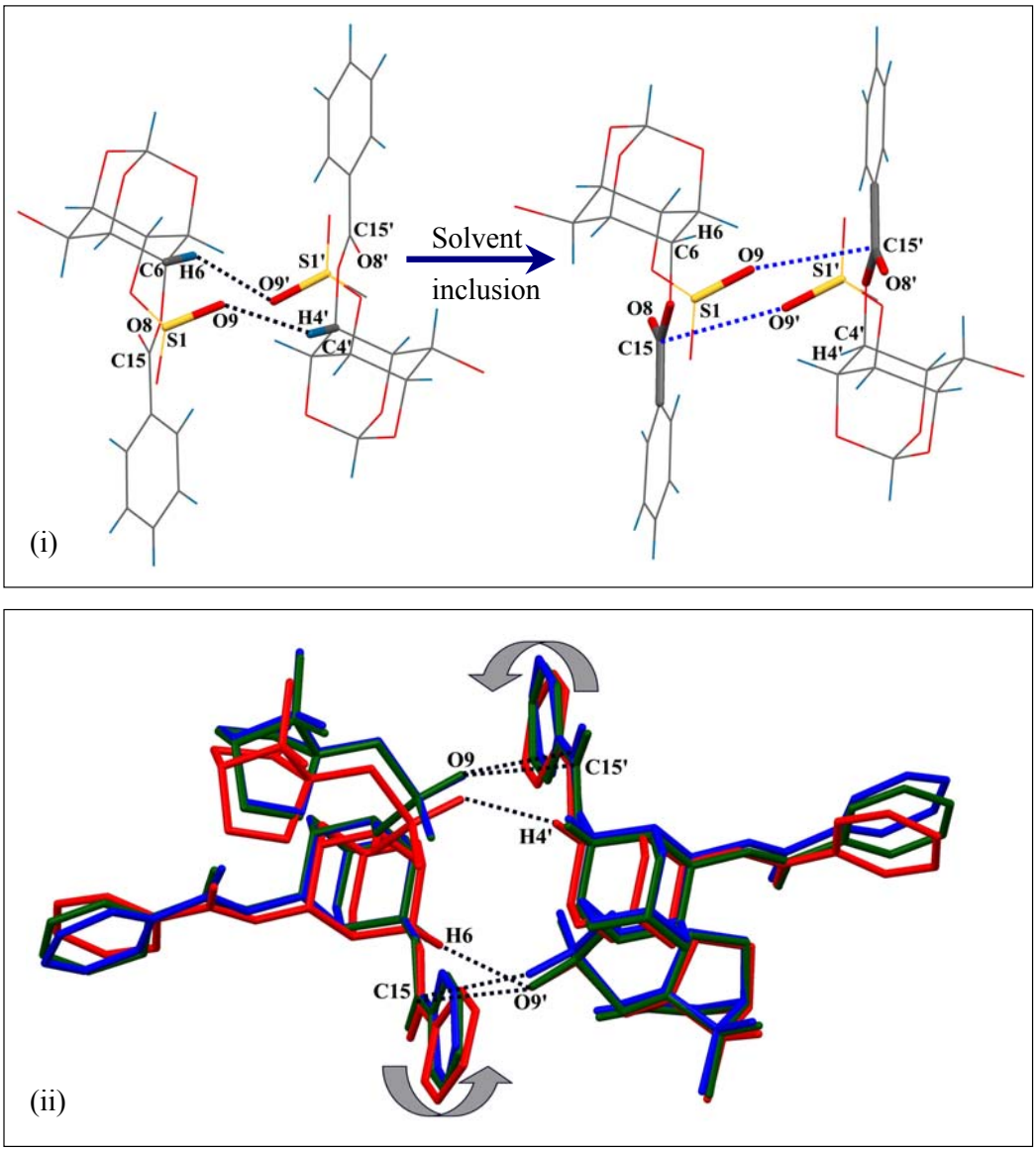


**Figure 2.2**: (i) Dimers of the Form-I (**8**) with C–H···O bridging cross over to S═O···C═O short contacts upon solvent inclusion [For clarity, the benzoyl groups (at *C2* and *C2*') and camphorsulphonyl groups (at *C4* and *C6*') are omitted]. (ii) Overlapping of dimers in Form I (red-**8**), II (blue-**8·DX**) and III (green-**8·BZ**) showing relative movement of molecules needed to switch between the two interactions.

**Table 2.2**: Geometrical parameters of S═O···C═O and C–H···O contacts for Forms I-III crystals of **8** as shown in figure 2.2.

| **Crystals** | **8** | **8·DX** | **8·DXTHF** | **8·BZ** | **8·DCM** |
|---|---|---|---|---|---|
| O9···C15' (Å) | 3.570(4) | 2.906(7) | 2.899(6) | 2.953(6) | 2.890(10) |
| O9'···C15 (Å) | 3.332(3) | 2.999(7) | 3.025(6) | 3.070(6) | 3.140(10) |
| O9···C15'–O8' (°) | 78.6(1) | 87.1(4) | 86.1(1) | 89.0(3) | 91.2(5) |
| O9'···C15–O8 (°) | 78.9(2) | 82.2(4) | 82.2(1) | 82.7(3) | 83.8(5) |
| S1═O9···C15' (°) | 165.1(2) | 160.3(4) | 160.1(1) | 156.0(3) | 151.3(4) |
| S1'═O9'···C15 (°) | 162.7(1) | 164.5(3) | 163.9(1) | 156.0(3) | 165.7(3) |
| C6–H6···O9' (Å) | 2.43 | 2.68 | 2.66 | 2.85 | 2.65 |
| C4'–H4'···O9 (Å) | 2.37 | 2.88 | 2.95 | 2.98 | 2.97 |
| C6–H6···O9' (°) | 139 | 121 | 122 | 123 | 122 |
| C4'–H4'···O9 (°) | 139 | 116 | 115 | 116 | 114 |

| **Crystals** | **8·HX** | **8·PY** | **8·THF** | **8·PYDX** |
|---|---|---|---|---|
| O9···C15' (Å) | 2.980(20) | 2.932(5) | 3.003(5) | 2.960(10) |
| O9'···C15 (Å) | 3.100(20) | 3.056(5) | 3.169(5) | 3.074(10) |
| O9···C15'–O8' (°) | 87.0(10) | 85.7(2) | 88.2(3) | 88.5(1) |
| O9'···C15–O8 (°) | 82.0(10) | 81.5(2) | 84.4(2) | 83.1(1) |
| S1═O9···C15' (°) | 162.0(10) | 157.4(2) | 167.4(3) | 163.7(1) |
| S1'═O9'···C15 (°) | 159.4(8) | 155.4(2) | 166.8(3) | 167.3(1) |
| C6–H6···O9' (Å) | 2.86 | 2.80 | 2.63 | 2.58 |
| C4'–H4'···O9 (Å) | 2.95 | 2.82 | 2.71 | 2.75 |
| C6–H6···O9' (°) | 125 | 126 | 125 | 124) |
| C4'–H4'···O9 (°) | 119 | 119 | 119 | 117 |

The geometrical parameters [Table 2.2] of dipolar S═O···C═O contacts observed in all inclusion crystals indicate that the interaction is of Type-I motif *i.e.* perpendicular interaction motif of dipoles.[112] The S═O···C═O and C–H···O interactions seem to be complementary, crystals with shorter S=O···C=O contacts have weaker C–H···O contacts (in Forms II and III) and *vice versa* (in Form-I) [Table 2.2]. When the diastereomers are associated *via* C–H···O contacts, the dimers are

closely packed and do not leave any space for the solvent inclusion [Fig. 2.3(i)]. However, molecular association *via* S═O···C═O contacts generates voids which are occupied by the guest solvents [Fig. 2.3(ii) and 2.3(iii)]. The choice between C–H···O and S═O···C═O contacts for the association of diastereomers seems to depend upon the medium of crystallization, although majority of solvents (6 out of 9) prefer the S═O···C═O association resulting in solvent inclusion crystals. However, the S═O···C═O contacts were observed only between the two diastereomers of **8**, the association in the crystal structure of separated diastereomer[115] was essentially *via* C–H···O interactions.

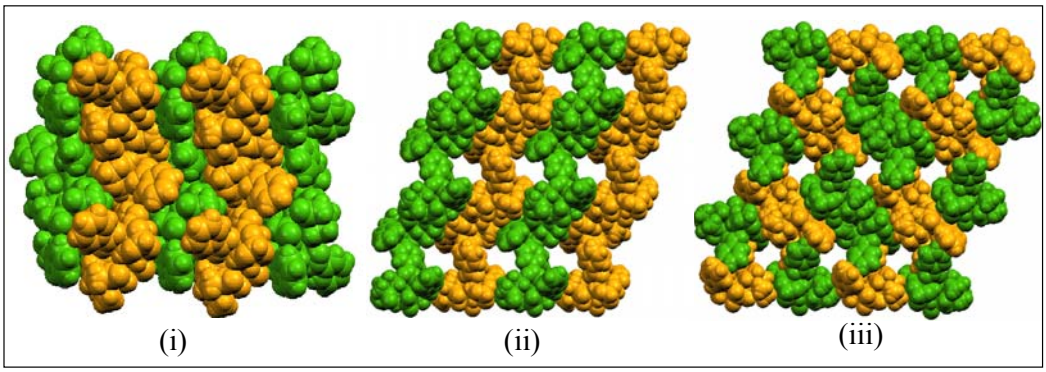


**Figure 2.3**: Molecular packing in (i) Form-I (**8**), (ii) Form-II (**8·DX**) and (iii) Form-III (**8·BZ**) crystals. Guest molecules are omitted in (ii) and (iii) to show the voids.

A comparison of the cell parameters of Forms I to III reveal conservation of the mode of molecular packing along the unique *b*- axis (~ 11.2 Å). The remarkable one-dimensional isostructucturality[116] along this axis, links the 'head-to-head' associated dimers *via* C–H···O interactions (C7–H7···O5' and C7'–H7'···O5) in all the crystal forms [Fig. 2.4]. There are additional C–H···O contacts in Forms II and III (C19–H19···O1 and C19'–H19'···O3') that bring the heads of the diastereomers even closer [Fig. 2.4(ii) and 2.4(iii)] in comparison to that in Form-I crystals [Fig. 2.4(i)]. Conserved supramolecular association in crystals is valuable in regressing to events in

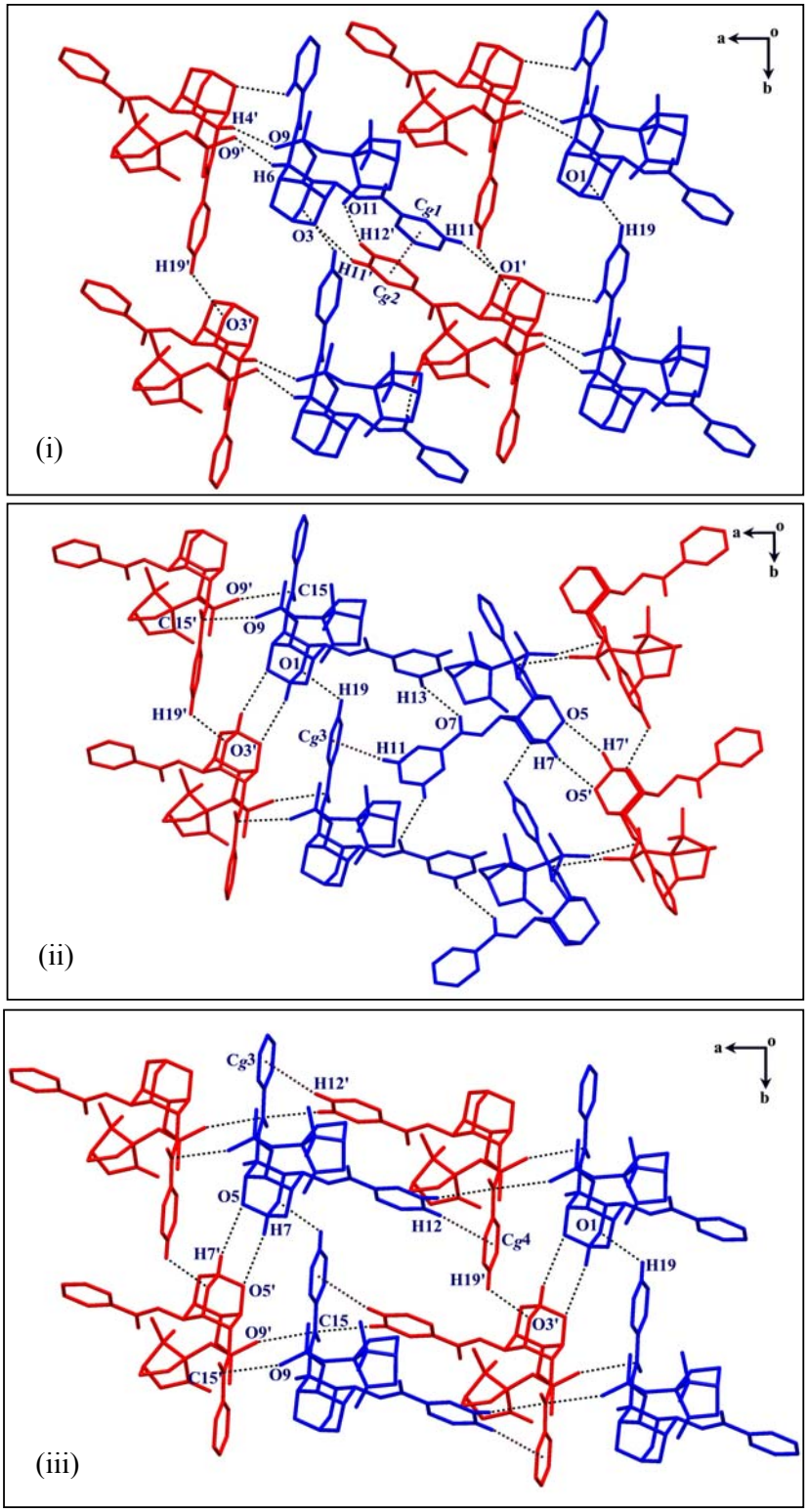


**Figure 2.4**: Isostructural layers of (i) Form-I, (ii) Form-II [**8·DX**] and (iii) Form-III [**8·PY**] crystals [only H-atoms involved in short contacts are shown].

early nucleation,[116] a stage difficult to observe experimentally. The different 'stitching' of these dimer-dimer chains along *a*-axis create voids to accommodate the guest in crystals of Forms II and III. In Forms I and III [Fig. 2.4(i) and 2.4(iii)], different diastereomers (blue-red) link the dimeric layers, whereas the same type (blue-blue and red-red) associate the dimeric rows in Form II [Fig. 2.4(ii)]. In solvent free Form-I, three C–H···O interactions, C11–H11···O1', C11'–H11'···O3 and C12'–H12'···O11 link two different dimeric layer and the phenyl rings attached to the C2 and C2' atoms (equatorial position) from different diastereomers C*g*1 [C9–C14] and C*g*2 [C9'–C14'] make moderate π···π interactions [C*g*1···C*g*2 = 4.031 Å, dihedral angle, α = 1.60°]. In Form-II, dimeric layers are linked *via* C13–H13···O7 and C–H···π [C11–H11···C*g*3 (C16–C21)] short contacts. Similar association exists between the (red-red) diastereomers as well [C13'–H13'···O7' and C11'–H11'···C*g*4 (C16'–C21')]. The dimers associated *via* S═O···C═O contacts in Form-III, make C–H···π [C12'–H12'···C*g*3 and C12–H12···C*g*4] contacts with the neighboring row of dimers [Table 2.3].

**Table 2.3**: Geometrical parameters of host-host interactions in Forms I, II and III of **8** as shown in figure 2.4.

| | D–H···A | D–H (Å) | H···A (Å) | D···A (Å) | D–H···A (°) |
|---|---|---|---|---|---|
| **8** | C19–H19···O1 [i] | 0.93 | 2.72 | 3.444(3) | 136 |
| Form-I | C19'–H19'···O3' [ii] | 0.93 | 2.74 | 3.450(4) | 134 |
| | C11–H11···O1' [ii] | 0.93 | 2.54 | 3.343(3) | 145 |
| | C11'–H11'···O3 [i] | 0.93 | 2.63 | 3.392(3) | 140 |
| | C12'–H12'···O11 [i] | 0.93 | 2.55 | 3.419(4) | 157 |
| **8·DX** | C19–H19···O1 [i] | 0.93 | 2.69 | 3.221(1) | 117 |
| Form-II | C19'–H19'···O3' [ii] | 0.93 | 2.62 | 3.209(1) | 122 |
| | C7–H7···O5' [iii] | 0.98 | 2.77 | 3.697(1) | 158 |
| | C7'–H7'···O5 [iv] | 0.98 | 2.79 | 3.722(1) | 160 |
| | C13–H13···O7 [v] | 0.93 | 2.68 | 3.313(1) | 126 |
| | C13'–H13'···O7' [vi] | 0.93 | 2.71 | 3.323(1) | 124 |

| | | | | | |
|---|---|---|---|---|---|
| | C11–H11···C*g*3 [v] | 0.93 | 2.83 | 3.651 | 149 |
| | C11'–H11'···C*g*4 [vi] | 0.93 | 2.87 | 3.718 | 153 |
| **8·DXTHF** | C19–H19···O1 [i] | 0.93 | 2.68 | 3.214(10) | 117 |
| Form-II | C19'–H19'···O3' [ii] | 0.93 | 2.59 | 3.214(12) | 125 |
| | C7–H7···O5' [iii] | 0.98 | 2.81 | 3.731(9) | 157 |
| | C7'–H7'···O5 [iv] | 0.98 | 2.80 | 3.737(9) | 159 |
| | C13–H13···O7 [v] | 0.93 | 2.75 | 3.360(10) | 124 |
| | C13'–H13'···O7' [vi] | 0.93 | 2.65 | 3.296(12) | 127 |
| | C11–H11···C*g*3 [v] | 0.93 | 2.92 | 3.709 | 144 |
| | C11'–H11'···C*g*4 [vi] | 0.93 | 2.82 | 3.681 | 155 |
| **8·BZ** | C19–H19···O1 [ii] | 0.93 | 2.64 | 3.291(8) | 127 |
| Form-III | C19'–H19'···O3' [i] | 0.93 | 2.69 | 3.305(8) | 124 |
| | C7–H7···O5' [vii] | 0.98 | 2.81 | 3.740(6) | 159 |
| | C7'–H7'···O5 [viii] | 0.98 | 2.83 | 3.773(6) | 161 |
| | C12'–H12'···C*g*3 [ix] | 0.93 | 3.32 | 4.064 | 139 |
| | C12–H12···C*g*4 [ix] | 0.93 | 3.37 | 4.110 | 138 |
| **8·DCM** | C19–H19···O1 [ii] | 0.93 | 2.64 | 3.177(1) | 118 |
| Form-III | C19'–H19'···O3' [i] | 0.93 | 2.71 | 3.271(1) | 120 |
| | C7–H7···O5' [vii] | 0.98 | 2.66 | 3.592(1) | 158 |
| | C7'–H7'···O5 [viii] | 0.98 | 2.66 | 3.606(1) | 163 |
| | C12'–H12'···C*g*3 [ix] | 0.93 | 3.18 | 3.930 | 139 |
| | C12–H12···C*g*4 [ix] | 0.93 | 3.11 | 3.870 | 141 |
| **8·HX** | C19–H19···O1 [ii] | 0.93 | 2.69 | 3.339(27) | 128 |
| Form-III | C19'–H19'···O3' [i] | 0.93 | 2.71 | 3.355(27) | 127 |
| | C7–H7···O5' [vii] | 0.98 | 2.78 | 3.718(20) | 161 |
| | C7'–H7'···O5 [viii] | 0.98 | 2.78 | 3.729(21) | 163 |
| | C12'–H12'···C*g*3 [ix] | 0.93 | 3.31 | 4.020 | 135 |
| | C12–H12···C*g*4 [ix] | 0.93 | 3.36 | 4.058 | 135 |
| **8·PY** | C19–H19···O1 [ii] | 0.93 | 2.63 | 3.233(1) | 123 |
| Form-III | C19'–H19'···O3' [i] | 0.93 | 2.61 | 3.215(1) | 123 |
| | C7–H7···O5' [vii] | 0.98 | 2.81 | 3.749(1) | 162 |
| | C7'–H7'···O5 [viii] | 0.98 | 2.82 | 3.768(1) | 163 |
| | C12'–H12'···C*g*3 [ix] | 0.93 | 3.18 | 3.930 | 139 |
| | C12–H12···C*g*4 [ix] | 0.93 | 3.11 | 3.870 | 141 |
| **8·THF** | C19–H19···O1 [ii] | 0.93 | 2.62 | 3.267(6) | 128 |
| Form-III | C19'–H19'···O3' [i] | 0.93 | 2.67 | 3.315(6) | 127 |
| | C7–H7···O5' [vii] | 0.98 | 3.01 | 3.956(6) | 162 |

| | | | | | |
|---|---|---|---|---|---|
| | C7'–H7'···O5 [viii] | 0.98 | 3.01 | 3.961(6) | 165 |
| | C12'–H12'···C*g*3 [ix] | 0.93 | 3.29 | 4.042 | 138 |
| | C12–H12···C*g*4 [ix] | 0.93 | 3.32 | 4.040 | 136 |
| **8·PYDX** | C19–H19···O1 [ii] | 0.93 | 2.73 | 3.247(12) | 116 |
| Form-III | C19'–H19'···O3' [i] | 0.93 | 2.74 | 3.272(10) | 117 |
| | C7–H7···O5' [vii] | 0.98 | 2.73 | 3.669(9) | 161 |
| | C7'–H7'···O5 [viii] | 0.98 | 2.76 | 3.717(9) | 165 |
| | C12'–H12'···C*g*3 [ix] | 0.93 | 3.28 | 3.997 | 133 |
| | C12–H12···C*g*4 [ix] | 0.93 | 3.31 | 4.006 | 134 |

Symmetry codes: (i) x, 1+y, z; (ii) x, -1+y, z; (iii) -x, -1/2+y, 1-z; (iv) -x, 1/2+y, 1-z; (v) 1-x, -1/2+y, 2-z; (vi) 1-x, 1/2+y, 2-z ; (vii) 3/2-x, 1/2+y, 1-z; (viii) 3/2-x, 1/2+y, 1-z; (ix) 2-x, y, 1-z.

Even though crystal forms I-III show similarity in organization along *b*-axis, there are differences in interactions with the neighboring host molecules along the *c*-axis. These differences arise essentially due to the modulation in the native structure upon guest inclusion.[101] The oxygen atom O11' of the camphor moiety make bifurcated C–H···O contacts in Form-I but trifurcated C–H···O contacts in Forms-II and III along the *c*-axis [Fig. 2.5]. In Form-I, the oxygen atom O11' of the camphor moiety makes bifurcated C–H···O contacts with the $2_1$-screw related molecules *via* C6'–H6'···O11' and C22'–H22*C*···O11' [Fig. 2.5(i)]; whereas in Form-II and III, the O11' atom makes trifurcated C–H···O contacts interactions with H6', H22*D* and H31*E* (H30*E* in Form-III) along *c*-axis as shown in figure 2.5(ii) and 2.5(iii). The O11 atom of the other diastereomer makes bifurcated C–H···O contacts in Form-I (with H12' and H22*A*) and Form-II (with H22*A* and H30*A*), but the same makes only C22-H22*A*···O11 in Form-III crystals. Also in Form-I, the carbonyl oxygen O8 of one of the diastereomers makes trifurcated C–H···O hydrogen bonding contacts with the $2_1$-screw related C13–H13, C14–H14 and C18–H18 from two different molecules along the *c*-axis. Similarly, the carbonyl oxygen O8' of the other diastereomer also makes

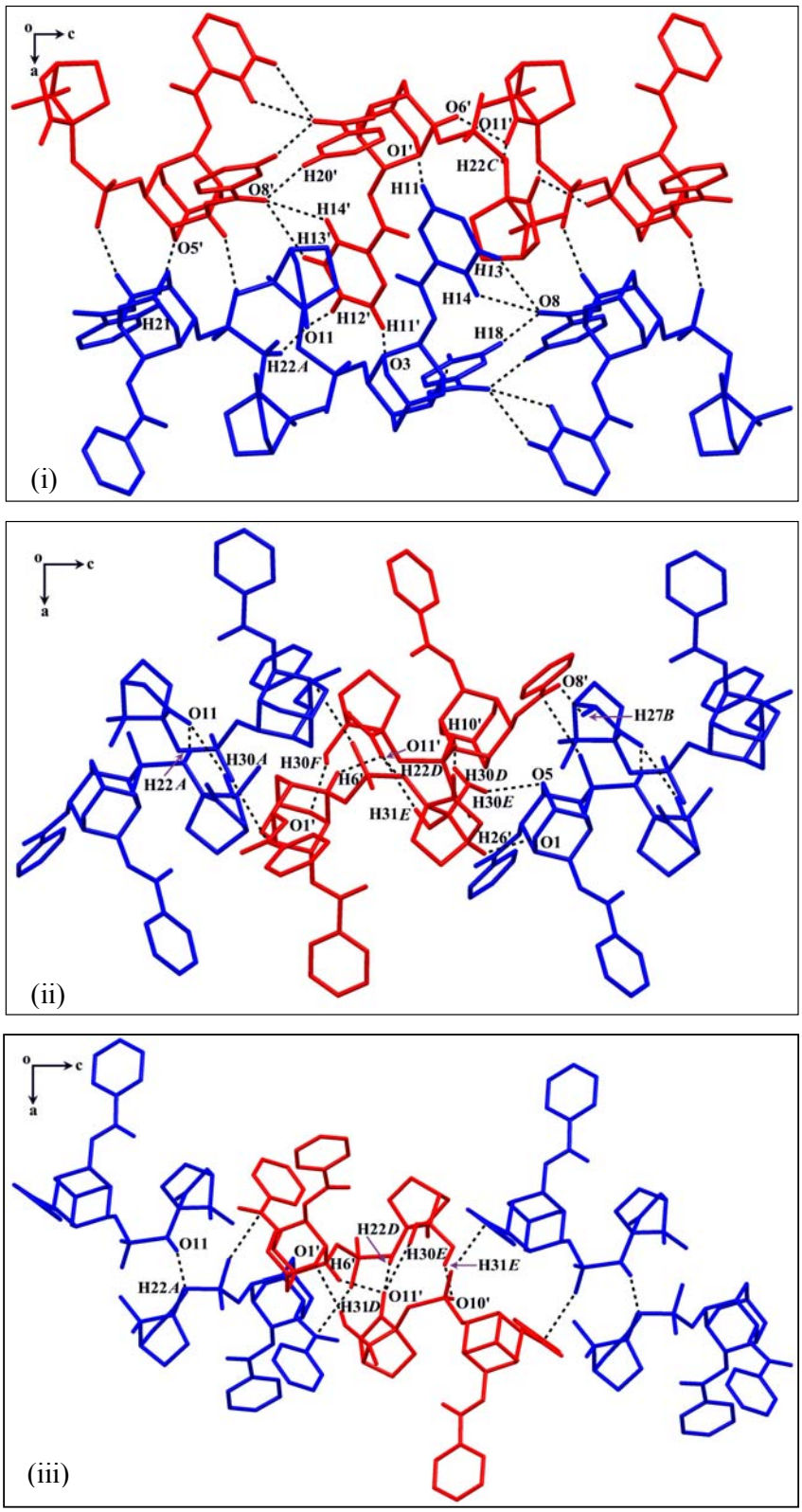


**Figure 2.5**: Molecular layers viewed down *b*-axis in (i) Form-I [**8**] (ii) Form-II [**8·DX**] and Form-III [**8·PY**], only H-atoms involved in short contacts are shown.

trifurcated C–H···O contacts with C13'–H13', C14'–H14' and C20'–H20' [Fig. 2.5(i)]. In the case of solvates (Forms II and III), the carbonyl oxygen atoms O8 and O8' take part in C–H···O contacts with the included guest molecules [Table 2.4]. There are additional C–H···O interactions in Forms II and III crystals that are given in the table 2.4.

**Table 2.4**: Geometrical parameters of host-host interactions in Forms I, II and III crystals of **8** as shown in figure 2.5.

| | D–H···A | D–H (Å) | H···A (Å) | D···A (Å) | D–H···A(°) |
|---|---|---|---|---|---|
| **8** | C13–H13···O8 [i] | 0.93 | 2.67 | 3.277(3) | 124 |
| Form-I | C14–H14···O8 [i] | 0.93 | 2.68 | 3.276(3) | 123 |
| | C18–H18···O8 [i] | 0.93 | 2.33 | 3.248(3) | 170 |
| | C13'–H13'···O8' [ii] | 0.93 | 2.68 | 3.304(3) | 125 |
| | C14'–H14'···O8' [ii] | 0.93 | 2.71 | 3.320(3) | 124 |
| | C20'–H20'···O8' [ii] | 0.93 | 2.38 | 3.291(4) | 166 |
| | C6'–H6'···O11' [iii] | 0.98 | 2.59 | 3.360(3) | 135 |
| | C22'–H22*C*···O11' [iii] | 0.97 | 2.40 | 3.222(3) | 159 |
| | C12'–H12'···O11 [iv] | 0.93 | 2.55 | 3.419(4) | 157 |
| | C22–H22*A*···O11 [v] | 0.97 | 2.71 | 3.615(3) | 156 |
| | C21–H21···O5' [vi] | 0.93 | 2.70 | 3.213(3) | 116 |
| **8·DX** | C6'–H6'···O11' [i] | 0.98 | 2.49 | 3.334(1) | 144 |
| Form-II | C22'–H22*D*···O11' [iii] | 0.97 | 2.25 | 3.182(1) | 161 |
| | C31'–H31*E*···O11' [iii] | 0.96 | 2.59 | 3.526(1) | 165 |
| | C22–H22*A*···O11 [vii] | 0.97 | 2.56 | 3.503(1) | 165 |
| | C30–H30*A*···O11 [vii] | 0.96 | 2.66 | 3.596(1) | 166 |
| | C30'–H30*D*···O10' [iii] | 0.96 | 2.70 | 3.405(1) | 130 |
| **8·DXTHF** | C6'–H6'···O11' [i] | 0.98 | 2.53 | 3.374(9) | 145 |
| Form-II | C22'–H22*D*···O11' [iii] | 0.97 | 2.25 | 3.187(10) | 162 |
| | C31'–H31*E*···O11' [iii] | 0.96 | 2.59 | 3.522(7) | 163 |
| | C22–H22*A*···O11 [vii] | 0.97 | 2.54 | 3.481(9) | 165 |
| | C30–H30*A*···O11 [vii] | 0.96 | 2.44 | 3.525(9) | 163 |
| | C30'–H30*D*···O10' [iii] | 0.96 | 2.59 | 3.522(10) | 163 |
| **8·BZ** | C6'–H6'···O11' [viii] | 0.98 | 2.64 | 3.421(5) | 137 |
| | C22'–H22*D*···O11' [ix] | 0.97 | 2.27 | 3.209(5) | 162 |

| | | | | | |
|---|---|---|---|---|---|
| Form-III | C30'–H30*E*···O11' [ix] | 0.96 | 2.62 | 3.535(7) | 160 |
| | C22–H22*A*···O11 [x] | 0.97 | 2.67 | 3.624(6) | 167 |
| | C31–H31*A*···O11 [x] | 0.96 | 2.63 | 3.572(9) | 167 |
| **8·DCM** | C6'–H6'···O11' [vii] | 0.98 | 2.52 | 3.338(9) | 142.6 |
| Form-III | C22'–H22*D*···O11' [ix] | 0.97 | 2.30 | 3.221(9) | 159 |
| | C30'–H30*E*···O11' [ix] | 0.96 | 2.67 | 3.597(12) | 162 |
| | C22–H22*A*···O11 [x] | 0.97 | 2.57 | 3.514(10) | 164 |
| | C22'–H22*C*···Cl1 [xi] | 0.97 | 2.91 | 3.762(6) | 147 |
| | C31'–H31*D*···O5 [xii] | 0.96 | 2.64 | 3.464(10) | 144 |
| | C31'–H31*E*···O1' [xi] | 0.96 | 2.60 | 3.437(8) | 146 |
| | C35–H35*A*···O8 [xiii] | 0.97 | 2.42 | 3.366(10) | 164 |
| **8·HX** | C6'–H6'···O11' [viii] | 0.98 | 2.52 | 3.373(17) | 145 |
| Form-III | C22'–H22*D*···O11' [ix] | 0.97 | 2.32 | 3.258(23) | 162 |
| | C30'–H30*E*···O11' [ix] | 0.96 | 2.62 | 3.542(28) | 161 |
| | C22–H22*A*···O11 [x] | 0.97 | 2.55 | 3.492(19) | 163 |
| | C31–H31*A*···O11 [viii] | 0.96 | 2.59 | 3.534(27) | 167 |
| | C31'–H31*D*···O1' [xi] | 0.96 | 2.70 | 3.557(20) | 149 |
| | C31'–H31*F*···O10' [xiv] | 0.96 | 2.71 | 3.449(24) | 134 |
| **8·PY** | C6'–H6'···O11' [viii] | 0.98 | 2.50 | 3.300(1) | 139 |
| Form-III | C22'–H22*D*···O11' [ix] | 0.97 | 2.25 | 3.174(4) | 159 |
| | C30'–H30*E*···O11' [ix] | 0.96 | 2.65 | 3.581(5) | 162 |
| | C22–H22*A*···O11 [x] | 0.97 | 2.62 | 3.558(4) | 162 |
| | C31'–H31*D*···O1' [xv] | 0.96 | 2.70 | 3.566(4) | 150 |
| | C31'–H31*E*···O10' [xiv] | 0.96 | 2.66 | 3.392(5) | 133 |
| **8·THF** | C6'–H6'···O11' [viii] | 0.98 | 2.50 | 3.319(4) | 141 |
| Form-III | C22'–H22*D*···O11' [ix] | 0.97 | 2.32 | 3.262(4) | 164 |
| | C30'–H30*E*···O11' [ix] | 0.96 | 2.61 | 3.543(6) | 165 |
| | C22–H22*A*···O11 [x] | 0.97 | 2.55 | 3.492(4) | 165 |
| | C30–H30*A*···O11 [viii] | 0.97 | 2.65 | 3.590(6) | 167 |
| | C31'–H31*D*···O5 [xiv] | 0.96 | 2.65 | 3.498(5) | 148 |
| | C31'–H31*E*···O1' [xiv] | 0.96 | 2.67 | 3.528(4) | 150 |
| **8·PYDX** | C6'–H6'···O11' [viii] | 0.98 | 2.53 | 3.369(8) | 144 |
| Form-III | C22'–H22*D*···O11' [ix] | 0.97 | 2.26 | 3.199(9) | 162 |
| | C30'–H30*E*···O11' [ix] | 0.96 | 2.63 | 3.552(9) | 162 |
| | C22–H22*A*···O11 [x] | 0.97 | 2.56 | 3.509(9) | 167 |
| | C30–H30*C*···O11 [xvi] | 0.96 | 2.71 | 3.659(13) | 171 |
| | C31–H31*A*···O3 [xvi] | 0.96 | 2.70 | 3.407(9) | 131 |
| | C31'–H31*E*···O1' [xvii] | 0.96 | 2.65 | 3.499(8) | 147 |

Symmetry codes: (i) 1-x, -1/2+y, 1-z; (ii) -x, 1/2+y, -z; (iii) -x, 1/2+y, 1-z; (iv) x, 1+y, z; (v) 1-x, 1/2+y, -z; (vi) 1+x, y, z; (vii) -x, 1/2+y, 2-z; (viii) 1/2-x, -1/2+y, -z; (ix) 3/2-x, -1/2+y, -z; (x) 3/2-x, -1/2+y, 1-z ; (xi) 1/2-x, 1/2+y, -z ; (xii) x, y, -1+z; (xiii) 1-x, y, 2-z ; (xiv) 1/2-x, -1/2+y,1-z ; (xv) 1/2-x, 1/2+y, 1-z; (xvi) 3/2-x, -1/2+y, 2-z; (xvii) 1/2-x, 1/2+y, 1-z.

### *2.3.4. Host-guest interactions in pseudopolymorphs of 8*

There are four different possible sites of inclusion of solvents in crystals of Forms II and III. In Form-II crystals, guest molecules occupy sites designated as *A*, *B*, *C* and *D* [*C* and *D* sites are located in the same cavity but designated to distinguish two different guest solvents, Fig. 2.6(i)]. In Form-II crystals, guests in sites *A* and *B* interact with the diastereomers of **8** *via* O···C═O and C–H···O contacts, whereas guests at sites *C* and *D* make only C–H···O contacts with the host molecule. In Form-III crystals [Fig. 2.6(ii)], guests in sites *A* make short contacts with one of the diastereomers (blue molecule) and the guests at sites *B* make closer interaction with the other diastereomer (red molecule). The guests in sites *C* and *D*, occupying the cavities on a 2-fold axis do not make any significant interactions with the host molecules. The guests at sites *C* and *D* have lower occupancies and exhibit varying extent of disorder. In all the cases, the oxygen atoms O8 and O8' (attached to carbons C15 and C15' involved in the S═O···C═O bridging) from the host molecules accept the protons from the C–H group of the guest molecules [Table 2.5]. Significant weak interactions between each of the guests and the host molecules are shown in figure 2.7.

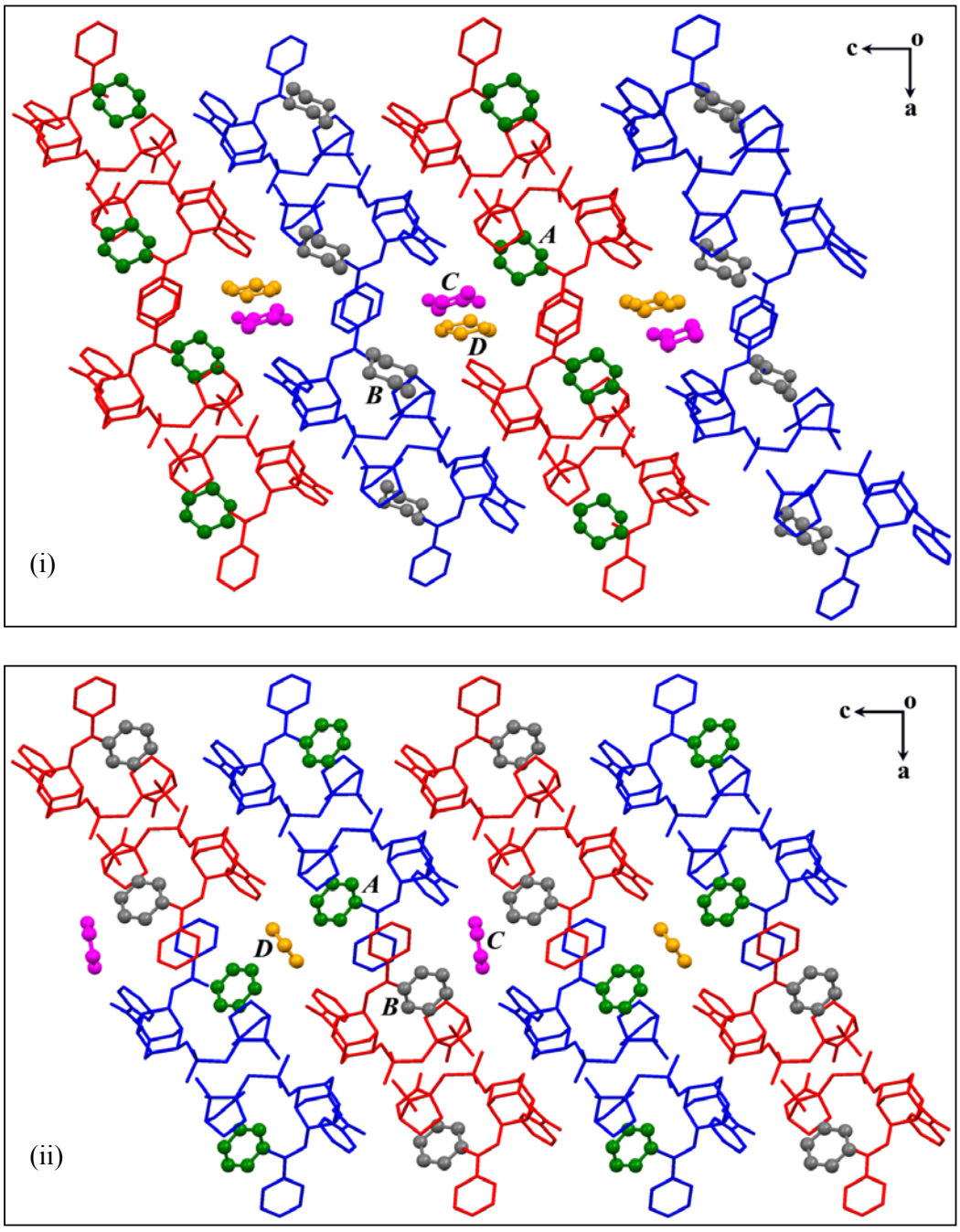


**Figure 2.6**: Molecular packing showing the four guest sites in (i) Form-II and (ii) Form-III crystals. The sites *C* and *D* in Form-II crystals located in the same cavity but designated to distinguish two different guests.

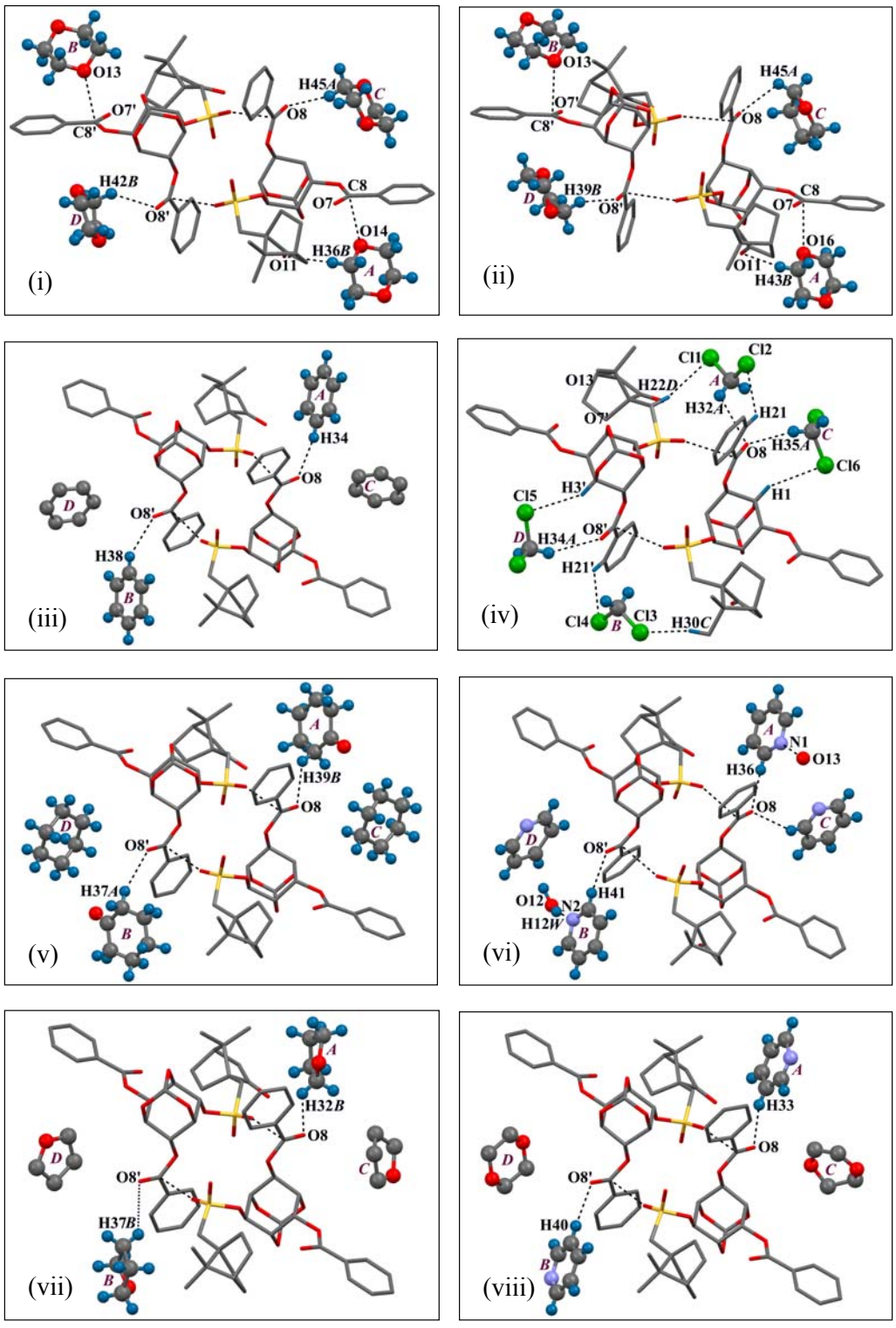


**Figure 2.7**: Significant host-guest interactions in pseudopolymorphs of **8**; (i) **8·DX**, (ii) **8·DXTHF**, (iii) **8·BZ**, (iv) **8·DCM**, (v) **8·HX**, (vi) **8·PY**, (vii) **8·THF** and (viii) **8·PYDX**.

**Table 2.5**: Geometry of C–H···O contacts made by the guests with the carbonyl oxygen O8 (O8') associated with the dimeric bridging as shown in figure 2.7.

| **Solvates** | D–H···A | D–H (Å) | H···A (Å) | D···A (Å) | D–H···A (°) |
|---|---|---|---|---|---|
| **8·DX** | C45–H45*A*···O8 [i] | 0.97 | 2.56 | 3.265(10) | 129 |
| Form-II | C42–H42*B*···O8' [ii] | 0.97 | 2.67 | 3.430(19) | 136 |
| **8·DXTHF** | C45–H45*A*···O8 [i] | 0.97 | 2.82 | 3.74(1) | 158 |
| Form-II | C39–H39*B*···O8' [i] | 0.97 | 2.80 | 3.40(2) | 121 |
| **8·BZ** | C34–H34···O8 [iii] | 0.93 | 2.44 | 3.351(6) | 129 |
| Form-III | C38–H38···O8' [i] | 0.93 | 2.61 | 3.441(7) | 136 |
| **8·DCM** | C35–H35*A*···O8 [iv] | 0.97 | 2.42 | 3.366(1) | 164 |
| Form-III | C34–H34*A*···O8' [v] | 0.97 | 2.80 | 3.689(2) | 152 |
| **8·HX** | C39–H39*B*···O8 [vi] | 0.97 | 2.55 | 3.33(5) | 137 |
| Form-III | C37–H37*A*···O8' [vii] | 0.97 | 2.64 | 3.58(3) | 161 |
| **8·PY** | C36–H36···O8 [viii] | 0.93 | 2.39 | 3.312(6) | 175 |
| Form-III | C46–H46···O8 [ix] | 0.93 | 2.56 | 3.368(2) | 144 |
| | C41–H41···O8' [x] | 0.93 | 2.43 | 3.341(6) | 168 |
| **8·THF** | C32–H32*B*···O8 [viii] | 0.97 | 2.72 | 3.38(2) | 165 |
| Form-III | C37–H37*B*···O8' [x] | 0.97 | 2.88 | 3.58(1) | 149 |
| **8·PYDX** | C33–H33···O8 [xi] | 0.93 | 2.55 | 3.33(5) | 137 |
| Form-III | C40–H40···O8' [iv] | 0.93 | 2.43 | 3.35(1) | 169 |

Symmetry codes: (i) x, y, z; (ii) 1-x, -1/2+y, 1-z; (iii) x, y, -1+z; (iv) 1-x, y, 2-z; (v) 1-x, y, 1-z; (vi) x, 1+y, z; (vii) x, -1+y, 1+z; (viii) 1/2-x, -1/2+y, 1-z; (ix) 1-x, -1+y, 1-z; (x) 1/2-x, -1/2+y, -z; (xi) 3/2-x, 1/2+y, 1-z.

(i) *Inclusion of dioxane in Form-II crystals* (**8·DX**)

Dioxane is the only guest, which produces a different cohesion of dimeric chains producing solvate in space group $P2_1$, whereas all the other solvates belong to space group *C2*. The dioxane molecules in site *A*, *C* and *D* take part in weak C–H···O interactions [Fig. 2.7(i), Table 2.5] with the host molecules. The oxygen atoms of the guests, O13 and O14, in sites *A* and *B* make O···C═O type short approach[96] almost perpendicular to the carbonyl carbon atoms C8' and C8 of the host molecules

respectively [O14···C8 = 3.04 Å, O14···C8═O7 = 102.6º and O13···C8' = 3.21 Å, O13···C8'═O7' = 106.4º]. These interactions were found to be similar to that of dipolar C═O···C═O interaction motif of Type-I.[96]

(ii) *Inclusion of dioxane-THF in Form-II crystals* (**8·DXTHF**)

Binary solvent systems were used to bring out an insight into guest preferences in crystals of **8**. Crystallization of **8** from a mixture of dioxane and THF resulted in the inclusion of both dioxane and THF, but the space group ($P2_1$) seems to be dictated by dioxane, which has dominance in the crystal lattice. Although, both the guests were present in the crystals, sites *A*, *B* and *D* are solely occupied by dioxane, whereas only site *C* contains THF. The guests in sites *C*, *D* and *A* take part in weak C–H···O interactions [Fig. 2.7(ii), Table 2.5] with the host molecules (same as seen in **8·DX**). The oxygen atoms of the dioxane O13 and O16 in sites *A* and *B* make short dipolar approaches to the C$sp^2$ carbon atoms C8' and C8 of the host molecules [O16···C8 = 3.07 Å, O14···C8═O7 = 99.7º and O13···C8' = 3.23 Å, O13···C8'═O7' = 108.5º] as seen in **8·DX**.

(iii) *Inclusion of benzene in Form-III crystals* (**8·BZ**)

The benzene molecules in sites *A* and *B* make C–H···O contacts [Fig. 2.7(iii), Table 2.5] with carbonyl oxygen atoms O8 and O8' of the host molecule respectively. Also the guests in site *A* (C32-C37) and site *B* (C38-C43) have off-centered π···π interactions [Fig. 2.8(i)] with the phenyl rings of the host molecule [C*g*1···C*g*5 = 4.1458 Å, α = 6.42º; C*g*2···C*g*6 = 4.0144 Å, α = 3.84º; C*g*1, C*g*2, C*g*5 and C*g*6 are the centroids of the phenyl rings C9-C14, C9'-C14', C38-C43 and C32-C37 respectively]. Guests exhibiting extensive orientational disorder in sites *C* and *D* do not make any notable interactions with the host molecules.

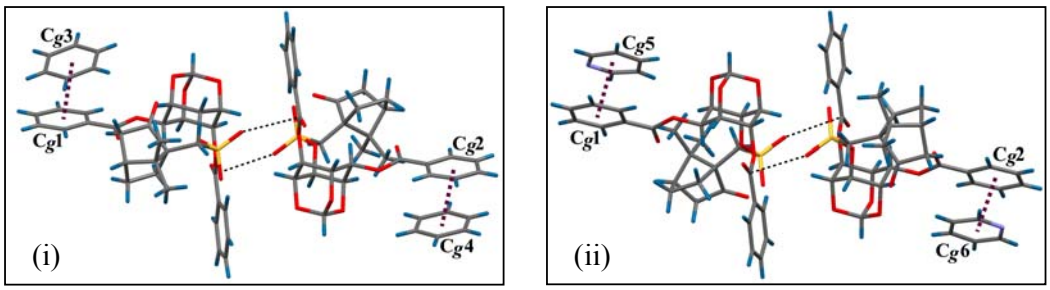


**Figure 2.8**: π···π interactions is made by the planar guests (i) benzene in **8·BZ** and (ii) pyridine in **8·PY** as well as **8·PYDX**.

(iv) *Inclusion of dichloromethane in Form-III crystals* (**8·DCM**)

In this structure, all the guest molecules make short contacts with the host molecules [Fig. 2.7(iv)]. In site *A*, DCM molecule is held by C32–H32*A*···O8 (2.78 Å & 115.4º), C22'–H22*D*···Cl1 (2.91 Å & 146.8º) and C21–H21···Cl2 (2.97 Å & 132.0º) interactions, whereas in site *B* the guest makes only C21'–H21'···Cl4 (2.83 Å, 132.9º), C30–H30···Cl3 (2.98 Å, 152.1º) contacts. The carbon atoms of DCM at *C* and *D* occupy special positions on a 2-fold axis, making C35–H35*A*···O8 (2.42 Å, 163.7º), C1–H1···Cl6 (3.00 Å, 140.8º) and C34–H34*A*···O8' (2.80 Å, 152.2º), C3'–H3'···Cl5 (2.98 Å, 149.0º) weak interactions with the host molecules at site *C* and *D* respectively.

(v) *Inclusion of cyclohexanone-cyclohexane in Form-III crystals* (**8·HX**)

The crystal structure of **8·HX** revealed the inclusion of cyclohexanone as well as cyclohexane (possibly came from the precipitant petroleum ether) unexpectedly. But inclusion of cyclohexane was not observed in crystals obtained from other solvents although petroleum ether was used for crystallization. Interestingly, both cyclohexanone and cyclohexane share sites *A* and *B* equally, which make weak C–H···O contacts [Fig. 2.7(v), Table 2.5] with the host molecule. The cyclohexane molecules in sites *C* and *D* do not make any significant short contact. Interestingly, no crystals were obtained when cyclohexane alone was used for crystallization.

(vi) *Inclusion of pyridine in Form-III crystals* (**8·PY**)

The guest molecules in sites *A*, *B* and *C* make C–H···O contacts [Fig. 2.7(vi), Table 2.5] with the host molecules. The molecular packing is almost similar to that of **8·BZ** (benzene) and the guests in sites *A* and *B* make moderate π···π interactions [Fig. 2.8(ii)] with the phenyl rings of the host molecules [C*g*1···C*g*7 = 3.9716 Å, α = 2.33º; C*g*2···C*g*8 = 3.8925 Å, α = 0.30º; C*g*1, C*g*2, C*g*7 and C*g*8 are the centroids of the aromatic rings C9-C14, C9'-C14', N2-C37-C41 and N1-C32-C36 respectively]. This crystal lattice also contains two water molecules (O12 and O13), which make two symmetric O–H···N contacts with the two pyridine molecules in sites *A* and *B*. The two-fold disordered pyridine in site *D* did not make any significant interactions with the host.

(vii) *Inclusion of tetrahydrofuran in Form-III crystals* (**8·THF**)

In these crystals, only the THF molecule in site *A* makes C32–H32B…O8 contact [Fig. 2.7(vii)] and the guest at site *B* makes a longer contact with O8' [Table 2.5]. This is in contrast to other solvates, where guests in site *B* always made short C–H···O8' contacts. However, the oxygen atom O13 of the guest molecule in site *B* makes bifurcated C–H···O contact with the host [H11'···O13 = 2.68 Å, C11'–H11'···O13 = 149º and H24*B*···O13 = 2.64 Å, C24–H24*B*···O13 = 136º]. The guest molecules in site *C* and *D* are highly disordered and are not held by any significant intermolecular interactions.

(viii) *Inclusion of pyridine-dioxane in Form-III crystals* (**8·PYDX**)

This solvate includes both the guests, but the space group (*C2*) seems to be dictated by pyridine, which has dominance in the crystal lattice. Although, both the guests were present in the crystal lattice, sites *A* and *B* are solely occupied by pyridine, which makes C–H···O contacts [Fig. 2.7(viii), Table 2.5] similar to that seen

in **8·PY**. Here also pyridine molecules in sites *A* and *B* make moderate π···π interactions with the host molecules [C*g*1···C*g*7 = 3.9723 Å, α = 2.69º; C*g*2···C*g*8 = 4.0138 Å, α = 5.62º; C*g*1, C*g*2, C*g*7 and C*g*8 are the centroids of the aromatic rings C9-C14, C9'-C14', N2-C37-C41 and N1-C32-C36 respectively]. Both the guests occupy site *C*, whereas site *D* contained only dioxane. However, the guests with low occupancies in sites *C* and *D* are highly disordered and do not make any significant interactions with the host molecules.

It is interesting to see how compound **8** accommodates guests to produce crystals of Forms II and III. The packing of molecules and the relationship between their unit cell parameters offers an insight into the growth of these crystalline modifications. The intercalation of the guest molecules in Forms II and III takes place only between the two rows without interrupting S═O···C═O bridged diastereomers [Fig. 2.9]. Expansions along *a*- and *c*-axis in Form-I, due to the inclusion of the dioxane guests produces Form-II, whereas almost doubling of a-axis with a different mode of inclusion of guests produces Form-III [Fig. 2.9(ii) and 2.9(iii)].

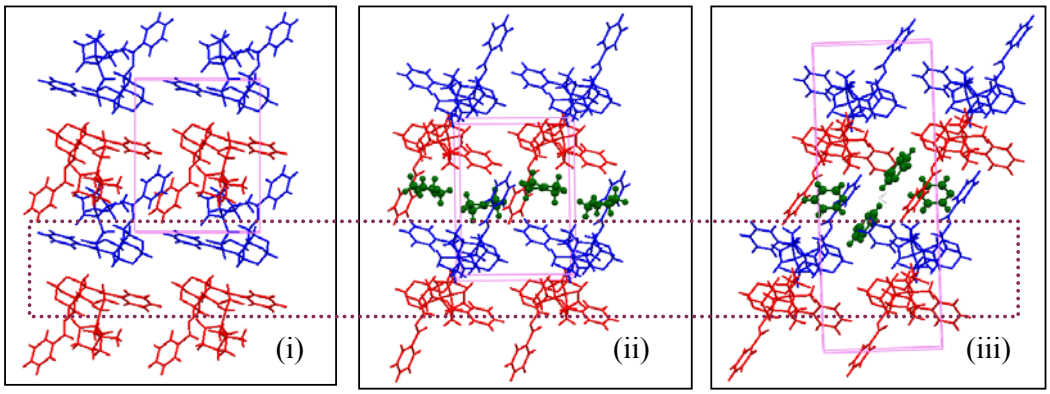


**Figure 2.9**: Molecular views down *c*-axis in Forms I, II and III. The dotted rectangle highlights unperturbed 1D- isostructurality of diastereomeric association.

Another remarkable feature of these pseudopolymorphs is the symmetry requirement of the included guests. All the guest molecules have 2-fold symmetry and

their electron count ranges from 40 to 60 as shown below [Chart 2.1]. In Form-III crystals, the guest molecules in sites *A* and *B* are distributed around the crystallographic 2-fold axis, whereas the 2-fold symmetry of guest molecules in sites *C* and *D* coincide with the crystallographic 2-fold axis (C2) [Fig. 2.10].

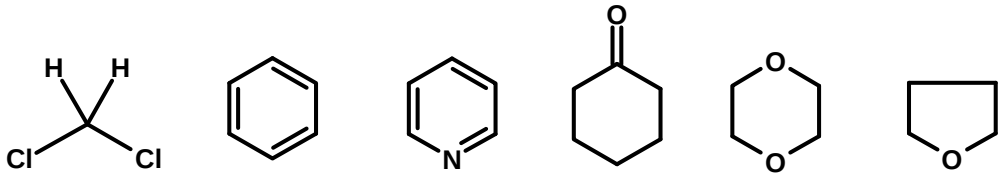


**Chart 2.1**

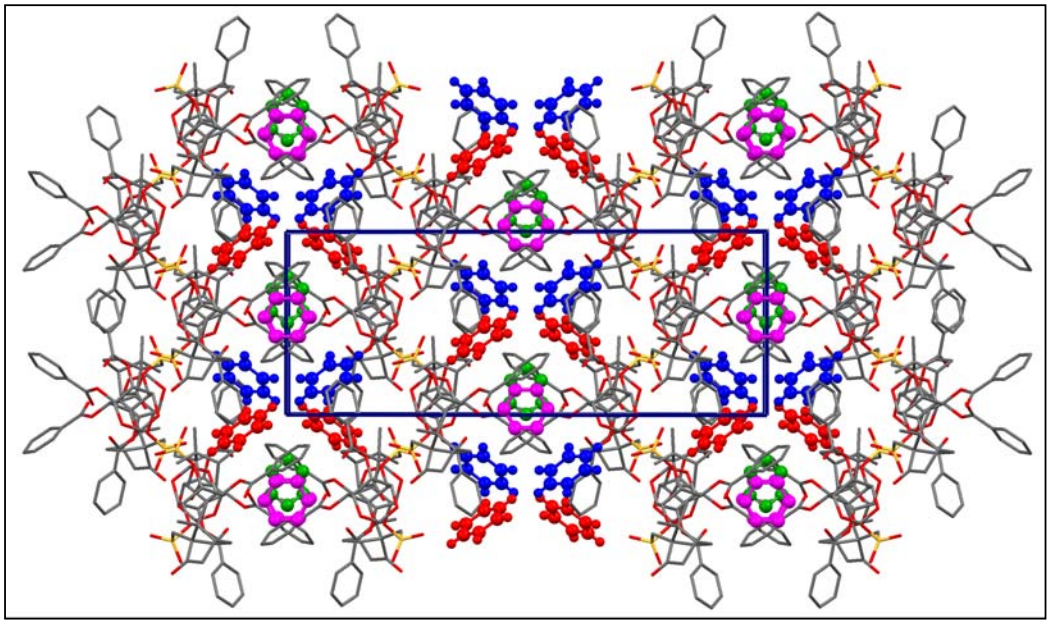

**Figure 2.10**: Molecular organization in Form-III crystals (**8·BZ**) viewed down *c*-axis revealing occupation by guests (shown in ball and stick model) on crystallographic 2-fold axis.

### *2.3.5. Subtle crossover of C–H···O to S═O···C═O interactions upon solvate formation*

It is intriguing to note the interplay between two types of weak interactions, C–H···O and S═O···C═O that associate the diastereomers of **8**. In solvent free of **8**,

the dimeric association is *via* C–H···O across the diastereomers (C4'–H4'···O9 and C6–H6···O9') and the parameters for S═O···C═O bridging are not very favorable. However, when crystals of **8** include guests, the S═O···C═O contacts get significantly shorter than the sum of the van der Waals radii of O and C atoms and the C–H···O contacts become weaker [Table 2.2]. This crossover is achieved by 'closing in' of the molecules of **8** so as to reach the S═O dipoles closer to the C$sp^2$ carbon atoms [Fig. 2.2(ii)]. Variations in the S═O···C═O contact geometries further correlate with the guest binding strengths. There are differences in the binding of the guests; the guests at site *A* are more tightly bound to the host molecules than the guests at site *B*. The stronger association of guest molecules *via* C–H···O contacts seems to weaken the S═O···C═O bridging and *vice versa* [Table 2.2 and 2.5]. For example, the pyridine molecule in site *A* makes stronger C–H···O contacts than pyridine included at site *B* and their S═O···C═O contacts show just mentioned anti correlation.

### *2.3.6. Structural modification in the orthoester position of 8*

In order to explore the dipolar S═O···C═O association of diastereomers further, the orthoester hydrogen was substituted with methyl and phenyl groups to obtain the orthoacetate **9** and the orthobenzoate **10** respectively [Scheme 2.2]. The crystallization experiments of **9** and **10** from different organic solvents / conditions did not give any polymorphs or inclusion complexes; suitable single crystals for the X-ray studies were obtained only from dichloromethane-methanol mixture [Table 2.1]. The crystal structure of **10** exhibited very high degree of orientational disorder and isotropic treatment of atoms in the least-square refinement was described in the experimental section [Fig. 2.11].

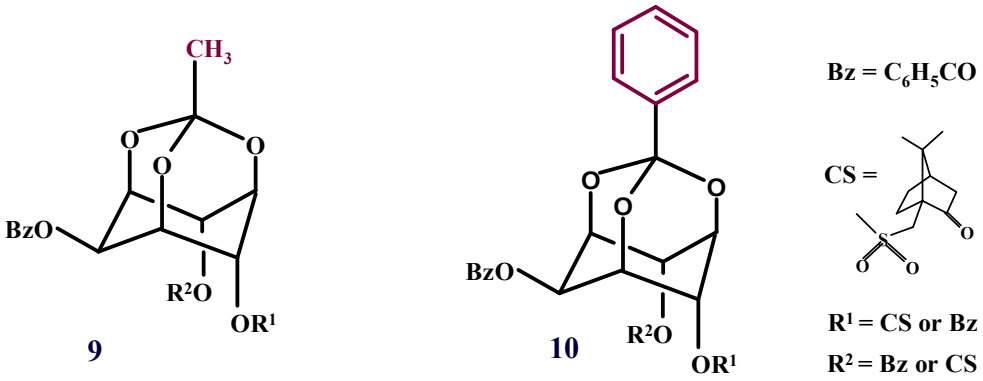


**Scheme 2.2** **Diastereomeric mixture**

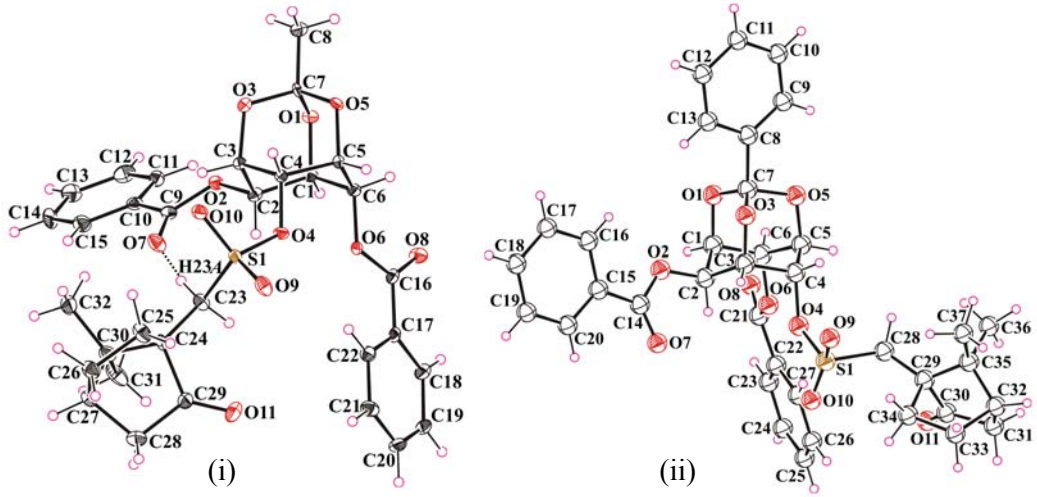


**Figure 2.11**: ORTEP plots of one of diastereomers with atom numbering scheme (i) **9** drawn at 30% probability ellipsoid and (ii) **10** with isotropic atoms.

The crystal structure of **9** showed a short intramolecular C–H···O interaction [Fig. 2.11] between H23*A* (H23*D*) atom of the camphorsulfonyl methylene group and O7 (O7') atom of the equatorial benzoyl group in both the diastereomers [Table 2.6]. This intramolecular interaction could be responsible for a different orientation of the camphor sulfonate group in **9** as compared to that in **8** [Fig. 2.12(i)]. However, the conformation of the disordered camphor moiety in the orthobenzoate derivative **10** is significantly different from **8** as well as **9** [Fig. 2.12(ii) and (iii)]. These differences in conformation also influence the diastereomeric association and their molecular organization in the crystal lattice as described below.

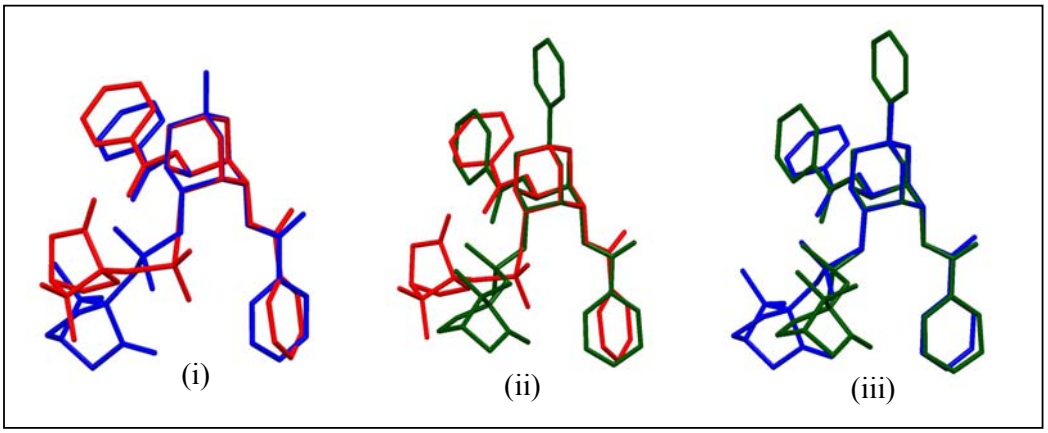


**Figure 2.12**: Molecular overlap plots of (i) **8** [red] and **9** [blue], (ii) **8** [red] and **10** [green], (iii) **9** [blue] and **10** [green].

2.3.6.1. *Dimeric association of diastereomers in **9** and **10***

As seen earlier, the association of molecules in the diastereomeric mixture of **8** that subtly switches from C–H···O to short S═O···C═O contacts on going from the solvent free crystal form to pseudopolymorphs. Interestingly, crystal structure of **9** also showed dimeric bridging *via* short S═O···C═O contacts [O9···C16' $^{i}$ = 3.144 (5) Å, O9···C16'=O8' $^{i}$ = 92.2 (1)º and S1=O9···C16' $^{i}$ = 123.6 (1)º; O9'···C16 $^{ii}$ = 3.556 (5) Å, O9'···C16=O8 $^{ii}$ = 94.7 (1)º and S1'=O9'···C16 $^{ii}$ = 103.6 (1)º; symmetry codes: (i) x+1, y, z; (ii) x-1, y, z] and C–H···O interactions [Fig. 2.13(i), Table 2.6]. However in **9**, the dipolar S═O···C═O contacts are of sheared parallel motif [Type-III] while in all the crystalline solvates of the orthoformate **8** [Fig. 2.2], these contacts were of perpendicular motif [Type-I, *details of different dipolar interaction motifs are given in Chapter 7*]. The crystals of the orthobenzoate, **10** on the other hand, are completely devoid of such S═O···C═O contacts, but the sulfonyl group is involved in only C–H···O interactions [Fig. 2.13(ii), Table 2.7] between the diastereomers.

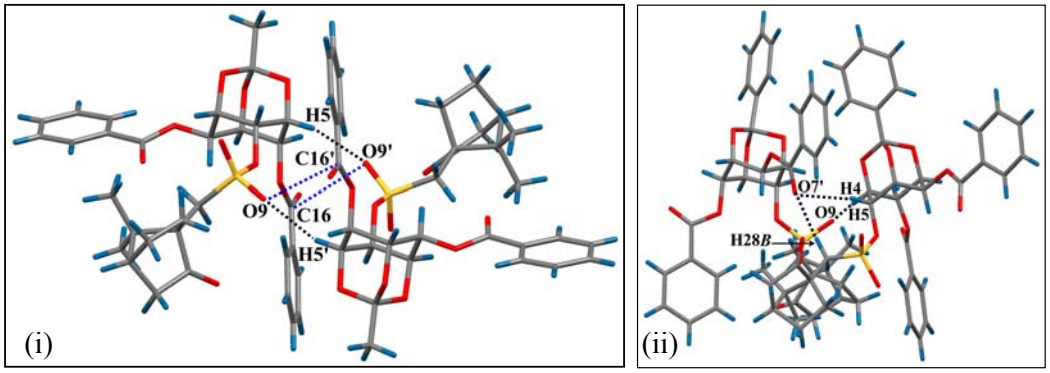


**Figure 2.13**: Diastereomeric association of diastereomers *via* S═O···C═O and C–H···O contacts in (i) **9** and (ii) C–H···O contacts in **10**.

*2.3.6.2. Molecular organization of* **9**

The diastereomers of **9** associated *via* S═O···C═O (and C–H···O) interactions are packed in the crystal lattice only *via* weak intermolecular interactions such as C–H···π and C–H···O by translation. These dimeric units translated diagonal to *a*- and *c*-axes make somewhat off-centered C–H···π interactions between the methyl H-atoms (H31*E* and H31*C*) of the camphor moiety and the phenyl ring of the axial benzoyl groups as shown in figure 2.14 [H31*E*···C*g*1$^{i}$ = 2.86 Å, C31'···C*g*1$^{i}$ = 3.724 Å, C31'–H31*E* = 0.96 Å and C31'–H31*E*···C*g*1$^{i}$ = 151º; H31*C*···C*g*2$^{ii}$ = 3.06 Å, C31···C*g*2$^{ii}$ = 3.943 Å, C31–H31*C* = 0.96 Å and C31–H31*C*···C*g*2$^{ii}$ = 153º; C*g*1 and C*g*2 are the centroids of the phenyl rings C17–22 and C17'–22' respectively; symmetry codes: (i) x, y, z+1; (ii) x, y, z-1]. These molecular rows are linked to unit translated ones along *b*-axis by very weak head-to-head C–H···O contacts forming layers as shown in figure 2.14 [H8*C*···O1' $^{vi}$ = 2.75 Å, C8···O1' $^{iii}$ = 3.644 (5) Å, C8–H8*C* = 0.96 Å and C8–H8*C*···O1' $^{iii}$ = 155º; H8*E*···O3 $^{iv}$ = 2.79 Å, C8'···O3 $^{iv}$ = 3.688 (5) Å, C8'–H8*E* = 0.96 Å and C8'–H8*E*···O3 $^{iv}$ = 156º; symmetry codes: (iii) x-1, y+1, z; (iv) x+1, y+1, z].

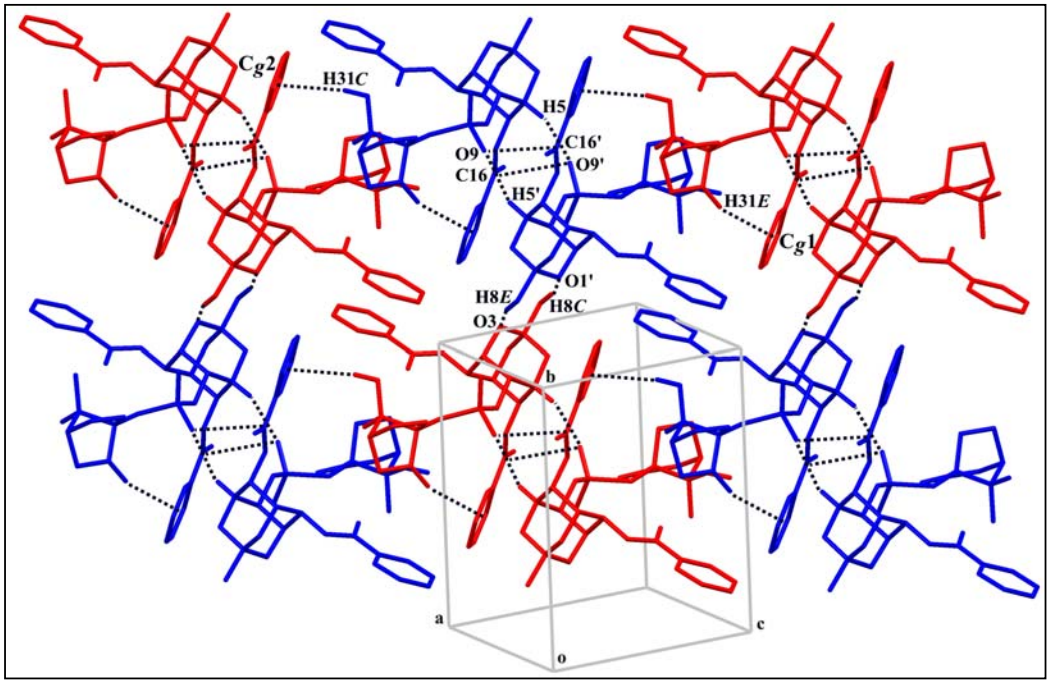


**Figure 2.14**: Layer of dimers linked *via* C–H···π (along diagonal) and C–H···O interactions (along *b*-axis) in crystals of **9**.

Although dimeric association is different in crystals of **9** compared to **8**, both the structures exhibit one-dimensional isostructurality in packing of these units although there are differences between dimer-dimer interactions [Fig. 2.4(i) and Fig. 2.14]. Also, the isostructurality in **8** and **9** is not only seen in one-dimension, but is also present in the second dimension (along *b*-axis) forming almost isostructural layers. Of course, there are differences in the weak interactions that are made between these layers; for example, in **9** the molecular chains are linked to unit translated chains along *b*-axis by head to head C8–H8*C*···O1', C8'–H8*E*···O3 contacts and also by head to tail C20'–H20'···O2' contact [Table 2.6]. In crystals of **8**, although these rows approach in head to head fashion, no head to head contacts were observed. But, these rows interact only in a head to tail manner *via* C19–H19···O1 contact along the *b*-axis [Fig. 2.4(i)]. However, the dimers interact diagonally *via* aromatic π···π stacking interaction and C–H···O interactions in **8**, whereas *via* C–H···π interactions in **9**.

**Table 2.6**: Geometrical parameters of C–H···O interactions in crystals of **9**.

| D–H···A | D–H (Å) | H···A (Å) | D···A (Å) | D–H···A (º) |
|---|---|---|---|---|
| C1–H1···O8' [i] | 0.98 | 2.33 | 3.275(5) | 161 |
| C5–H5···O9' [ii] | 0.98 | 2.41 | 3.153(5) | 132 |
| C8–H8*C*···O1' [ii] | 0.96 | 2.75 | 3.644(6) | 155 |
| C12–H12···O10 [iii] | 0.93 | 2.72 | 3.495(6) | 142 |
| C23–H23*A*···O7[i] | 0.97 | 2.43 | 3.348(6) | 158 |
| C28–H28*B*···O11' [iv] | 0.97 | 2.45 | 3.297(6) | 146 |
| C3'–H3'···O8[i] | 0.98 | 2.35 | 3.310(5) | 167 |
| C5'–H5'···O9[v] | 0.98 | 2.63 | 3.351(5) | 130 |
| C8'–H8*E*···O3 [vi] | 0.96 | 2.76 | 3.658(7) | 155 |
| C18'–H18'···O1[i] | 0.93 | 2.71 | 3.485(6) | 142 |
| C20'–H20'···O2' [vii] | 0.93 | 2.79 | 3.648(6) | 152 |
| C23'–H23*D*···O7' [i] | 0.97 | 2.63 | 3.252(5) | 122 |

Symmetry codes: (i) x, y, z; (ii) –1+x, y, z; (iii) 1+x, y, z; (iv) -1+x, y, -1+z; (v) 1+x, y, z; (vi) 1+x, -1+y, z; (vi) x, 1+y, z

The difference in stacking of the isostructural layers in **8** and **9** develops along the third dimension [Fig. 2.15]. In triclinic crystals of **9**, the successive dimeric units are related by unit translation in both the dimensions, whereas in **8** they have $2_1$-screw axis relation (monoclinic) along *b*-axis. In **9**, the unit translated dimers are linked *via* C8'–H8*E*···O3 and C8–H8*C*···O1' contacts along the *b*-axis and along diagonal to *ac*-plane *via* two C–H···O interactions namely, C1–H1···O8' and C3'–H3'···O8 interactions [Fig. 2.15, Table 2.6]. As discussed earlier, in **8** the $2_1$-screw axis related dimers are associated *via* bifurcated C–H···O (C22'–H22*C*···O11', C6'–H6'···O11') and trifurcated C–H···O (C13–H13···O8, C14–H14···O8 and C18–H18···O8) interaction[7] in *bc*-plane [Fig. 2.5(i)].

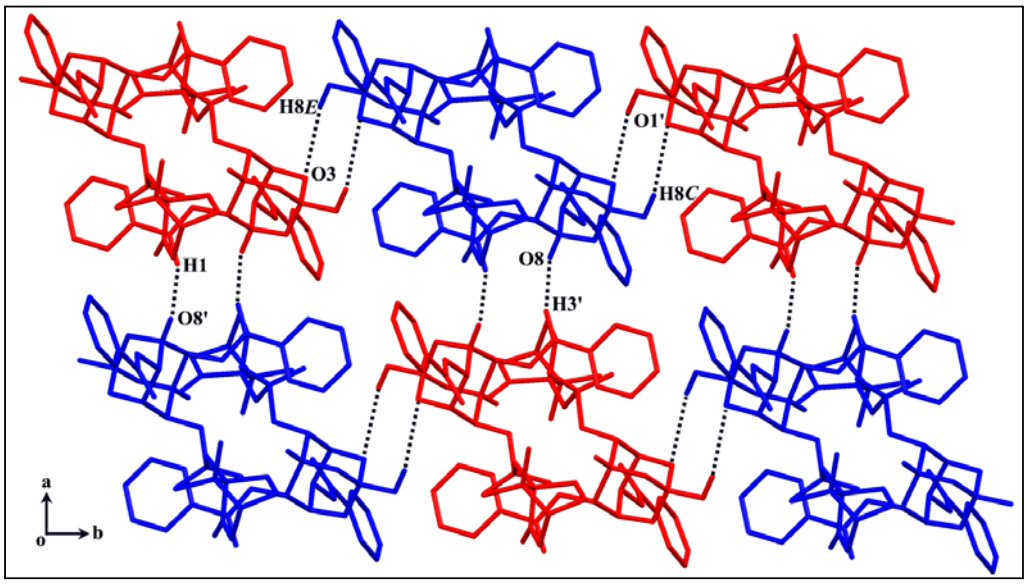


**Figure 2.15**: Molecular layers of **9** in the third dimension.

*2.3.6.3. Molecular organization of* **10**

As seen above, the pseudo-centrosymmetric diastereomeric association *via* S═O···C═O (and C–H···O) interactions were observed in **8** and **9**, but a different type of dimeric association *via* C–H···O interactions between the orthoester bridge and the axial benzoyl group [Fig. 2.16] is seen in **10**. There are four C–H···O contacts namely C1–H1···O8', C23–H23···O3', C3'–H3'···O8 and C27–H27'···O1 [Table 2.7] that bind the diastereomers of **10** in their crystals.

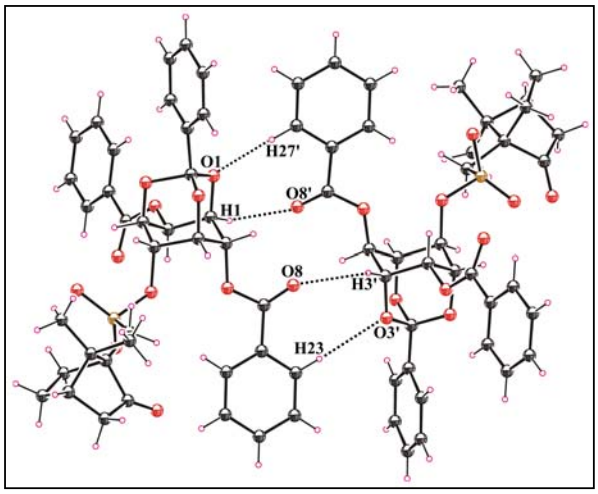


**Figure 2.16**: Diastereomeric association of molecules in crystals of **10**.

**Table 2.7**: Geometrical parameters of C–H···O interactions (isotropic refinement of atoms) in crystals of **10** as shown in figure 2.16.

| D–H···A | D–H (Å) | H···A (Å) | D···A (Å) | D–H···A (º) |
|---|---|---|---|---|
| C1–H1···O8' [i] | 0.97 | 2.42 | 3.272 | 147 |
| C1'–H1'···O5 [ii] | 0.98 | 2.71 | 3.618 | 153 |
| C3'–H3'···O8 [iii] | 0.98 | 2.53 | 3.196 | 124 |
| C4–H4···O7' [iv] | 0.97 | 2.51 | 3.352 | 146 |

Symmetry codes: (i) 1-x, 1/2+y, 1-z; (ii) -1+x, y, z; (iii) 1-x, -1/2+y, 2-z; (iv) 1+x, y, z

The dimers of **10** are translated along *b*-axis *via* C–H···O contacts [*shown in figure* 2.13(ii)] forming molecular chains [Fig.2.17]. These strings form two-dimensional layer along *c*-axis *via* weak C–H···O interactions between the camphor oxygen O11 and the orthobenzoate hydrogen H12 [Fig.2.17, Table 2.8].

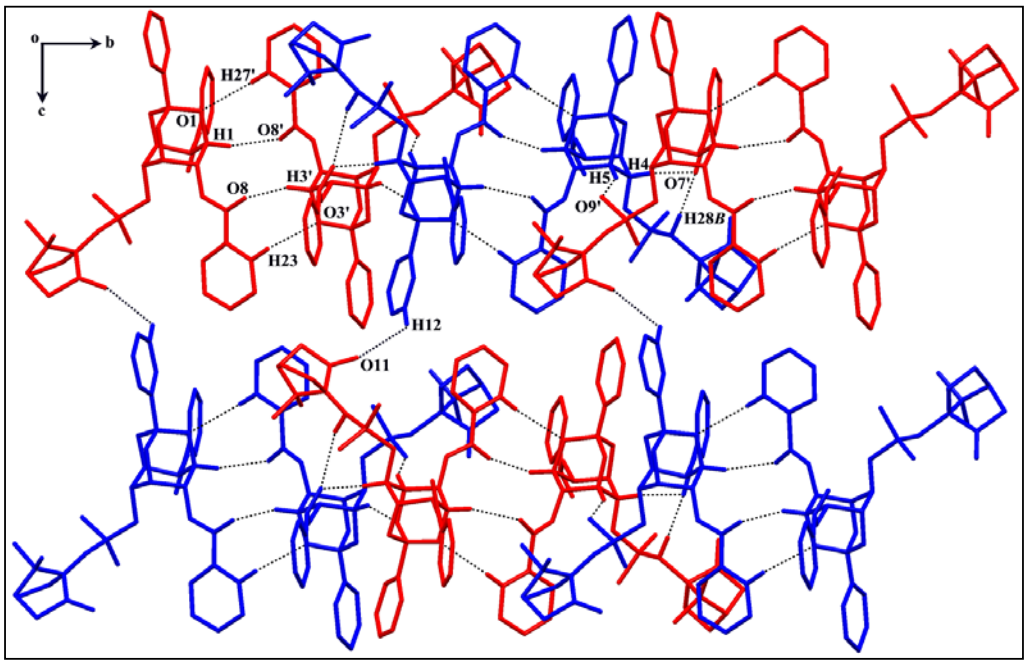


**Figure 2.17**: Layer of dimers of **10** linked *via* C–H···O interactions viewed down *a*-axis.

These 2D-layers weave in the third dimension along *a*-axis *via* weak C–H···O interactions involving the sulfonyl oxygens O9 and O9' [C5'–H5'···O9, C6'–H6'···O7

and C28–H28*D*···O7 as well as *via* C1'–H1'···O5 and C5–H5···O9', Fig. 2.18].

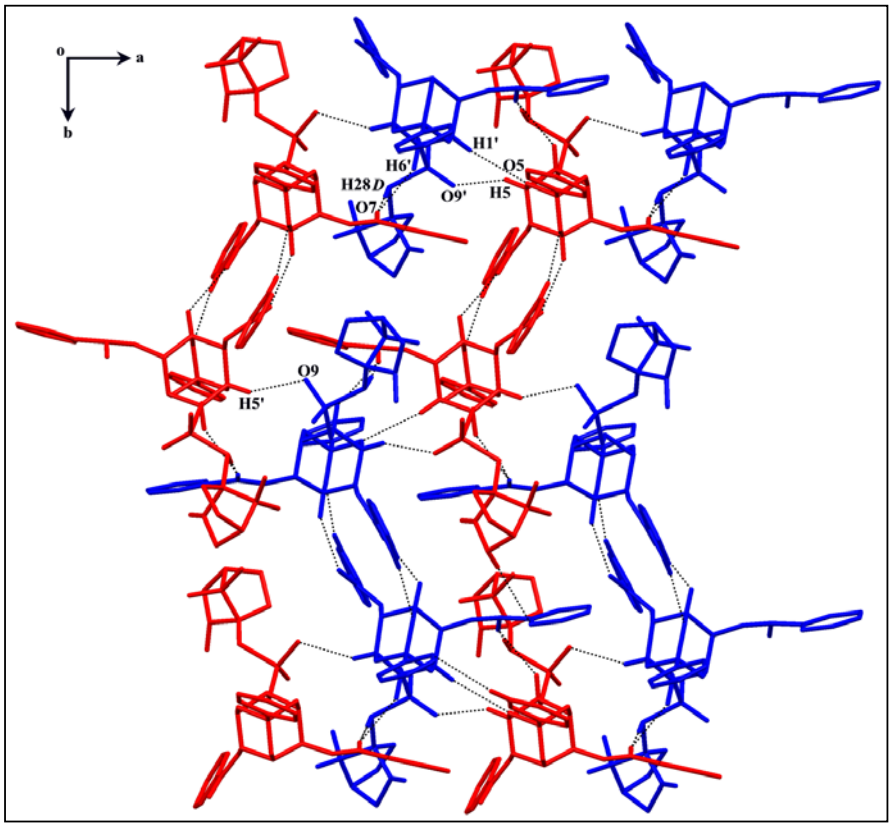


**Figure 2.18**: Molecular layer formation of **10** *via* C–H···O interactions.

**Table 2.8**: Geometrical parameters of C–H···O interactions (isotropic refinement of atoms) in **10**.

| D–H···A | D–H (Å) | H···A (Å) | D···A (Å) | D–H···A (º) |
|---|---|---|---|---|
| C5–H5···O9' [i] | 0.98 | 2.21 | 3.096 | 150 |
| C5'–H5'···O9 [ii] | 0.98 | 2.42 | 3.288 | 148 |
| C6'–H6'···O7 [ii] | 0.98 | 2.37 | 3.275 | 152 |
| C12–H12···O11 [iii] | 0.93 | 2.84 | 3.472 | 126 |
| C23–H23···O3' [iv] | 0.93 | 2.65 | 3.572 | 172 |
| C27'–H27'···O1 [v] | 0.93 | 2.62 | 3.532 | 168 |
| C28–H28B···O7' [i] | 0.97 | 2.66 | 3.597 | 162 |
| C28'–H28D···O7 [ii] | 0.97 | 2.10 | 3.065 | 177 |

Symmetry codes: (i) 1+x, y, z; (ii) x, y, z; (iii) x, y, 1+z; (iv) 1-x, 1/2+y, 2-z. (v) 1-x, -1/2+y, 2-z.

'Morphotropism', is a phenomenon[117] that is concerned with the isostructurality in crystal lattice upon different substitutions. It is rather extraordinary that crystals of racemic 2,4-di-*O*-benzoyl *myo*-inositol 1,3,5-orthoformate and its orthoacetate and orthobenzoate analogs showed almost three-dimensional isostructuality in their molecular organization in the crystal lattices belonging to monoclinic space groups.[118] However, the systems **8**, **9** and **10**, with similar molecular structural changes do not exhibit isostructural molecular organization to the third dimension in their crystals. As described earlier, two-dimensional isostructurality exists only between **8** and **9**, but molecular organization in crystals of **10** is quite different.

### *2.3.7. Structural modification by substitution of acetyl group in myo-inositol ring*

As described above, the orthoester modification of methyl group resulted in the diastereomeric association *via* different motif of S═O···C═O contacts. In order to explore the dipolar contacts and their polymorphic modifications, other related molecules 2,4(6)-di-*O*-acetyl-6(4)-*O*-camphorsulfonyl-*myo*-inositol 1,3,5-orthoformate (**11**) and 2-*O*-benzoyl-4(6)-*O*-acetyl-6(4)-*O*-camphorsulfonyl-*myo*-inositol 1,3,5-orthoformate (**12**) were prepared by substituting the *C2-O*- and *C4-O*-benzoyl group with acetyl group [Scheme 2.3]. It was thought that the C$sp^2$=O group is still present in the acetate substitution, which may give the opportunity of S=O group to interact with carbonyl dipole.

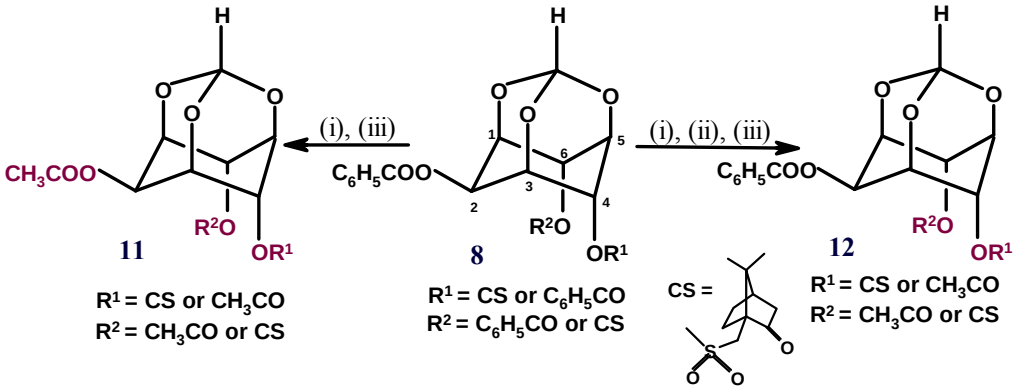


**Scheme 2.3** *Reagents and conditions*: (i) *iso*-$BuNH_2$, MeOH, 80 $^0$C; (ii) 1*eq*. $C_6H_5COCl$, Pyridine, rt; (iii) *excess* $(CH_3CO)_2O$, pyridine, rt.

The crystallization of **11** and **12** from most of the organic solvents / conditions did not give any polymorphs or inclusion complexes. Monoclinic ($P2_1$) crystals of **11** were always produced from most of the solvents but **12** failed to yield any crystals. The crystal structure of **11** showed that the diastereomers form dimers *via* head to head centrosymmetric C–H···O interactions [Fig. 2.19, Table 2.9] but did not show any intra/intermolecular dipolar S═O···C═O interactions.

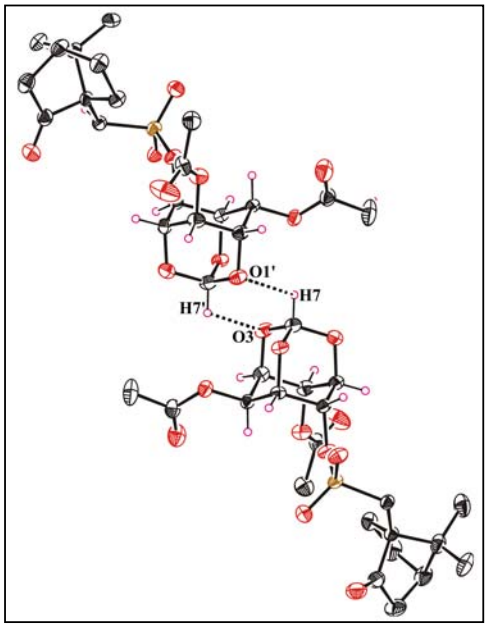


**Figure 2.19**: ORTEP of **11** showing dimer formation of diastereomers *via* head-to-head C–H···O interactions.

It is interesting to note that each of the diastereomers make its own helical molecular assembly bridged essentially *via* dipolar C═O···C═O and C–H···O interactions [Fig. 2.20(i) and 2.20(ii)].[119] In diastereomer-1 (2,6-di-*O*-acetyl-4-*O*-camphorsulfonyl-*myo*-inositol 1,3,5-orthoformate), the $2_1$-screw axis related molecules binds *via* dipolar C10═O8···C8═O7 contacts, C2–H2···O8 and C18–H18*A*···O1 interactions [Fig. 2.20(iii), Table 2.9] to form helical assembly. Similar helical strings are also made by the diastereomer-2 (2,4-di-*O*-acetyl-6-*O*-

camphorsulfonyl-*myo*-inositol 1,3,5-orthoformate) by linking the molecules with dipolar C10'═O8'···C8'═O7' contacts but with different C-H…O interactions, such as C1'–H1'···O8', C2'–H2'···O8', C3'–H3'···O10' and C5'–H5'···O7' [Fig. 2.20(iv), Table 2.9]. The dipolar C═O···C═O interactions in both the diastereomeric chains showed a perpendicular approach [Type-III motif[96]] and O···C distances were shorter [3.011(5) and 3.151(5) Å] than the sum of the van der Waals radii of O and C atoms (3.22 Å). The geometrical parameters of C═O···C═O interactions are O8···C8═O7 = 88.7º, O8'···C8'═O7' = 87.5º, C10═O8···C8 = 136.7º and C10'═O8'···C8' = 128.1º for the Type-III motif. It is noteworthy that the solvent free crystals of **9** and **11** exhibited dipolar interactions of sheared parallel motif (Type-III) whereas, the solvent inclusion crystals of **8** showed perpendicular interaction motif (Type-I).[112]

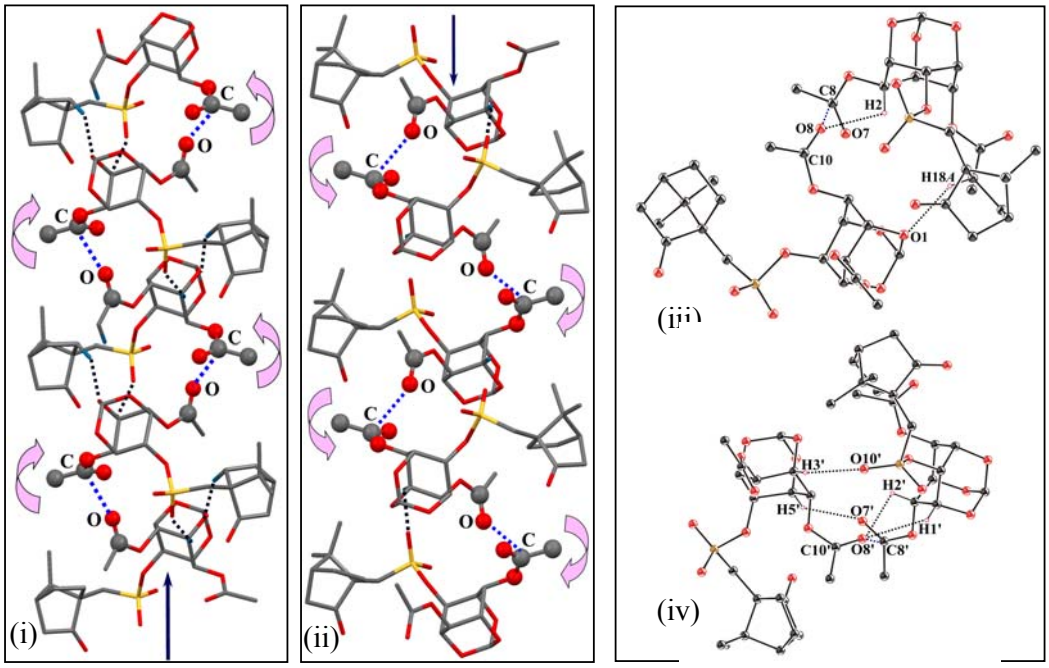


**Figure 2.20**: Helical arrangement in (i) diastereomer-1 and (ii) diastereomer-2 of **11**. Molecular association *via* dipolar C═O···C═O and C–H···O interactions in (iii) diastereomer-1 and (iv) diastereomer-2 of **11**.

**Table 2.9**: Geometrical parameters of C–H···O interactions in **11** (Fig. 2.19).

| D–H···A | D–H (Å) | H···A (Å) | D···A (Å) | D–H···A (º) |
|---|---|---|---|---|
| C7–H7···O1' [i] | 0.98 | 2.65 | 3.198(4) | 116 |
| C7'–H7'···O3 [ii] | 0.98 | 2.61 | 3.175(5) | 117 |
| C2–H2···O8 [iii] | 0.98 | 2.68 | 3.120(4) | 108 |
| C18–H18*A*···O1 [iii] | 0.97 | 2.52 | 3.411(4) | 153 |
| C1'–H1'···O8' [iv] | 0.98 | 2.66 | 3.297(5) | 123 |
| C2'–H2'···O8' [iv] | 0.98 | 2.68 | 3.104(5) | 107 |
| C3'–H3'···O10' [iv] | 0.98 | 2.40 | 3.117(5) | 130 |
| C5'–H5'···O7' [iv] | 0.98 | 2.67 | 3.486(5) | 141 |

Symmetric codes: (i) x, y, -1+z; (ii) x, y, 1+z. (iii) 1-x, -1/2+y, 1-z; (iv) -x, 1/2+y, 2-z.

The neighboring helices are bridged *via* C–H···O interactions to form a layered arrangement (red and blue) as shown in figure 2.21. The helices are linked *via* dimeric head-to-head C–H···O interactions [shown in figure 2.19] and C16'–H16'···O10 along *a*-axis [Fig. 21]. Similarly, each helical strings [Fig. 2.20(i) and (ii)] further binds to *b*-axis *via* C16–H16···O9' and C17–H17*A*···O1' interactions [Table 2.10].

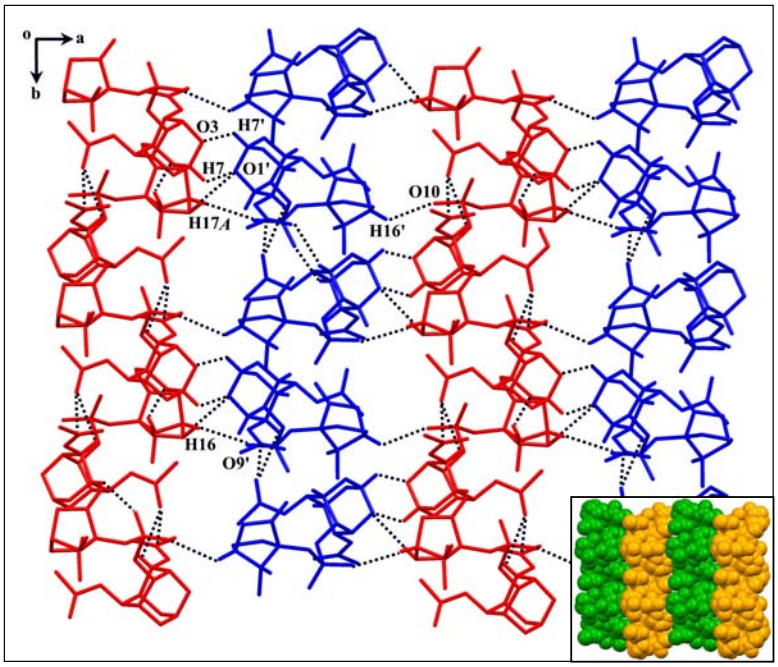


**Figure 2.21**: Helical assembly of **11** viewed down *c*-axis. Inset showed CPK view of **11** with close packing of helices.

**Table 2.10**: Geometry parameters of C–H···O interactions in **11** as shown in figure 2.21.

| D–H···A | D–H (Å) | H···A (Å) | D···A (Å) | D–H···A (º) |
|---|---|---|---|---|
| C16'–H16'···O10 [i] | 0.98 | 2.64 | 3.250(6) | 121 |
| C16–H16···O9' [ii] | 0.98 | 2.66 | 3.411(5) | 134 |
| C17–H17*A*···O1' [iii] | 0.97 | 2.65 | 3.601(5) | 168 |

Symmetry codes: (i) -x, 1/2+y, 1-z; (ii) 1-x, -1/2+y, 2-z; (iii) 1-x, -1/2+y, 1-z.

These layers are differently stitched in the third dimension *via* C–H···O interactions [Fig. 2.22]. The helical assembly of each diastereomers [Fig. 2.20(i) and (ii)] linked along *c*-axis *via* bifurcated C–H···O interactions between camphor sulfonyl proton, H12*C* with carbonyl oxygens O7 and O11of the other diastereomer and also *via* C12–H12*A*···O11' and C21–H21*C*···O7' [Fig. 2.22, Table 2.11].

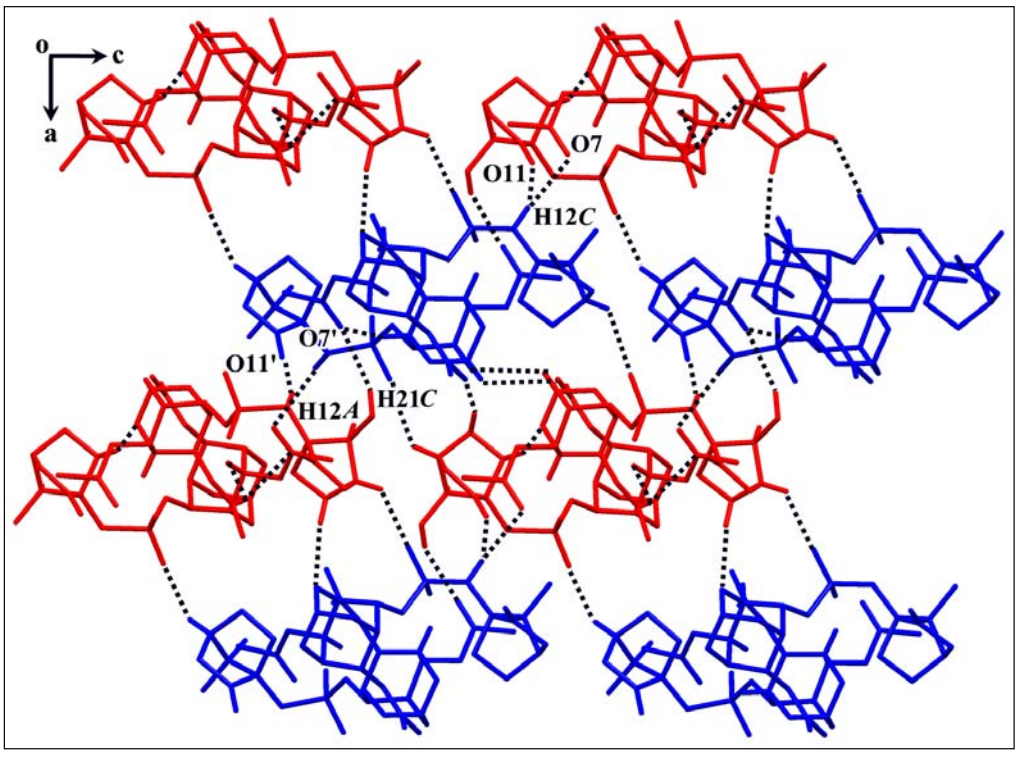


**Figure 2.22**: Molecular layer formation of **11** viewed down *b*-axis.

**Table 2.11**: Geometrical parameters of C–H···O interactions in **11** (Fig. 2.22).

| D–H···A | D–H (Å) | H···A (Å) | D···A (Å) | D–H···A (º) |
|---|---|---|---|---|
| C12'–H12*C*···O7 [i] | 0.97 | 2.69 | 3.465(4) | 138 |
| C12'–H12*C*···O11 [ii] | 0.97 | 2.65 | 3.453(5) | 140 |
| C12–H12*A*···O11' [iii] | 0.97 | 2.66 | 3.591(4) | 161 |
| C21–H21*C*···O7' [iv] | 0.94 | 2.61 | 3.509(5) | 160 |

Symmetry codes: (i) x, 1+y, z; (ii) x, 1+y, z; (iii) x, y, z; (iv) -x, -1/2+y, 2-z.

## 2.4 Conclusions

The molecular association *via* S═O···C═O short contacts between the diastereomers is observed and this bond dipolar interaction recognized for the first time. The mode of association among the diastereomers of **8** decides the observed inclusion behavior. When the dimer is formed *via* C–H···O hydrogen bonds, a very close packing of molecules results (Form-I), which does not allow the inclusion of guest molecules. However, a slight change in the relative orientation of the two diastereomers and bridging *via* S═O···C═O interactions leads to the formation of solvates (Form-II and Form-III crystals). The C–H···O and S═O···C═O interactions are complementary; when the C–H···O contact is stronger the S═O···C═O is weaker. Similarly, when the guest binding in **8** *via* C–H···O is stronger, the S═O···C═O contact is weaker. This complimentary S═O···C═O and C–H···O intermolecular interactions are also observed in crystals of **9** with different geometries, whereas the orthobenzoate, **10** associated without these dipolar contacts. The crystals of **11** choose dipolar C═O···C═O interactions for the helical assembly of diastereomers.

# Chapter 3

## Interplay of Weak Interactions on Molecular Conformation: Concomitant Dimorphism in Racemic 2,4-Di-*O*-Bezoyl-6-*O*-Tosyl-*myo*-Inositol-1,3,5-Orthoacetate *via* Intramolecular Dipolar S═O···C═O Interactions

# Chapter 3

## 3.1. Introduction

The studies of concomitant polymorphs, in which two or more crystal forms are grown under the same experimental conditions, are of great interest because they represent a special situation of equilibrium arising due to different inter/intramolecular interactions. Several mechanisms have been proposed for their formation; due to competing processes of homogeneous nucleation of different polymorphs[24c] or solvent mediated conversion of one polymorph to another[120] or the heterogeneous nucleation (cross nucleation) of one polymorph on another.[121] If concomitant crystallization occurs for a compound, its recognition and control is a challenging task. Therefore, one should investigate thoroughly the factors that influence the preferential crystallization to obtain the desired form or morphology. This chapter describes one such interesting case of conformational polymorphs that occur concomitantly.

As seen in the previous chapter (*Chapter 2*), a slight orientational change in the molecular association of diastereomers **8** *via* dipolar S═O···C═O interactions resulted in the formation of pseudopolymorphs. Related compounds, racemic 2,4-di-*O*-benzoyl-6-*O*-tosyl-*myo*-inositol 1,3,5-orthoesters [**13**, **14** and **15**, Scheme 3.1] were synthesized by replacing the bulky chiral camphorsulfonate with a flexible tosyl group, which was expected to adopt different orientations in the crystalline state. One of our main objectives in undertaking the structural investigations of these derivatives was also to examine the occurrence of these dipolar S═O···C═O short contacts in molecular association and their preferred motifs of interaction.

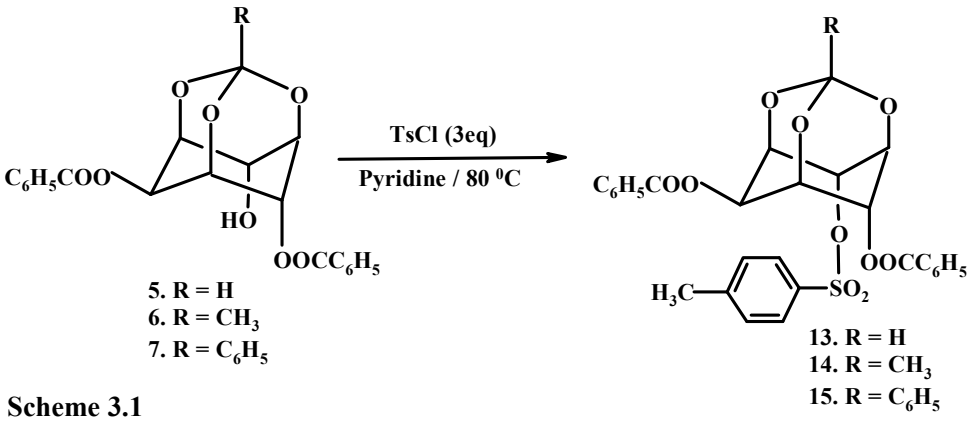


**Scheme 3.1**

## 3.2. Experimental section

### *3.2.1. Synthesis*

*3.2.1.1. Preparation of racemic 2,4-di-O-benzoyl-6-O-tosyl-myo-inositol 1,3,5-orthoformate* (**13**)

Racemic 2,4-di-*O*-benzoyl *myo*-inositol 1,3,5-orthoformate (0.398 g, 1 mmol) was dissolved in pyridine (10 ml), added tosyl chloride (0.570 g, 3 mmol) and the mixture stirred at 80˚C for 36 h. The pyridine was evaporated from the reaction mixture under reduced pressure and the gummy residue obtained worked up and finally purified by column chromatography (0.508 g, 92 %).[111]

Data for **13**:

**M.P.**: 163-164 °C

**IR ($CHCl_3$)ν**: 1710 (C═O) $cm^{-1}$

**$^1$H NMR (200 MHz, $CDCl_3$)**: **δ** 2.40 (s, 3H, ArMe), 4.45-4.65 (m, 3H, Ins H), 5.26-5.34 (m, 1H, Ins H), 5.52-5.58 (m, 1H, Ins H), 5.61-5.69 (m, 1H, Ins H), 5.80-5.85 (m, 1H, Ins H), 7.22 (d, *J* = 3.8 Hz, 2H, ArH), 7.35-7.75 (m, 8H, ArH), 8.00-8.20 (m, 4H, ArH) ppm.

**$^{13}$C NMR (50 MHz, $CDCl_3$)**: **δ** 21.8, 63.3, 67.3, 67.5, 69.3, 69.8, 72.2, 103.2, 128.1, 128.8, 129.5, 129.7, 130.1, 130.2, 130.3, 132.4, 133.8, 145.9, 165.1, 165.9 ppm.

**Anal. Calcd for $C_{28}H_{24}O_{10}S$**: C, 60.86; H, 4.38; Found: C, 60.68; H, 4.65 %.

*3.2.1.2. Preparation of racemic 2,4-di-O-benzoyl-6-O-tosyl-myo-inositol 1,3,5-orthoacetate* (**14**)

Racemic 2,4-di-*O*-benzoyl *myo*-inositol 1,3,5-orthoacetate (0.412 g, 1 mmol) and tosyl chloride (0.570 g, 3 mmol) were dissolved in pyridine (8 mL) and the reaction mixture stirred at 80 ˚C for 60 h. The solvent was evaporated under reduced pressure and the residue obtained was worked up with ethyl acetate and purified by column chromatography to obtain **14** (0.269 g, 48 %).

Data for **14**:

**M.P.**: 184-185 °C

**IR ($CHCl_3$)ν**: 1726 (C=O) $cm^{-1}$

**$^1$H NMR (200 MHz, $CDCl_3$)**: **δ** 1.53 (s, 3H, $O_3CMe$), 2.40 (s, 3H, ArMe), 4.44-4.52 (m, 2H, Ins H), 4.56-5.63 (m, 1H, Ins H), 5.22-5.29 (m, 1H, Ins H), 5.50 (t, 1H, *J* =1.64 Hz, Ins H), 5.72-5.78 (m, 1H, Ins H), 7.20-7.72 (m, 10H, ArH), 8.02- 8.16 (m, 4H, ArH) ppm.

**$^{13}$C NMR (50 MHz, $CDCl_3$)**: **δ** 21.6, 23.9, 62.2, 67.1, 67.2, 69.7, 70.1, 72.2, 109.2, 127.9, 128.4, 128.5, 128.6, 129.3, 129.9, 130.0, 130.1, 132.2, 133.5, 133.5, 145.6, 165.0, 165.8 ppm.

**Anal. Calcd for $C_{29}H_{26}O_{10}S$**: C, 61.48; H, 4.63. Found: C, 61.27; H, 4.36 %.

*3.2.1.3. Preparation of racemic 2,4-di-O-benzoyl-6-O-tosyl myo-inositol 1,3,5-orthobenzoate* (**15**)

A mixture of racemic 2,4-di-*O*-benzoyl *myo*-inositol 1,3,5-orthobenzoate (0.474 g, 1 mmol), tosyl chloride (0.570 g, 3 mmol) and pyridine (10 mL) was stirred at 80 ˚C for 96 h. The solvent was evaporated under reduced pressure and the residue was worked up with ethyl acetate and purified by column chromatography using ethyl acetate-petroleum ether (1:9) as eluent to obtain **15** as colorless solid (0.398 g, 63 %).

Data for **15**:

**M.P.**: 167-168 °C

**IR ($CHCl_3$)ν**: 1726 (C=O) $cm^{-1}$

**$^1$H NMR (200 MHz, $CDCl_3$)**: **δ** 2.41 (s, 3H, ArMe), 4.64-4.72 (m, 2H, Ins H), 4.75-4.83 (m, 1H, Ins H), 5.38-5.44 (m, 1H, Ins H), 5.63 (t, 1H, *J* = 2.54 Hz, Ins H), 5.90-5.96 (m, 1H, Ins H), 7.23-7.73 (m, 15H, ArH), 8.05-8.23 (m, 4H, ArH) ppm.

**$^{13}$C NMR (50 MHz, $CDCl_3$)**: **δ** 21.9, 62.5, 67.5, 68.2, 70.8, 71.2, 72.5, 108.2, 125.6, 128.2, 128.4, 128.8, 128.9, 129.6, 130.2, 130.4, 132.5, 133.9, 136.2, 146.0, 165.4, 166.1 ppm.

**Anal. Calcd for $C_{34}H_{28}O_{10}S$**: C, 64.96; H, 4.49. Found (%): C, 64.62; H, 4.53 %.

### *3.2.2. Crystallization*

Slow evaporation of a solution of **13**, **14** or **15** in organic solvents such as dichloromethane, chloroform, acetonitrile, ethyl acetate (containing light petroleum ether as precipitant), at room temperature produced crystals (needles of **13** and **15**, plates of **14)**. The concomitant dimorphs of **14** (plates: Form-I and needles: Form-II) were obtained by slow evaporation of a solution of **14** (0.05 g) in dichloromethane (2 mL) and methanol (five drops) in a closed container at room temperature [Fig. 3.1]. The melt crystallization experiments of monoclinic crystals of **13**, **14** and **15** were also carried out, which did not yield any crystals.

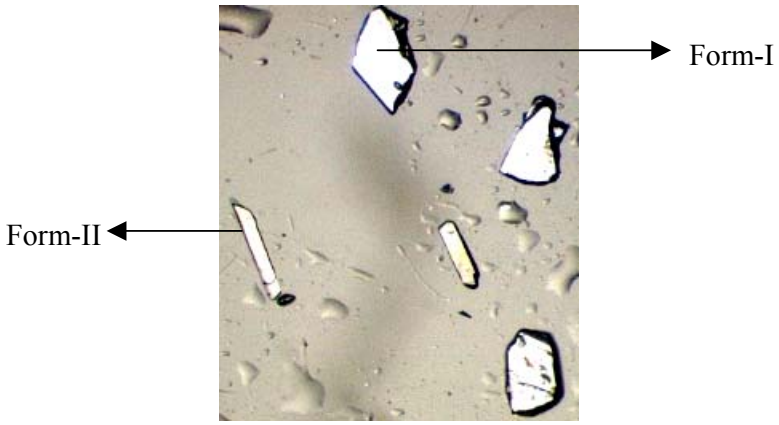


**Figure 3.1**: Photomicrograph of concomitant polymorphs of **14**.

### *3.2.3. Thermal Analysis*

Differential Scanning Calorimetric (DSC) analysis was performed on Mettler Toledo DSC instrument for the crystalline samples of **13**, Form-I of **14** and **15**. About 6-8 mg of the crystalline samples were placed in an aluminum pan and heated from 40 to 190 °C at the rate of 5 °C/minute. An empty pan was used as the reference; dry nitrogen was used for purging (50 mL/min). All the DSC curves showed a single endothermic peak corresponding to the melting point of the sample [Fig. 3.2]. DSC studies of Form-II crystals of **14** could not be carried out due to their low yield.

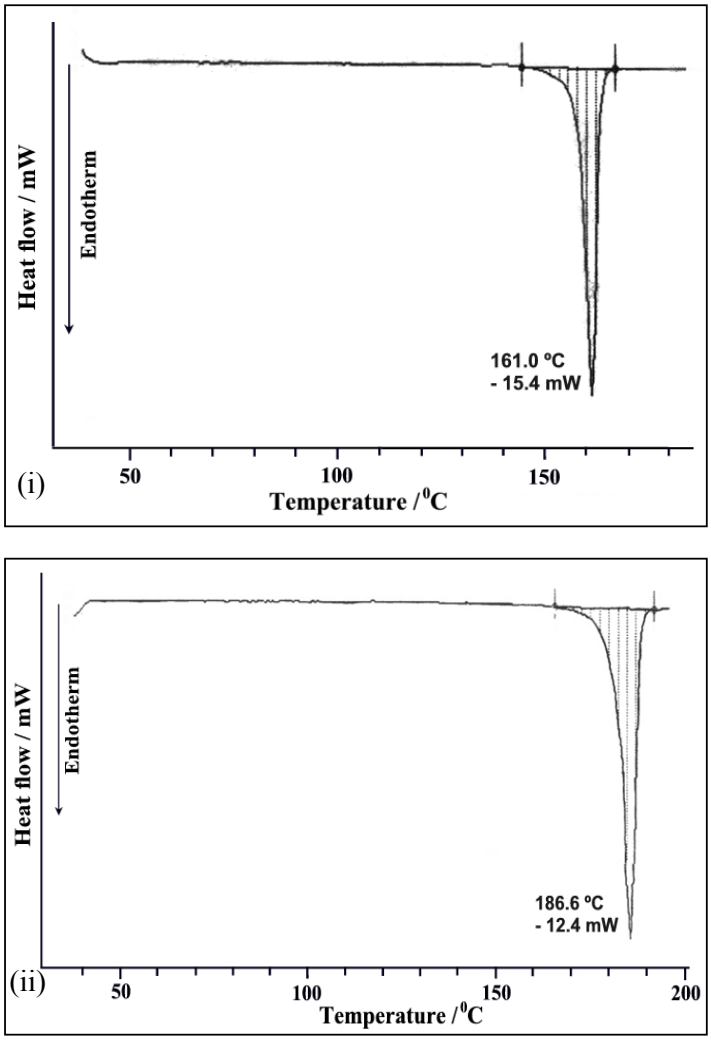


**Figure 3.2**: DSC plots of (i) **13**, (ii) Form-I of **14** and (iii) **15** crystals.

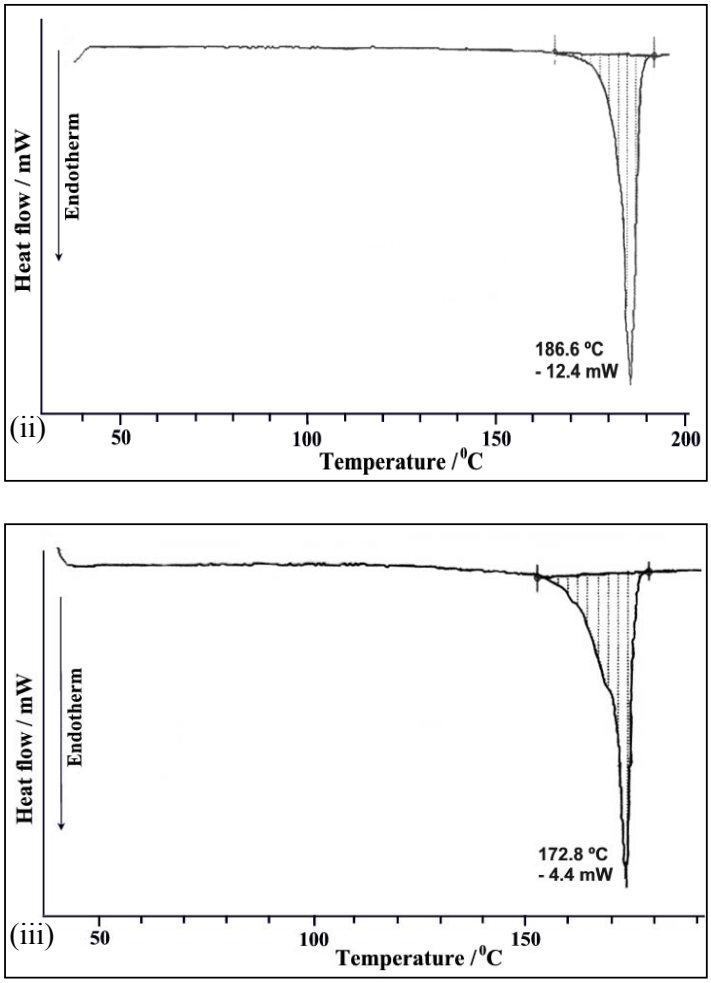


**Figure 3.2**: Continued. DSC plots of (ii) Form-I of **14** and (iii) **15** crystals.

### *3.2.4. Crystallographic Details*

X-ray intensity data for crystals of **13**, **14** (Forms I and II) and **15** were collected on a Bruker SMART APEX CCD diffractometer in omega and phi scan mode, $\lambda_{MoK\alpha}$ = 0.71073 Å at room temperature. All the intensities were corrected for Lorentzian, polarization and absorption effects using Bruker's *SAINT* and *SADABS* programs. All the crystal structures were solved by Direct methods using program *SHELXS-97*; the full-matrix least squares refinements on $F^2$ were carried out by using *SHELXL-97*. Hydrogen atoms were included in the refinement as per the riding model. Table 3.1 summarizes the crystal data for all the compounds.

**Table 3.1**: Summary of crystallographic data for **13**, dimorphs of **14** and **15**.

| Crystal data | **13** | Form-I (**14**) | Form-II (**14**) | **15** |
|---|---|---|---|---|
| Chemical Formula | $C_{28}H_{24}O_{10}S$ | $C_{29}H_{26}O_{10}S$ | $C_{29}H_{26}O_{10}S$ | $C_{34}H_{28}O_{10}S$ |
| $M_r$ | 552.53 | 566.56 | 566.56 | 628.62 |
| Temperature/K | 298(2) | 298(2) | 298(2) | 298(2) |
| Morphology | Thin needles | Plate | Thin needles | Needles |
| Colour | Colorless | Colorless | Colorless | Colorless |
| Crystal size (mm) | 0.74 × 0.04 × 0.03 | 0.48 × 0.37 × 0.04 | 0.42 × 0.06 × 0.02 | 0.64 × 0.20 × 0.07 |
| Crystal system | Monoclinic | Monoclinic | Triclinic | Monoclinic |
| Space group | *P2₁/c* | *P2₁/n* | *P-1* | *C2/c* |
| *a* (Å) | 15.311(6) | 15.3915(19) | 7.107(3) | 22.30(4) |
| *b* (Å) | 13.352(5) | 10.6781(13) | 13.831(7) | 19.15(3) |
| *c* (Å) | 12.882(5) | 16.722(2) | 15.272(7) | 14.72(3) |
| $\alpha$ (°) | 90 | 90 | 65.826(8) | 90 |
| $\beta$ (°) | 91.594(7) | 95.776(2) | 77.644(8) | 107.00(5) |
| $\gamma$ (°) | 90 | 90 | 76.627(10) | 90 |
| *V* (Å$^3$) | 2632.5(18) | 2734.4(6) | 1320.3(11) | 5949.9(13) |
| *Z* | 4 | 4 | 2 | 8 |
| $D_x$ (Mg m$^{-3}$) | 1.394 | 1.376 | 1.425 | 1.389 |
| $\mu$ (mm$^{-1}$) | 0.181 | 0.177 | 0.183 | 0.168 |
| *F(000)* | 1152 | 1184 | 592 | 2624 |
| $T_{min}$ | 0.877 | 0.920 | 0.927 | 0.900 |
| $T_{max}$ | 0.995 | 0.992 | 0.996 | 0.988 |
| $\theta_{max}$ (°) | 25.0 | 25.0 | 25.0 | 25.0 |
| *h* (min, max) | (-18, 16) | (-18, 18) | (-8, 8) | (-26, 26) |
| *k* (min, max) | (-15, 15) | (-12, 12) | (-16, 16) | (-15, 22) |
| *l* (min, max) | (-15, 15) | (-19, 17) | (-18, 18) | (-15, 17) |
| No. of refl$^n$ collected | 18309 | 18018 | 12755 | 12035 |
| No. of unique refl$^n$ | 4615 | 4800 | 4654 | 5256 |
| No. of observed refl$^n$ | 2551 | 3277 | 2595 | 2359 |
| No. of parameters | 354 | 363 | 363 | 407 |
| $R_{int}$ | 0.153 | 0.033 | 0.080 | 0.068 |
| $R_1$_obs, $R_1$_all | 0.146, 0.224 | 0.046, 0.074 | 0.132, 0.216 | 0.058, 0.160 |
| $wR_2$_obs, $wR_2$_all | 0.357, 0.396 | 0.104, 0.118 | 0.226, 0.260 | 0.102, 0.127 |
| GoF | 1.16 | 1.01 | 1.18 | 0.93 |
| $\Delta\rho_{max}$, $\Delta\rho_{min}$ (e Å$^{-3}$) | 0.49, –0.47 | 0.26, –0.21 | 0.34, –0.32 | 0.18, –0.15 |

### *3.2.5. Computational Studies*

Single point *ab initio* energy calculation on Forms I and II of **14** (dimorphs) were performed using the 'Gaussian 03' suite of programs.[122] In each case, single point energies of isolated molecules were computed with the *Hartree-Fock* theory at 6-31G(*d*,*f*) level to correlate the relative energies of dimorphs without taking into account of any intermolecular interactions.

## 3.3. Results and Discussion

The tosylates **13**, **14** and **15** produced solvent free crystals from different organic solvents/conditions; the orthoacetate **14** yielded concomitant dimorphs from dichloromethane-methanol mixture with different morphologies [Fig. 3.1]. Majority of the crystals were plates (Form-I: monoclinic, $P2_1/n$) while very few were thin needles (Form-II: triclinic, *P-1*). The DSC analysis of **13**, **14** (Form-I) and **15** revealed only a single endotherm attributed to their melting, indicating no thermal phase transformations in the crystals [Fig. 3.2].

Crystal structure analysis of **13**, **14** (Forms I and II) and **15** revealed different conformations of the tosyl group due to rotation around *O6–S1* bond [Fig. 3.3]; the *C6–O6–S1–C22* (*C23* in **14** or *C28* in **15**) torsion angles were found to be 80.6º, 91.2º, 165.5º and 160.6º respectively. As seen from the torsion angles, the conformations of the tosyl group in **13** and **15** are quite different; interestingly conformational dimorphs of **14** adopt two different orientations for the tosyl group, one of them [Form-I, Fig. 3.4(ii)] is similar to the conformation of molecules in **13** [Fig. 3.4(i)] and the other [Form-II, Fig. 3.4(iii)] is similar to the conformation of molecules in **15** [Fig. 3.4(iv)]. It is noteworthy that a marked difference in orientation of the tosyl group (~ 74º difference in torsion angle) in crystals of Forms I and II of **14** [Fig. 3.4(ii) and 3.4(iii)] was observed under identical crystallization conditions. Although the conformations in **15** and Form-II crystals of **14** are similar, the

intramolecular interactions made by the tosyl group with the benzoyl group are quite different. The molecules in Form-II crystals (of **14**) make intramolecular S═O···C═O dipolar short contacts between the tosyl group and the C4-*O*-benzoyl group [Fig. 3.3(iii)]; a difference of ~ 5º in the orientation of tosyl group changes this interaction to intramolecular π···π interaction in crystals of **15** [Fig. 3.3(iv)]. The geometry of intramolecular S═O···C═O contacts [S1═O10···C16═O8 = 3.157(8) Å, ∠O10···C16═O8 = 94º, ∠S1═O10···C16= 116º] observed here is of interaction motif Type-III *i.e.* sheared parallel motif.[112] These dipolar contacts are changed to stacking

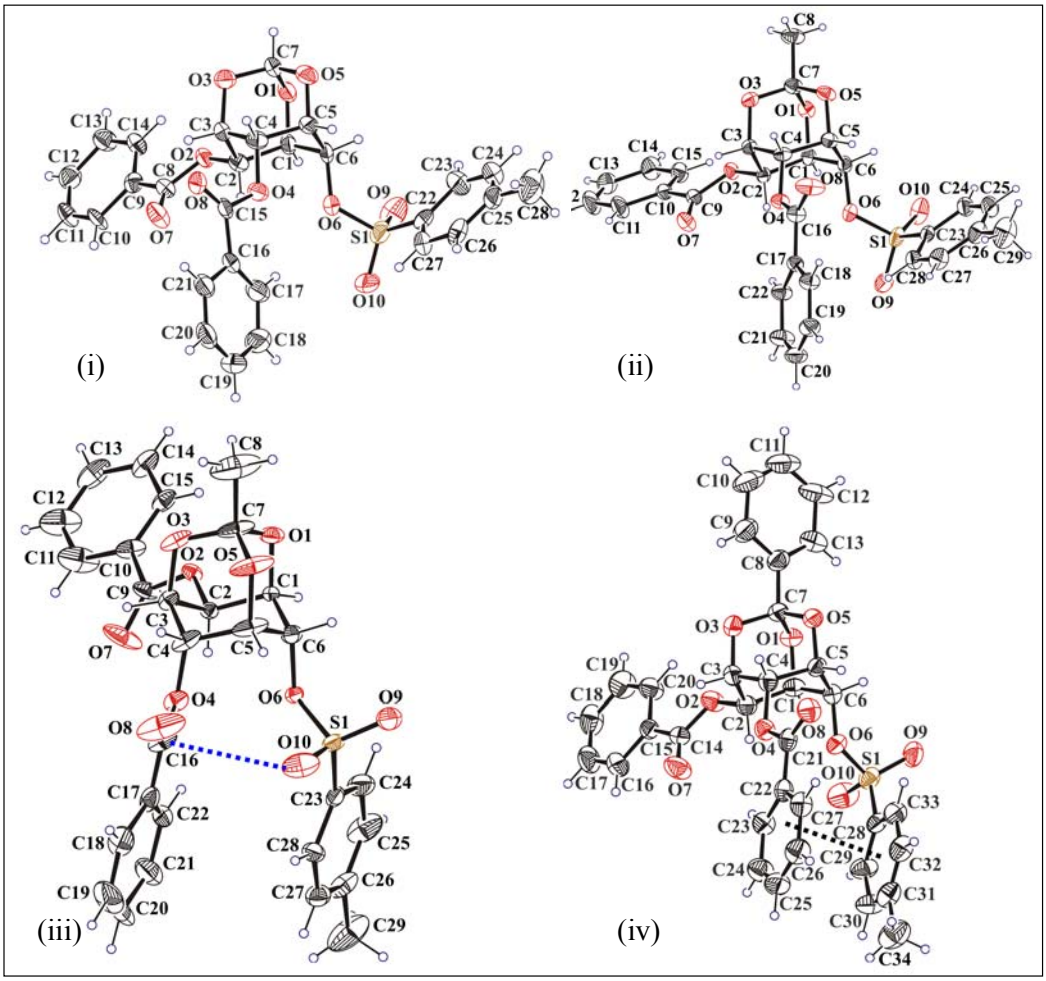


**Figure 3.3**: ORTEP view of (i) **13**, (ii) Form-I of **14**, (iii) Form-II of **14** [blue dashed line indicates dipolar S═O···C═O contact] and (iv) **15** [black dashed line indicates π···π interaction] with 30% probability displacement ellipsoids.

interactions in crystals of **15** with parameters, C*g*2···C*g*3 = 3.819 Å and dihedral angle, $\alpha$ = 3.69º [C*g*2 and C*g*3 are the centroid of the phenyl rings benzoyl (C22-27) and tosyl (C28-33) groups respectively]. These observations suggest the multiple choice of weaker non-covalent interaction in crystals *i.e.* S═O···C═O contacts as in **14** or π···π interactions in **15**, with a very slight change in the orientation of tosyl and benzoyl groups.

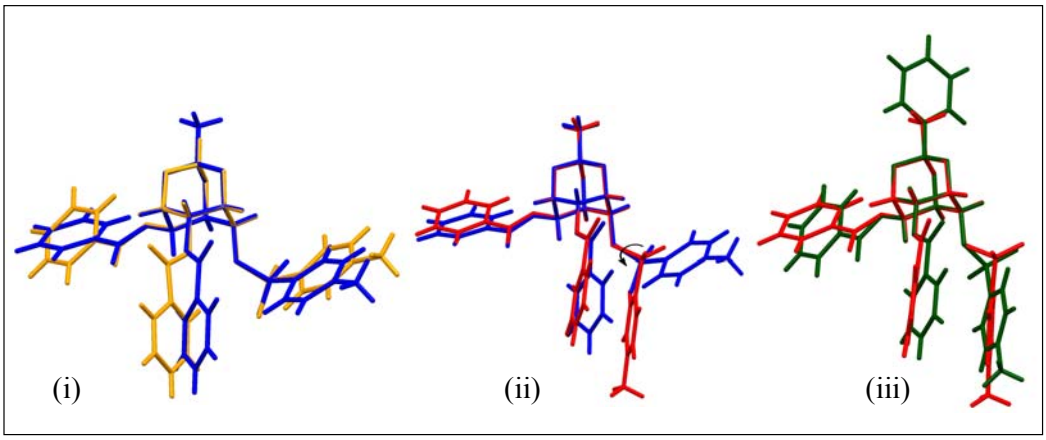


**Figure 3.4**: Molecular overlap of (i) **13** (orange) and Form-I of **14** (blue); (ii) Form-I (blue) and Form-II (red) of **14** and, (iii) Form-II of **14** (red) and **15** (green).

### *3.3.1. Conformational Analysis of Tosyl Group in Organic Crystals*

As seen above, the conformation of tosyl group varied drastically along *O–S* bond upon substitution of the orthoester H by $CH_3$ or $C_6H_5$ (phenyl) groups. Therefore, we carried out statistical analysis to find the orientational preference for tosyl group in the crystalline state. The CSD version 5.29 was used for the torsion angle (*X–X–S–C, X=any element*) in the crystal structures of organic compounds containing tosyl groups. All the searches were carried out with error free structures with 3D co-ordinates and restricted entries of disorders, ionic, polymeric and structures elucidated from X-ray powder diffraction data. There are 1610 entries of organic compounds with tosyl groups in the CSD; out of which 950 (60 %) were

included in a torsion angle range of 70 and 90º [Fig. 3.5]. The conformation of the tosyl group in **13** and Form I crystals of **14** is similar to the preferred orientation seen in the CSD search, but the tosyl group in Form-II crystals of **14** and **15** is similar to the less prevalent orientation seen in the CSD search (~160º). Also there are only eight cases of tosylated derivatives exhibiting polymorphism in the CSD [Appendix]. The relative difference in the orientation of the tosyl group in these polymorphs is slight (maximum of ~ 12º), whereas in the conformational dimorphs of **14** (Forms I and II) reported here this relative difference is significant (74º). The single point energy calculations of dimorphs (isolated molecule) show an energy barrier of ~ 55 kJ/mol, which could be because of the larger orientational difference of tosyl group. It is noteworthy that the lower energy crystal form (Form-I) was obtained from most of the solvents which was also a major product among the concomitant crystals. However, the competitive intra/intermolecular interactions of molecules resulted in the formation of high energetic form (Form-II) during crystal formation.

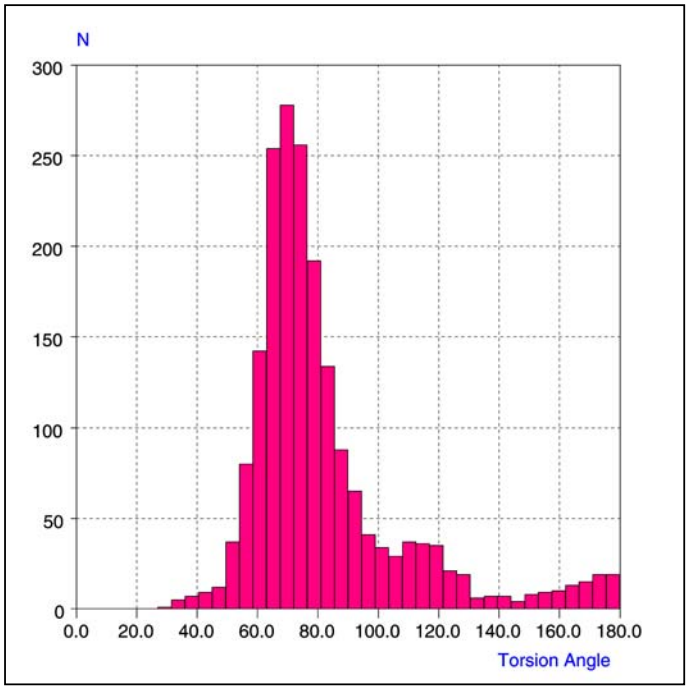


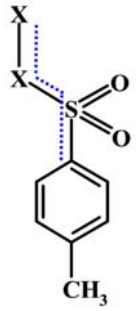


[X = any element attached to sulfur]

**Figure 3.5**: Histogram of X–X–S–C torsion angle in the tosyl derivatives.

### *3.3.2. Dimeric Association in 13-15*

Although the molecular conformations in **13**, **14** and **15** differ; the molecules are associated to form dimers *via* centrosymmetric C–H···O interactions in the crystal lattice. The dimer formation in **13** involves the binding of inositol proton *H3* and *C6*-benzoyl oxygen *O8* [Fig. 3.6(i)]; whereas in Form-I of **14** dimers are formed by the interaction of the inositol ring proton *H1* with the sulfonyl oxygen *O10* [Fig. 3.6(ii)]. In Form-II crystals of **14**, centrosymmetric dimer is formed between the inositol proton *H6* and the orthoester oxygen *O1* [Fig. 3.6(iii)] but interestingly the formation of dimers in **15** involve the inositol proton (*H5*) and the orthoester oxygen (*O5*) as well as the *C6*–benzoyl oxygen (*O8*) and the tosyl groups (*H32*) [Fig. 3.6(iv), Table 3.2].

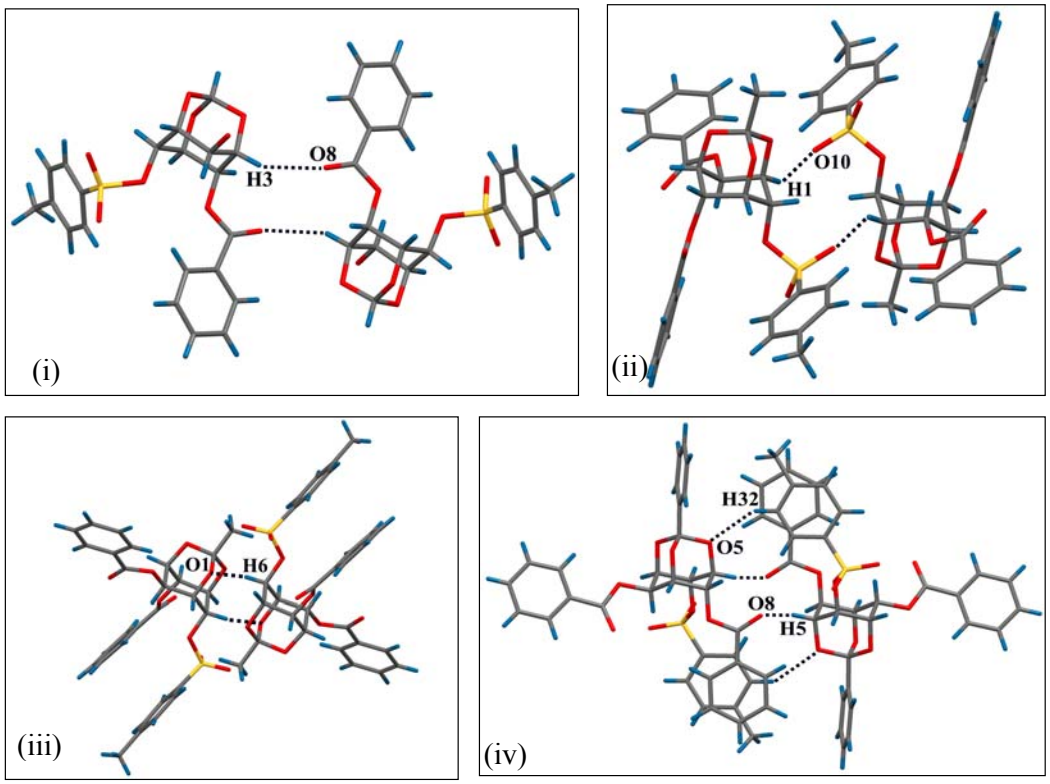


**Figure 3.6**: Dimeric association of molecules in (i) **13** (2-*O*-benzoyl group is not shown for clarity), (ii) Form-I of **14**, (iii) Form-II of **14** and (iv) **15** (2-benzoyl group is not shown for clarity).

**Table 3.2**: Geometrical parameters for hydrogen bonding interactions (Fig. 3.6).

| Crystal | D–H···A | D–H (Å) | H···A (Å) | D···A (Å) | D–H···A (°) |
|---|---|---|---|---|---|
| **13** | C3–H3···O8 [i] | 0.98 | 2.53 | 3.367(10) | 144 |
| Form-I (**14**) | C1–H1···O10 [ii] | 0.98 | 2.50 | 3.328(3) | 142 |
| Form-II (**14**) | C6–H6···O1 [iii] | 0.98 | 2.55 | 3.391(9) | 144 |
| **15** | C5–H5···O8 [iv] | 0.98 | 2.43 | 3.253(4) | 142 |
| | C32–H32···O5 [iv] | 0.93 | 2.67 | 3.444(5) | 141 |

Symmetric codes: (i) -x+1, -y+1, -z; (ii) -x, -y, -z ; (iii) 2-x, 1-y, 1-z ; (iv) 2-x, 1-y, 2-z .

### *3.3.3. Molecular Chain Formation in 13-15*

The dimers of **13**, **14** and **15** form 1D molecular chains *via* weak C–H···O, C–H···π and π···π interactions. Dimers of **13** are linked centrosymmetrically *via* C28–H28*A*···O10 interactions diagonal to *ab*-plane [Fig. 3.7(i) and Table 3.4]; whereas in **15** and dimorphs of **14** the dimers are linked *via* C–H···O and π···π interactions [Fig. 3.7(ii), (iii) and (iv), Table 3.3] involving the *C2*–benzoyl group. In Form-I crystals of **14**, the dimers bind *via* centrosymmetric π···π stacking interactions [C═O···C*g*1] and C13–H13···O9 interactions, but in Form-II crystals they are bound *via* π···π [C*g*1···C*g*1] and C13–H13···O3 interactions. The linking of the dimers in **15** is similar to that in Form-II crystals, *via* π···π [C*g*1···C*g*1] and C18–H18···O10 contacts.

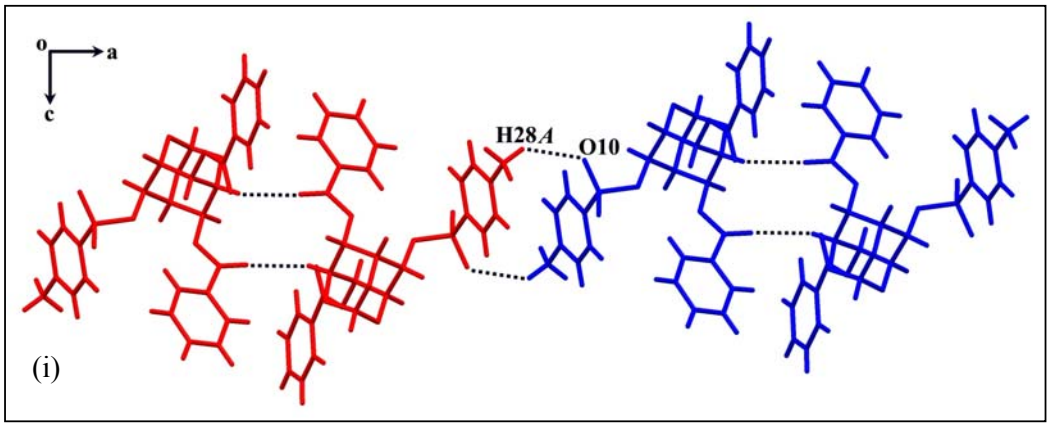


**Figure 3.7**: Molecular chain formation in (i) **13** (ii) Form-I of **14**, (iii) Form-II of **14** and (iv) **15**.

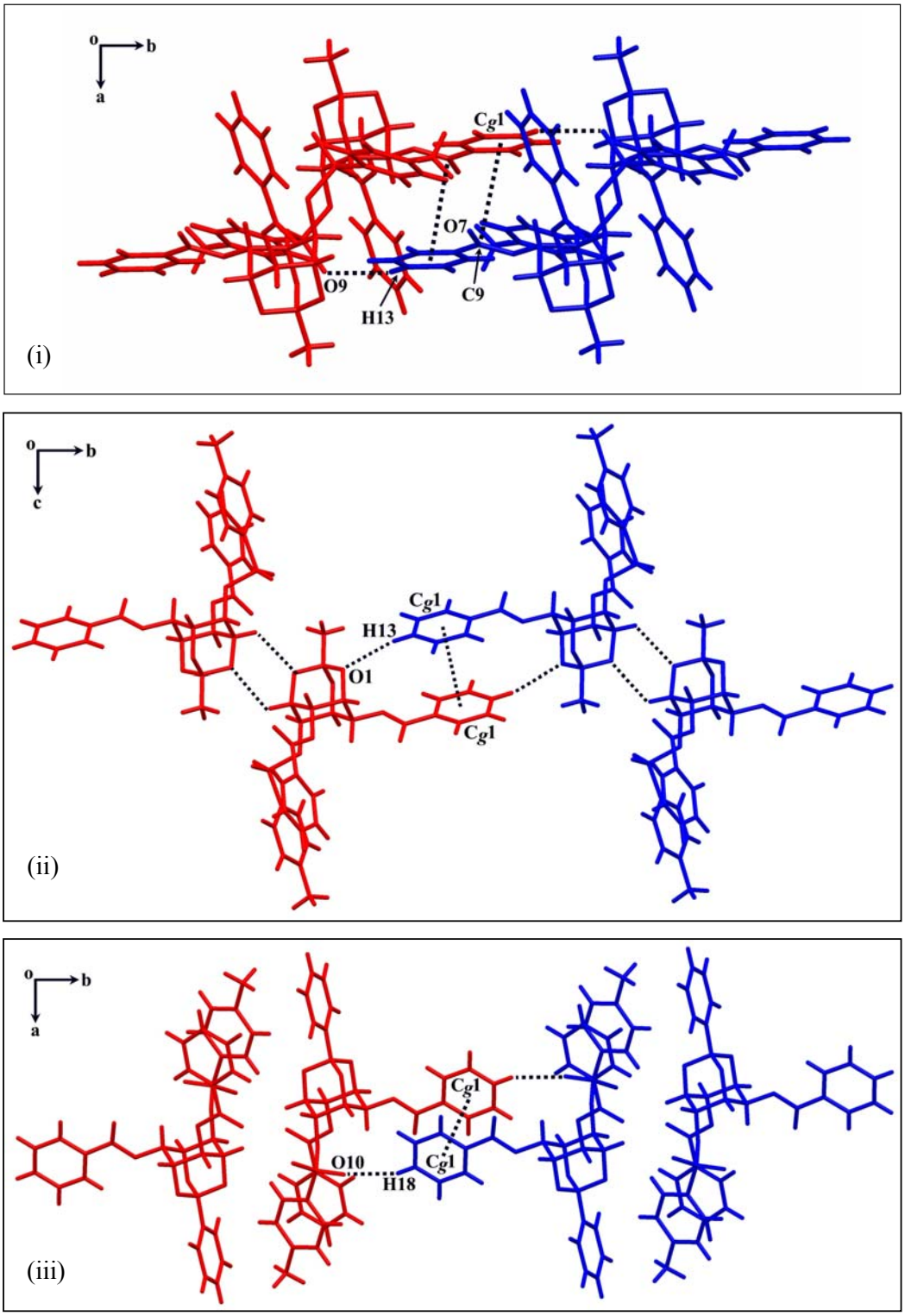


**Figure 3.7**: Continued. Molecular chain formation in (ii) Form-I of **14**, (iii) Form-II of **14** and (iv) **15** *via* C–H···O and π···π interactions.

**Table 3.3**: Geometrical parameters of π···π interactions as shown in figure 3.7.

| Crystals | Y–X/Cg···Cg | Y-X/Cg···Cg | Y-X···Cg/ α | Phenyl Rings |
|---|---|---|---|---|
| Form-I (**14**) | C9═O7···Cg1$^{i}$ | 3.825 Å | 80º | Cg1: C10-C15 |
| Form-II (**14**) | Cg1···Cg1$^{i}$ | 3.743 Å | 0.00º | Cg1: C10-C15 |
| **15** | Cg1···Cg1$^{i}$ | 3.856 Å | 0.03º | Cg1: C15-C20 |

Symmetric code: (i) -x, -y, 1-z.

### *3.3.4. Molecular Organization in 13-15*

#### *3.3.4.1. Molecular organization in* **13**

The molecular chains are linked to form a 2D-molecular net along *c*-axis *via* weak C–H···π interactions [Fig. 3.8(i)]. These layers form cavities (~ 16 x 8 Å$^2$) which are penetrated by the adjacent layer. This achieves a close packing in the crystal lattice *via* dipolar (ether) O1···C15═O8 contacts and C14–H14···O5 interactions [Table 3.4]. Thus, the overall packing results from the cross-linking of molecular chains in the crystal lattice without leaving any voids for solvent inclusion [Fig. 3.8(ii) and (iii)].

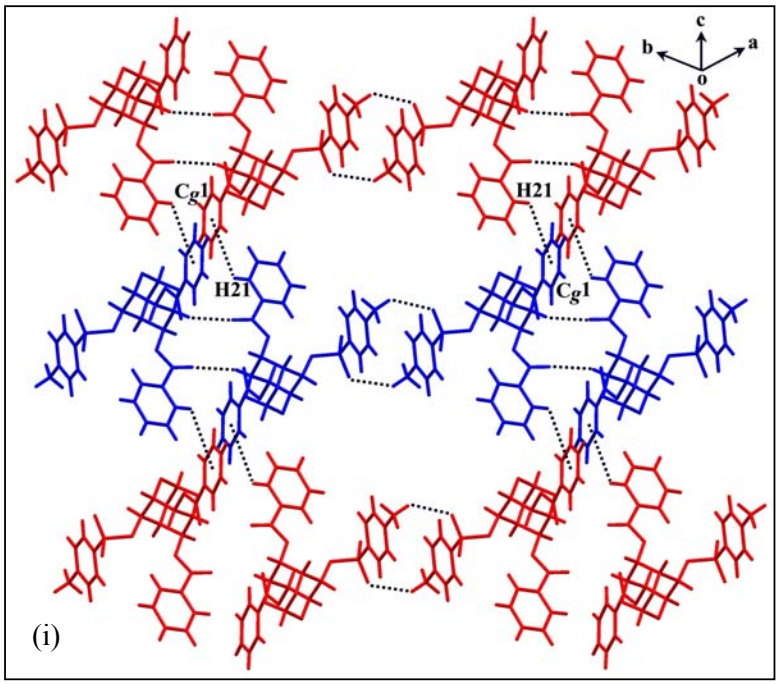


**Figure 3.8**: (i) Molecular layer of **13** viewed down *b*-axis.

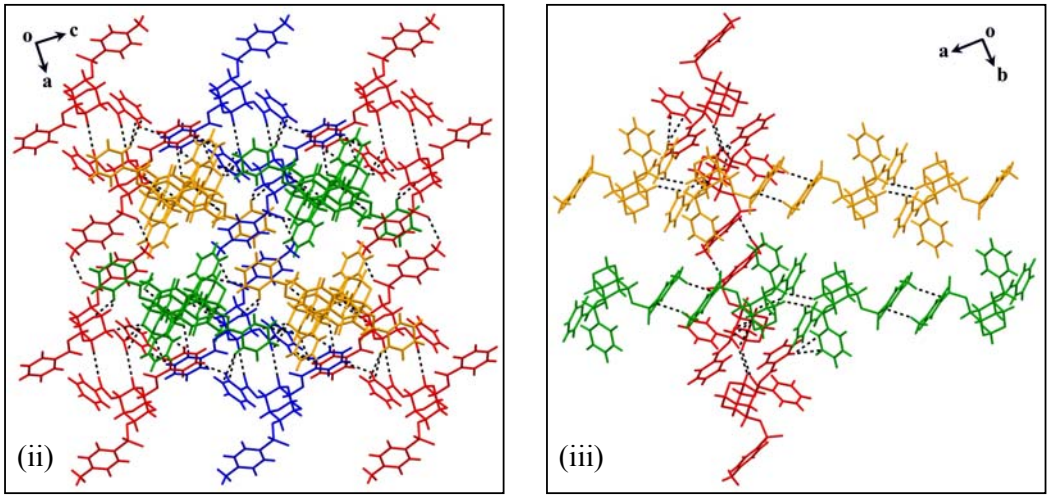


**Figure 3.8**: Continued. Cross linked molecular layers (ii) viewed down *b*-axis (ii) viewed down *c*-axis.

**Table 3.4**: Geometrical parameters for intermolecular interactions [Fig. 3.7(i) & 3.8].

| Crystal | D–H···A | D–H (Å) | H···A (Å) | D···A (Å) | D–H···A (°) |
|---|---|---|---|---|---|
| **13** | C3–H3···O8 [i] | 0.98 | 2.53 | 3.367(10) | 144 |
| | C14–H14···O5 [ii] | 0.93 | 2.70 | 3.403(11) | 133 |
| | C28–H28A···O10 [iii] | 0.96 | 2.66 | 3.445(17) | 139 |
| | C21–H21···Cg1 [iv] | 0.93 | 3.84 | 4.395(12) | 122 |
| | O1···C15═O8 [ii] | - | - | 2.916(10) | 83.8 |

Symmetry codes: (i) -x+1, -y+1, -z; (ii) x, -y+3/2, z+1/2; (iii) -x, -y+2, -z; (iv) x, y, z+1.

*3.3.4.2. Molecular organization in dimorphs of* **14**

The molecular strings of dimorphs [Fig. 3.7(ii) & (iii)] are weaved differently to form two-dimensional layers as shown in figure 3.9. In Form-I crystals of **14**, the molecular strings related by $2_1$-screw axis are bound together *via* C3–H3···O5 interactions to form 2D-layer along *b*-axis [Fig. 3.9(i)], whereas in Form-II crystals of **14**, the molecular chains are linked to the unit-translated strings *via* C19–H19···O7 contacts along *c*-axis. It is noteworthy that the molecular strings in Form-I crystals are stitched to each other by orthoester oxygen (O5) and the inositol proton (H3) but in

Form-II crystals, they are linked together by *C2*-benzoyl oxygen (O7) and *C4*-benzoyl hydrogen (H19) [Table 3.5].

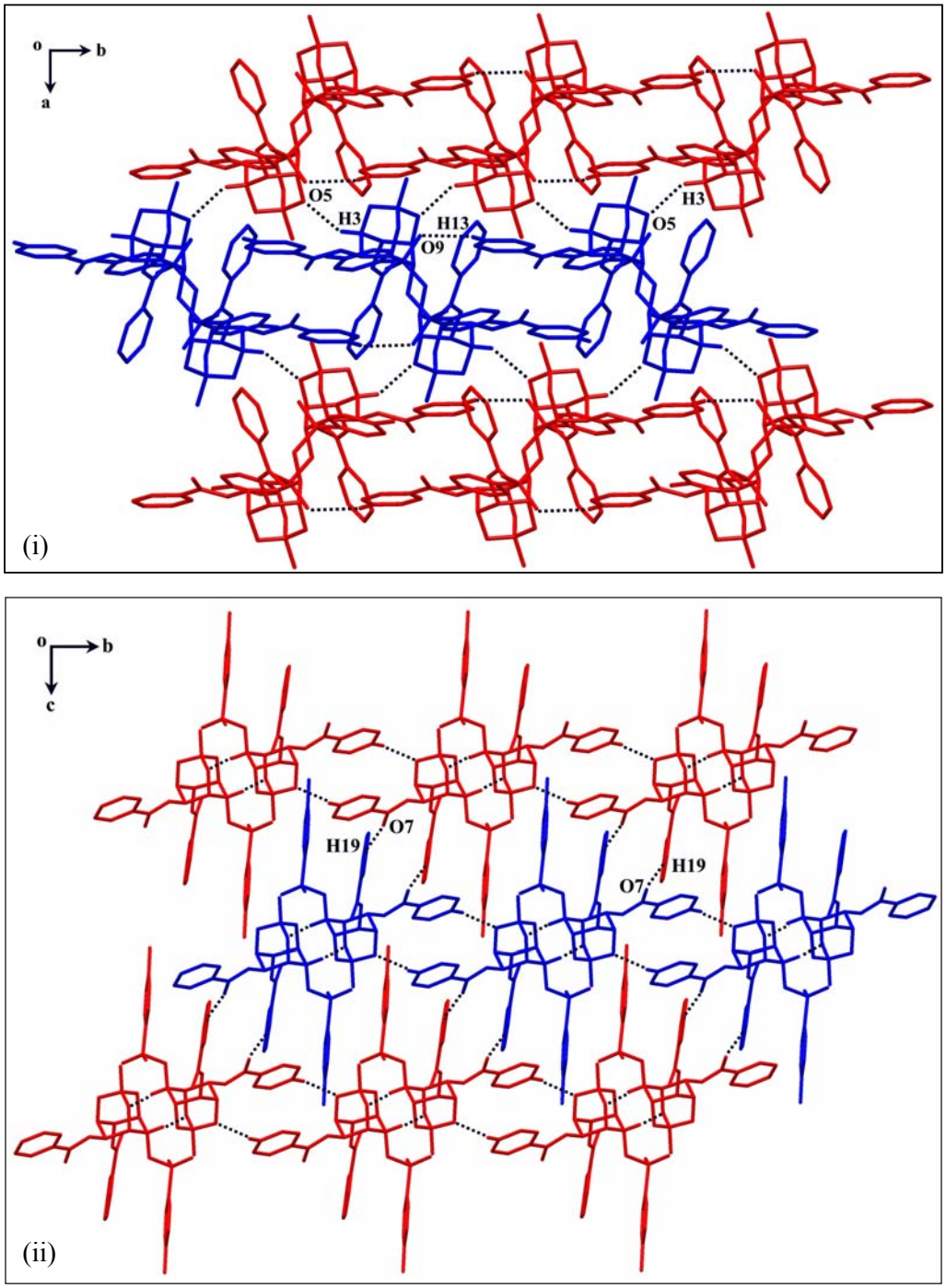


**Figure 3.9**: Molecular layer formation of **14** in (i) Form-I of **14** viewed down *c*-axis and (ii) Form-II of **14** viewed down *a*-axis.

**Table 3.5**: Geometrical parameters for intermolecular C–H···O interactions in dimorphs of **14** as shown in figures 3.9 and 3.10.

| Crystal | D–H···A | D–H (Å) | H···A (Å) | D···A (Å) | D–H···A (°) |
|---|---|---|---|---|---|
| Form-I (**14**) | C1–H1···O10 [i] | 0.98 | 2.50 | 3.328(3) | 142 |
| | C3–H3···O5 [ii] | 0.98 | 2.36 | 3.231(3) | 148 |
| | C13–H13···O9 [iii] | 0.93 | 2.51 | 3.259(4) | 138 |
| | C18–H18···O8 [iv] | 0.93 | 2.65 | 3.284(3) | 126 |
| Form-II (**14**) | C1–H1···O8 [v] | 0.98 | 2.44 | 3.134(10) | 127 |
| | C2–H2···O8 [v] | 0.98 | 2.69 | 3.089(9) | 105 |
| | C5–H5···O5 [vi] | 0.98 | 2.64 | 3.170(9) | 114 |
| | C13–H13···O3 [vii] | 0.93 | 2.64 | 3.546(10) | 165 |
| | C19–H19···O7 [viii] | 0.93 | 2.37 | 3.173(15) | 145 |

Symmetry codes: (i) -x, -y, -z; (ii) 1/2-x, 1/2+y, 1/2-z; (iii) -x 1-y, -z; (iv) -x, -y, 1-z; (v) 1+x, y, z; (vi) 1-x, 1-y, 1-z; (vii) 2-x, 2-y, 1-z; (viii) 1-x, 2-y, -z.

In Form-I crystals of **14**, these molecular layers are associated in the third dimension *via* centrosymmetric C–H···O interactions between the inositol proton *H1* and tosyl oxygen *O10* [Fig. 3.10(i)]. But in Form-II crystals, the 2D-layers are weaved very closely *via* centrosymmetric C6–H6···O1 contacts and bifurcated C–H···O interactions between the *C4*-benzoyl oxygen *O8* and inositol ring protons *H1* and *H2* [Fig. 3.10(ii), Table 3.5]. It is interesting to note that the tosyl oxygen atoms (O9 and O10) in Form-II crystals do not take part in any significant intermolecular interaction except for intramolecular dipolar S═O···C═O contact. As a result of intra and inter molecular interactions, the tosyl groups are packed more closely to the axial benzoyl groups in Form-II crystals resulting in denser crystal packing (1.425 $Mgm^{-3}$) compared to Form I crystals (1.376 $Mgm^{-3}$).

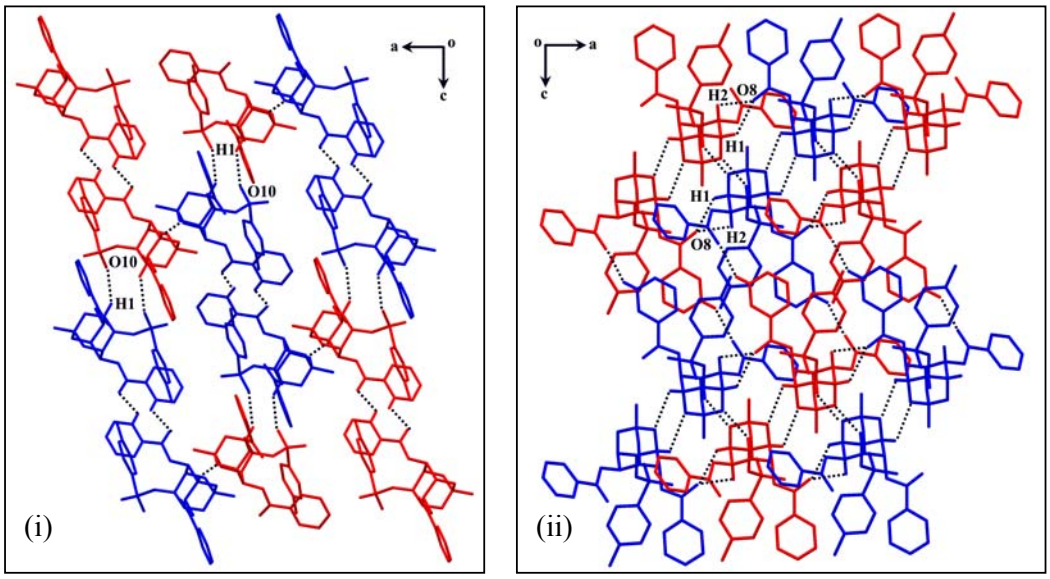


**Figure 3.10**: Molecular layer formation of **14** in (i) Form-I viewed down *c*-axis and (ii) Form-II viewed down *a*-axis.

*3.3.4.3. Molecular organization in* **15**

The molecular strings of **15** are unit translated along *a*-axis to form 2D layer *via* C11–H11···O7 interaction and C–H···π contact between the axial phenyl H-atom (H24) and the phenyl ring of the orthobenzoate group [C24–H24···C*g*2 = 2.81 Å, C24···C*g*2 = 3.668 Å, ∠C24–H24···C*g*2 = 154º, C*g*2 = the centroid of C8-C13 ring, symmetric code: 1/2+x, 1/2-y, 1/2+z] [Fig. 3.11(i)]. These molecular layers form discrete molecular columns along *c*-axis *via* bifurcated C–H···O interactions *i.e*. each dimeric unit [shown blue or red in Fig. 3.11(ii)] is linked to each other *via* C6–H6···O9 and C27–H27···O9 contacts [Table 3.6].

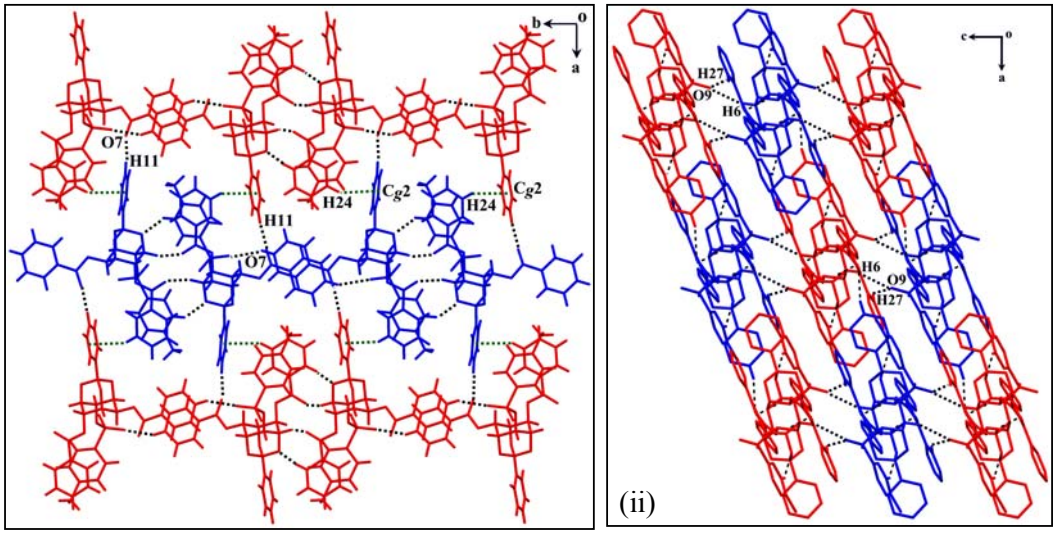


**Figure 3.11**: Molecular layers of **15** viewed (i) down *c*-axis and (ii) down *b*-axis.

**Table 3.6**: Geometrical parameters of intermolecular C–H···O interactions shown in figure 3.11.

| Crystal | D–H···A | D–H (Å) | H···A (Å) | D···A (Å) | D–H···A (°) |
|---|---|---|---|---|---|
| **15** | C5–H5···O8 [i] | 0.98 | 2.43 | 3.253(4) | 142 |
| | C6–H6···O9 [ii] | 0.98 | 2.50 | 3.413(4) | 156 |
| | C11–H11···O7 [iii] | 0.93 | 2.34 | 3.294(7) | 165 |
| | C18–H18···O10 [iv] | 0.93 | 2.52 | 3.383(5) | 154 |
| | C27–H27···O9 [v] | 0.93 | 2.58 | 3.361(5) | 142 |
| | C32–H32···O5 [ii] | 0.93 | 2.67 | 3.444(5) | 141 |

Symmetry codes: (i) 2-x, 1-y, 2-z ; (ii) 1-x, y, 5/2-z ; (iii) 1/2+x, 1/2-y, 1/2+z ; (iv) 2-x, -y, 2-z ; (v) x, 1-y, -1/2+z.

It is interesting to note that the tosyl oxygen atoms make intermolecular C–H···O interactions in **13**, **15** and Form-I crystals of **14**, whereas in Form-II of **14** tosyl oxygen is only involved in dipolar S═O···C═O contacts. This can be viewed as competition between the weak hydrogen bonding interactions as well as dipolar S═O···C═O contacts in the molecular recognition process to yield polymorphs for **14**. The former contacts favored in the formation of Form-I crystals of **14**, whereas the

later preferred results in Form-II crystals of **14**. Also, significant conformational differences were observed for **15** and Form-II crystals of **14** indicating the influence of weaker non-covalent interactions in modifying the overall molecular conformation during crystal growth.

### 3.4. Conclusions

Conformationally flexible tosyl group can adopt different conformations as seen in crystal structures of **13**, **14** and **15**. The different orientations of the tosyl group are possible due to the free rotation around *S–O* bond resulting in different patterns of weak intra as well as intermolecular interactions. Only **14** exhibited conformational dimorphism, the two distinct conformations are similar to structures of **13** and **15**. However, the Form-II crystals of **14** revealed intramolecular dipolar S═O···C═O interactions, whereas a slight orientational difference (~ 5º) changes these contacts to intramolecular π···π contacts in **15**. It is noteworthy that the interplay of different intra and intermolecular weak interactions could alter the conformation of flexible molecules significantly, observed in many pharmaceutical compounds.[30]

# Chapter 4

## Isostructural Molecular Strings *via* Conserved Dipolar O···C═O Contacts in Conformational Polymorphs of Racemic 2,4-Di-*O*-Acetyl- 6-*O*-Tosyl *myo*-Inositol 1,3,5-Orthoesters

# Chapter 4

## 4.1. Introduction

Isostructurality implies the similarity in the crystal structures of different compounds, on the other hand polymorphism means the existence of different crystal structures of the same compound. These two phenomena represent the two ends of the structural property. However, fascinating cases of polymorphs which lie between these extremes having one- and two-dimensional isostructurality have been reported by Kálmán *et al*. recently.[116] Ofcourse in the strict sense, conformational polymorphs cannot have isostructurality because of the different molecular conformations.[117] But, the present chapter describe interesting examples of the existence of isostructural molecular chains (despite the difference in the orientation of the tosyl group) associated *via* weak O···C=O dipolar interactions in the dimorphs of two *myo*-inositol derivatives.

As seen in *Chapter 3*, relatively less conformational freedom because of the bulky benzoyl groups in racemic 2,4-di-*O*-benzoyl-6-*O*-tosyl *myo*-inositol 1,3,5-orthoesters resulted in conformational polymorphs only for orthoacetate (**14**) derivative. The acetyl derivatives (**16**, **17** and **18**) were prepared and investigated to see if more rotational freedom for the tosyl group would yield conformational polymorphs. Thus, racemic 2,4-di-*O*-acetyl-6-*O*-tosyl-*myo*-inositol 1,3,5-orthoesters (**16**, **17** and **18**) were synthesized from the corresponding benzoates [Scheme 4.1]. As anticipated, conformational polymorphism was indeed observed for both **16** and **17**.

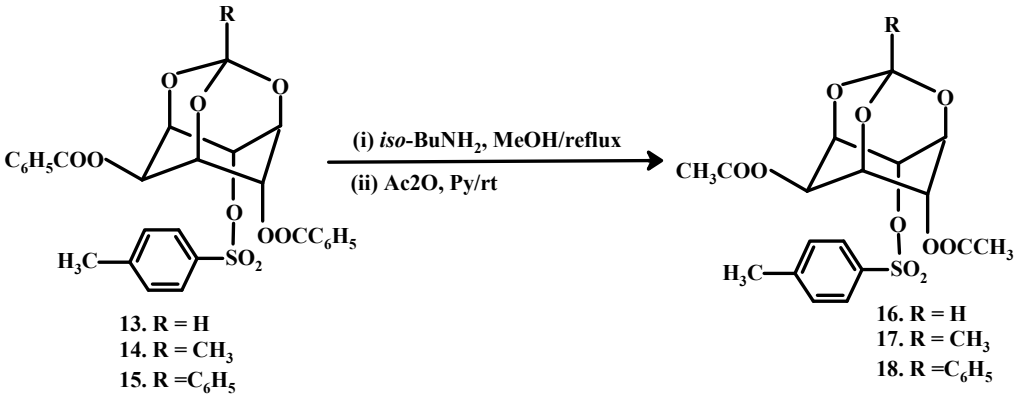


**13. R = H**
**14. R = $CH_3$**
**15. R = $C_6H_5$**

**16. R = H**
**17. R = $CH_3$**
**18. R = $C_6H_5$**

**Scheme 4.1**

## 4.2. Experimental section

### *4.2.1. Synthesis*

*4.2.1.1. Preparation of 2,4-di-O-acetyl-6-O-tosyl myo-inositol 1,3,5-orthoformate*(**16**)

Racemic 2,4-di-*O*-benzoyl-6-*O*-tosyl *myo*-inositol 1,3,5-orthoformate (0.552 g, 1 mmol) was heated with *iso*-butylamine (5 mL) in methanol (8 mL) under reflux for 5 h. The residue obtained after removal of volatile liquids was dissolved in pyridine (2 mL) and cooled to 0 °C; a solution of acetic anhydride (3 mL, 3.15 mmol) in pyridine (1 mL) was added drop wise, and the mixture stirred for 24 h at ambient temperature. The solvents were evaporated from the reaction mixture under reduced pressure and the residue obtained was worked up with ethyl acetate. The diacetate **16** was obtained as a colorless solid (0.410 g, 96 %) after column chromatography using ethyl acetate-petroleum ether (3:7) mixture as eluent.

Data for **16**:

**M.P.**: 119-121°C

**IR ($CHCl_3$)ν**: 1712 $cm^{-1}$

**$^1$H NMR (200 MHz, $CDCl_3$)**: **δ** 2.10 (s, 3H, MeCO), 2.25 (s, 3H, MeCO), 2.50 (s, 3H, ArMe), 4.15-4.25 (m, 1H, Ins H), 4.30-4.40 (m, 1H, Ins H), 5.55-4.65 (m, 1H, Ins H), 5.00-5.15 (m, 1H, Ins H), 5.20-5.30 (d, *J* =6.0 Hz, 1H, Ins H), 5.40-5.50 (m, 1H,

Ins H), 5.55 (d, *J* = 1.5 Hz, $O_3CH$), 7.40 (d, *J* = 4.0 Hz, 2H, Ar H), 7.76 (d, *J* = 4.2 Hz, 2H, ArH) ppm.

**$^{13}$C NMR (50 MHz, $CDCl_3$)**: **δ** 20.3, 20.6, 21.4, 62.3, 66.2, 66.7, 68.8, 71.8, 102.5, 127.6, 129.9, 132.0, 145.5, 169.2, 169.8 ppm.

**Anal. Calcd for $C_{18}H_{20}O_{10}S$**: C, 50.46; H, 4.71; Found: C, 50.43; H, 4.40 %.

*4.2.1.2. Preparation of 2,4-di-O-acetyl-6-O-tosyl myo-inositol 1,3,5-orthoacetate* (**17**)

The racemic diacetate **17** was prepared as above from the racemic 2,4-di-*O*-benzoyl-6-*O*-tosyl *myo*-inositol 1,3,5-orthoacetate (0.566 g, 1 mmol), using *iso*-butylamine (5 mL), methanol (8 mL), pyridine (3 mL) and acetic anhydride (4 mL, 4.20 mmol). The crude product was column chromatographed (eluent: ethyl acetate-petroleum ether 2:8) to isolate **17** as a colorless solid (0.415 g, 94 %).

Data for **17**:

**M.P.**: 138-139 °C

**IR** ($CHCl_3$)**ν**: 1747 $cm^{-1}$ (C=O)

**$^1$H NMR** (200 MHz, $CDCl_3$): **δ** 1.45 (s, 3H, $O_3CMe$), 2.09 (s, 3H, MeCO), 2.18 (s, 3H, MeCO), 2.47 (s, 3H, ArMe), 4.15-4.21 (m, 1H, Ins H), 4.29-4.35 (m, 1H, Ins H), 4.47-4.53 (m, 1H, Ins H), 4.97-5.03 (m, 1H, Ins H), 5.16 (t, *J* = 3.6 Hz, 1H, Ins H), 5.38-5.44 (m, 1H, Ins H), 7.39 (m, 2H, Ar H), 7.81 (m, 2H, Ar H) ppm.

**$^{13}$C NMR** (50 MHz, $CDCl_3$): **δ** 20.6, 21.0, 21.6, 23.8, 61.7, 66.6, 66.9, 69.6, 69.8, 72.3, 109.0, 128.0, 130.2, 132.3, 145.8, 169.7, 170.2 ppm.

**Anal. Calcd for $C_{19}H_{22}O_{10}S$**: C, 51.58; H, 5.01. Found: C, 51.71; H, 4.92 %.

*4.2.1.3. Preparation of 2,4-di-O-acetyl-6-O-tosyl myo-inositol 1,3,5-orthobenzoate* (**18**)

The racemic diacetate **18** was prepared as above from the racemic 2,4-di-*O*-benzoyl-6-*O*-tosyl *myo*-inositol 1,3,5-orthobenzoate (0.628 g, 1 mmol), using *iso*-butylamine (5 mL), methanol 8 mL), pyridine (4 mL) and acetic anhydride (4 mL,

4.20 mmol). The crude product was flash column chromatographed (eluent: ethyl acetate-petroleum ether 2:8) to isolate **18** as a colorless gum (0.470 g, 93 %).

Data for **18**:

**M.P.**: 57-59 °C

**IR** ($CHCl_3$)**ν**: 1759 $cm^{-1}$(C=O)

**$^1$H NMR** (200 MHz, $CDCl_3$): **δ** 2.13 (s, 3H, MeCO), 2.18 (s, 3H, MeCO), 2.47 (s, 3H, ArMe), 4.35-4.41 (m, 1H, Ins H), 4.48-4.54 (m, 1H, Ins H), 4.66-4.72 (m, 1H, Ins H), 5.13-5.19 (m, 1H, Ins H), 5.28 (t, *J* = 1.8 Hz, 1H, Ins H), 5.55-5.61 (m, 1H, Ins H), 7.32-7.44 (m, 5H, Ar H), 7.55-7.63 (m, 2H, ArH) 7.83 (m, 2H, ArH) ppm.

**$^{13}$C NMR** (50 MHz, $CDCl_3$): **δ** 20.6, 20.9, 21.6, 61.8, 67.0, 67.3, 70.3, 70.5, 72.3, 107.7, 125.3, 128.0, 128.1, 129.9, 130.2, 132.2, 135.8, 145.8, 169.7, 170.3 ppm.

**Anal. Calcd for $C_{24}H_{24}O_{10}S$**: C, 57.14; H, 4.79. Found: C, 56.95; H, 4.80 %.

### *4.2.2. Crystallization*

Crystallization was carried out by diffusing vapors of light petroleum ether to a solution of **16** and **17** in common organic solvents such as acetone, dichloromethane, ethyl acetate, dioxane, nitromethane yielded plate like crystals of **16** and **17** (Form-I) at room temperature. However, thin flat crystals of **16** were obtained from chloroform (Form-II of **16**) and similar crystals were seen for **17** from tetrahydrofuran (Form-II of **17**). The crystallization of the orthobenzoate **18** from various solvents resulted in gummy solids.

### *4.2.3. Thermal Analysis*

Differential Scanning Calorimetry (DSC) analysis was performed on TA DSC instrument for the Form I and II crystals of **16** and **17**. About 3-6 mg of the crystalline samples were placed in an aluminium pan and heated from 40 to 150 °C at a rate of 1°C/minute. An empty pan was used as the reference and dry nitrogen used for purging (50 mL/min). The DSC curves of Form-I crystals **16** and **17** showed two

sharp endothermic peaks, the first endotherm (at 112°C for Form-I of **16** and 134°C for Form-I of **17**) indicated the probable structural phase transformation, whereas the second endotherm is attributed to the melting of the crystal. The DSC plot of Form-II crystals of **16** and **17** showed only one endothermic peak corresponding to their melting point [Fig. 4.1].

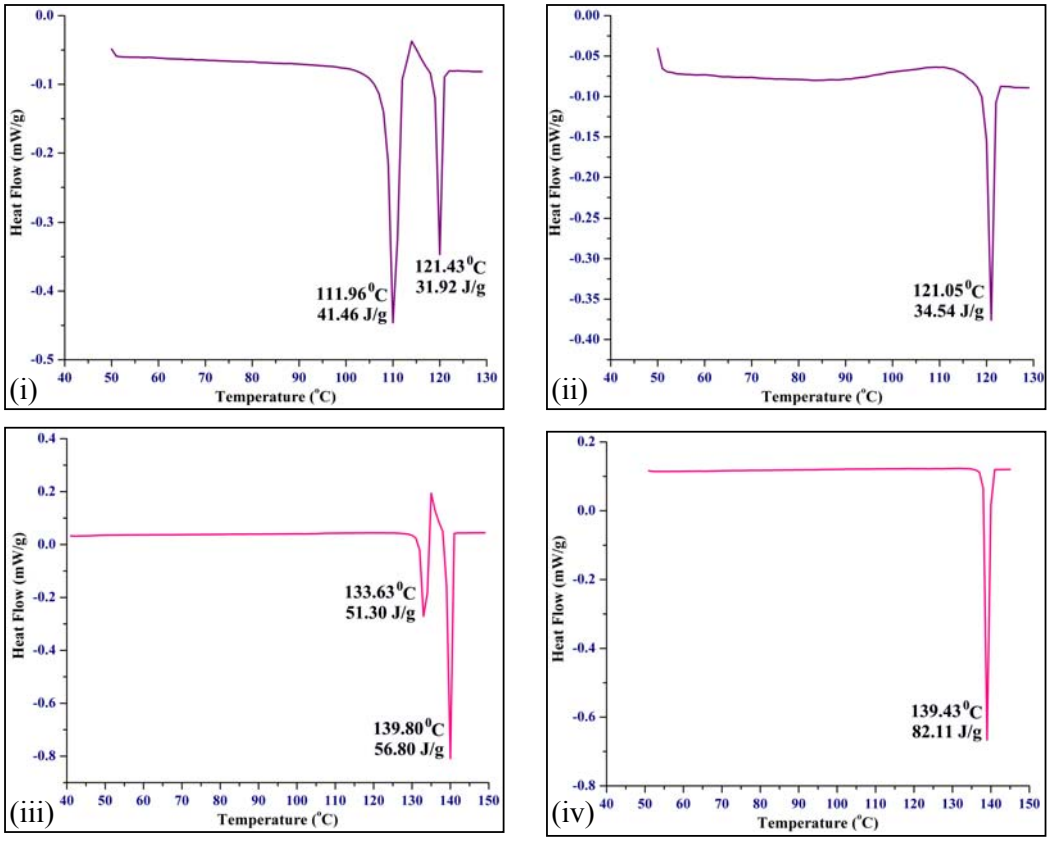


**Figure 4.1**: DSC plot of (i) Form-I of **16**, (ii) Form-II of **16**, (iii) Form-I of **17** and (iv) Form-II of **17** crystals.

### *4.2.4. Hot Stage Microscopy*

The DSC results as described above, prompted us to carry out Hot Stage Microscopic (HSM) analysis for Form-I crystals of **16** and **17**. The Form-I crystal of **16** was heated from the room temperature at the rate of 1ºC per minute. The crystals started melting slowly ~ 110ºC and further heating showed the formation of thin

needle shaped crystals in the melt ~111.8 ºC. On continuing the heating resulted in the gradual growth of thin needles, which melted completely ~121 ºC [Fig. 4.2]. However, Form-I crystals of **17** when heated on the HSM did not show any discrete phase change until melting. The first and second endotherms are closer in **17** (133ºC and 139ºC) as compared to those in **16** (111ºC and 121ºC). Therefore, it is possible that the HSM experiments could not capture the transformed phase in case of **17**.

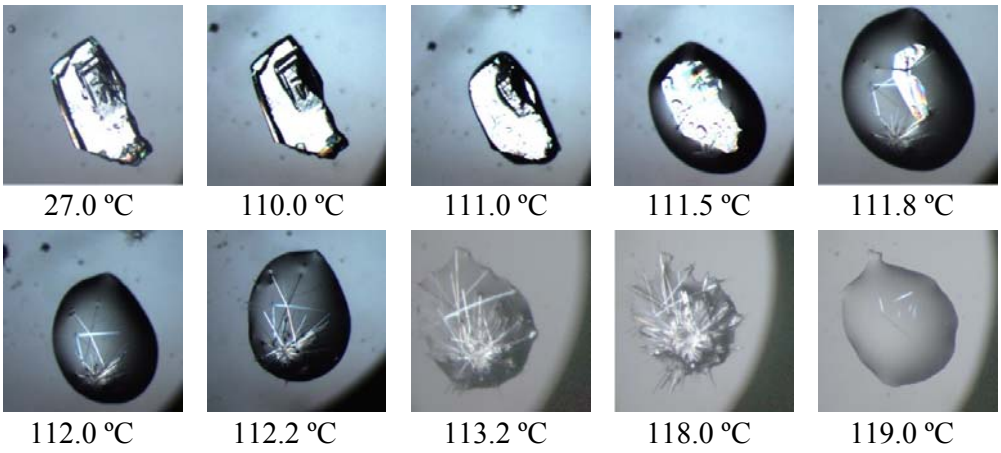


**Figure 4.2**: Hot stage photomicrographs of Form-I crystals of **16**.

### *4.2.5. Crystallographic Details for the dimorphs of 16 and 17*

X-ray intensity data were collected on a Bruker SMART APEX CCD diffractometer in omega and phi scan mode, $\lambda_{MoK\alpha}$ = 0.71073 Å at room temperature. All the intensities were corrected for Lorentzian, polarization and absorption effects using Bruker's *SAINT* and *SADABS* programs. The crystal structures were solved by Direct methods using program SHELXS-97; the full-matrix least squares refinements on $F^2$ were carried out by using SHELXL-97. Hydrogen atoms were included in the refinement as per the riding model. Table 4.1 summarizes the crystal data for all the compounds.

**Table 4.1**: Summary of crystallographic data for dimorphs of **16** and **17**.

| Crystal data | Form-I of **16** | Form-II of **16** | Form-I of **17** | Form-II of **17** |
|---|---|---|---|---|
| Chemical Formula | $C_{18}H_{20}O_{10}S$ | $C_{18}H_{20}O_{10}S$ | $C_{19}H_{22}O_{10}S$ | $C_{19}H_{22}O_{10}S$ |
| $M_r$ | 428.40 | 428.40 | 442.43 | 442.43 |
| Temperature/K | 298(2) | 298(2) | 298(2) | 298(2) |
| Morphology | Plate | Thin plate | Flat | Thin plate |
| Colour | Colorless | Colorless | Colorless | Colorless |
| Crystal size (mm) | 0.62 × 0.26 × 0.16 | 0.28 × 0.16 × 0.02 | 0.55 × 0.14 × 0.13 | 0.53 × 0.15 × 0.04 |
| Crystal system | Monoclinic | Orthorhombic | Triclinic | Monoclinic |
| Space group | $P2_1/c$ | *Pbca* | *P*-1 | $P2_1/c$ |
| *a* (Å) | 16.4270(17) | 6.206(2) | 6.2596(8) | 9.2713(11) |
| *b* (Å) | 6.1377(6) | 14.602(5) | 9.8947(12) | 35.728(4) |
| *c* (Å) | 19.2741(19) | 42.099(13) | 17.022(2) | 6.1772(8) |
| $\alpha$ (°) | 90 | 90 | 87.723(2) | 90 |
| $\beta$ (°) | 91.317(2) | 90 | 89.460(2) | 90.872(2) |
| $\gamma$ (°) | 90 | 90 | 76.195(2) | 90 |
| *V* (Å$^3$) | 1942.8(3) | 3815(2) | 1023.0(2) | 2045.9(4) |
| *Z* | 4 | 8 | 2 | 4 |
| $D_x$ (Mg m$^{-3}$) | 1.465 | 1.492 | 1.436 | 1.436 |
| $\mu$ (mm$^{-1}$) | 0.222 | 0.226 | 0.213 | 0.213 |
| *F(000)* | 896 | 1792 | 464 | 928 |
| $T_{min}$ | 0.875 | 0.940 | 0.892 | 0.895 |
| $T_{max}$ | 0.965 | 0.996 | 0.973 | 0.992 |
| $\theta_{max}$ (°) | 25.0 | 25.0 | 25.0 | 25.1 |
| *h* (min, max) | (-19, 19) | (-7, 7) | (-7, 7) | (-11, 11) |
| *k* (min, max) | (-7, 7) | (-17, 17) | (-11, 11) | (-42, 42) |
| *l* (min, max) | (-22, 22) | (-50, 50) | (-20, 20) | (-7, 7) |
| No. of refl$^n$ collected | 13355 | 17512 | 9894 | 19352 |
| No. of unique refl$^n$ | 3422 | 3352 | 3610 | 3621 |
| No. of observed refl$^n$ | 3062 | 1379 | 3110 | 2319 |
| No. of parameters | 265 | 265 | 275 | 275 |
| $R_{int}$ | 0.021 | 0.193 | 0.019 | 0.085 |
| $R_1$_obs, $R_1$_all | 0.040, 0.045 | 0.075, 0.208 | 0.044, 0.051 | 0.084, 0.133 |
| $wR_2$_obs, $wR_2$_all | 0.103, 0.106 | 0.141, 0.185 | 0.114, 0.119 | 0.140, 0.149 |
| GoF | 1.05 | 1.00 | 1.06 | 1.20 |
| $\Delta\rho_{max}$, $\Delta\rho_{min}$ (e Å$^{-3}$) | 0.23, –0.25 | 0.30, –0.23 | 0.35, –0.24 | 0.27, –0.19 |

### *4.2.6. Computational Studies*

Single point *ab initio* energy calculation on dimorphs of **16** and **17** were performed using the 'Gaussian 03' suite of programs.[122] In each case, energies of isolated molecules were computed with the *Hartree-Fock* theory at the 6-31G*(d,f)* level, so that the data obtained relates to the intrinsic conformational preferences without accounting the effect of intermolecular interactions.

## 4.3. Results and Discussion

As mentioned earlier, **16** and **17** crystallized in two different forms but all attempts to obtain crystals of **18** failed. Crystallization of **16** from most of the solvents yielded monoclinic crystals (Form-I, $P2_1/c$) but crystals from chloroform-petroleum ether mixture were orthorhombic (Form-II, *Pbca*). Similarly triclinic crystals (Form-I, *P*-1) of **17** were obtained from most of the organic solvents while diffusing vapors of petroleum ether into a THF solution of **17** yielded monoclinic needles (Form-II, $P2_1/c$). As seen in the polymorphs of the dibenzoate (**14** in *Chapter 3*), the dimorphs of acetates **16** and **17** differ mainly in the orientation of tosyl group along *O–S* bond [Fig. 4.3]. A major orientational change of tosyl group was observed for the dimorphs of **16** [*C–O–S–C* torsion angles 86º and 142º], whereas only a slight change in the conformation of **17** [81º and 84º] resulted in polymorphic modification [*see molecular overlap figure of dimorphs*, Fig. 4.3]. It is rather intriguing that conformation of the tosyl group in Form-I crystals of **16** and Forms I and II of **17** belongs to the preferred orientation of tosyl group as suggested by the CSD analysis [*Chapter 3*, page no. 90], whereas orientation adopted by the tosyl group in Form-II crystals of **16** is the less preferred one. As observed in case of **14** [*Chapter 3*, page no. 89], this less probable conformation showed stabilization *via* intramolecular S═O···C═O short contacts in Form-II crystals of **16** also [Fig. 4.3(ii)]. The geometrical parameters of dipolar S═O···C═O short contacts [O10···C10 = 3.040 (8) Å, O10···C10═O8 = 96.2 (4)º and

S1═O10···C10 = 118.8 (4)º] in **16.2** crystals indicated the interaction motif is of the Type-III *i.e.* sheared parallel motif.[112]

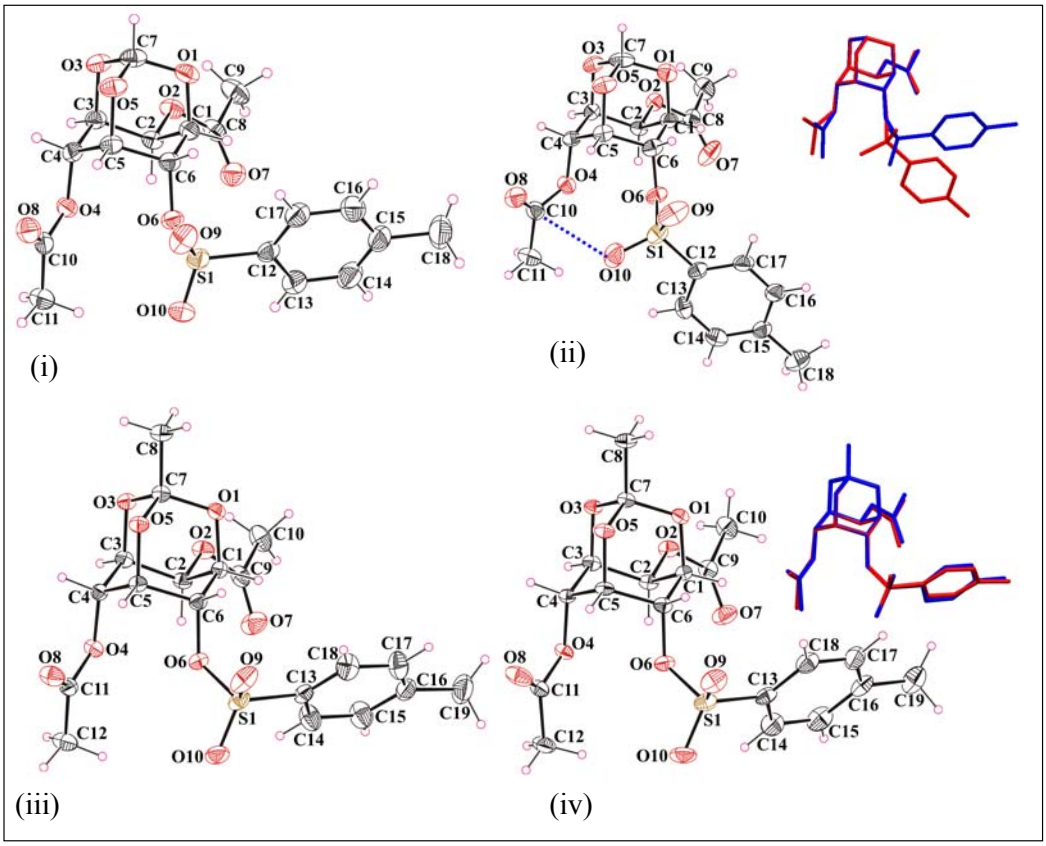


**Figure 4.3**: ORTEP view of dimorphs of (i) Form-I of **16**, (ii) Form-II of **16** [blue dashed line indicates intramolecular S═O···C═O short contact], (iii) Form-I of **17** and (iv) Form-II of **17** with atom numbering scheme, displacement ellipsoids drawn at 30% probability level. Inset shows molecular overlapping plot of dimorphs [color scheme, blue: Form-I and red: Form-II crystals].

The single point energy calculation of Form-I crystals of **16** was found to be ~ 9 kJ/mol lower than that of Form-II, could be due to the larger orientational change of the tosyl group. However, slight conformational changes (3º) in dimorphs of **17** have a relatively smaller energy difference (~ 2 kJ/mol).

### *4.3.1. Conserved One-Dimensional Isostructurality via O···C=O Interactions*

Although the diacetate molecules **16** and **17** have different orientation of tosyl group in their dimorphic modifications, an interesting common feature observed is the identical intermolecular association *via* dipolar O···C=O interactions between the orthoester ether oxygen (O1) and the equatorial carbonyl carbon (C8) [Fig. 4.4, Table 4.2] to form 1D molecular chains. The molecules in these chains are also linked *via* C3–H3···O5 interactions having better geometry in Form-I crystals of **16**, **17** and Form-II crystals of **17** as compared to that in Form-II crystals of **16** [Table 4.3]. Additionally, the molecules of **17** make C8–H8*B*···O2, C10–H10*C*···O1 and C18–H18···O7 interactions that are longer in Form-I crystals as compared to Form-II crystals of **17**. It is noteworthy that the Form-I crystals of **16** and Form-II crystals of **17** make similar C–H···O interactions involving the *C2*-benzoyl oxygen (O7) with the tosyl aromatic proton (H17 in Form-I of **16** and H18 in Form-II of **17**), whereas these interactions are longer in other two forms [Table 4.3].

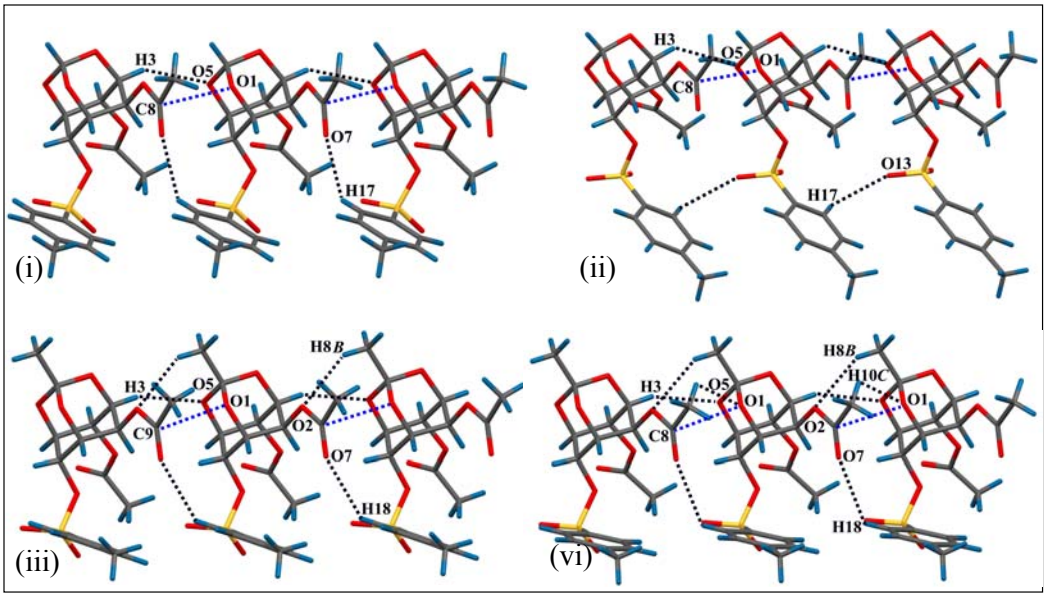


**Figure 4.4**: Identical molecular chain formation *via* O···C=O and C–H···O interactions in (i) Form-I of **16**, (ii) Form-II of **16**, (iii) Form-I of **17** and (iv) Form-II of **17**crystals.

**Table 4.2**: Geometrical parameters of O···C═O interactions as shown in figure 4.4.

| Crystals | O···C═O | O···C (Å) | O···C═O (º) |
|---|---|---|---|
| Form-I of **16** | O1···C8═O7 [i] | 2.968(2) | 98.2 |
| Form-II **16** | O1···C8═O7 [ii] | 3.080(7) | 94.1 |
| Form-I of **17** | O1···C9═O7 [ii] | 3.162(3) | 98.1 |
| Form-II of **17** | O1···C9═O7 [iii] | 3.150(5) | 97.7 |

Symmetry codes: (i) x, y+1, z; (ii) x+1, y, z; (iii) x, y, z+1

**Table 4.3**: Geometrical parameters for hydrogen bonding interactions (Fig. 4.4).

| Crystals | D–H···A | D–H (Å) | H···A (Å) | D···A (Å) | D–H···A (°) |
|---|---|---|---|---|---|
| Form-I of **16** | C3–H3···O5 [i] | 0.98 | 2.58 | 3.367(2) | 138 |
| | C17–H17···O7 [ii] | 0.93 | 2.68 | 3.217(3) | 118 |
| Form-II of **16** | C3–H3···O5 [iii] | 0.98 | 2.75 | 3.497(7) | 134 |
| | C13–H13···O9 [iii] | 0.93 | 2.75 | 3.164(8) | 108 |
| Form-I of **17** | C3–H3···O5 [iv] | 0.98 | 2.64 | 3.540(2) | 154 |
| | C8–H8*B*···O2 [iii] | 0.96 | 2.77 | 3.628(3) | 150 |
| | C18–H18···O7 [iii] | 0.93 | 2.75 | 3.359(4) | 124 |
| Form-II of **17** | C3–H3···O5 [v] | 0.98 | 2.54 | 3.448(4) | 153 |
| | C8–H8*B*···O2 [vi] | 0.96 | 2.71 | 3.567(5) | 148 |
| | C10–H10*C*···O1 [v] | 0.96 | 2.61 | 3.286(5) | 128 |
| | C18–H18···O7 [vi] | 0.93 | 2.67 | 3.402(6) | 136 |

Symmetry codes: (i) x, y+1, z; (ii) x, y-1, z; (iii) x+1, y, z; (iv) x-1, y, z; (v) x, y, z+1; (vi) x, y, z-1.

The superimposition of the molecular chains in the conformational polymorphs clearly indicates the isostructurality in one-dimension except for the orientation of tosyl group [Fig. 4.5]. The tosyl groups in these chains are involved in different C–H···O interactions which perhaps adopted different conformations in their dimorphic crystals.

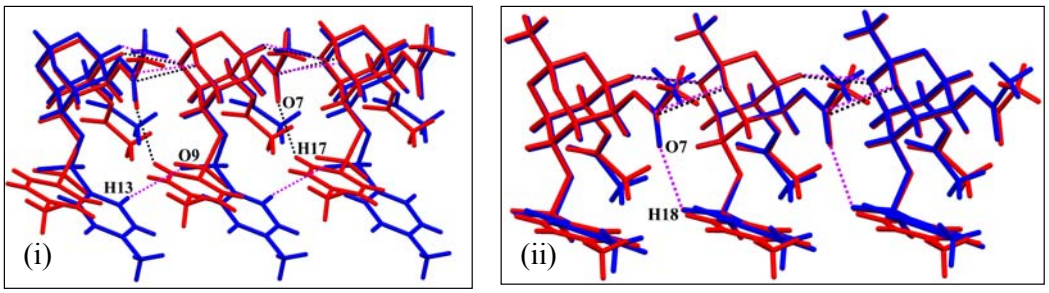


**Figure 4.5**: Molecular overlap figure of (i) dimorphs of **16** [ red: Form-I; blue: Form-II] and (ii) dimorphs of **17** [ red: Form-I; blue: Form-II].

### *4.3.2. CSD Survey of Dipolar (ether)O···C═O Interaction*

It is remarkable to see that the molecular association *via* (ether)O···C═O interactions is retained in both the dimorphic modifications of the orthoester derivatives **16** and **17**. This brings out the significance of the O···C═O contacts in the aggregation of molecules, irrespective of different substitutions in the orthoester position or even change in molecular conformation. In order to investigate these dipolar interactions more, a survey of the Cambridge Structural Database [CSD, Version 5.29][78] was carried out to see the geometrical preferences for the (ether)O···C═O intermolecular interactions. All the searches were carried out for organic compounds with geometrical parameters cut-off value of less than 3.22 Å (sum of the van der Waals radii of carbon and oxygen) for inter atomic distance (*D*) and angle (*A*) ranging 0-180°. The filters were used to restrict entries of *R*-factor <0.10, error-free co-ordinates, disordered, ionic, polymeric and X-ray powder diffraction structures. Interestingly, a sizable number of hits (790) was found and majority of hits (575) were between 80-100° [Fig. 4.6], indicating the preferred perpendicular approach of oxygen to the carbonyl carbon [Type-II motif].[78] The observed molecular association *via* (ether)O···C═O interactions of dimorphs of **16** and **17** showed the same preferences [94-98°]. However, the optimum angle for the approach of a nucleophile (O or N) to an electrophile (C═O) during chemical reaction

has been suggested to be ~107°.[123] It is also reported in the literature that the energy contribution of such dipolar interactions were similar to that of weak hydrogen bonding.[96]

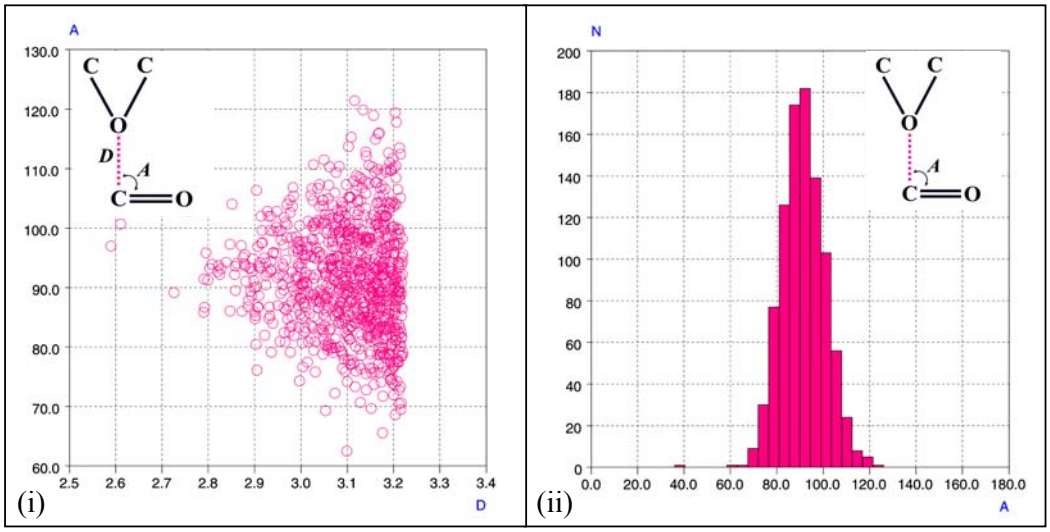


**Figure 4.6**: CSD analysis of (ether) O···C═O interactions (i) scatter plot of distance O···C [*d* in Å] *vs*. angle O···C═O [*A* in °] (ii) histogram of angle O···C═O, *A*.

### *4.3.3. Molecular Organization in Dimorphs of 16 and 17*

It is interesting to see how these isostructural molecular strings link differently in the crystal lattice. In Form-I crystals of **16**, the identical molecular strings make centrosymmetric head to head C7–H7···O3 interaction to form a bilayer [Fig. 4.7(i)]; whereas in Form-II crystals of **16**, the identical strings are linked in a head to head fashion by the same C–H···O interactions but *via* $2_1$-screw axis relationship [Fig. 4.7(ii)]. Almost similar bilayer formation is observed for Forms I and II crystals of **17** with centrosymmetric and $2_1$-screw relation respectively, linking the strings *via* C8–H8*C*···O8 and C12–H12*C*···O8 interactions [Fig. 4.7(iii) and (iv)]. The strings in Form-II crystals of **16** make additional binding *via* C9–H9*C*···O1 interaction and *via* C4–H4···O5, dipolar C11═O8···C11═O8 interactions in Form-II crystals of **17**.

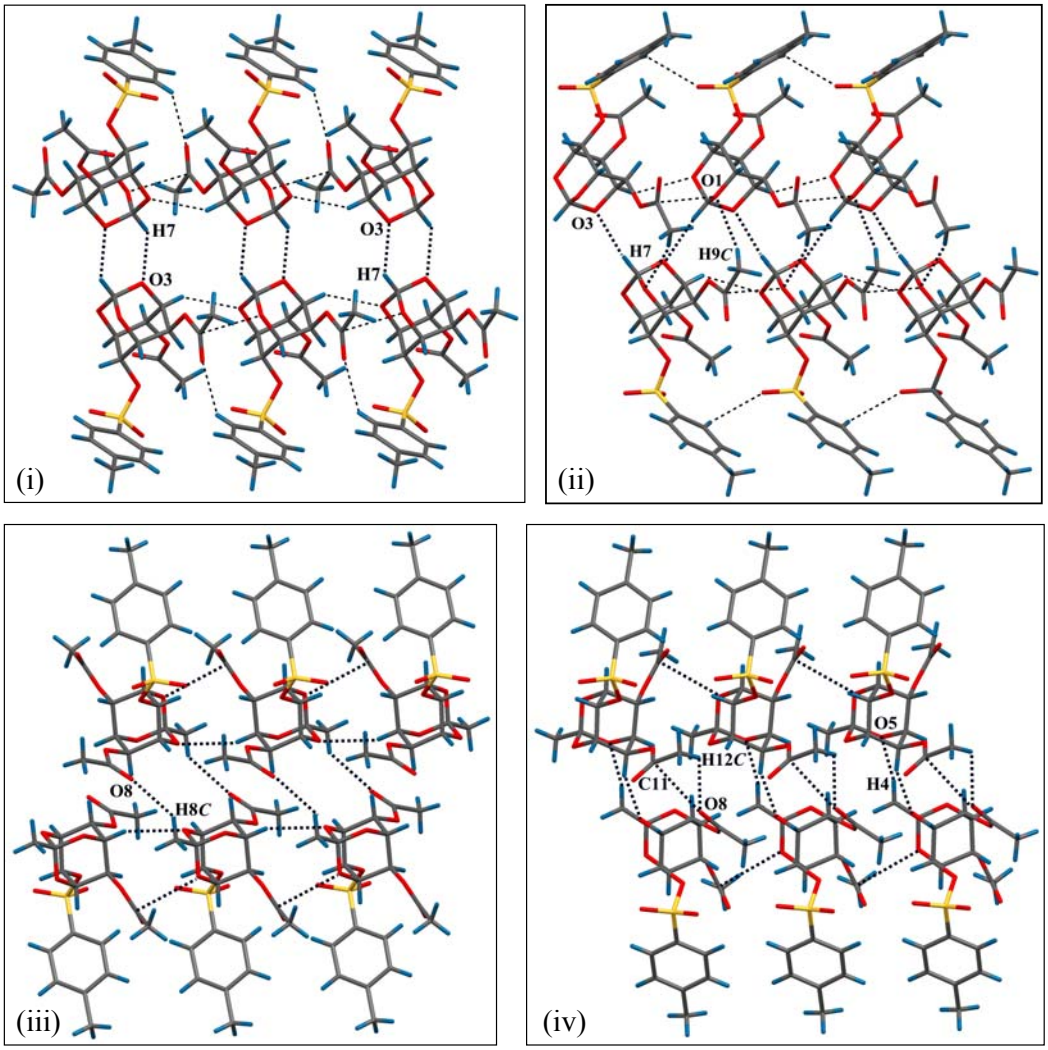


**Figure 4.7**: Head to head molecular bilayer formation *via* C–H···O and O···C═O interactions in (i) Form-I crystals of **16**, (ii) Form-II crystals of **16**, (iii) Form-I crystals of **17** and (iv) Form-II crystals of **17**.

These bilayers are linked to the *ac*-plane *via* C18–H18*A*···O10 interaction in Form-I crystals of **16**, along *c*-axis *via* weak C14–H14···π (Cg) interaction in Form-II crystals of **16**, along *c*-axis *via* centrosymmetric C15–H15···O10 interaction in Form-I crystals of **17** and *via* centrosymmetric C19–H19*B*···O7 interaction along *b*-axis in Form-II crystals of **17** [Fig. 4.8, Table 4.4].

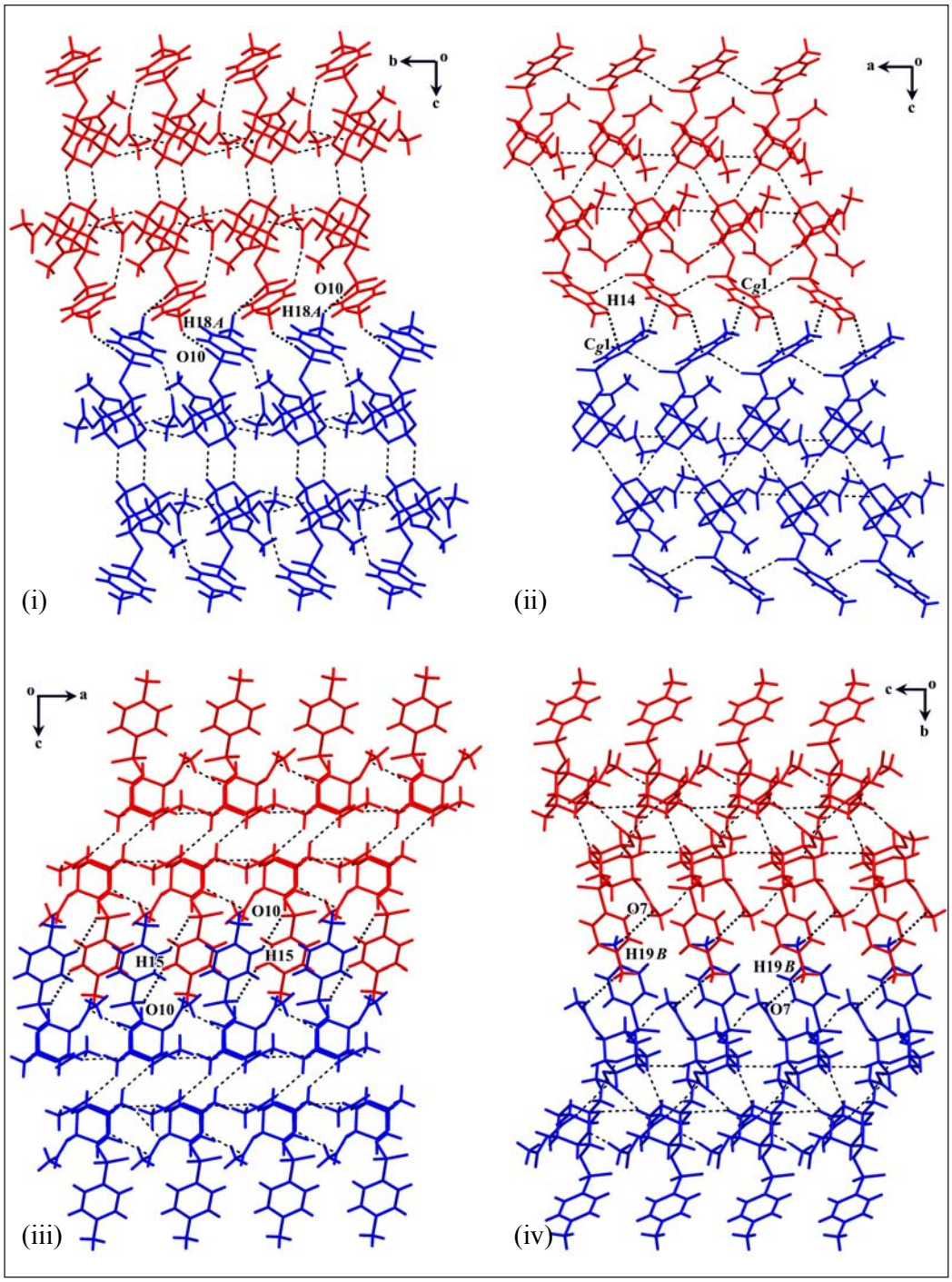


**Figure 4.8**: Molecular layer formation in (i) Form-I crystals of **16**, (ii) Form-II crystals of **16**, (iii) Form-I crystals of **17** and (iv) Form-II crystals of **17**.

**Table 4.4**: Hydrogen bonding interactions as shown in figures 4.7 and 4.8.

| Crystals | D–H···A | D–H (Å) | H···A (Å) | D···A (Å) | D–H···A (°) |
|---|---|---|---|---|---|
| Form-I of **16** | C7–H7···O3 [i] | 0.98 | 2.58 | 3.393(2) | 141 |
| | C18–H18*A*···O10 [ii] | 0.96 | 2. 86 | 3.478(4) | 123 |
| Form-II of **16** | C7–H7···O3 [iii] | 0.98 | 2.47 | 3.412(7) | 162 |
| | C9–H9*C*···O1 [iv] | 0.96 | 2.79 | 3.717(7) | 163 |
| | C14–H14···Cg1 [v] | 0.93 | 3.209 | 3.938(8) | 137 |
| Form-II of **17** | C8–H8*C*···O8 [vi] | 0.96 | 2.62 | 3.359(3) | 134 |
| | C15–H15···O10 [vii] | 0.93 | 2.80 | 3.515(3) | 134 |
| Form-II of **17** | C4–H4···O5 [ii] | 0.98 | 2.65 | 3.469(4) | 142 |
| | C12–H12*C*···O8 [ii] | 0.96 | 2.66 | 3.195(6) | 116 |
| | C11–O8···C11 [viii] | 1.18 | 3.111(6) | | 95.7, 164.6 |
| | C19–H19*B*···O7 [ix] | 0.96 | 2.91 | 3.720(7) | 143 |

Symmetry codes: (i) -x, -y+1, -z+1; (ii) x, -y+3/2, z+1/2; (iii) x-1/2, y, -z+1/2; (iv) x+1/2, y, -z+1/2; (v) x+1/2, -y+1/2, -z; (vi) -x+2, -y, -z+2; (vii) x+1/2, -y+1/2, -z; (viii) x, -y+3/2, z-1/2; (ix) -x+1, -y+2, -z+1.

These molecular layers are linked differently in the third dimension to achieve close packing in the crystal lattice. In Form-I crystals of **16**, the bilayer [Fig. 4.7] extends along *a*-axis *via* C3–H3···O8 and C9–H9*A*···O10 interactions, whereas in Form-II crystals of **16** these make C16–H16···O10, C1–H1···O8 and C17–H17···O8 interactions along *b*-axis [Fig. 4.9, Table 4.5]. In case of Forms I and II crystals of **17**, bilayers are translated along *b*- and *a*-axis respectively with different orientation of the tosyl group. It is noteworthy that these bilayers have similar orientation of tosyl group in Form-I crystals of **16** and **17** (tosyl group pointing opposite direction) whereas in Form-II crystals of **16** and **17**, the tosyl groups are pointing in the same direction [*see arrows shown in* Fig. 4.9]. As explained earlier, the bilayers translated centrosymmetrically along the third dimension are shown in figure 4.9. It is remarkable to see that centrosymmetric C–H···O interaction between the adjacent

layers through the tosyl groups links the bilayer in **16.1**, **17.1** and **17.2** but the biayers are linked *via* weak C14–H14···π (C*g*) interaction in **16.2** [Table 4.5].

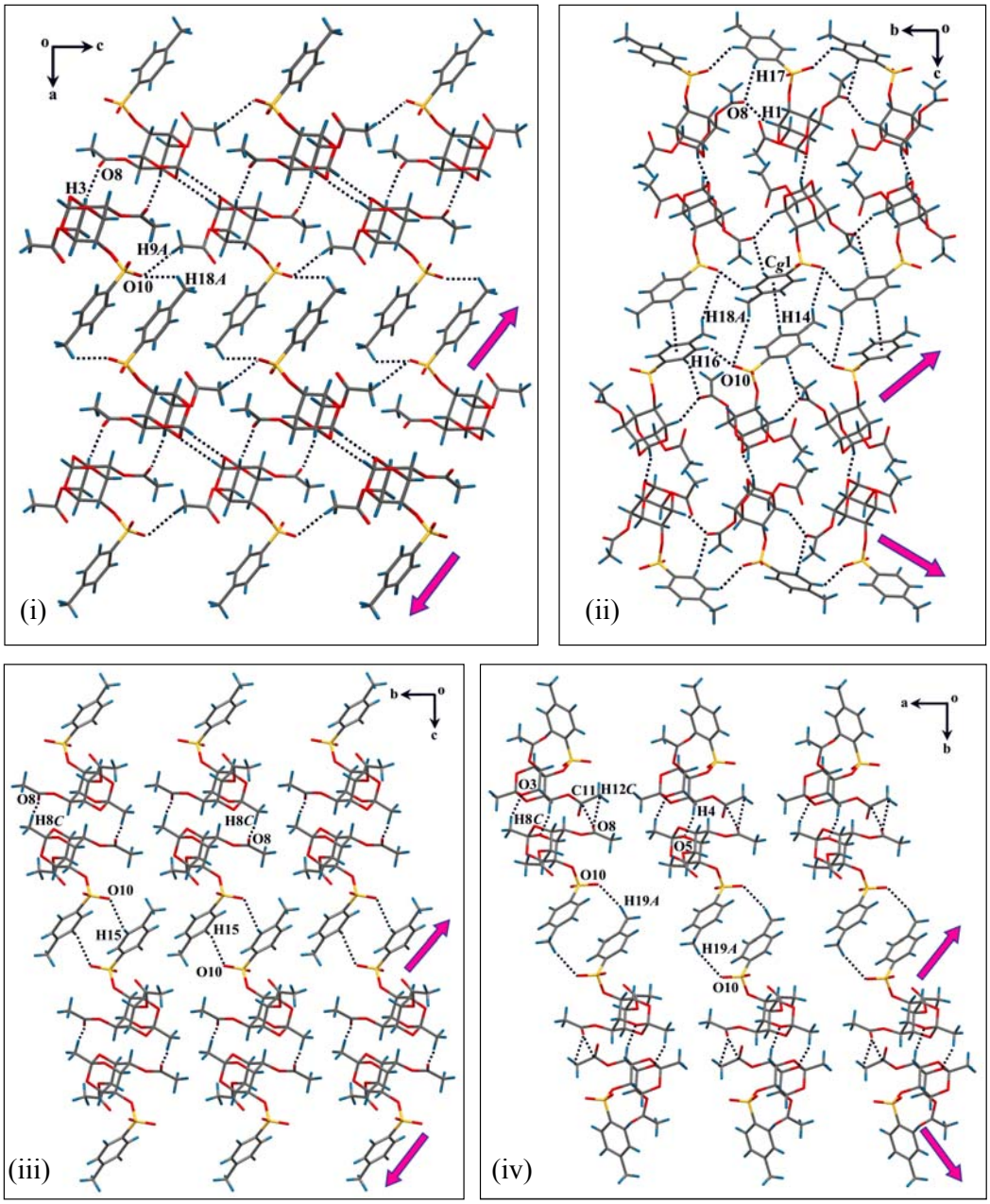


**Figure 4.9**: Molecular layer formation on the third dimension in (i) Form-I crystals of **16**, (ii) Form-II crystals of **16**, (iii) Form-I crystals of **17** and (iv) Form-II crystals of **17**. Arrows indicating the orientation of tosyl group in the bilayer.

**Table 4.5**: Geometrical parameters of hydrogen bonding interactions as shown in figure 4.9.

| Crystals | D–H···A | D–H (Å) | H···A (Å) | D···A (Å) | D–H···A (°) |
|---|---|---|---|---|---|
| Form-I of **16** | C3–H3···O8 [i] | 0.98 | 2.50 | 3.326(2) | 142 |
| | C9–H9A···O10 [ii] | 0.96 | 2.60 | 3.518(3) | 159 |
| | C18–H18A···O10 [iii] | 0.96 | 2. 86 | 3.478(4) | 123 |
| Form-II of **16** | C1–H1···O8 [iv] | 0.98 | 2.47 | 3.224(7) | 134 |
| | C7–H7···O3 [v] | 0.98 | 2.47 | 3.412(7) | 162 |
| | C14–H14···Cg1 [vi] | 0.93 | 3.209 | 3.938(8) | 137 |
| | C16–H16···O10 [iv] | 0.93 | 2.65 | 3.398(8) | 138 |
| | C17–H17···O8 [iv] | 0.93 | 2.68 | 3.311(7) | 126 |
| | C18–H18A···O10 [vii] | 0.96 | 3.03 | 3.894(8) | 150 |
| Form-I of **17** | C8–H8C···O8 [viii] | 0.96 | 2.62 | 3.359(3) | 134 |
| | C15–H15···O10 [ix] | 0.93 | 2.80 | 3.515(3) | 134 |
| Form-I of **17** | C4–H4···O5 [ii] | 0.98 | 2.65 | 3.469(4) | 142 |
| | C8–H8C···O3 [x] | 0.96 | 2.60 | 3.462(5) | 150 |
| | C19–H19A···O10 [xi] | 0.96 | 2.54 | 3.452(6) | 160 |

Symmetry codes: (i) -x, y+1/2, -z+1/2; (ii) x, -y+3/2, z+1/2; (iii) -x+1, y-1/2, -z+1/2; (iv) -x+3/2, y-1/2, z; (v) x-1/2, y, -z+1/2; (vi) 3/2-x, -y, 1/2+z; (vii) x, -y+3/2, z+1/2; (viii) -x+2, -y,-z+2; (ix) x+1/2, -y+1/2, -z; (x) x, -y+3/2, z-1/2; (xi) -x, -y+2, -z+1.

### *4.3.4. Possible Pathways of Nucleation of Polymorphs of 16 and 17*

The common identical molecular strings [Fig. 4.4] are stitched differently, leading to two different paths of nucleation resulting in dimorphs. Although the nucleation process cannot be visualized, we are proposing a probable sequence of events extrapolated from the final observed structures (in the form of a cartoon diagram) that result from the dynamic equilibrium between various weak interactions in solution [Fig. 4.10]. The first step is the formation of one-dimensional strings *via* O···C═O interactions [**Step 1**, then their centrosymmetric [**Step 2i**] and screw related [**Step 2ii**] adhesions *via* C–H···O interactions [also dipolar C═O···C═O contacts in

**17.2**] to form bilayer. These bilayers further extend the crystal lattice *via* C–H···O interactions in **16.1**, **17.1** and **17.2**, whereas *via* C–H···π adhesions in **16.2** [**Steps 3i** and **3ii**].

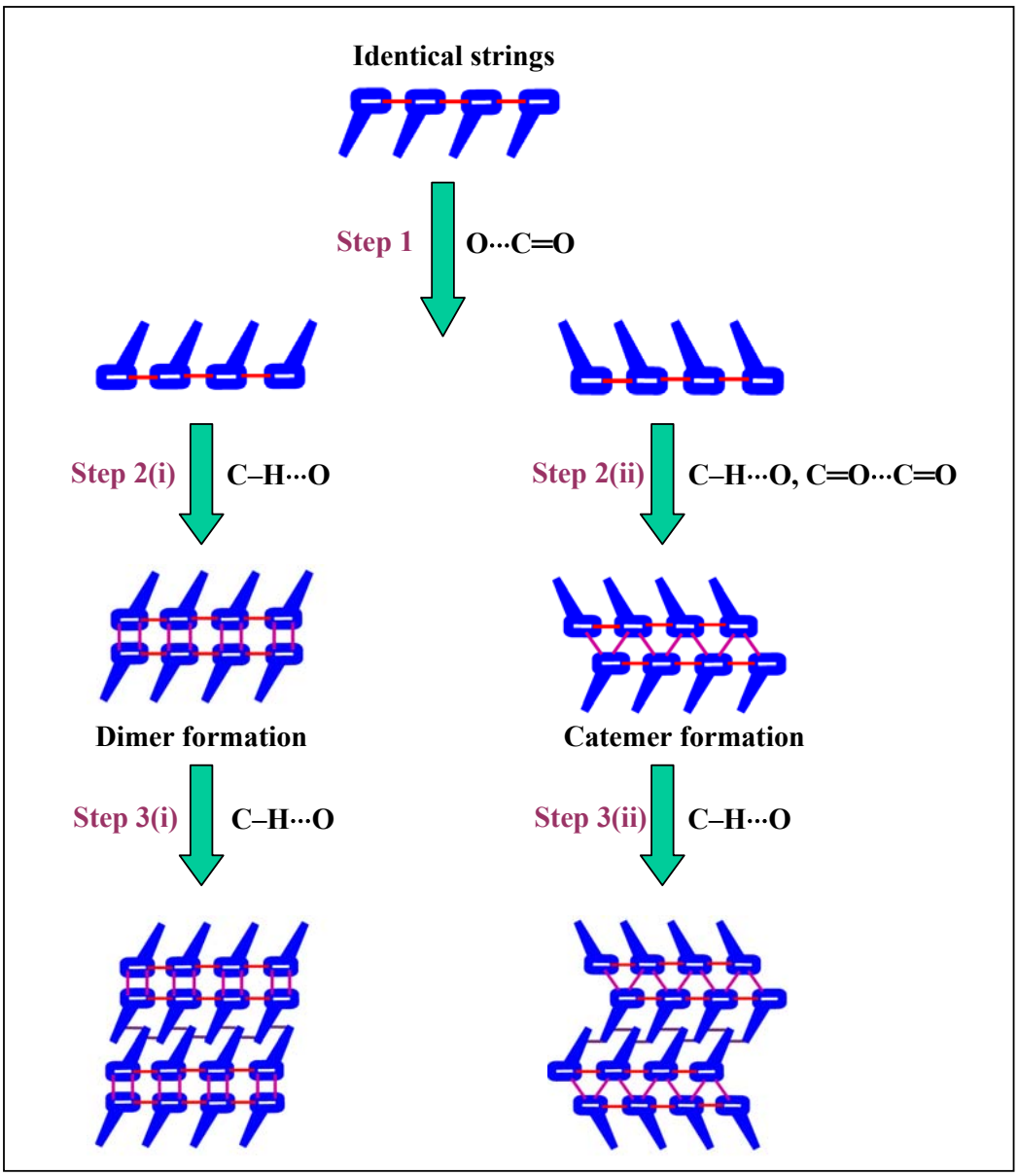


**Figure 4.10**: Cartoon diagram of the proposed pathways of polymorph formation in **16** and **17**.

## 4.4. Conclusions

The sterically smaller substitution of acetyl group, as proposed exhibits dimorphic modification for **16** and **17** having different molecular conformations. All polymorphic crystal forms showed one-dimensional isostructural strings (except tosyl group orientation) in their crystals *via* dipolar O···C═O interactions. The Form-II crystals of **16** adopt an extended conformation, perhaps due to stabilization from the intramolecular S═O···C═O interactions between the tosyl and axial benzoyl group.

# Chapter 5

## Effect of Molecular Conformation on Solvatomorphic Behavior in 2-*O*-Tosyl-4,6-Di-*O*-Acetyl-*myo*-Inositol 1,3,5-Orthoesters

# Chapter 5

## 5.1. Introduction

Many organic compounds exhibit solvatomorphism by including solvent molecules in their crystal lattice. A solvent can be associated with a crystalline solid in different ways. In some inherently stable crystals, small guests are included in their crystal lattice to achieve close packing; whereas in some other cases crystals are stable only in the presence of certain guests.[49] Formation of inclusion crystals involves molecular recognition processes that result from a number of non-covalent interactions during crystallization. It was seen in *Chapter 2*, a slight orientational change of diastereomeric association was enough to produce inclusion crystals of **8**. The present chapter reports structures of three tosylated orthoesters; only the orthoacetate derivative with a different conformation of tosyl group exhibits solvatomorphic behavior that accommodates a range of solvent molecules.

As described in the previous chapters (*Chapter 3* and *4*), the orientational change of tosyl group at the *C6-O6* position of the inositol ring was responsible for the formation of conformational polymorphs in **14**, **16** and **17**. In order to examine the polymorphic behavior of related molecules, racemic 2-*O*-tosyl-4,6-di-*O*-acetyl- *myo*-inositol 1,3,5-orthoesters (**19-21**) having conformationally flexible tosyl group at different (equatorial position, *C2-O-* of inositol), were synthesized [Scheme 5.1]. The tosyl group in **19-21** indeed adopted different orientations in the crystal lattice, but did not yield any conformational polymorphs.

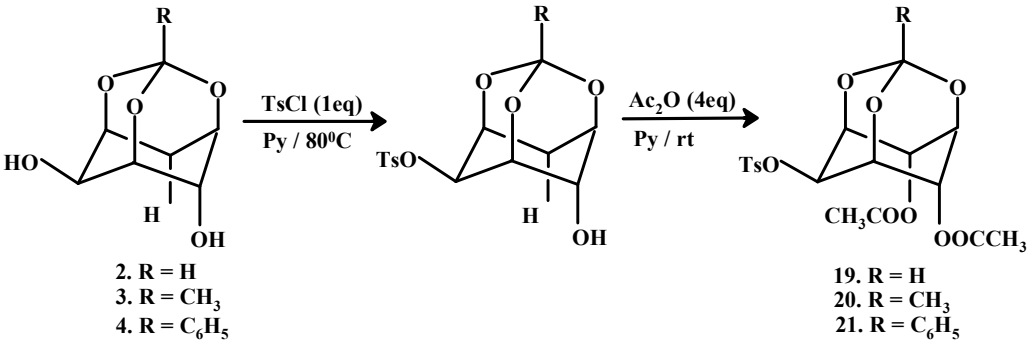


**2. R = H**
**3. R = $CH_3$**
**4. R = $C_6H_5$**

**19. R = H**
**20. R = $CH_3$**
**21. R = $C_6H_5$**

**Scheme 5.1**

## 5.2. Experimental section

### *5.2.1. Synthesis*

*5.2.1.1. Preparation of 2-O-tosyl 4,6-di-O-acetyl myo-inositol 1,3,5-orthoformate* (**19**)

A mixture of *myo*-inositol 1,3,5-orthoformate **2** (0.190 g, 1 mmol), tosyl chloride (0.200 g, 1.05 mmol) and pyridine (8 mL) was heated at 80 °C for 48 h. The reaction mixture was concentrated under reduced pressure and the residue worked up as usual. The product was purified by column chromatography to get 2-*O*-tosyl *myo*-inositol 1,3,5-orthoformate (0.300 g, 87 %). The 2-*O*-tosyl derivative (0.172 g, 0.5 mmol) and acetic anhydride (0.2 mL, 2.10 mmol) were dissolved in pyridine (6 mL) and the mixture stirred at room temperature for 8 h. The solvent was evaporated from the reaction mixture under reduced pressure and the residue worked up as usual. The product was purified by flash column chromatography to get 2-*O*-tosyl 4,6-di-*O*-acetyl *myo*-inositol 1,3,5-orthoformate (0.205 g, 96 %) as colorless solid.

Data for **19**:

**M.P.**: 175-176 °C

**IR** ($CHCl_3$)**ν**: 1751 $cm^{-1}$

**$^1$H NMR** (200 MHz, $CDCl_3$): **δ** 2.09 (s, 6H, MeCO), 2.47 (s, 3H, ArMe), 4.25-4.31 (m, 2H, Ins H), 4.52-4.58 (m, 1H, Ins H), 4.94-4.98 (m, 1H, Ins H), 5.46 (t, *J* = 3.9

Hz, 2H, Ins H), 5.52 (d, *J* = 1.5 Hz, $O_3CH$), 7.34-7.42 (m, 2H, ArH), 7.82-7.89 (m, 2H, ArH) ppm.

**$^{13}$C NMR** (50 MHz, $CDCl_3$): **δ** 20.5, 21.6, 65.8, 67.5, 68.8, 69.1, 71.8, 102.7, 127.7, 129.9, 133.3, 145.5, 168.7 ppm.

**Anal. Calcd for $C_{18}H_{20}O_{10}S$**: C, 50.47; H, 4.71; Found: C, 50.23; H, 4.55 %.

*5.2.1.2. Preparation of 2-O-tosyl 4,6-di-O-acetyl myo-inositol 1,3,5-orthoacetate* (**20**)

2-*O*-tosyl *myo*-inositol 1,3,5-orthoacetate was prepared as above from *myo*-inositol orthoacetate **3** (0.204 g, 1 mmol), tosyl chloride (0.200 g, 1.05 mmol) and pyridine (8 mL). Subsequently 2-*O*-tosyl-*myo*-inositol 1,3,5-orthoacetate (0.179 g, 0.5 mmol) was acetylated as above using in pyridine (6 mL) and acetic anhydride (0.2 mL, 4 mmol) to get the diacetate **20** (0.208 g, 94 %) as a colorless solid.

Data for **20**:

**M. P.**: 177-178 °C

**IR** ($CHCl_3$)**ν**: 1755 $cm^{-1}$(C=O)

**$^1$H NMR** (200 MHz, $CDCl_3$) **δ**: 1.45 (s, 3H, $O_3CMe$), 2.07 (s, 6H, MeCO), 2.47 (s, 3H, ArMe), 4.23-4.28 (m, 2H, Ins H), 4.45-4.51 (m, 1H, Ins H), 4.85-4.89 (m, 1H, Ins H), 5.40 (t, *J* = 1.9 Hz, 2H, Ins H), 7.33-7.41 (m, 2H, ArH), 7.81-7.88 (m, 2H, ArH) ppm.

**$^{13}$C NMR** (50 MHz, $CDCl_3$) **δ**: 20.6, 21.6, 23.8, 66.0, 67.6, 68.1, 69.8, 109.1, 127.8, 130.0, 133.5, 145.4, 168.8 ppm.

**Anal. Calcd for $C_{19}H_{22}O_{10}S$**: C, 51.58; H, 5.01; Found: C, 51.56; H, 5.03 %.

*5.2.1.3. Preparation of 2-O-tosyl 4,6-di-O-acetyl myo-inositol 1,3,5-orthobenzoate* (**21**)

2-*O*-tosyl *myo*-inositol 1,3,5-orthobenzoate was prepared as above from *myo*-inositol orthobenzoate **4** (0.266 g, 1 mmol), tosyl chloride (0.200 g, 1.05 mmol) and pyridine (8 mL). The 2-*O*-tosyl *myo*-inositol 1,3,5-orthobenzoate derivative (0.211 g,

0.5 mmol) so obtained was acetylated with acetic anhydride (0.2 mL, 4 mmol) in pyridine (6 mL) as above to get the diacetate **21** (0.115 g, 91 %) as a colorless solid.

Data for **21**:

**M. P.**: 188-190 °C

**IR** ($CHCl_3$)**ν**: 1755 $cm^{-1}$(C=O)

**$^1$H NMR** (200 MHz, $CDCl_3$) **δ**: 2.11 (s, 6H, MeCO), 2.46 (s, 3H, ArMe), 4.43-4.50 (m, 2H, Ins H), 4.65-4.73 (m, 1H, Ins H), 5.01 (t, *J* = 1.9 Hz, 1H, Ins H), 5.58 (m, 2H, Ins H), 7.31-7.41 (m, 5H, ArH), 7.54-7.62 (m, 2H, ArH), 7.82-7.90 (m, 2H, ArH).

**$^{13}$C NMR** (50 MHz, $CDCl_3$) **δ**: 20.6, 21.6, 66.8, 67.7, 68.2, 70.5, 107.8, 125.3, 127.7, 128.0, 129.8, 129.9, 133.6, 135.8, 145.4, 168.8.

**Anal. Calcd for $C_{24}H_{24}O_{10}S$**: C, 57.14; H, 4.79. Found: C, 57.23; H, 4.97 %.

### *5.2.2. Crystallization*

Crystallization experiments were carried out by diffusing vapor of light petroleum ether (bp 40-60 °C) in to a solution of **19** or **20** or **21** in common organic solvents, at room temperature. Solvent free crystals of **19** and **21** were obtained from acetone, acetonitrile, chloroform, dichloromethane, dioxane, nitromethane and tetrahydrofuran. However, **20** produced inclusion crystals from various solvents such as acetone (**20·AC**), acetonitrile (**20·AN**), chloroform (**20·CF**), dichloromethane (**20·DCM**), dioxane (**20·DX**), nitromethane (**20·NM**), tetrahydrofuran (**20·THF**), pyridine (**20·PY**), dichloroethane (**20·DCE**) and ethyl acetate (**20·EA**). All solvated crystals were stable from 2 to 6 days in the open atmosphere; longer exposure led to the formation of a powder.

### *5.2.3. Crystallographic Details*

X-ray intensity data for **19**, **21** and solvated crystals of **20** were collected on a Bruker SMART APEX CCD diffractometer in omega and phi scan mode, $\lambda_{MoK\alpha}$ =

0.71073 Å at room temperature. The inclusion crystals were coated with oil to avoid exposure to the atmosphere. All the intensities were corrected for Lorentzian, polarization and absorption effects using Bruker's *SAINT* and *SADABS* programs. The crystal structures were solved by Direct methods using program *SHELXS-97*; the full-matrix least squares refinements on $F^2$ were carried out by using *SHELXL-97*. Hydrogen atoms were included in the refinement as per the riding model. Table 5.1 summarizes the crystal data for all the compounds.

Full-matrix least-squares refinements of solvatomorphs of **20** were carried out by applying geometrical constraint options (DFIX and DANG) in *SHELXL97* to retain the molecular geometries of low occupied and disordered entities. Geometrical constraint, DFIX was applied to guest molecules in **20·AC**, **20·CF**, **20·DCE**, **20·DCM**, **20·EA** and **20·THF** crystals, whereas for **20·DX** both the constraints DFIX and DANG were used. All the included guest solvents were kept isotropic in the solvatomorphs of **20** due to lower occupancies (0.125-0.375), except for **20·AN**, **20·NM** and **20·DCM**, which had higher occupancies (0.5).

Some of the included guests, such as halogenated solvents and acetone showed statistical disorder in their crystal lattice. In **20·AC** crystals, O11 and C20 atoms of the acetone guest were disordered over two positions (O11' and C20') having occupancies 0.5 and 0.125 respectively. The guest in **22·CF** showed two different sites for chloroform molecule with occupancies of 0.25 and 0.0625 respectively. In **22·DCM** crystals, two positions of chlorine atoms were assigned 0.5 (Cl1 and Cl2) and 0.0625 (Cl1' and Cl2') occupancies. The chlorine atoms (Cl1 and Cl2) of the dichloroethane guest in **22·DCE** crystals exhibited extensive disorder over sites Cl1, Cl1', Cl1", Cl2 and Cl2' which were assigned occupancies of 0.5, 0.15, 0.5, 0.375 and 0.125 respectively.

**Table 5.1**: Summary of crystallographic data for **19**, **21** and solvatomorphs of **20**.

| Crystal data | **19** | **20·AC** | **20·AN** | **20·CF** |
|---|---|---|---|---|
| Chemical Formula | $C_{18}H_{20}O_{10}S$ | $C_{19}H_{22}O_{10}S$ 0.38 ($C_3H_6O$) | $C_{19}H_{22}O_{10}S$ 0.5 ($CH_3CN$) | $C_{19}H_{22}O_{10}S$ 0.32 ($CHCl_3$) |
| $M_r$ | 428.40 | 465.44 | 462.95 | 481.13 |
| Temperature/K | 298 | 298 | 298 | 298 |
| Morphology | Plate | Thin Plate | Plate | Thin Plate |
| Colour | Colorless | Colorless | Colorless | Colorless |
| Crystal size (mm) | 0.49 × 0.29 × 0.13 | 0.33 × 0.14 × 0.05 | 0.62 × 0.12 × 0.10 | 0.59 × 0.25 × 0.06 |
| Crystal system | Triclinic | Monoclinic | Monoclinic | Monoclinic |
| Space group | *P-1* | *P2₁/c* | *P2₁/c* | *P2₁/c* |
| *a* (Å) | 8.5756(6) | 8.200(2) | 8.1948(14) | 8.1940(16) |
| *b* (Å) | 11.0381(8) | 13.855(4) | 13.941(2) | 13.848(3) |
| *c* (Å) | 11.2005(8) | 21.255(6) | 20.911(3) | 21.345(4) |
| $\alpha$ (°) | 100.426(1) | 90 | 90 | 90 |
| $\beta$ (°) | 103.123(1) | 91.628(6) | 91.544(3) | 91.681(3) |
| $\gamma$ (°) | 99.660(1) | 90 | 90 | 90 |
| *V* (Å$^3$) | 991.04(12) | 2413.9(12) | 2388.1(7) | 2420.9(8) |
| *Z* | 2 | 4 | 4 | 4 |
| $D_x$ (Mg m$^{-3}$) | 1.436 | 1.281 | 1.288 | 1.320 |
| $\mu$ (mm$^{-1}$) | 0.217 | 0.186 | 0.186 | 0.292 |
| *F(000)* | 448 | 974 | 972 | 1003 |
| $T_{min}$ , $T_{max}$ | 0.901, 0.972 | 0.941, 0.991 | 0.893, 0.982 | 0.846, 0.983 |
| $\theta_{max}$ (°) | 25.3 | 25.0 | 25.0 | 25.0 |
| *h* (min, max) | (-10, 10) | (-9, 9) | (-9, 9) | (-9, 9) |
| *k* (min, max) | (-13, 13) | (-16, 16) | (-16, 16) | (-16, 16) |
| *l* (min, max) | (-13, 13) | (-25, 25) | (-24, 24) | (-25, 25) |
| No. of refl$^n$ collected | 9864 | 17070 | 16815 | 21717 |
| No. of unique refl$^n$ | 3581 | 4248 | 4208 | 4254 |
| No. of observed refl$^n$ | 3179 | 2719 | 3112 | 3776 |
| No. of parameters | 274 | 299 | 303 | 307 |
| No. of restraints | 0 | 5 | 0 | 6 |
| $R_{int}$ | 0.020 | 0.079 | 0.044 | 0.037 |
| $R_1$_obs, $R_1$_all | 0.042, 0.046 | 0.091, 0.140 | 0.079, 0.108 | 0.106, 0.117 |
| $wR_2$_obs, $wR_2$_all | 0.110, 0.114 | 0.203, 0.230 | 0.193, 0.208 | 0.274, 0.282 |
| GoF | 1.03 | 1.15 | 1.17 | 1.24 |
| $\Delta\rho_{max}$, $\Delta\rho_{min}$ (e Å$^{-3}$) | 0.41, –0.22 | 0.46, –0.26 | 0.42, –0.22 | 0.87, –0.44 |

**Table 5.1**: Continued.

| Crystal data | **20·DCE** | **20·DCM** | **20·DX** | **20·EA** |
|---|---|---|---|---|
| Chemical Formula | $C_{19}H_{22}O_{10}S$ 0.5($C_2H_4Cl_2$) | $C_{19}H_{22}O_{10}S$ 0.5 ($CH_2Cl_2$) | $C_{19}H_{22}O_{10}S$ 0.13 ($C_4H_8O_2$) | $C_{19}H_{22}O_{10}S$ 0.25($C_4H_8O_2$) |
| $M_r$ | 516.47 | 493.75 | 453.44 | 462.44 |
| Temperature/K | 298 | 298 | 298 | 298 |
| Morphology | Plate | Plate | Plate | Plate |
| Colour | Colorless | Colorless | Colorless | Colorless |
| Crystal size (mm) | 0.32 × 0.20 × 0.10 | 0.30 × 0.23 × 0.22 | 0.53 × 0.19 × 0.11 | 0.74 × 0.39 × 0.30 |
| Crystal system | Monoclinic | Monoclinic | Monoclinic | Monoclinic |
| Space group | $P2_1/c$ | $P2_1/c$ | $P2_1/c$ | $P2_1/c$ |
| $a$ (Å) | 8.2496(13) | 8.2606(13) | 8.2463(16) | 8.2376(9) |
| $b$ (Å) | 13.876(2) | 13.881(2) | 13.855(4) | 13.692(2) |
| $c$ (Å) | 21.133(3) | 21.106(3) | 21.710(4) | 21.155(2) |
| $\alpha$ (°) | 90.00 | 90 | 90 | 90.00 |
| $\beta$ (°) | 91.796(3) | 90.597(3) | 90.753(4) | 91.696 (2) |
| $\gamma$ (°) | 90.00 | 90 | 90 | 90.00 |
| $V$ (Å$^3$) | 2417.8(7) | 2420.0(7) | 2504.8(8) | 2385.0 (5) |
| $Z$ | 4 | 4 | 4 | 4 |
| $D_x$ (Mg m$^{-3}$) | 1.419 | 1.355 | 1.202 | 1.288 |
| $\mu$ (mm$^{-1}$) | 0.378 | 0.321 | 0.176 | 0.187 |
| *F(000)* | 1071 | 1029 | 952 | 968 |
| $T_{min}$ , $T_{max}$ | 0.963, 0.889 | 0.933, 0.910 | 0.912, 0.981 | 0.946, 0.874 |
| $\theta_{max}$ (°) | 25.0 | 25.0 | 25.0 | 25.0 |
| $h$ (min, max) | (-9, 9) | (-9, 9) | (-9, 9) | (-9, 9) |
| $k$ (min, max) | (-16, 16) | (-16, 16) | (-16, 16) | (-16, 16) |
| $l$ (min, max) | (-25, 25) | (-25, 23) | (-25, 25) | (-25, 25) |
| No. of refl$^n$ collected | 22760 | 17218 | 21103 | 16711 |
| No. of unique refl$^n$ | 4263 | 4245 | 4399 | 4185 |
| No. of observed refl$^n$ | 3292 | 3655 | 3162 | 3450 |
| No. of parameters | 300 | 317 | 299 | 296 |
| No. of restraints | 6 | 4 | 15 | 2 |
| $R_{int}$ | 0.030 | 0.024 | 0.035 | 0.021 |
| $R_1$_obs, $R_1$_all | 0.073, 0.088 | 0.066, 0.075 | 0.076, 0.098 | 0.063, 0.072 |
| $wR_2$_obs, $wR_2$_all | 0.213, 0.229 | 0.181, 0.189 | 0.217, 0.240 | 0.188, 0.200 |
| GoF | 1.04 | 1.08 | 1.07 | 1.08 |
| $\Delta\rho_{max}$, $\Delta\rho_{min}$ (e Å$^{-3}$) | 0.98, –0.98 | 0.58, –0.18 | 0.60, –0.30 | 0.99, –0.21 |

**Table 5.1**: Continued.

| Crystal data | **20·NM** | **20·PY** | **20·THF** | **21** |
|---|---|---|---|---|
| Chemical Formula | $C_{19}H_{22}O_{10}S$ 0.5 ($CH_3NO_2$) | $C_{19}H_{22}O_{10}S$ 0.38 ($C_5H_5N$) | $C_{19}H_{22}O_{10}S$ 0.13($C_4H_8O$) | $C_{24}H_{24}O_{10}S$ |
| $M_r$ | 472.95 | 475.21 | 448.43 | 504.49 |
| Temperature/K | 298 | 298 | 298 | 298 |
| Morphology | Plate | Plate | Plate | Thin plate |
| Colour | Colorless | Colorless | Colorless | Colorless |
| Crystal size (mm) | 0.47 × 0.29 × 0.20 | 0.21 × 0.16 × 0.11 | 0.57 × 0.28 × 0.19 | 0.69 × 0.17 × 0.07 |
| Crystal system | Monoclinic | Monoclinic | Monoclinic | Monoclinic |
| Space group | $P2_1/c$ | $P2_1/c$ | $P2_1/c$ | $P2_1/c$ |
| $a$ (Å) | 8.2695(12) | 8.216(3) | 8.2092(10) | 12.3019(14) |
| $b$ (Å) | 13.941(2) | 13.960(4) | 13.848(3) | 8.2155(10) |
| $c$ (Å) | 20.726(3) | 21.620(7) | 21.613(3) | 23.551(3) |
| $\alpha$ (°) | 90 | 90 | 90 | 90 |
| $\beta$ (°) | 91.395(2) | 91.697(6) | 91.406(2) | 91.306(2) |
| $\gamma$ (°) | 90 | 90 | 90 | 90 |
| $V$ (Å$^3$) | 2378.5(6) | 2478.5(14) | 2482.3(5) | 2379.6(5) |
| $Z$ | 4 | 4 | 4 | 4 |
| $D_x$ (Mg m$^{-3}$) | 1.321 | 1.274 | 1.200 | 1.408 |
| $\mu$ (mm$^{-1}$) | 0.191 | 0.181 | 0.176 | 0.193 |
| *F(000)* | 992 | 997 | 940 | 1056 |
| $T_{min}$ , $T_{max}$ | 0.915, 0.963 | 0.980, 0.963 | 0.906, 0.967 | 0.878, 0.987 |
| $\theta_{max}$ (°) | 25.0 | 25.0 | 25.0 | 25.0 |
| $h$ (min, max) | (-9, 9) | (-9, 9) | (-9, 9) | (-14, 14) |
| $k$ (min, max) | (-16, 16) | (-16, 16) | (-16, 16) | (-9, 9) |
| $l$ (min, max) | (-24, 24) | (-25, 25) | (-25, 25) | (-28, 13) |
| No. of refl$^n$ collected | 20561 | 23466 | 23525 | 11497 |
| No. of unique refl$^n$ | 4183 | 4348 | 4359 | 4179 |
| No. of observed refl$^n$ | 3592 | 3373 | 3620 | 3082 |
| No. of parameters | 312 | 285 | 295 | 319 |
| No. of restraints | 0 | 0 | 5 | 0 |
| $R_{int}$ | 0.022 | 0.047 | 0.024 | 0.037 |
| $R_1$_obs, $R_1$_all | 0.066, 0.072 | 0.098, 0.119 | 0.067, 0.076 | 0.056, 0.082 |
| $wR_2$_obs, $wR_2$_all | 0.212, 0.221 | 0.241, 0.257 | 0.206, 0.222 | 0.114, 0.123 |
| GoF | 1.08 | 1.13 | 1.06 | 1.08 |
| $\Delta\rho_{max}$, $\Delta\rho_{min}$ (e Å$^{-3}$) | 0.77, –0.28 | 0.81, –0.27 | 0.90, –0.24 | 0.35, –0.22 |

### *5.2.4. Thermal Analysis (DSC/DTA/TGA)*

Differential Scanning Calorimetry (DSC) analysis was performed on Mettler Toledo DSC instrument for the crystalline samples of **19** and **21**. The Differential Thermal Analysis (DTA) and Thermo-Gravimetric Analysis (TGA) of all the inclusion crystals of **20** were performed using a Seiko DTA/TG 320 instrument. About 3-6 mg of the crystalline sample was placed in an aluminium pan and heated from 40 to 200 $^{\circ}$C at a rate of 10 $^{\circ}$C/minute. An empty pan was used as the reference and dry nitrogen used for purging (50 mL/min).

## 5.3. Results and discussion

The tosylate **19** yielded triclinic, *P-1* crystals from most of the solvents, whereas **20** and **21** gave crystals that belonged to monoclinic, $P2_1/c$ space group. It is interesting to note that structurally different (such as linear, planar, halogenated, cyclic, aromatic, Chart 5.1) solvent molecules with electron count ranging from 22-50 numbers were included in the crystal lattice.

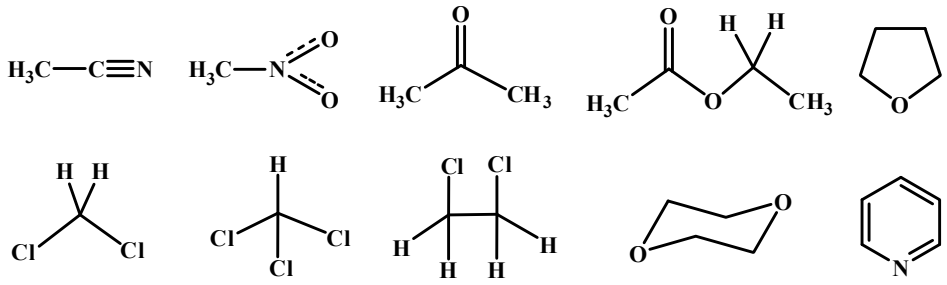

Chart 5.1

The dimorphic modifications of **14**, **16** and **17** (*Chapters 3* and *4*) resulted mainly due to the orientational change of the tosyl group about *O–S* bond at *C6*-position of inositol ring. Here also, the molecules adopted different conformations essentially due to rotation about the same bond, although the tosyl is substituted at *C2*- position of inositol ring. The conformation of the molecules in **19** and **21** is almost the same**,** whereas the conformation of the molecules of **20** in its inclusion

crystals differs from those of **19** and **21** due to the different orientations of *C2–O2–*tosyl and *C6–O6–*acetyl groups [Fig. 5.1(i)-(iii)]. The torsion angle *C2–O2–S1–C8 (C9* or *C14*) of the tosyl group was 68.89º in **19**, 71.89º in **21** and ~ 60º in all the inclusion crystals of **20**. However, the variation in the torsion angle of tosyl group is very little (deviating ~ 4º) among the inclusion crystals of **20** [Fig. 5.1(iv), Table 5.2]. The carbonyl oxygen at *C6-O6-* in the crystal structure of **19** is disordered over two positions O10 and O10' [Fig. 5.1(i)] with occupancy 0.55 and 0.45 respectively.

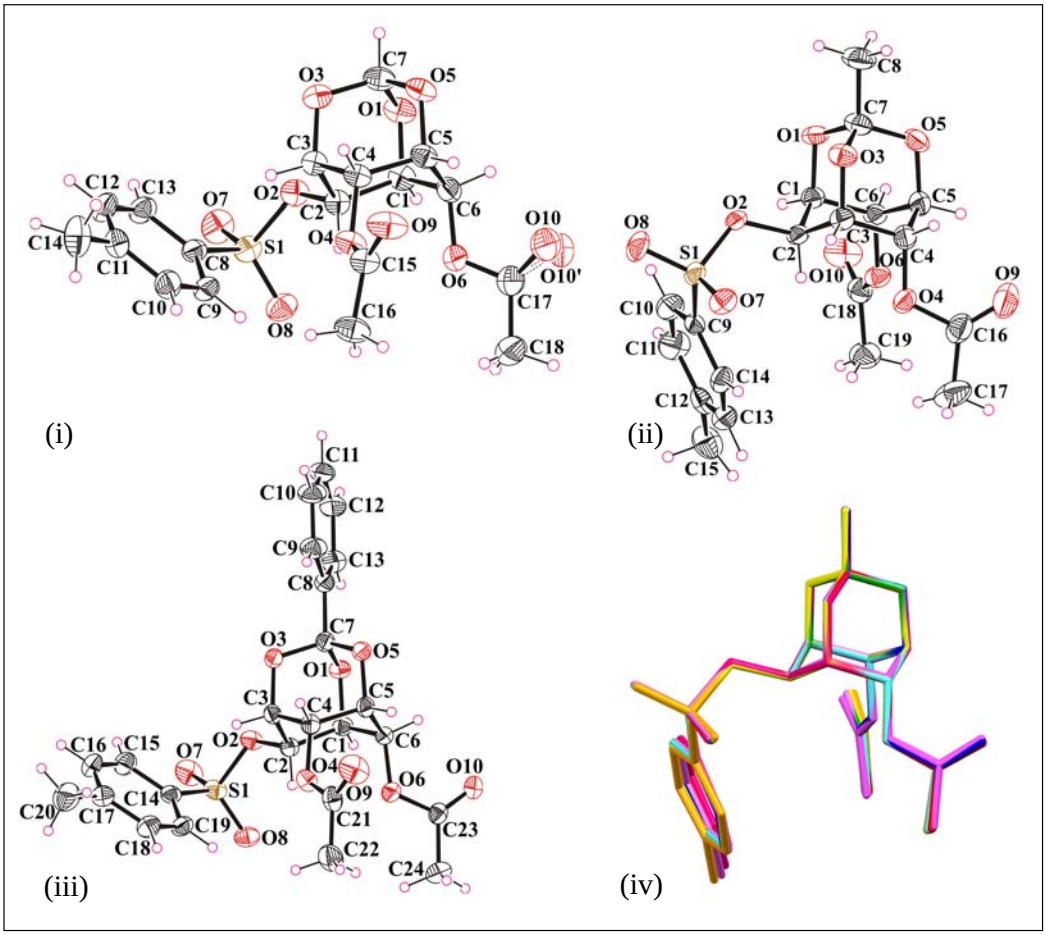


**Figure 5.1**: ORTEP diagram drawn at 30 % probability displacement ellipsoids of (i) **19**, (ii) **20·AC** and (iii) **21** with atom numbering scheme. (iv) Overlap plots of solvatomorphs of **20** [color scheme, blue: **20·AC**, red: **20·AN**, green: **20·CF**, purple: **20·DCE**, violet: **20·DCM**, orange: **20·DX**, pink: **20·EA**, rose: **20·NM**, skyblue: **20·PY** and yellow: **20·THF**].

**Table 5.2**: Torsion angle, *C2–O2–S1–C9* of tosyl group in solvatomorphs of **20**.

| 20·AC | 20·AN | 20·CF | 20·DCE | 20·DCM | 20·DX | 20·EA | 20·NM | 20·PY | 20·THF |
|---|---|---|---|---|---|---|---|---|---|
| 58.7º | 56.6º | 58.8º | 57.8º | 57.8º | 59.4º | 58.5º | 55.6º | 59.7º | 59.6º |

### 5.3.1. Thermal Analysis of 19, 21 and solvatomorphs of 20

The DSC curves of crystals of **19** [Fig. 5.2(i)] and **21** [Fig. 5.2(ii)] showed a single endotherm attributed to their melting, indicating no phase transformation in the crystals. The DTA plot of solvent free compound, **20** (obtained after column chromatography and confirmed by $^{1}$H NMR) showed only a single melting endothermic peak ~ 173.6 °C [Fig. 5.2(iii)], whereas DTA of solvated crystals showed a rather broad endotherm before the melting endothermic peak [Fig. 5.2(iv)-(xii)]. The first endotherm indicates phase transformation possibly due to escape of the guest solvent molecules from the crystal lattice. The melting endotherm (at ~176°C), however, was found to be the same for all the inclusion crystals. Thermogravimetric analyses of the solvates showed a continuous weight loss of ~ 10 % in the temperature range 60-130 °C, due to the release of the included solvent from the crystal lattice.

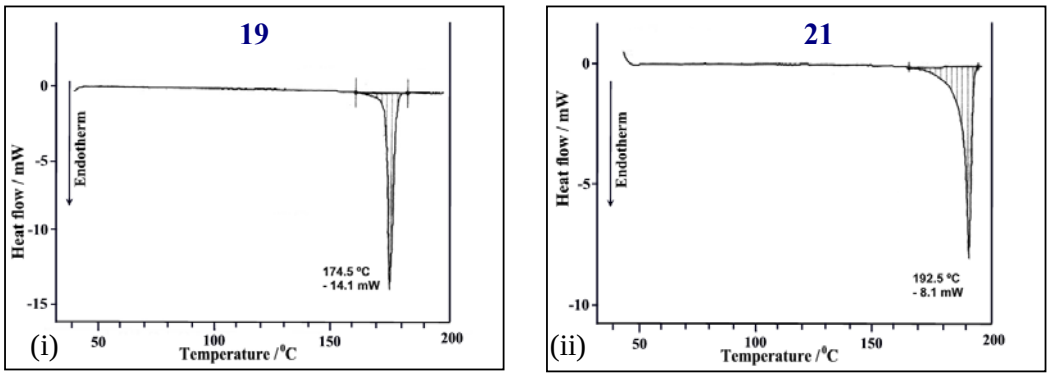


**Figure 5.2**: DSC plots of (i) crystals of **19** and (ii) crystals of **21**. DTA/TGA curves of (iii) **20** and (iv-xii) inclusion crystals of **20**.

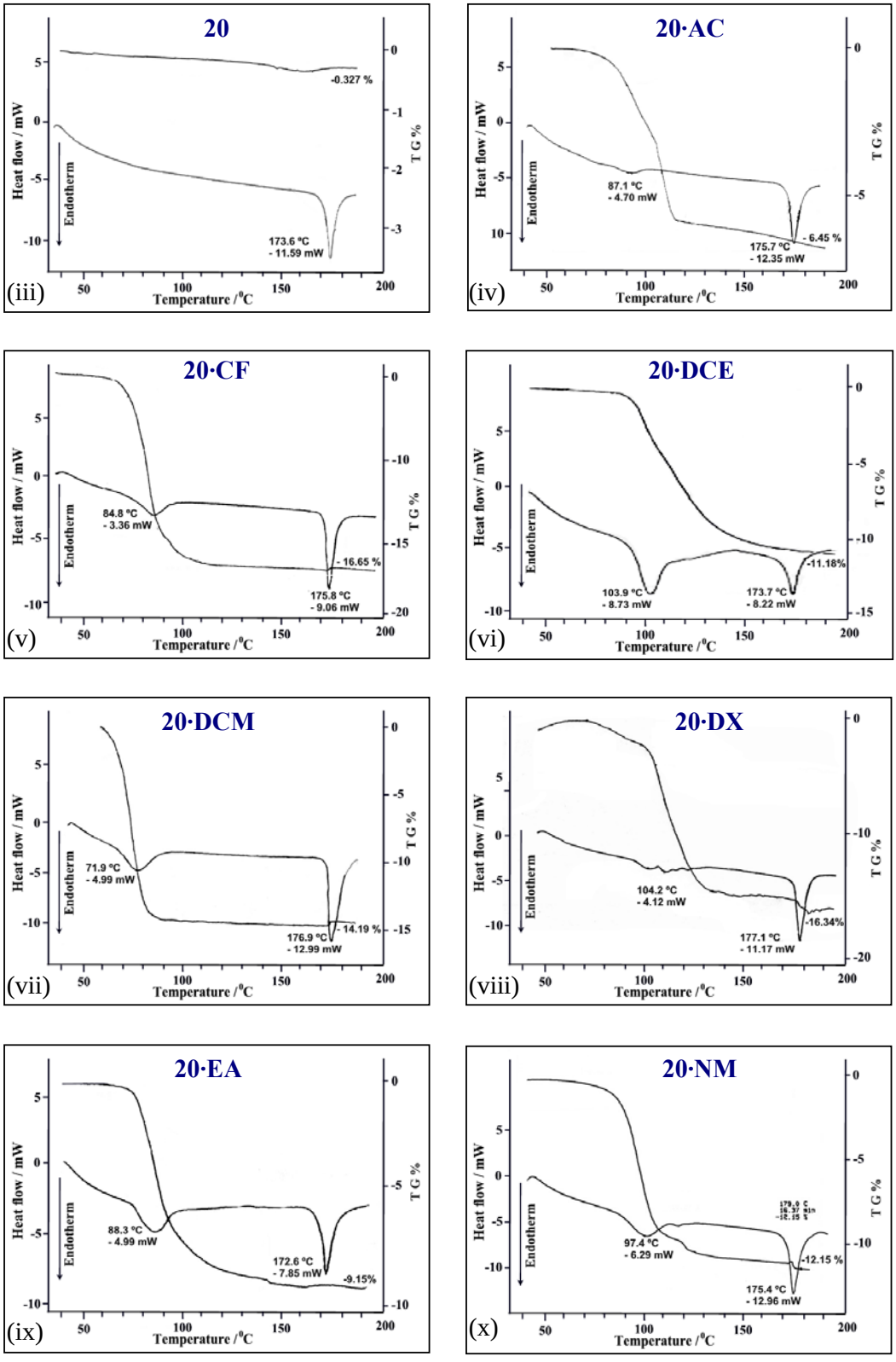


**Figure 5.2**: Continued. (iii)-(xii) DTA/TGA curves of inclusion crystals of **20**.

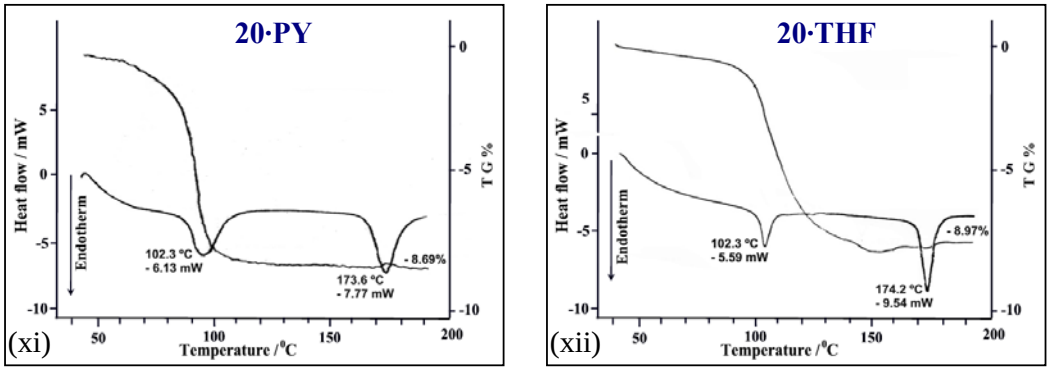


**Figure 5.2**: Continued. (xi)-(xii) DTA/TGA curves of inclusion crystals of **20**.

### 5.3.2. Molecular Organization in Crystals of 19

The molecules of **19** are linked sideways by centrosymmetric C–H···O interactions involving orthoformate hydrogen *H7* with carbonyl oxygen *O9* of the *C4–O4–* acetyl group and inositol ring hydrogen *H4* with ether oxygen *O5* of the orthoformate bridge, forming dimeric assembly [Fig. 5.3(i)]. These dimers upon unit translation along *a*-axis, form molecular chains making C7–H7···O1 and C1–H1···O9 interactions as shown in figure 5.3(ii) [Table 5.3].

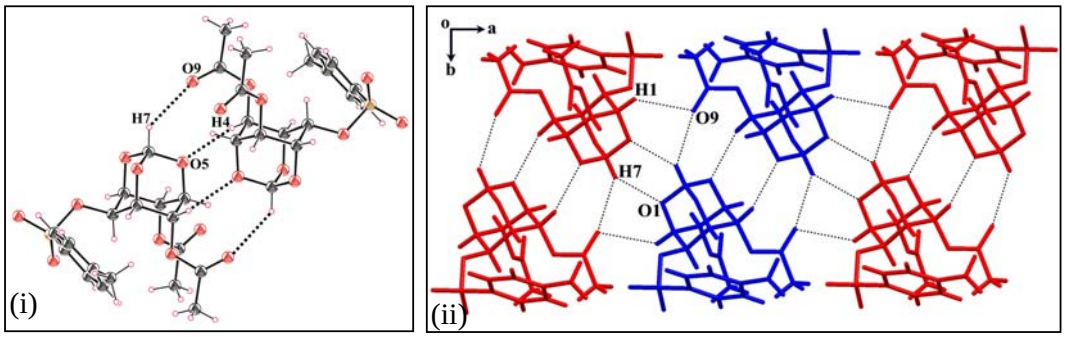


**Figure 5.3**: (i) Dimer formation *via* centro-symmetric C–H···O interactions and (ii) molecular chain formation along *a*-axis *via* C1–H1···O9 and C7–H7···O1 interactions in crystals of **19**.

**Table 5.3**: Geometrical parameters of hydrogen bonding interactions in crystals of **19** as showed in figures 5.3 and 5.4.

| | D–H···A | D–H (Å) | H···A (Å) | D···A (Å) | D–H···A (°) |
|---|---|---|---|---|---|
| **19** | C1–H1···O9 [i] | 0.98 | 2.64 | 3.346(2) | 129 |
| | C4–H4···O5 [ii] | 0.98 | 2.49 | 3.371(2) | 149 |
| | C7–H7···O1 [iii] | 0.98 | 2.47 | 3.222(2) | 133 |
| | C7–H7···O9 [ii] | 0.98 | 2.60 | 3.391(2) | 138 |
| | C9–H9···O8 [iv] | 0.93 | 2.41 | 3.329(2) | 171 |
| | C18–H18*A*···O9 [v] | 0.96 | 2.50 | 3.426(3) | 163 |

Symmetry codes: (i) 1+x, y, z ; (ii) 1-x, -y, -z ; (iii) 2-x, -y, -z ; (iv) 2-x, 1-y, 1-z ; (v) 1-x, 1-y1, -z.

The neighboring molecular chains are linked along the *b*-axis centrosymmetrically *via* bifurcated C–H···O interactions between the sulfonyl oxygen *O8* and hydrogens *H9* and *H16B* forming a two-dimensional layer [Fig. 5.4, Table 5.3].

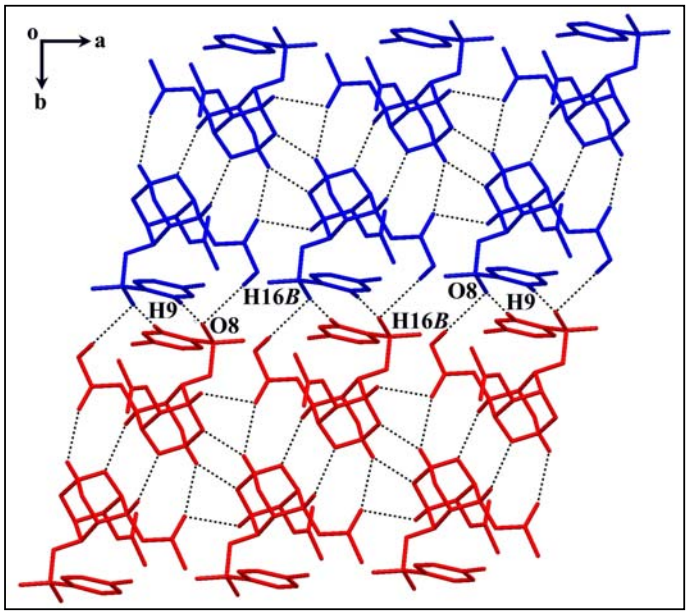


**Figure 5.4**: Molecular layer formation *via* C–H···O interactions in crystals of **19**.

These molecular layers are extended in the third dimension *via* three C–H···O interactions, C12–H12···O2, C16–H16*A*···O10 and C18–H18*A*···O9 [Fig. 5.5 (i), Table 5.4]. The overall molecular packing was found to be compact in the crystal lattice, which does not leave any cavities/voids for solvent inclusion [Fig. 5.5 (ii)].

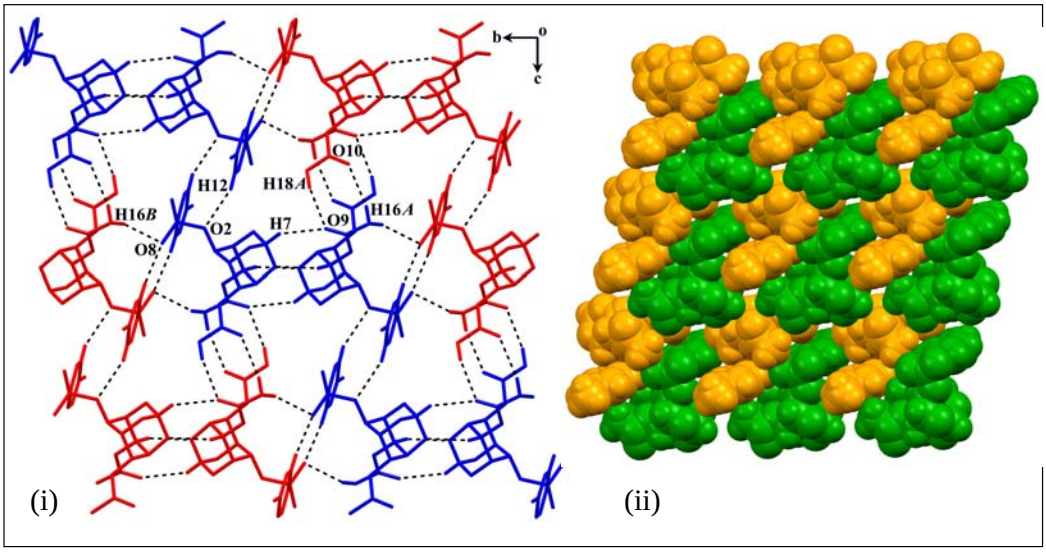


**Figure 5.5**: Molecular layer of **19** (i) linked *via* C–H···O interactions viewed down *a*-axis; (ii) CPK plot viewed down *c*-axis.

**Table 5.4**: Intermolecular hydrogen-bonding geometry in crystals of **19** as showed in figure 5.5.

| Crystals | D–H···A | D–H (Å) | H···A (Å) | D···A (Å) | D–H···A (°) |
|---|---|---|---|---|---|
| **19** | C12–H12···O2 [i] | 0.93 | 2.71 | 3.456(3) | 137 |
| | C14–H14C···O5 [ii] | 0.96 | 2.64 | 3.443(3) | 141 |
| | C16–H16A···O10 [iii] | 0.96 | 2.63 | 3.458(5) | 145 |
| | C16–H16B···O8 [iv] | 0.96 | 2.65 | 3.551(3) | 158 |

Symmetry codes: (i) 2-x, -y, 1-z ; (ii) x, y, 1+z ; (iii) 1-x, 1-y1, -z ; (iv) 2-x, 1-y, 1-z.

### 5.3.3. Molecular Organization in the Inclusion Crystals of 20

As seen above, the molecules of **19** formed centrosymmetric dimers that achieved closest possible packing in their crystal lattice. However, with methyl

substitution at *C7*, the conformation of the molecule changed in **20**, to form a helical assembly around the crystallographic $2_1$-screw axis (*b*-axis). The successive molecules along the helical axis (*b*-axis) are linked by four C-H···O interactions *via* C3–H3···O10, C6–H6···O7, C14–H14···O5 and C17–H17*C*···O1 [Fig. 5.6, Table 5.5].

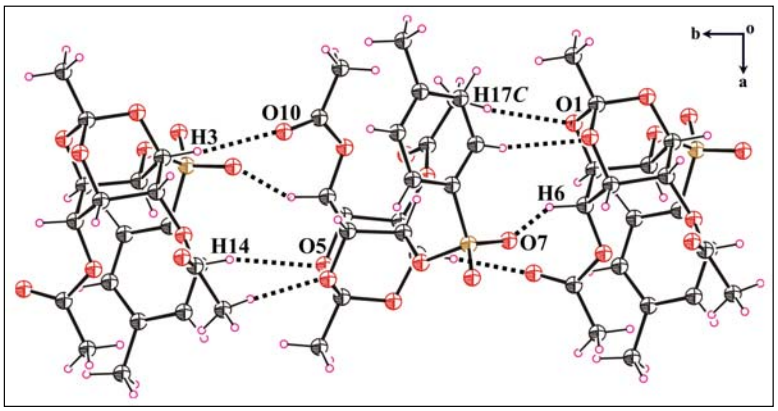


**Figure 5.6**: Molecular chain formation along *b*-axis through C–H···O interactions in solvatomorphs of **20**.

**Table 5.5**: Geometric parameters of hydrogen bonding interactions [Fig. 5.6].

| Crystals | D–H···A | D–H (Å) | H···A (Å) | D···A (Å) | D–H···A (°) |
|---|---|---|---|---|---|
| **20·AC** | C3–H3···O10 [i] | 0.98 | 2.53 | 3.415(6) | 150 |
| | C6–H6···O7 [ii] | 0.98 | 2.55 | 3.214(5) | 125 |
| | C14–H14···O5 [i] | 0.93 | 2.60 | 3.488(6) | 160 |
| | C17–H17*C*···O1 [i] | 0.96 | 2.54 | 3.373(7) | 146 |
| **20·AN** | C3–H3···O10 [i] | 0.98 | 2.49 | 3.408(5) | 155 |
| | C6–H6···O7 [ii] | 0.98 | 2.48 | 3.171(4) | 128 |
| | C14–H14···O5 [i] | 0.93 | 2.63 | 3.526(5) | 161 |
| | C17–H17*C*···O1 [i] | 0.96 | 2.50 | 3.456(6) | 175 |
| **20·CF** | C3–H3···O10 [i] | 0.98 | 2.48 | 3.387(7) | 153 |
| | C6–H6···O7 [ii] | 0.98 | 2.52 | 3.204(6) | 127 |
| | C14–H14···O5 [i] | 0.93 | 2.64 | 3.516(6) | 157 |
| | C17–H17*C*···O1 [i] | 0.96 | 2.55 | 3.392(7) | 146 |
| **20·DX** | C3–H3···O10 [i] | 0.98 | 2.55 | 3.433(12) | 150 |
| | C6–H6···O7 [ii] | 0.98 | 2.63 | 3.286(10) | 125 |

| | | | | | |
|---|---|---|---|---|---|
| **20·DX** | C14–H14···O5 [i] | 0.93 | 2.61 | 3.489(11) | 157 |
| | C17–H17*C*···O1 [i] | 0.96 | 2.52 | 3.421(13) | 157 |
| **20·NM** | C3–H3···O10 [i] | 0.98 | 2.46 | 3.373(4) | 155 |
| | C6–H6···O7 [ii] | 0.98 | 2.44 | 3.152(3) | 129 |
| | C14–H14···O5 [i] | 0.93 | 2.65 | 3.547(3) | 162 |
| | C17–H17*C*···O1 [i] | 0.96 | 2.63 | 3.474(5) | 147 |
| **20·THF** | C3–H3···O10 [i] | 0.98 | 2.56 | 3.450(4) | 152 |
| | C6–H6···O7 [ii] | 0.98 | 2.58 | 3.250(3) | 126 |
| | C14–H14···O5 [i] | 0.93 | 2.61 | 3.482(4) | 157 |
| | C17–H17*C*···O1 [i] | 0.96 | 2.47 | 3.421(4) | 172 |
| **20·DCM** | C3–H3···O10 [i] | 0.98 | 2.59 | 3.477(4) | 151 |
| | C6–H6···O7 [ii] | 0.98 | 2.57 | 3.227(4) | 125 |
| | C14–H14···O5 [i] | 0.93 | 2.56 | 3.447(4) | 160 |
| | C17–H17*C*···O1 [i] | 0.96 | 2.45 | 3.411(5) | 178 |
| **20·PY** | C3–H3···O10 [i] | 0.98 | 2.51 | 3.414(7) | 154 |
| | C6–H6···O7 [ii] | 0.98 | 2.55 | 3.236(5) | 127 |
| | C14–H14···O5 [i] | 0.93 | 2.65 | 3.532(6) | 158 |
| | C17–H17*C*···O1 [i] | 0.96 | 2.46 | 3.413(7) | 171 |
| **20·DCE** | C3–H3···O10 [i] | 0.98 | 2.49 | 3.395(5) | 153 |
| | C6–H6···O7 [ii] | 0.98 | 2.50 | 3.185(4) | 127 |
| | C14–H14···O5 [i] | 0.93 | 2.62 | 3.500(5) | 159 |
| | C17–H17*C*···O1 [i] | 0.96 | 2.47 | 3.421(6) | 173 |
| **20·EA** | C3–H3···O10 [i] | 0.98 | 2.49 | 3.359 (4) | 147 |
| | C6–H6···O7 [ii] | 0.98 | 2.54 | 3.204 (3) | 125 |
| | C14–H14···O5 [i] | 0.93 | 2.62 | 3.509 (4) | 160 |
| | C17–H17*C*···O1 [i] | 0.96 | 2.36 | 3.319 (5) | 176 |

Symmetry codes: (i) -x+1, y-1/2, -z+1/2; (ii) -x+1, y+1/2, -z+1/2.

These helices are packed discretely that leave voids between them that are included by the guest solvent molecules. Crystals in which the chirality is maintained around crystallographic $2_1$-axis (resulting in helical packing of molecules) are termed as 'pseudoracemates.'[124] The neighboring helices (with opposite chirality) are

centrosymmetrically related *via* rather weak π···π stacking interactions (C*g*1···C*g*1) between the phenyl rings (C*g*1 = C9-14) of the tosyl groups and by somewhat longer C-H···O (C15–H15*C*···O9) interactions, [Fig. 5.7, Table 5.6]. The dimensions of the cavity that houses weakly coordinated guest molecules are ~ 8 x 7 $Å^2$. The helical assembly across crystallographic two-fold axis *via* C-H···O bonding is consistent feature in the organization of the host molecules in all the solvates of **20**. The lack of guest specificity in solvatomorphs of **20** suggests that the role of guest solvent could be more for 'space filling' to achieve the close packing. It is interesting that varying guest solvents accommodate themselves in these voids without affecting the host architecture. The adaptability of the host and the guest selectivity has always been an area under investigation because of its direct applicability in drug binding *via* non-covalent interactions, molecular separations and molecular recognition *via* selective inclusions.[100,101]

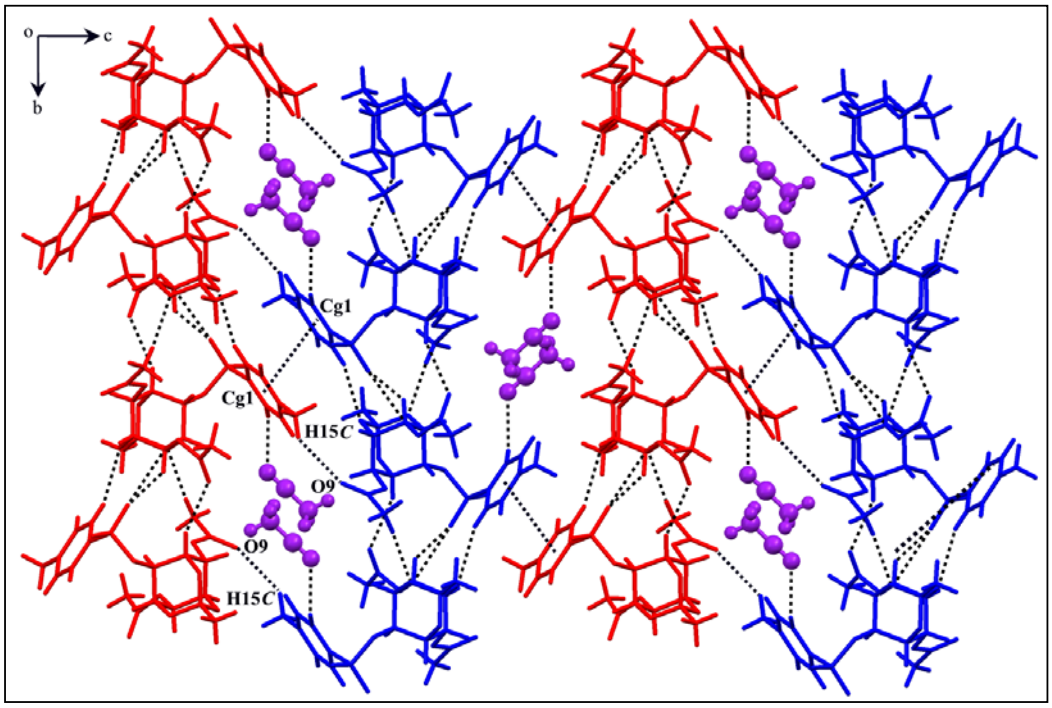


**Figure 5.7**: Molecular layer with included solvent molecules (violet) viewed down *a*-axis in **20·AN**.

**Table 5.6**: Geometrical parameters of weak interactions that linking the chiral helices in the solvatomorphs of **20** as shown in figure 5.7.

| Crystals | D–H···A / Cg···Cg | D–H (Å) | H···A (Å) | D···A / Cg···Cg (Å) | D–H···A / α (º) |
|---|---|---|---|---|---|
| **20·AC** | C15–H15*C*···O9 [i] | 0.96 | 2.82 | 3.523(9) | 131 |
| | C*g*1···C*g*1 [ii] | | | 3.843 | 0.02 |
| **20·AN** | C15–H15*C*···O9 [i] | 0.96 | 2.79 | 3.623(7) | 145 |
| | C*g*1···C*g*1 [ii] | | | 3.807 | 0.00 |
| **20·CF** | C15–H15*C*···O9 [i] | 0.96 | 2.86 | 3.593(10) | 134 |
| | C*g*1···C*g*1 [ii] | | | 3.802 | 0.00 |
| **20·DX** | C15–H15*C*···O9 [i] | 0.96 | 2.72 | 3.649(16) | 162 |
| | C*g*1···C*g*1 [ii] | | | 3.845 | 0.00 |
| **20·NM** | C15–H15*C*···O9 [i] | 0.96 | 2.86 | 3.640(5) | 139 |
| | C*g*1···C*g*1 [ii] | | | 3.823 | 0.03 |
| **20·THF** | C15–H15*C*···O9 [i] | 0.96 | 2.87 | 3.627(6) | 137 |
| | C*g*1···C*g*1 [ii] | | | 3.836 | 0.04 |
| **20·DCM** | C15–H15*C*···O9 [i] | 0.96 | 2.62 | 3.423(6) | 141 |
| | C*g*1···C*g*1 [ii] | | | 3.837 | 0.00 |
| **20·PY** | C15–H15*C*···O9 [i] | 0.96 | 2.86 | 3.580(10) | 133 |
| | C*g*1···C*g*1 [ii] | | | 3.847 | 0.00 |
| **20·DCE** | C15–H15*C*···O9 [i] | 0.96 | 2.73 | 3.591(7) | 150 |
| | C*g*1···C*g*1 [ii] | | | 3.7983 | 0.00 |
| **20·EA** | C15–H15*C*···O9 [i] | 0.96 | 2.65 | 3.504 (6) | 149 |
| | C*g*1···C*g*1 [ii] | | | 3.879 | 0.00 |

Symmetry codes: (i) x, -y+1/2, z-1/2; (ii) 1-x, -y, -z.

In the third dimension, these helical strings (viewed down *b*-axis) showed 'dancing pair' like organization of the molecules [red or blue moiety in Fig. 5.8]. The unit translated dancing pair of molecules along the *a*-axis associate to form columnar assembly. These columns are linked *via* two weak C–H···O interactions namely C19–H19*C*···O1 and C13–H13···O8 (this interaction shifted to C15–H15*A*···O8 in **20·AC**,

**20·DCM** and **20·NM** due to very slight change in the orientation of tosyl group). These columns along the *c*-axis are linked exclusively *via* centrosymmetric π···π stacking interactions creating cavities to accommodate the guest solvents [Fig. 5.8, Table 5.7].

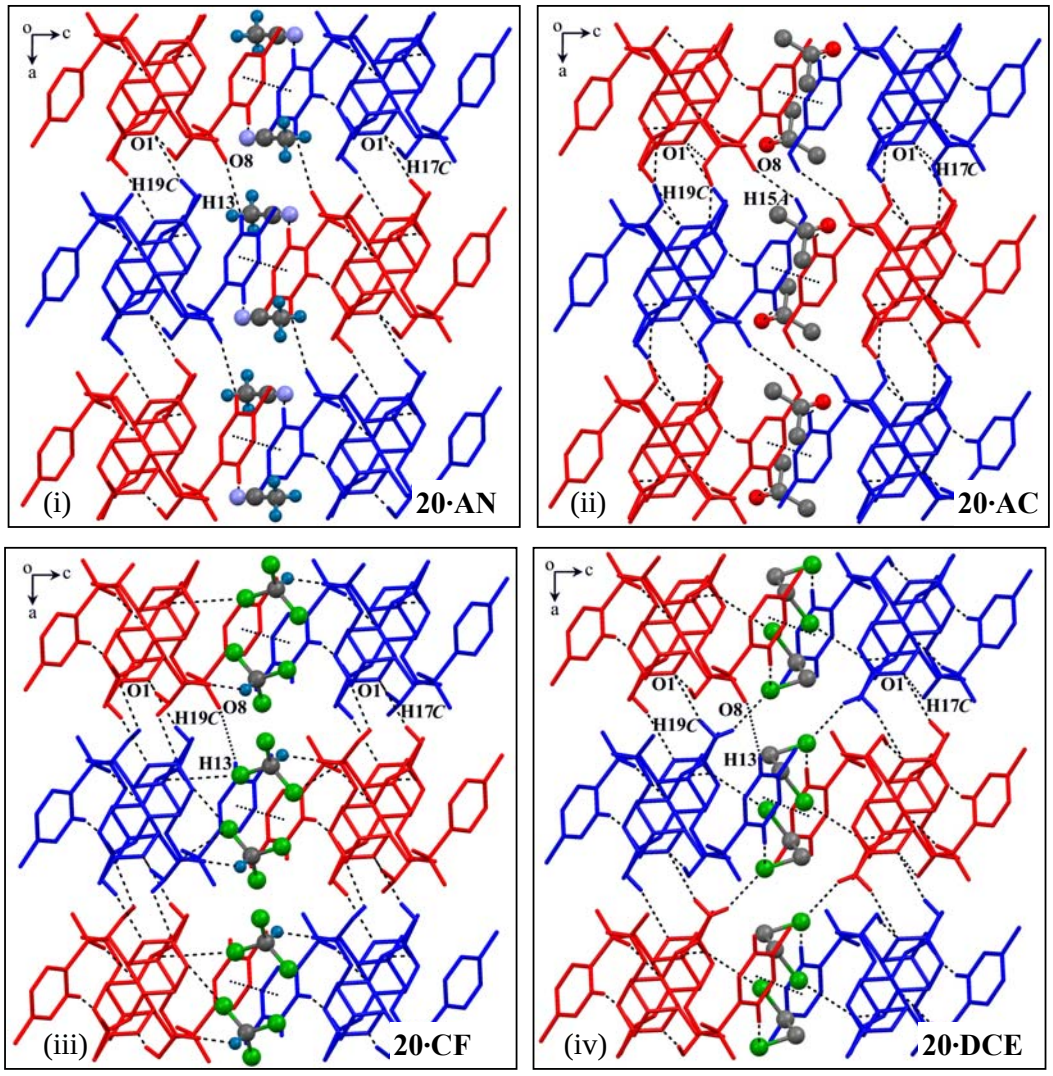


**Figure 5.8**: Molecular layer viewed down *b*-axis in the solvatomorphs of **20**. Solvent inclusion of (i) acetonitrile [**20·AN**], (ii) acetone [**20·AC**], (iii) chloroform [**20·CF**], (iv) 1,2-dichlororethane [**20·DCE**], (v) dichloromethane [**20·DCM**], (vi) dioxane [**20·DX**], (vii) ethyl acetate [**20·EA**], (viii) nitromethane [**20·NM**], (ix) pyridine [**20·PY**] and (x) tetrahydrofuran [**20·THF**].

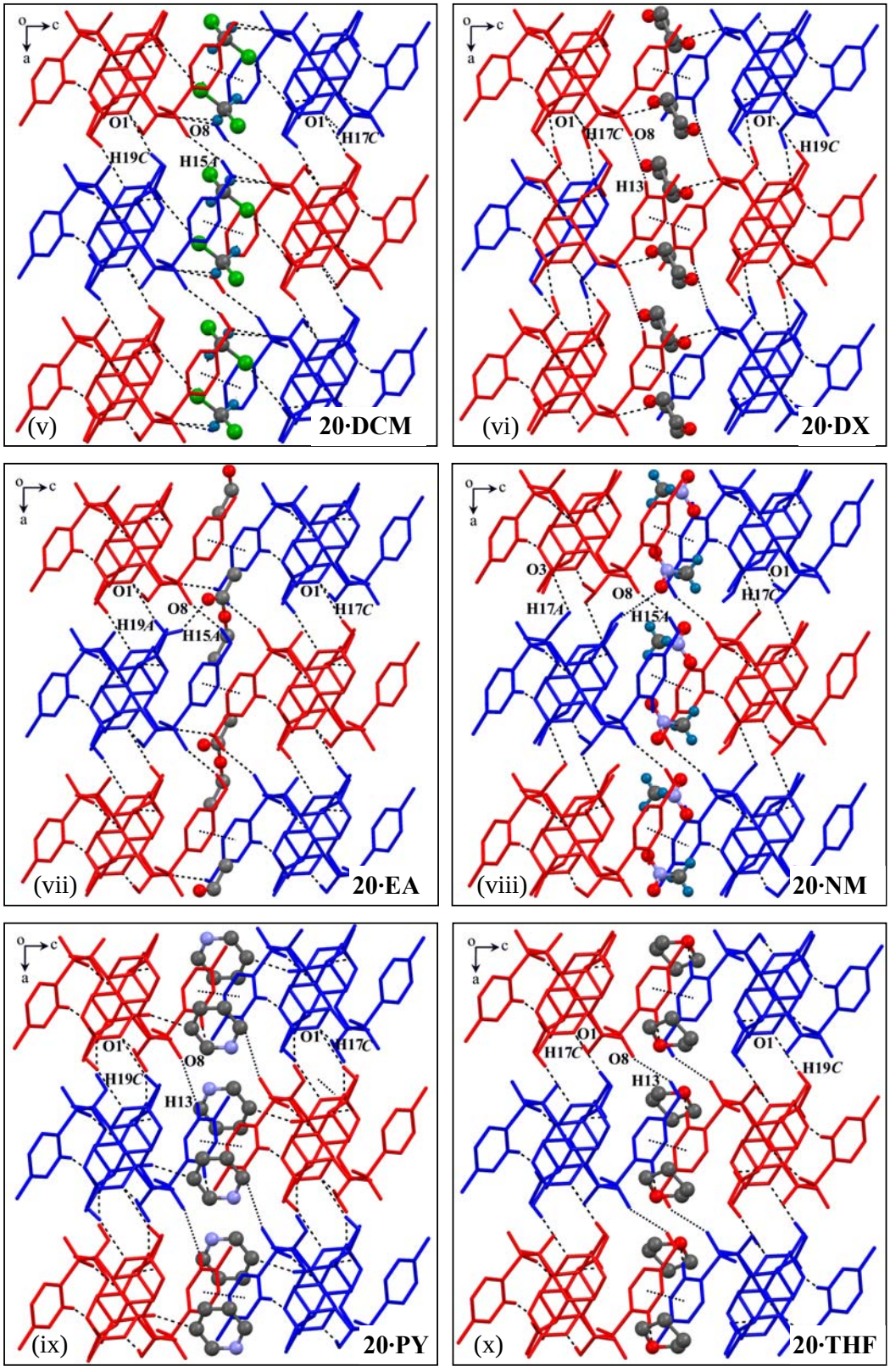


**Figure 5.8**: Continued.

**Table 5.7**: Hydrogen bonding interaction geometry in solvatomorphs of **20** as shown in figure 5.8.

| Crystals | D–H···A | D–H (Å) | H···A (Å) | D···A (Å) | D–H···A (º) |
|---|---|---|---|---|---|
| **20·AC** | C13–H13···O8 $^{i}$ | 0.93 | 2.73 | 3.453(6) | 135 |
| | C19–H19C···O1 $^{i}$ | 0.96 | 2. 60 | 3.559(7) | 174 |
| **20·AN** | C13–H13···O8 $^{i}$ | 0.93 | 2.72 | 3.446(5) | 136 |
| | C19–H19C···O1 $^{i}$ | 0.96 | 2. 61 | 3.547(6) | 165 |
| **20·CF** | C13–H13···O8 $^{i}$ | 0.93 | 2.72 | 3.459(7) | 137 |
| | C19–H19C···O1 $^{i}$ | 0.96 | 2.62 | 3.551(8) | 162 |
| **20·DX** | C13–H13···O8 $^{i}$ | 0.93 | 2.80 | 3.524(12) | 136 |
| | C19–H19C···O1 $^{i}$ | 0.96 | 2. 69 | 3.650(14) | 177 |
| **20·NM** | C13–H13···O8 $^{i}$ | 0.93 | 2.76 | 3.476(4) | 134 |
| | C19–H19C···O1 $^{i}$ | 0.96 | 2.81 | 3.582(4) | 138 |
| **20·THF** | C13–H13···O8 $^{i}$ | 0.93 | 2.74 | 3.471(4) | 136 |
| | C19–H19C···O1 $^{i}$ | 0.96 | 2.63 | 3.592(4) | 176 |
| **20·DCM** | C13–H13···O8 $^{i}$ | 0.93 | 2.78 | 3.493(4) | 135 |
| | C19–H19C···O1 $^{i}$ | 0.96 | 2.71 | 3.593(5) | 154 |
| **20·PY** | C13–H13···O8 $^{i}$ | 0.93 | 2.76 | 3.501(6) | 137 |
| | C19–H19C···O1 $^{i}$ | 0.96 | 2.67 | 3.576(7) | 158 |
| **20·DCE** | C13–H13···O8 $^{i}$ | 0.93 | 2.75 | 3.490(5) | 137 |
| | C19–H19C···O1 $^{i}$ | 0.96 | 2. 67 | 3.588(6) | 161 |
| **20·EA** | C13–H13···O8 $^{i}$ | 0.93 | 2.73 | 3.462(4) | 136 |
| | C19–H19C···O1 $^{i}$ | 0.96 | 2. 64 | 3.596(5) | 172 |

Symmetry code: (i) x+1, y, z

### *5.3.3.1. Host-Guest Interactions in solvatomorphs of 20*

The fact that **20** crystallizes only by inclusion of solvent molecules, and we have been unsuccessful in obtaining solvent free crystals of **20**, suggest the role of solvent molecules in crystal formation. The structural analysis of all the solvatomorphs indicates only one site for the guest in the crystal lattice. It is noteworthy that the included guest solvents make different weak interactions with the host molecules and the significant interactions are shown in figure 5.9 [Table 5.8].

The acetone guest in **20·AC** makes bifurcated C–H···O interactions to the host [Fig. 5.9(i), Table 5.8] whereas acetonitrile linked *via* C–H···N contacts in **20·AN** crystals [Fig. 5.9(ii), Table 5.8]. Additionally, the acetonitrile guests themselves bind *via* weak C–H···π interactions between the methyl (H20*A*) and the cyanide group (C21≡N1) in the voids. It is interesting to note that all halogenated solvent molecules (chloroform in **20·CF**, 1,2-dichloroethane in **20·DCE** and dichloromethane in **20·DCM** linked to the host *via* C–H···O interaction as well as halogen bonding (C–Cl···O) in their crystals [Fig. 5.9(iii)-(v), Table 5.8]. In **20·DX** and **20·EA**, the dioxane and ethyl acetate guests make only C–H···O interaction to the host molecule [Fig. 5.9(vi)-(vii), Table 5.8]. However, the nitromethane molecules bind to the host molecule *via* three weak C–H···O interactions namely, C19–H19*A*···O11, C20–H20*B*···O10 and C20–H20*C*···O9 in **20·NM** [Fig. 5.9(viii), Table 5.8]. In case of **20·PY** and **20·THF** crystals, the guests (pyridine and tetrahydrofuran) linked to the host *via* bifurcated C–H···O interactions [Fig. 5.9(ix)-(x), Table 5.8].

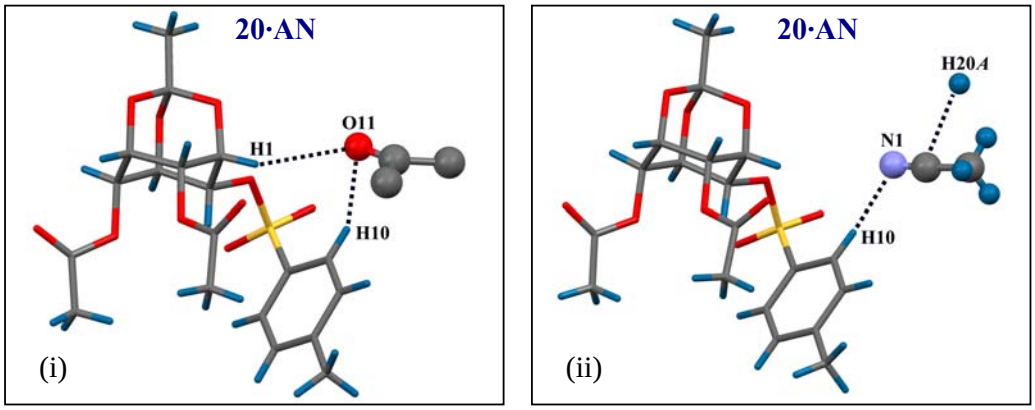


**Figure 5.9**: Significant host-guest interactions in solvatomorphs of **20**. (i) Acetone in **20·AC**; (ii) acetonitrile in **20·AN**; (iii) chloroform in **20·CF**; (iv) 1,2-dichloromethane in **20·DCE**; (v) dichloromethane in **20·DCM**; (vi) dioxane in **20·DX**; (vii) ethyl acetate in **20·EA**; (viii) nitromethane in **20·NM**; (ix) pyridine in **20·PY** and (x) tetrahydrofuran in **20·THF**.

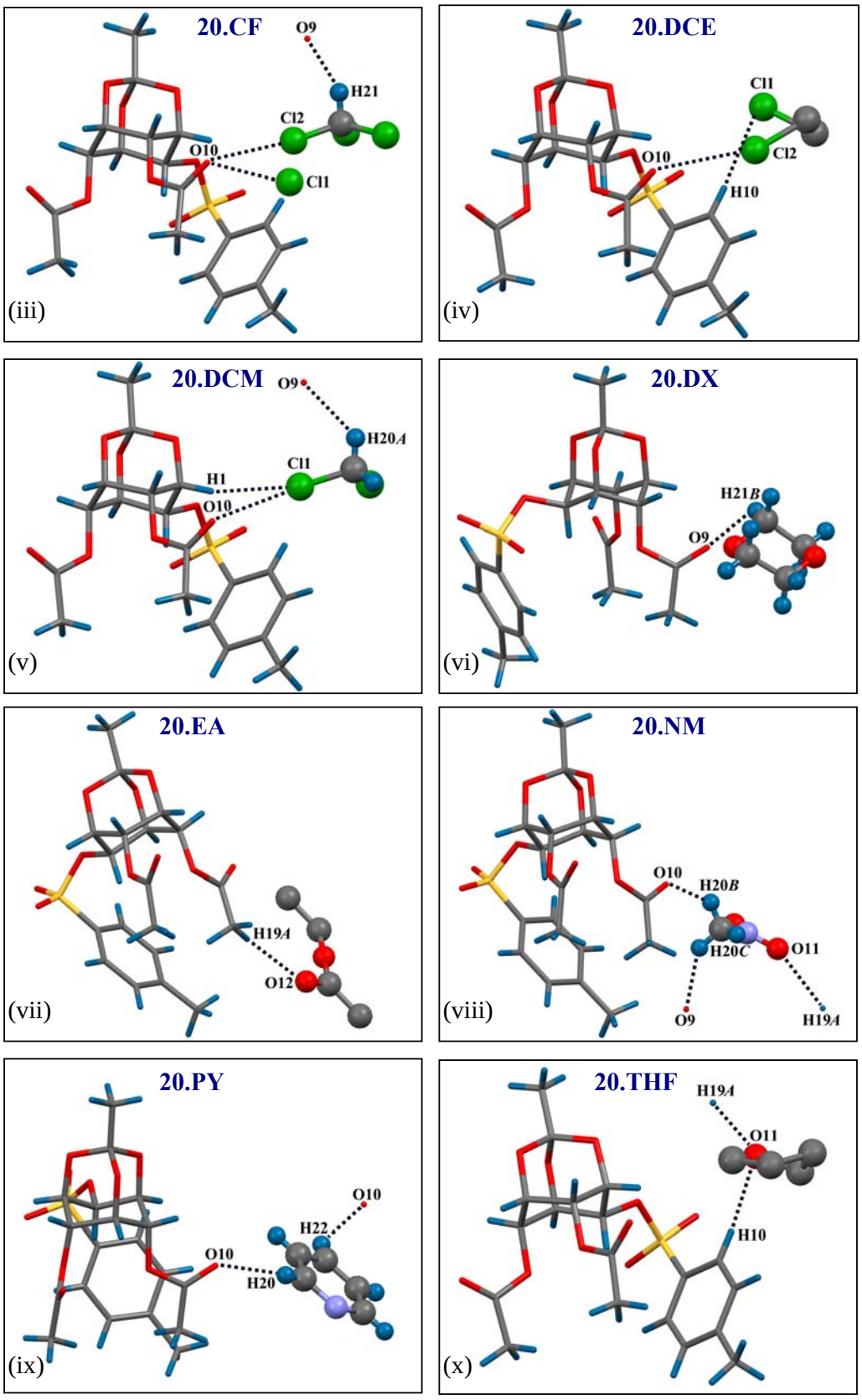


**Figure 5.9**: Continued. Significant host-guest interactions in solvatomorphs of **20**.

**Table 5.6**: Geometrical parameters of host-guest interactions in solvatomorphs of **20** as shown in figure 5.9.

| Crystals | D–H···A | D–H (Å) | H···A (Å) | D···A (Å) | D–H···A (º) |
|---|---|---|---|---|---|
| **20·AC** | C10–H10···O11 [i] | 0.93 | 2.71 | 3.391(16) | 131 |
| | C1–H1···O11 [i] | 0.98 | 2.76 | 3.657(15) | 152 |
| **20·AN** | C10–H10···N1 [i] | 0.93 | 2.61 | 3.342(10) | 136 |
| | C20–H20A···C21 [ii] | 0.98 | 2.48 | 3.171(4) | 128 |
| **20·CF** | C21–H21···O9 [iii] | 0.98 | 2.29 | 3.12(3) | 143 |
| | C21–Cl1···O10 [iv] | | 2.797 | | 166 |
| | C21–Cl2···O10 [v] | | 3.119 | | 172 |
| **20·DCE** | C10-H10···Cl1 [vi] | 0.93 | 2.93 | 3.731(7) | 145 |
| | C21-Cl2···O10 [vii] | - | 3.226(7) | - | 161 |
| **20·DCM** | C1–H1···Cl1 [i] | 0.98 | 3.00 | 3.942(5) | 163 |
| | C20–H20A···O9 [iv] | 0.97 | 2.63 | 3.343(12) | 131 |
| | C21–Cl1···O10 [viii] | | 3.235 | | 163 |
| **20·DX** | C21–H21B···O9 [ix] | 0.97 | 2. 65 | 3.35(10) | 129 |
| **20·EA** | C19–H19A···O12 [vi] | 0.96 | 2.53 | 3.373(12) | 147 |
| **20·NM** | C19–H19A···O11 [x] | 0.96 | 2.73 | 3.615(7) | 154 |
| | C20–H20B···O10 [xi] | 0.96 | 2.74 | 3.281(6) | 116 |
| | C20–H20C···O9 [vi] | 0.96 | 2.76 | 3.453(6) | 130 |
| **20·PY** | C20–H20···O10 [xii] | 0.93 | 2.41 | 3.246(9) | 149 |
| | C22–H22···O10 [xii] | 0.93 | 2.71 | 3.500(9) | 143 |
| **20·THF** | C10–H10···O11 [ii] | 0.93 | 2.62 | 3.426(17) | 146 |
| | C19–H19A···O11 [xi] | 0.96 | 2.80 | 3.620(16) | 144 |

Symmetry codes: (i) -x+1, y-1/2, -z+1/2; (ii) x+1, -y+3/2, z+1/2; (iii) -x, y-1/2, -z+3/2; (iv) x, y+1, z; (v) -x, -y+1, 1-z; (vi) x, y, z; (vii) 1-x, 2-y, -z; (viii) –x+1, y+1/2, -z+1/2; (ix) -x+1, y+1/2, -z+3/2; (x) -x+2, y+1/2, -z+1/2; (xi) x, -y+3/2, z+1/2; (xii) 1-x, 1-y, 2-z.

### 5.3.4. Molecular Organization in Crystals of 21

The crystal structure analysis of **21** revealed interesting centrosymmetric dimeric association *via* dipolar S=O···C=O and C–H···O contacts [Fig. 5.10, Table

5.7]. The sulfonyl oxygen *O7* and *O8* make short contacts with the carbonyl carbon, *C23* and inositol ring proton H1 respectively of the molecule related by inversion. Geometrical parameters [O7···C23 = 3.194 (3) Å, O7···C23=O10 = 84.4 (2)° and S1=O7···C23 = 147.9 (2)°; symmetry code: 1-x, 1-y, 1-z] for the approach of the S=O dipole towards the C=O group indicates a Type-I (perpendicular) interaction motif.[112] A similar dipolar S=O···C=O contact with Type-I motif was observed in the diastereomers of **8** resulting in the inclusion of solvents whereas solvent free form of **9** had shown Type-III interaction motif in their crystals (*Chapter 2* and *7*). However in both cases (**8** and **9**) these interactions participating S=O was also involved in C–H···O interactions (complementary, *Chapter 2*, page no. 46). The 'stand alone' S=O···C=O contacts in **21** is the only example that evidences for the existence of these bond dipolar interactions, without masked by any other intermolecular contribution.

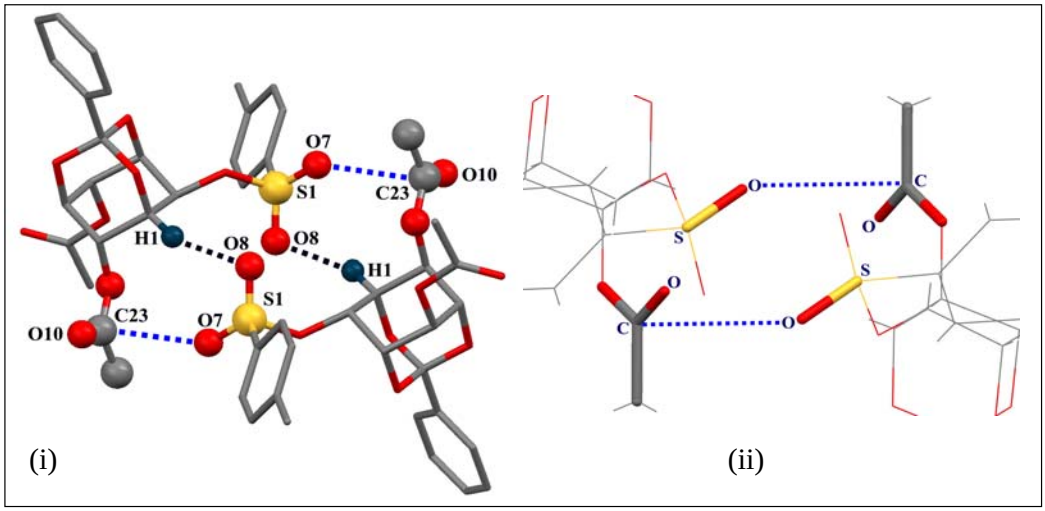


**Figure 5.10**: (i) Dimeric bridging *via* of S=O···C=O contacts (blue dashed lines) and C–H···O interactions (black dashed lines) in the crystals of **21**; (ii) Type-I dipolar S=O···C=O interaction motif in **21**.

The dimers associated *via* S=O···C=O and C–H···O contacts are linked to form molecular chains *via* weak C–H···O interactions along *c*-axis. The orthoester oxygen

*O3* makes contacts with *H16* of the tosyl group along *c*-axis. These chains translated to form 2D molecular layer *via* centrosymmetric C–H···O interactions between the carbonyl oxygen O10 and inositol ring proton H5 along *a*-axis [Fig. 5.11, Table 5.7].

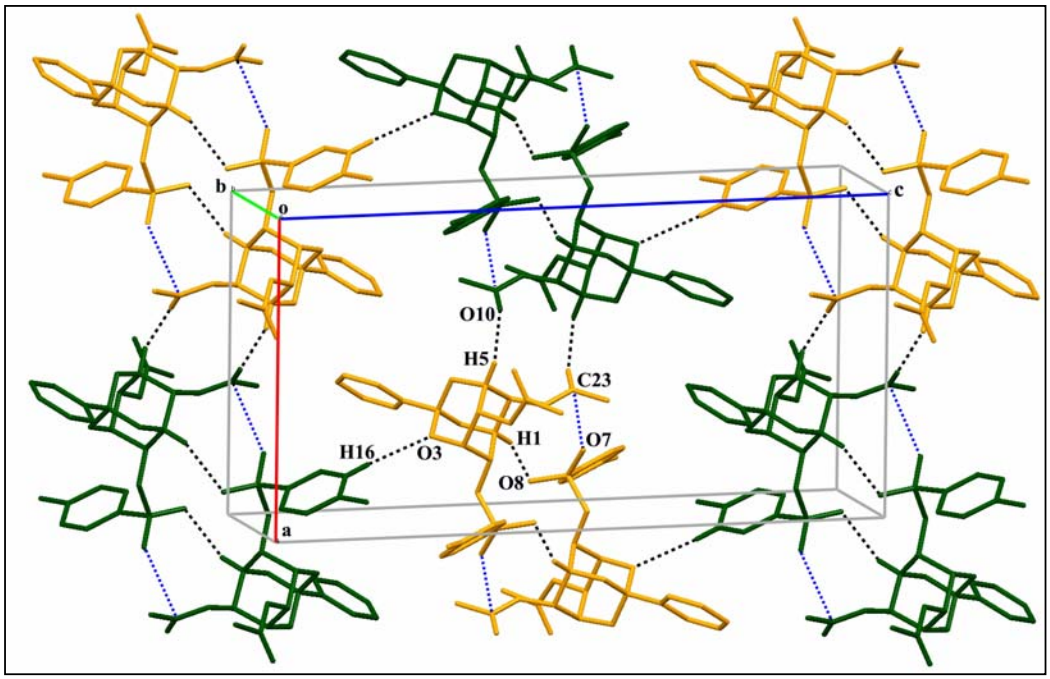


**Figure 5.11**: Molecular layer formation viewing down *b*-axis *via* C–H···O interactions in the crystals of **21**.

**Table 5.7**: Geometrical parameters of intermolecular hydrogen bonds in **21**.

| Crystals | D–H···A | D–H (Å) | H···A (Å) | D···A (Å) | D–H···A (°) |
|---|---|---|---|---|---|
| **21** | C1–H1···O8 [i] | 0.98 | 2.56 | 3.490 (3) | 159 |
| | C5–H5···O10 [ii] | 0.98 | 2.58 | 3.153 (3) | 117 |
| | C16–H16···O3 [iii] | 0.93 | 2.68 | 3.590 (4) | 168 |
| | C19–H19···O8 [iv] | 0.93 | 2.72 | 3.299 (3) | 121 |
| | C22–H22C···O10 [v] | 0.96 | 2.63 | 3.435 (4) | 142 |
| | C24–H24B···O9 [vi] | 0.96 | 2.46 | 3.360 (3) | 156 |

Symmetry codes: (i) 2-x, 2-y, 1-z (ii) 1-x, 2-y, 1-z (iii) 2-x, -1/2+y, 1/2-z (iv) 2-x, 1-y, 1-z (v) x, -1+y, z (vi) 1- x, 1-y, 1-z.

These molecular layers [Fig. 5.11] are packed closely *via* C22–H22*C*···O10 and C24–H24*B*···O9 interactions in the third dimension without leaving voids for solvent inclusion or polymorphic phase change upon heating [Fig. 5.12, Table 5.7].

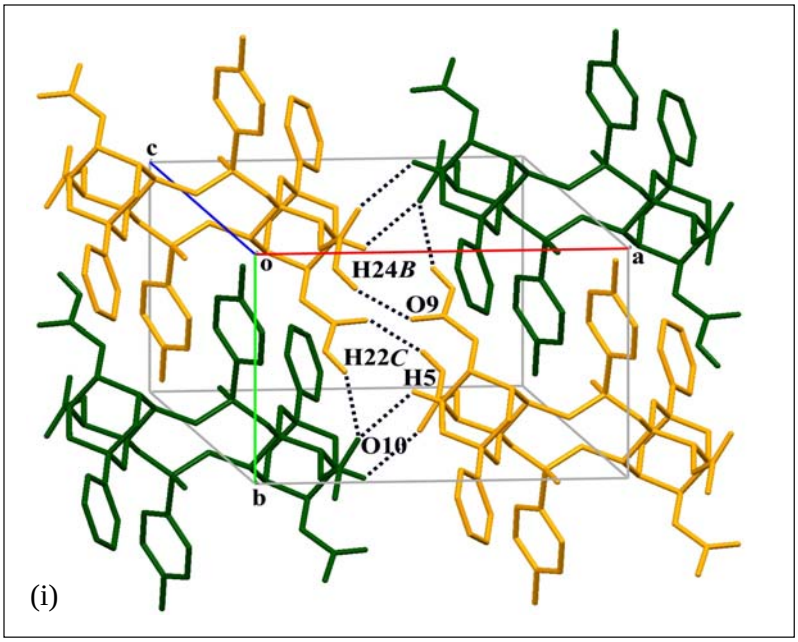


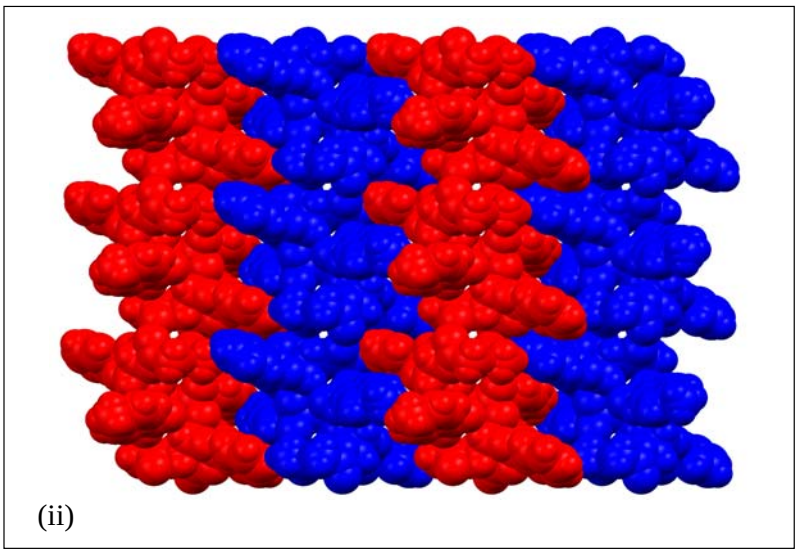


**Figure 5.12**: (i) Molecular packing of **21** viewing down *c*-axis *via* C–H···O interactions; (ii) CPK view of **21** viewed down *b*-axis.

### 5.4. Effect of Molecular Conformation on Solvent Inclusion Behavior

It is intriguing to note that the orientational change of tosyl as well as acetyl groups in the inclusion crystals of **20** is subtly modified to accommodate the guest solvents; whereas the tosyl group in the crystals of **19** and **21** achieved a 'close packing' without leaving any void for the inclusion of solvents [Fig. 5.13].

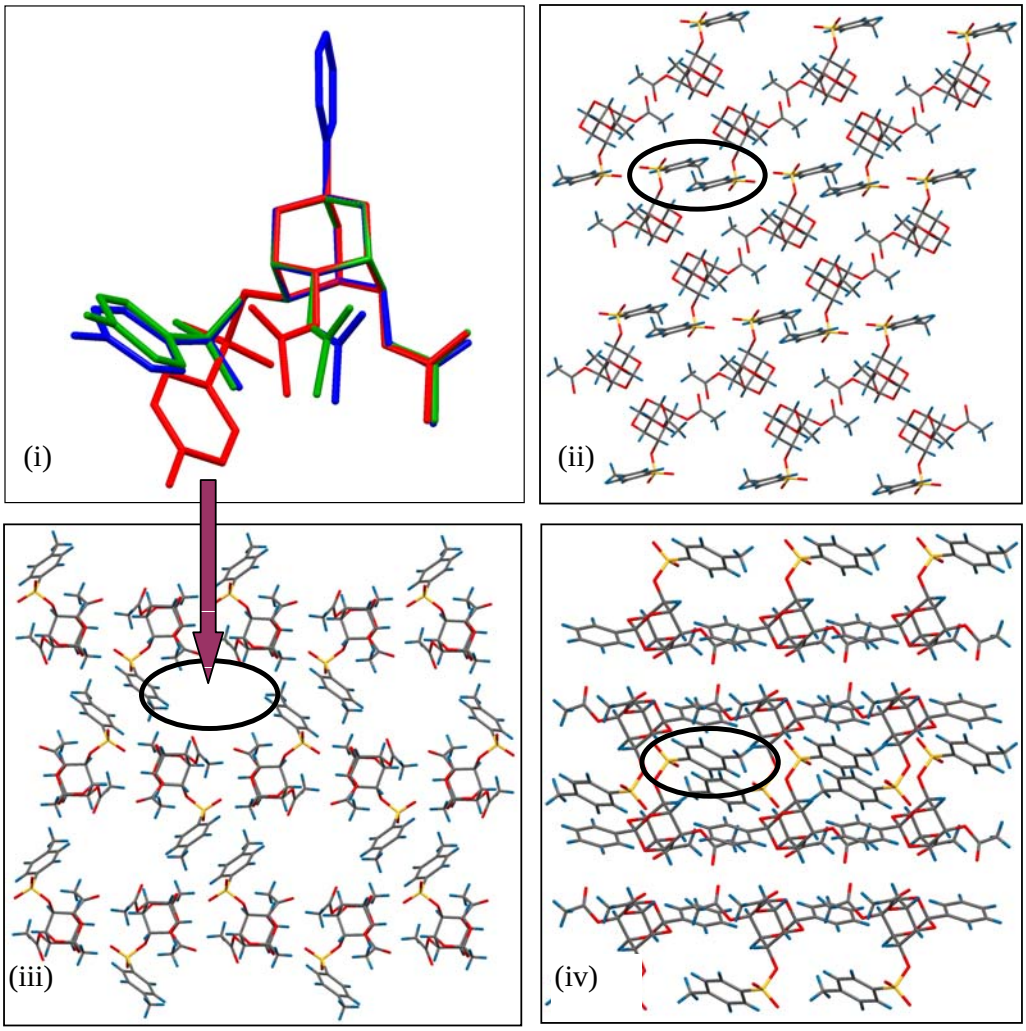


**Figure 5.13**: Molecular packing showing that orientational change of tosyl group created voids for guest inclusion in **20** and a close packing in crystals of **19** and **21**. (i) molecular overlap of **19** [green], **20·AC** [red] and **21** [blue]; (ii) molecular layer in **19** [down *c*-axis] (iii) molecular layer in **20** with voids [down *c*-axis] and (iv) molecular layer in **21**[down *c*-axis].

## 5.5. Conclusions

A comparison of the conformation of individual molecules in crystals of **19**, **20** and **21** reveal that a slight orientational change in **20** can create different packing to accommodate solvent molecules in its crystal lattice. Isomorphic crystal structures of **20** were observed in all the inclusion crystals with structurally different guest molecules. The only example of independent S=O···C=O contact is observed in **21**, in all other cases the same dipoles were also engaged in other weak interactions such as C–H···O.

# Chapter 6

## Solvatopolymorphism in 1,2,3,4(6),5-Penta-*O*-Acetyl-6(4)-*O*-[(1*S*)-10-Camphorsulfonyl]-*myo*-Inositol: Conserved Molecular Association of Diastereomers *via* Trifurcated C–H···O Interactions

# Chapter 6

## 6.1. Introduction

As seen in *Chapters 2* and *5*, solvents were incorporated in the crystal lattices as a result of either different molecular associations or conformational modifications of *myo*-inositol orthoesters. However, all of them contained a rigid adamantane like *myo*-inositol orthoester bridge. In order to explore (pseudo) polymorphic behavior possibly with the involvement of dipolar interactions, hexa-*O*-substituted *myo*-inositol derivatives were synthesized [Scheme 6.1]. Thus, diastereomeric mixture of 1,2,3,4(6),5-penta-*O*-acetyl-6(4)-*O*-[(1*S*)-10-camphorsulfonyl]-*myo*-inositol (**22**) and racemic 1,2,3,4,5-penta-*O*-acetyl-6-*O*-tosyl-*myo*-inositol (**23**) were prepared, the former showed solvent inclusion behavior. This chapter describes an interesting case of solvatopolymorphism[32] in **22** with the inclusion of dichloromethane molecules.

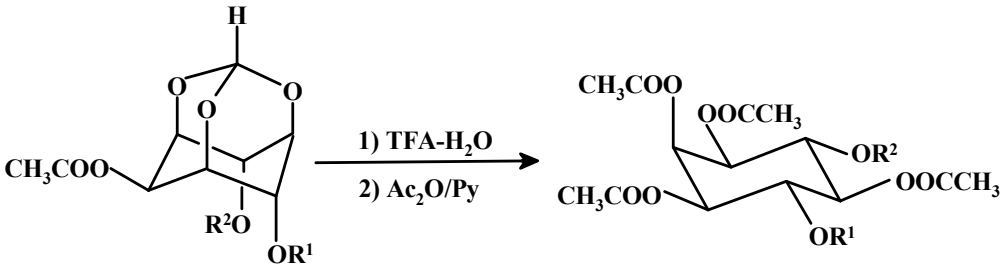


**11. $R^1$ = CS ($CH_3CO$), $R^2$ = $CH_3CO$ (CS)**
**16. $R^1$ = $CH_3CO$ (Ts), $R^2$ = Ts ($CH_3CO$)**

**11 & 22 : Diastereomeric mixture**

**22. $R^1$ = CS ($CH_3CO$), $R^2$ = $CH_3CO$ (CS)**
**23. $R^1$ = $CH_3CO$ (Ts), $R^2$ = Ts ($CH_3CO$)**

**16 & 23 : Racemic**

**Scheme 6.1**

## 6.2. Experimental Section

### *6.2.1. Synthesis*

*6.2.1.1. Preparation of 1,2,3,4(6),5-penta-O-acetyl-6(4)-O-[(1S)-10-camphor-sulfonyl]-myo-inositol* (**22**, diastereomeric mixture)

The camphorsulfonate **11** (0.244 g, 0.5 mmol) was stirred with 4:1 (v/v) mixture of trifluroacetic acid (TFA) and water at room temperature for 24 h. TFA and water were evaporated under reduced pressure and the residue obtained was dissolved in dry pyridine (4 mL). A solution of acetic anhydride (0.2 mL, 2.10 mmol) in pyridine (2 mL) was added drop-wise and the mixture stirred for 12 h. The solvents were evaporated from the reaction mixture under reduced pressure and the residue obtained worked up with ethyl acetate. Colorless solid (**22**) was obtained after column chromatography using ethyl acetate-petroleum ether as eluent (0.229 g, 76 %).

Data for **22**:

**M.P.**: 173-174 °C

**IR** ($CHCl_3$)**ν**: 1755 $cm^{-1}$ (C=O)

**$^1$H NMR** (200 MHz, $CDCl_3$): **δ** 0.86 (s, 3H, Me), 1.12 (s, 3H, Me), 1.36-1.48 (m, 1H), 1.59-1.68 (m, 1H), 2.04 (s, 3H, MeCO), 2.02 (s, 3H, MeCO), 2.10 (2s, 3H), 2.13 (2s, 3H, MeCO), 2.14, 2.16 (2s, 3H, MeCO), 2.21, 2.22 (2s, 3H, MeCO), 2.32-2.50 (m, 2H), 2.96-3.06 (d, 1H), 3.48-362 (2d, 1H), 5.06-5.19 (m, 3H, InsH), 5.20-5.32 (m, 1H, InsH), 5.48 (t, *J*= 10.0 Hz, 1H, Ins H), 5.61-5.65 (m, 1H, Ins H) ppm.

**$^{13}$C NMR** (50 MHz, $CDCl_3$): **δ** 19.6,19.8, 19.9, 20.3, 20.4, 20.9, 20.7, 24.9 ($CH_2$), 25.0 ($CH_2$), 26.7 ($CH_2$), 42.3 ($CH_2$), 42.7, 47.6, 47.7, 48.8 ($CH_2$), 57.8, 57.9, 67.9, 68.0, 68.3, 69.3, 70.0, 70.1, 169.3, 169.4, 169.5, 169.6, 169.7, 169.8, 214.0 ppm.

**Anal. Calcd for $C_{26}H_{36}O_{14}S$**: C, 51.65; H, 6.00; Found: C, 51.79; H, 6.17 %.

*6.2.1.2. Preparation of racemic 1,2,3,4,5-penta-O-acetyl-6-O-tosyl-myo-inositol* (**23**)

Racemic 2,4-di-*O*-acetyl 6-*O*-tosyl *myo*-inositol 1,3,5-orthoformate (**16**, 0.428

g, 1mmol) was stirred with 4:1 (v/v) mixture of TFA and water at room temperature for 24h. The residue obtained after the removal of solvents, dissolved in dry pyridine (5 mL) and followed by the addition of acetic anhydride (0.3 mL, 3.15 mmol) in pyridine (3 mL). The reaction mixture was stirred for 12 h. The solvents were evaporated under reduced pressure and residue obtained was worked up using ethyl acetate and finally purified by column chromatography (0.447 g, 82 %).

Data for **23**:

**M.P.**: 191-192 °C

**IR** ($CHCl_3$)**ν**: 1759 $cm^{-1}$

**$^1$H NMR** (200 MHz, $CDCl_3$): **δ** 1.88 (s, 3H, MeCO), 1.94 (s, 3H, MeCO), 1.99 (s, 3H, MeCO), 2.01 (s, 3H, MeCO), 2.23 (s, 3H, MeCO), 2.44 (s, 3H, ArMe), 5.01-5.15 (m, 2H, Ins H), 4.17-5.31 (m, 2H, Ins H), 5.37-5.53 (m, 1H, Ins H), 5.58 (t, *J* = 2.5 Hz, 1H, Ins H), 7.23-7.39 (m, 2H, ArH), 7.66-7.82 (m, 2H, ArH) ppm.

**$^{13}$C NMR** (50 MHz, $CDCl_3$): **δ** 20.2, 20.3, 20.4, 20.6, 21.5, 67.8, 68.1, 68.3, 69.3, 69.9, 127.4, 129.7, 134.1, 144.9, 169.2, 169.3, 169.4, 169.6 ppm.

**Anal. Calcd for $C_{23}H_{28}O_{13}S$**: C, 50.73; H, 5.18; Found: C, 50.63; H, 5.11 %.

### *6.2.2. Crystallization*

Crystallization experiments were carried out by diffusing vapors of light petroleum ether (bp 40-60°C) into a solution of **22** and **23** in the desired organic solvents at room temperature. Very thin needles of **22** were produced from dioxane, dimethyl formamide and tetrahydrofuran, not suitable for single crystal X-ray studies. However, suitable plate like inclusion crystals of **22** were obtained from dichloromethane (**22·1DCM**), acetonitrile (**22·AN**), nitromethane (**22·NM**), acetone (**22·AC**), chloroform (**22·CF**) and 1,2-dichloroethane (**22·DCE**) by diffusing petroleum ether (boiling range 40-60°C) to their respective solutions at room temperature. Mixtures of solvents in different ratios (1:1, 1:3 and 3:1) were also used

for exploring the guest selectivity. These experiments did not yield any crystals except in acetone-dichloromethane (3:1), which also gave plates (**22·2DCM**). There are three different types of solvated crystals obtained for **22**, Form-I: triclinic crystals (space group *P1*) from dichloromethane (**22·1DCM**); Form-II: triclinic crystals (space group *P1*) from acetonitrile (**22·AN**) and nitromethane (**22·NM**), and Form-III: monoclinic crystals (space group $P2_1$) from acetone (**22·AC**), chloroform (**22·CF**), 1,2-dichloroethane (**22·DCE**) and acetone-dichloromethane mixture (**22·2DCM**). All the solvated crystals of **22** were stable in open atmosphere for ~2-4 days, after which they slowly disintegrated into powder. We were unable to obtain solvent free crystals of **22**. The tosylate **23** gave always solvent free, colorless crystals from all the solvents used for **22**.

### *6.2.3. Crystallographic Details*

X-ray intensity data were collected on a Bruker SMART APEX CCD diffractometer in omega and phi scan mode, $\lambda_{MoK\alpha}$ = 0.71073 Å at room temperature for the crystals of **23**. Due to the moderate stability (~ 2-4 days), crystals of all the solvatomorphs of **22** were coated with oil (to prevent atmospheric contact) and the data measured at low temperature (133 K) using OXFORD LN2 cryosystem. All the intensities were corrected for Lorentzian, polarization and absorption effects using Bruker's *SAINT* and *SADABS* programs. The crystal structures were solved by Direct methods using program *SHELXS-97*; the full-matrix least squares refinements on $F^2$ were carried out by using *SHELXL-97*. Hydrogen atoms were included in the refinement as per the riding model. Table 6.1 summarizes the crystal data for all the compounds and the ORTEP views of **22** and **23** are shown below [Fig. 6.1].

**Table 6.1**: Summary of crystallographic data for **23** and solvatomorphs of **22**.

| Crystal data | **22·1DCM** Form-I | **22·AN** Form-II | **22·NM** Form-II | **22·AC** Form-III |
|---|---|---|---|---|
| Chemical Formula | $C_{26}H_{36}O_{14}S$ 0.25 ($CH_2Cl_2$) | $C_{26}H_{36}O_{14}S$ $CH_3CN$ 0.5 ($H_2O$) | $C_{26}H_{36}O_{14}S$ $CH_3NO_2$ 0.25 ($H_2O$) | $C_{26}H_{36}O_{14}S$ 0.75($C_3H_6O$) |
| $M_r$ | 622.84 | 653.66 | 665.65 | 648.17 |
| Morphology | Plate | Plate | Plate | Plate |
| Colour | Colorless | Colorless | Colorless | Colorless |
| Crystal size (mm) | 0.45 × 0.29 × 0.22 | 0.60 × 0.44 × 0.35 | 0.69 × 0.49 × 0.13 | 0.62 × 0.59 × 0.38 |
| Crystal system | Triclinic | Triclinic | Triclinic | Monoclinic |
| Space group | *P1* | *P1* | *P1* | $P2_1$ |
| $a$ (Å) | 11.499 (5) | 12.404 (4) | 12.401 (4) | 13.597 (4) |
| $b$ (Å) | 11.793 (5) | 12.492 (4) | 12.587 (4) | 14.351 (4) |
| $c$ (Å) | 12.374 (5) | 13.331 (4) | 13.250 (4) | 17.818 (5) |
| $\alpha$ (°) | 94.564 (7) | 99.188 (5) | 98.697 (5) | 90 |
| $\beta$ (°) | 101.799 (7) | 109.620 (5) | 108.729 (5) | 91.466 (5) |
| $\gamma$ (°) | 105.126 (7) | 116.837 (4) | 117.919 (4) | 90 |
| $V$ (Å$^3$) | 1569.9 (11) | 1612.8 (9) | 1614.5 (9) | 3475.7 (18) |
| $Z$, $D_x$ (Mg m$^{-3}$) | 2, 1.318 | 2, 1.346 | 2, 1.369 | 4, 1.239 |
| $\mu$ (mm$^{-1}$) | 0.210 | 0.170 | 0.174 | 0.157 |
| *F(000)* | 658 | 692 | 704 | 1376 |
| $T_{min}$ , $T_{max}$ | 0.911, 0.955 | 0.905, 0.943 | 0.889, 0.978 | 0.909, 0.943 |
| $\theta_{max}$ (°) | 25.0 | 25.0 | 25.0 | 25.0 |
| $h$ (min, max) | -13, 13 | -14, 14 | -14, 14 | -16, 10 |
| $k$ (min, max) | -14, 13 | -14, 14 | -14, 14 | -17, 16 |
| $l$ (min, max) | -14, 14 | -15, 15 | -15, 15 | -21, 21 |
| No. of refl$^n$ collected | 14953 | 15615 | 14462 | 17415 |
| No. of unique refl$^n$ | 10787 | 11129 | 10684 | 11744 |
| No. of observed refl$^n$ | 7137 | 10663 | 10050 | 9729 |
| No. of parameters | 780 | 817 | 894 | 801 |
| $R_{int}$ | 0.062 | 0.030 | 0.055 | 0.031 |
| $R_1$_obs, $R_1$_all | 0.078, 0.117 | 0.040, 0.041 | 0.080, 0.082 | 0.063, 0.075 |
| $wR_2$_obs, $wR_2$_all | 0.189, 0.221 | 0.104, 0.106 | 0.229, 0.232 | 0.170, 0.185 |
| GoF | 1.01 | 1.04 | 1.08 | 1.03 |
| $\Delta\rho_{max}$, $\Delta\rho_{min}$ (e Å$^{-3}$) | 0.48, –0.55 | 0.28, –0.21 | 0.83, –0.43 | 0.60, –0.34 |
| Flack parameter | 0.11 (12) | 0.02 (5) | 0.08 (13) | –0.01 (10) |

**Table 6.1**: Continued.

| Crystal data | **22·CF** Form-III | **22·DCE** Form-III | **22·2DCM** Form-III | **23** |
|---|---|---|---|---|
| Chemical Formula | $C_{26}H_{36}O_{14}S$ 0.75 ($CHCl_3$) | $C_{26}H_{36}O_{14}S$ $C_2H_4Cl_2$ | $C_{26}H_{36}O_{14}S$ $CH_2Cl_2$ | $C_{23}H_{28}O_{13}S$ |
| $M_r$ | 703.00 | 703.56 | 689.53 | 544.51 |
| Morphology | Plate | Plate | Plate | Plate |
| Colour | Colorless | Colorless | Colorless | Colorless |
| Crystal size (mm) | 0.63 × 0.47 × 0.28 | 0.49 × 0.29 × 0.18 | 0.39 × 0.23 × 0.07 | 0.69 x 0.17 x 0.11 |
| Crystal system | Monoclinic | Monoclinic | Monoclinic | Monoclinic |
| Space group | $P2_1$ | $P2_1$ | $P2_1$ | $P2_1/n$ |
| $a$ (Å) | 13.857 (3) | 13.39 (2) | 13.463 (2) | 15.1420 (18) |
| $b$ (Å) | 14.298 (3) | 14.35 (3) | 14.451 (3) | 6.8671 (8) |
| $c$ (Å) | 17.717 (4) | 17.54 (3) | 17.848 (3) | 25.753 (3) |
| $\alpha$ (°) | 90 | 90 | 90 | 90 |
| $\beta$ (°) | 90.651 (4) | 91.55 (2) | 91.363 (3) | 100.053 (2) |
| $\gamma$ (°) | 90 | 90 | 90 | 90 |
| $V$ (Å$^3$) | 3510.2 (14) | 3372 (11) | 3471.4 (11) | 2636.7 (5) |
| $Z$, $D_x$ (Mg m$^{-3}$) | 4, 1.330 | 4, 1.386 | 4, 1.319 | 4, 1.372 |
| $\mu$ (mm$^{-1}$) | 0.343 | 0.319 | 0.308 | 0.188 |
| *F(000)* | 1471 | 1480 | 1448 | 1144 |
| $T_{min}$ , $T_{max}$ | 0.813, 0.910 | 0.859, 0.945 | 0.889, 0.979 | 0.980, 0.882 |
| $\theta_{max}$ (°) | 25.0 | 25.0 | 25.0 | 25.0 |
| $h$ (min, max) | -16, 16 | -15, 15 | -16, 16 | -13, 18 |
| $k$ (min, max) | -17, 17 | -17, 17 | -17, 17 | -8, 8 |
| $l$ (min, max) | -21, 21 | -20, 20 | -21, 21 | -30, 30 |
| No. of refl$^n$ collected | 42287 | 26497 | 25077 | 12545 |
| No. of unique refl$^n$ | 12340 | 10755 | 11847 | 4622 |
| No. of observed refl$^n$ | 9723 | 8320 | 9192 | 3600 |
| No. of parameters | 867 | 843 | 807 | 340 |
| $R_{int}$ | 0.037 | 0.048 | 0.060 | 0.030 |
| $R_1$_obs, $R_1$_all | 0.064, 0.080 | 0.052, 0.068 | 0.079, 0.097 | 0.074, 0.172 |
| $wR_2$_obs, $wR_2$_all | 0.173, 0.189 | 0.123, 0.130 | 0.209, 0.229 | 0.095, 0.183 |
| GoF | 1.03 | 0.98 | 1.02 | 1.12 |
| $\Delta\rho_{max}$, $\Delta\rho_{min}$ (e Å$^{-3}$) | 0.69, –0.27 | 0.50, –0.37 | 0.80, –0.77 | 0.41, –0.33 |
| Flack parameter | 0.05 (8) | 0.09 (6) | 0.06 (11) | - |

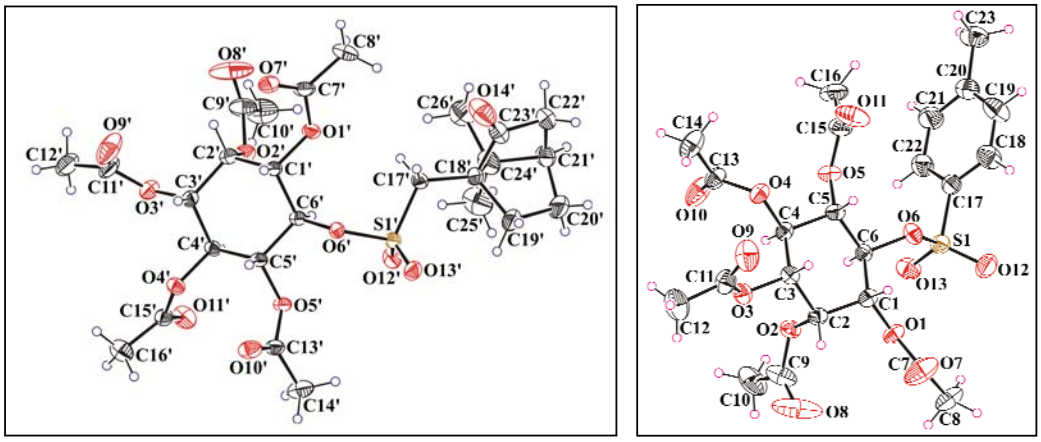


**Figure 6.1**: (i) ORTEP view of **22** (in **22·AC)** with numbering scheme (30 % probability displacement ellipsoids of diastereomer-2). The diastereomer-1, which has camphor sulfonyl group at *C4* and acetyl group at *C6* position of the inositol ring, has unprimed atom labels. (ii) ORTEP view of **23** with 30 % probability ellipsoids level.

Full-matrix least-squares refinements of Forms I and III crystals were carried out by applying geometrical and anisotropic displacement constraints (DFIX, DANG, SIMU and DELU) in *SHELXL97* to retain their molecular geometries close to their ideal values. These constraints were applied particularly to the guest molecules in **22·1DCM** and **22·CF**, and camphorsulfonate group of the host in **22·DCE** and **22·2DCM** crystals. Traces of water molecules (O15 and O16) in **22·AN** were picked up in the difference Fourier, which were assigned occupancies of 0.35 and 0.15 respectively. A single water molecule (O1*W*) having a lower occupancy (0.25) was also located along with nitromethane in the difference Fourier in **22·NM**.

Most of the included guest solvents in Forms II and III showed statistical disorder in their crystal lattice. The oxygen atoms O17 and O18 of the nitromethane guest in site *A* [*see* Fig. 6.8, *in page no*.173] disordered over two positions (O17' and O18') having 0.5 occupancy each, whereas in site *B* [*see* Fig. 6.8, *in page no*.173], all the atoms are disordered over two positions with equal occupancies in **22·NM**. In **22·AC**, the oxygen atoms (O15 and O16) of both the acetone molecules indicated two

positions (O15' and O16') with occupancies 0.25 and 0.375 respectively. The guest in site *A* of **22·CF** crystals also showed two different locations for chloroform molecule with occupancies 0.5 and 0.25 respectively. In **22·DCE** crystals, two positions of chlorine atoms were assigned in the site *B* with occupancies 0.875 (for Cl3 and Cl4) and 0.125 (for Cl3' and Cl4') respectively.

### *6.2.4. Thermal Analysis*

The DTA/TGA of solvated crystals of **22** were carried out (using a Seiko DTA/TGA 320 instrument) to examine the thermal stability of the solvent included crystals. Since we were unable to obtain solvent free crystals of **22**, powder form of **22** (obtained after column chromatography, dried under reduced pressure) was used for thermal analysis to compare with the solvated form. The powder form of **22** free of solvents was established by its $^{1}$H NMR spectrum.

## 6.3. Results and Discussion

### 6.3.1. Crystallization of 22 and 23

Depending on the crystal system, three different types of solvated crystals of **22** were obtained [Table 6.1]. In order to investigate the role of solvent in yielding different crystal forms (triclinic or monoclinic), we carried out crystallization of **22** in mixture of solvents. A 1:1 mixture of acetone (which gave Form-III) and dichloromethane (which gave Form-I) did not produce any crystals. Interestingly, the same solvent mixture in a ratio 3:1 gave monoclinic Form-III crystals, but it included dichloromethane molecules as guests, which were obtained only as Form-I type crystals! This cross over reveals the enigmatic way in which nucleation event takes place. The formation of Form-III crystals with dichloromethane inclusion can be viewed as a phenomenon wherein the nucleation (of Form-III crystals) is initiated by acetone, but the voids are filled by dichloromethane.

### 6.3.2. Thermal Analysis (DTA/TGA) of 22

The DTA/TGA plots of solvatomorphs of **22** are shown in figure 6.2. DTA curves showed a sharp melting endotherm at 174 °C for the powdered form of **22** (solvent free, confirmed by $^{1}$H NMR), whereas all the inclusion complexes showed an endothermic peak (100-120 °C) before the melting endotherm indicating a probable phase transformation due to the escape of guest solvent molecules from the crystal lattice. The thermo-gravimetric analyses of all the solvatomorphs showed a continuous weight loss of 9-20 % in the temperature range 60-160 °C, due to the loss of included solvents from the crystal lattice. All the solvates showed a final endotherm corresponding to the melting of solvent free powder of **22** [Fig. 6.2].

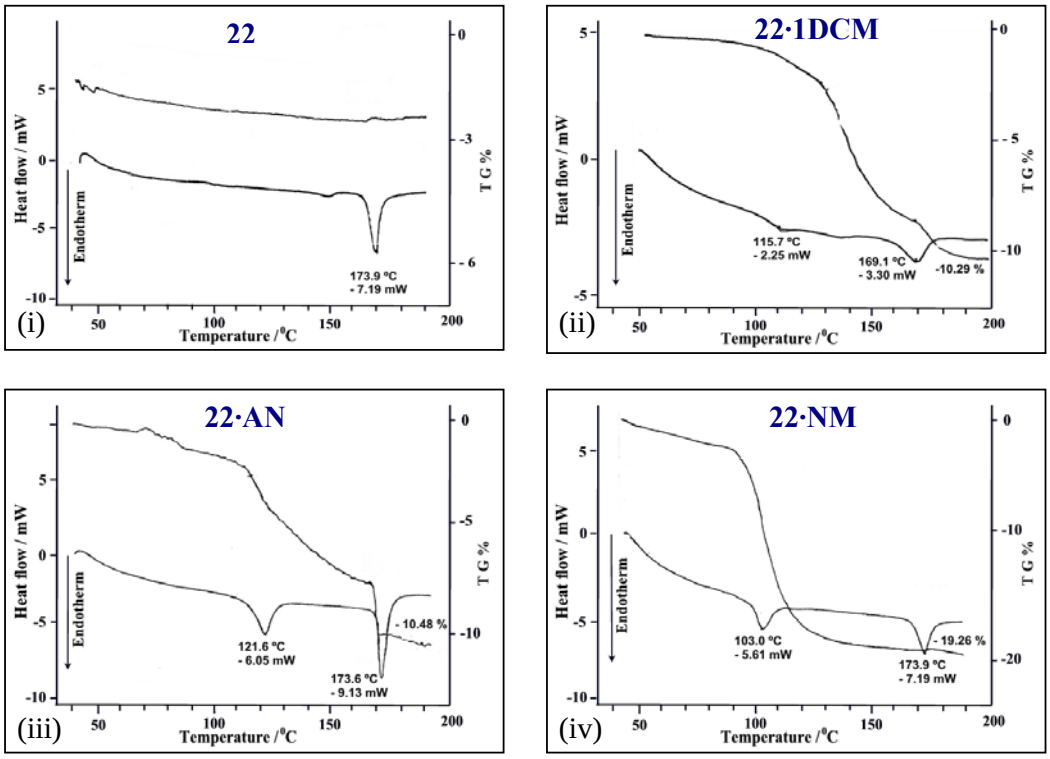


**Figure 6.2**: DTA/TGA plots of (i) **22** [powder] and (ii-viii) solvatomorphs of **22**.

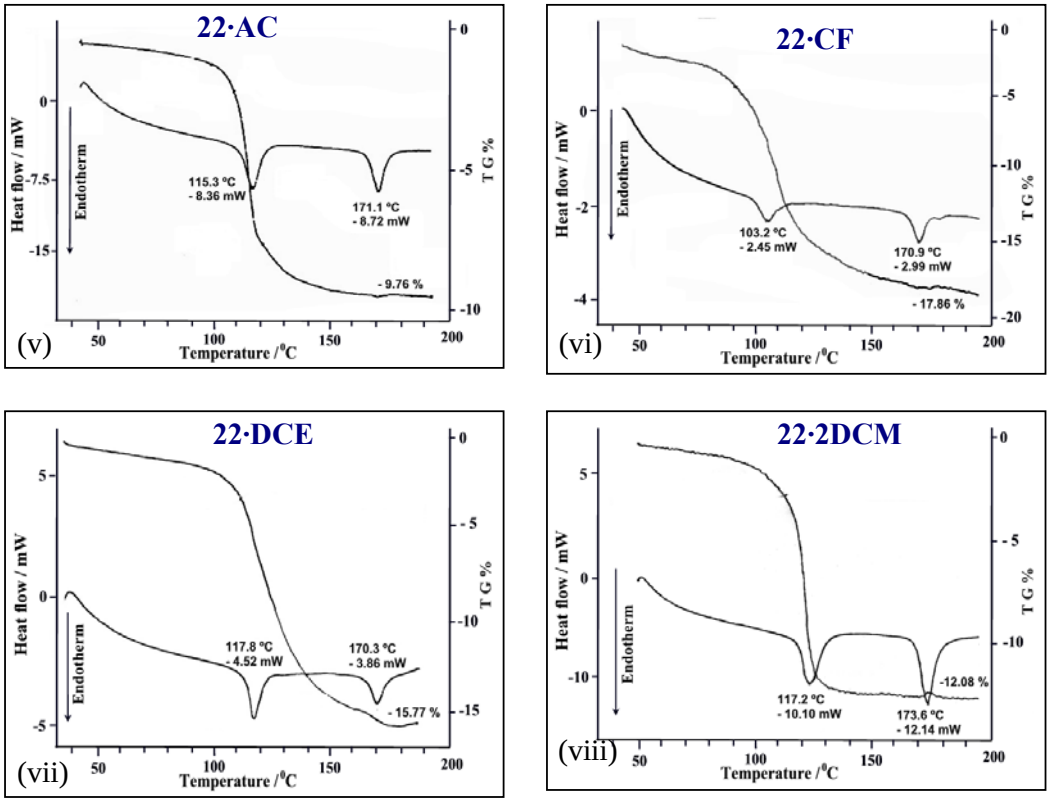


**Figure 6.2**: Continued. (v)-(viii) DTA/TGA plots of solvatomorphs of **22**.

### 6.3.3. Molecular Organization in Solvatomorphs of 22

The differences in the relative orientations of the two diastereomers in different crystals were revealed by the overlapping diagram and torsion angles *O4–S1–C17–C18* [Fig. 6.3 and Table 6.2]. The crystal structure analysis of solvatomorphs of **22** showed a slight change in the molecular conformation of host molecules depending on the included solvent. The orientation of the camphorsulfonate group of the diastereomer-1 in Form-III crystals (except **22·DCE**) deviates from that in the Form-I and II crystals. The corresponding deviation in torsion angles *O4–S1–C17–C18* were found to be ~ 20° between Form-III and Form I (and From II) crystals [Table 6.2]. A similar relative orientational change was also observed for *C1*-, *C2*- and *C5*-*O*-acetyl groups in Form-I, II and III crystals [Fig. 6.3(i)]. It is noteworthy that the conformation of the diastereomer-1 in **22·DCE** deviates rest of the Form-III

crystals *i.e.* the orientation of the molecule is matching with the conformation of Form-I and II crystals. However, the conformation of the diastereomer-2 deviates slightly (a maximum of ~ 5°) for camphorsulfonyl group and *C2*'-, *C3*'- and *C4*'-*O*-acetyl groups [Fig. 6.3(ii)].

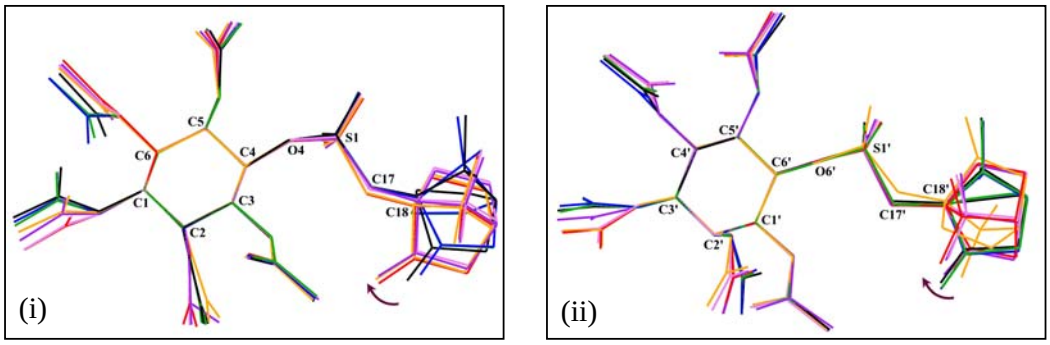


**Figure 6.3**: Molecular overlap of solvatomorphs of **22** (i) diastereomer-1 and (ii) diastereomer-2 [Black: **22·1DCM**, Blue: **22·AN**, Green: **22·NM**, Red: **22·AC**, Purple: **22·CF**, Orange: **22·DCE**, Violet: **22·2DCM**].

**Table 6.2**: Torsion angle of camphorsulfonyl group in diastereomer-1 and 2 of solvatomorphs of **22**.

| Solvated crystals | **22·1DCM** | **22·AN** | **22·NM** | **22·AC** | **22·CF** | **22·DCE** | **22·2DCM** |
|---|---|---|---|---|---|---|---|
| O4-S1-C17-C18 | 156° | 155° | 157° | 180° | 177° | 155° | 179° |
| O6'-S1'-C17'-C18' | 176° | 174° | 174° | 180° | 173° | 178° | 177° |

### *6.3.4. Host-Host Organization in Solvatomorphs of 22*

An interesting feature in all the solvated crystals of **22** is the well-conserved dimeric association of diastereomers *via* pseudo-centrosymmetric C–H···O interactions. Three axial hydrogen atoms (H1, H3, H5 and H1', H3', H5') of *myo*-inositol ring from one of the diastereomers make trifurcated C–H···O interactions with the sulfonyl oxygens (O13' and O13) of the other diastereomer and *vice versa* [Fig.

6.4]. However, there is a slight variation in the geometry of these trifurcated interactions in the crystals because of other weak interactions between the dimers [Table 6.3]. These trifurcated interactions between the diastereomers appear similar to an adamantane type framework, formed between enantiomers in the racemic crystals as observed earlier.[50] It is interesting that the propensity to form the same (pseudo) centrosymmetric association exists even between the diastereomers.

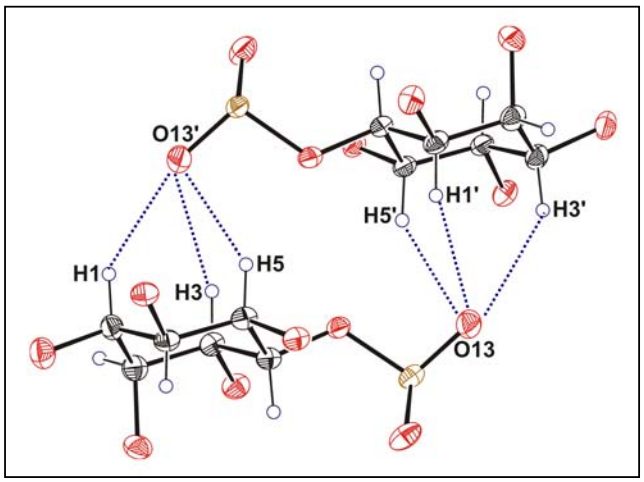


**Figure 6.4**: Conserved dimeric association of diastereomers of **22** *via* trifurcated C–H···O interactions in its crystals. Camphor and acetyl groups are not shown for clarity.

**Table 6.3**: Geometrical parameters of trifurcated C–H···O interactions (Fig. 6.4).

| Crystals | D–H···A | D–H (Å) | H···A (Å) | D···A (Å) | D–H···A (°) |
|---|---|---|---|---|---|
| **22·1DCM** | C1–H1···O13' | 0.98 | 2.80 | 3.601(8) | 139 |
| | C3–H3···O13' | 0.98 | 2.54 | 3.382(10) | 145 |
| | C5–H5···O13' | 0.98 | 2.54 | 3.385(9) | 145 |
| | C1'–H1'···O13 | 0.98 | 2.49 | 3.325(10) | 143 |
| | C3'–H3'···O13 | 0.98 | 2.73 | 3.539(8) | 140 |
| | C5'–H5'···O13 | 0.98 | 2.48 | 3.322(8) | 144 |
| **22·AN** | C1–H1···O13' | 0.98 | 2.79 | 3.583(5) | 139 |
| | C3–H3···O13' | 0.98 | 2.57 | 3.434(3) | 147 |
| | C5–H5···O13' | 0.98 | 2.62 | 3.455(4) | 143 |

| | | | | | |
|---|---|---|---|---|---|
| | C1'–H1'···O13 | 0.98 | 2.53 | 3.381(3) | 145 |
| | C3'–H3'···O13 | 0.98 | 2.69 | 3.498(5) | 140 |
| | C5'–H5'···O13 | 0.98 | 2.59 | 3.413(4) | 142 |
| **22·NM** | C1–H1···O13' | 0.98 | 2.78 | 3.589(12) | 140 |
| | C3–H3···O13' | 0.98 | 2.60 | 3.460(8) | 147 |
| | C5–H5···O13' | 0.98 | 2.65 | 3.484(10) | 143 |
| | C1'–H1'···O13 | 0.98 | 2.56 | 3.403(8) | 145 |
| | C3'–H3'···O13 | 0.98 | 2.64 | 3.461(11) | 141 |
| | C5'–H5'···O13 | 0.98 | 2.60 | 3.423(9) | 142 |
| **22·AC** | C1–H1···O13' | 0.98 | 2.55 | 3.405(1) | 146 |
| | C3–H3···O13' | 0.98 | 2.59 | 3.434(1) | 144 |
| | C5–H5···O13' | 0.98 | 2.74 | 3.537(1) | 139 |
| | C1'–H1'···O13 | 0.98 | 2.50 | 3.357(1) | 146 |
| | C3'–H3'···O13 | 0.98 | 2.61 | 3.415(1) | 140 |
| | C5'–H5'···O13 | 0.98 | 2.76 | 3.543(1) | 137 |
| **22·CF** | C1–H1···O13' | 0.98 | 2.46 | 3.382(6) | 158 |
| | C3–H3···O13' | 0.98 | 2.85 | 3.654(6) | 139 |
| | C5–H5···O13' | 0.98 | 2.85 | 3.727(5) | 137 |
| | C1'–H1'···O13 | 0.98 | 2.67 | 3.487(6) | 141 |
| | C3'–H3'···O13 | 0.98 | 2.46 | 3.338(6) | 149 |
| | C5'–H5'···O13 | 0.98 | 2.86 | 3.630(5) | 136 |
| **22·DCE** | C1–H1···O13' | 0.98 | 2.46 | 3.328(6) | 147 |
| | C3–H3···O13' | 0.98 | 2.51 | 3.362(7) | 145 |
| | C5–H5···O13' | 0.98 | 2.82 | 3.591(7) | 136 |
| | C1'–H1'···O13 | 0.98 | 2.46 | 3.402(7) | 160 |
| | C3'–H3'···O13 | 0.98 | 2.89 | 3.720(8) | 144 |
| | C5'–H5'···O13 | 0.98 | 2.66 | 3.495(7) | 143 |
| **22·2DCM** | C1–H1···O13' | 0.98 | 2.54 | 3.405(8) | 148 |
| | C3–H3···O13' | 0.98 | 2.58 | 3.436(7) | 146 |
| | C5–H5···O13' | 0.98 | 2.85 | 3.624(7) | 137 |
| | C1'–H1'···O13 | 0.98 | 2.47 | 3.335(7) | 147 |
| | C3'–H3'···O13 | 0.98 | 2.56 | 3.384(8) | 142 |
| | C5'–H5'···O13 | 0.98 | 2.83 | 3.586(7) | 135 |

The organization of these dimers, linked differently in the lattice creates different sites for the solvent inclusion. In Form-I crystals, these dimeric units were translated to form molecular chains *via* C8–H8*A*···O7', C2'–H2'···O7, C12'–H12*D*···O9 and C12'–H12*F*···O13' interactions along *c*-axis [Fig. 6.5(i), Table 6.4]. A similar organization is also seen in Form-II crystals along *b*-axis which makes two additional interactions namely C20–H20*B*···O8 and C2–H2···O9' [Fig. 6.5(ii), Table 6.4]. These chains translated along *a*-axis form molecular layers *via* C10'–H10*F*···O11 and C20'–H20*C*···O5 interactions in Form-I, whereas they are formed C10–H10*B*···O12' in Form-II. In Form-III crystals, the dimers that are translated along *b*-axis make C8–H8*B*···O11' and C12'–H12*F*···O11 interactions which are further linked to form a layer *via* C21–H21···O5 and bifurcated C–H···O interactions between H20*A* and H22*B* with O12 as shown in figure 6.5(iii).

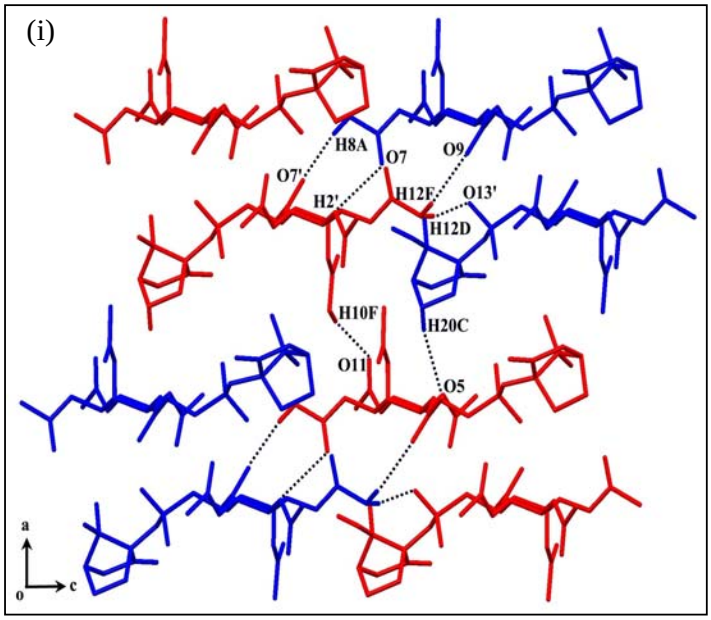


**Figure 6.5**: Layer formation of diastereomers in (i) Form-I, (ii) Form-II and (iii) Form-III crystals of **22**.

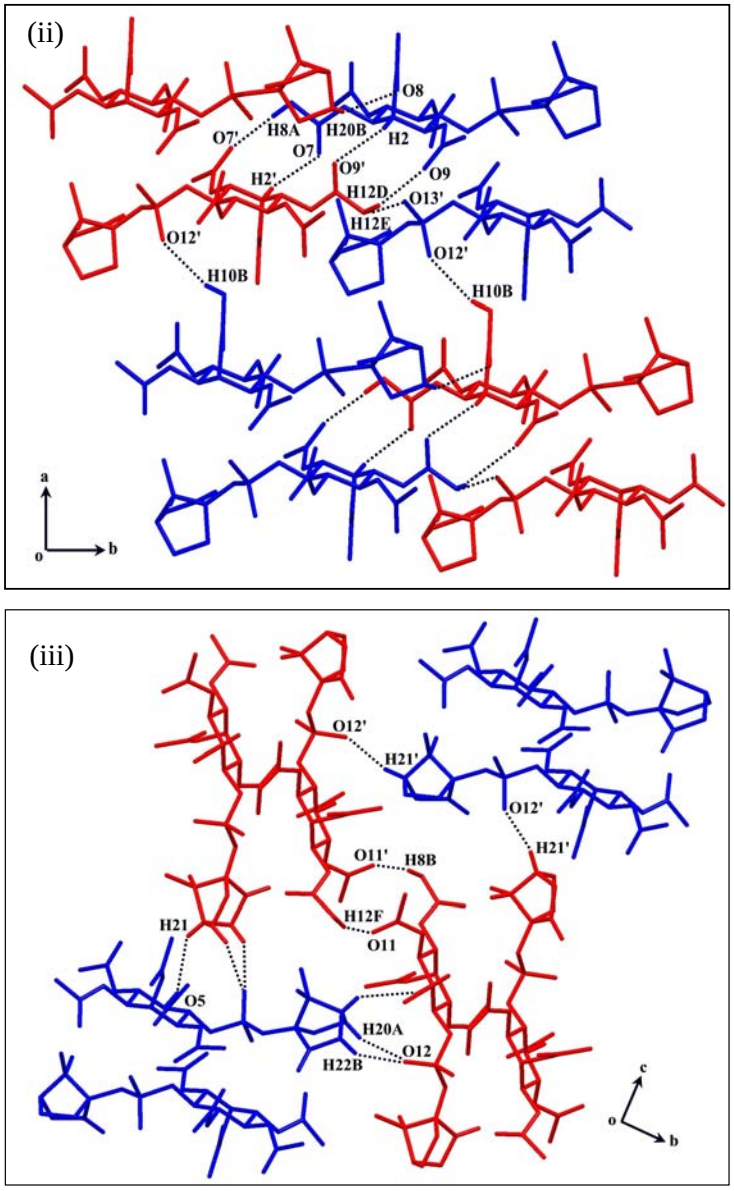


**Figure 6.5**: Continued.

**Table 6.4**: Geometrical parameters of C–H···O interactions as shown in figure 6.5.

| | D–H···A | D–H (Å) | H···A (Å) | D···A (Å) | D–H···A (°) |
|---|---|---|---|---|---|
| **22·1 DCM** | C2–H2'···O7 [i] | 0.98 | 2.68 | 3.467(10) | 138 |
| | C8–H8*A*···O7' [ii] | 0.96 | 2.52 | 3.439(13) | 160 |
| | C10'–H10*F*···O1 [iii] | 0.96 | 2.73 | 3.634(13) | 158 |
| | C12'–H12*D*···O13 [iii] | 0.96 | 2.51 | 3.447(11) | 166 |
| | C12'–H12*F*···O9' [i] | 0.96 | 2.57 | 3.375(13) | 142 |

| | | | | | |
|---|---|---|---|---|---|
| | C14–H14*A*···O14 [iv] | 0.96 | 2.39 | 3.326(14) | 166 |
| | C20'–H20*C*···O5 [v] | 0.97 | 2.71 | 3.558(12) | 147 |
| **22·AN** | C2–H2···O9' [vi] | 0.98 | 2.70 | 3.485(4) | 138 |
| | C2'–H2'···O7 [vii] | 0.98 | 2.60 | 3.393(4) | 158 |
| | C8–H8*A*···O7' [vi] | 0.96 | 2.47 | 3.382(3) | 138 |
| | C10–H10*B*···O12' [viii] | 0.96 | 2.67 | 3.509(6) | 146 |
| | C12'–H12*D*···O9 [vii] | 0.96 | 2.56 | 3.368(3) | 142 |
| | C12'–H12*F*···O13' [ix] | 0.96 | 2.48 | 3.431(5) | 169 |
| | C20–H20*B*···O8 [ix] | 0.97 | 2.68 | 3.386(4) | 130 |
| **22·NM** | C2–H2···O9' [vi] | 0.98 | 2.72 | 3.511(9) | 138 |
| | C2'–H2'···O7 [vii] | 0.98 | 2.59 | 3.388(1) | 139 |
| | C8–H8*A*···O7' [vi] | 0.96 | 2.51 | 3.386(7) | 151 |
| | C10–H10*B*···O12' [viii] | 0.96 | 2.78 | 3.594(8) | 144 |
| | C12'–H12*D*···O9 [vii] | 0.96 | 2.48 | 3.369(7) | 154 |
| | C12'–H12*F*···O13' [ix] | 0.96 | 2.48 | 3.369(7) | 154 |
| | C20–H20*B*···O8 [ix] | 0.97 | 2.69 | 3.411(10) | 132 |
| **22·AC** | C8–H8*B*···O11' [ix] | 0.96 | 2.46 | 3.365(1) | 156 |
| | C12–H12*A*···O14' [x] | 0.96 | 2.52 | 3.360(1) | 146 |
| | C12'–H12*F*···O11 [ii] | 0.96 | 2.59 | 3.405(1) | 143 |
| | C20–H20*A*···O12 [xi] | 0.97 | 2.83 | 3.705(1) | 150 |
| | C21–H21···O5 [xi] | 0.98 | 2.89 | 3.530(1) | 124 |
| | C21'–H21'···O12' [xii] | 0.98 | 2.39 | 3.304(1) | 155 |
| | C22–H22*A*···O8' [ii] | 0.97 | 2.62 | 3.553(1) | 161 |
| | C22–H22*B*···O12 [iv] | 0.97 | 2.51 | 3.449(1) | 163 |
| **22·CF** | C8–H8*B*···O11' [ix] | 0.96 | 2.47 | 3.429(6) | 175 |
| | C12–H12*A*···O14' [x] | 0.96 | 3.11 | 3.523(6) | 108 |
| | C12'–H12*F*···O11 [ii] | 0.96 | 2.40 | 3.350(9) | 168 |
| | C20–H20*A*···O12 [xi] | 0.97 | 2.60 | 3.444(12) | 146 |
| | C21–H21···O5 [xi] | 0.98 | 2.83 | 3.610(10) | 137 |
| | C21'–H21'···O12' [xii] | 0.98 | 2.42 | 3.273(9) | 146 |
| | C22–H22*A*···O8' [ii] | 0.97 | 2.69 | 3.640(9) | 166 |
| | C22–H22*B*···O12 [iv] | 0.97 | 2.53 | 3.398(9) | 149 |
| **22·DCE** | C8–H8*B*···O11' [ix] | 0.96 | 2.47 | 3.426(8) | 176 |
| | C12–H12*A*···O14' [x] | 0.96 | 2.51 | 3.386(8) | 151 |
| | C12'–H12*F*···O11 [ii] | 0.96 | 2.47 | 3.382(9) | 159 |

| | | | | | |
|---|---|---|---|---|---|
| | C20–H20*A*···O12 [xi] | 0.97 | 2.86 | 3.510(9) | 125 |
| | C21–H21···O5 [xi] | 0.98 | 2.83 | 3.466(8) | 124 |
| | C21'–H21'···O12' [xii] | 0.98 | 2.44 | 3.308(8) | 147 |
| | C22–H22*A*···O8' [ii] | 0.97 | 2.66 | 3.613(8) | 167 |
| | C22–H22*B*···O12 [iv] | 0.97 | 2.81 | 3.732(9) | 160 |
| **22·2 DCM** | C8–H8*B*···O11' [ix] | 0.96 | 2.41 | 3.361(11) | 169 |
| | C12–H12*A*···O14' [x] | 0.96 | 2.40 | 3.347(9) | 168 |
| | C12'–H12*F*···O11 [ii] | 0.96 | 2.47 | 3.382(9) | 159 |
| | C20–H20*A*···O12 [xi] | 0.97 | 2.55 | 3.396(20) | 146 |
| | C21–H21···O5 [xi] | 0.98 | 2.65 | 3.452(13) | 140 |
| | C21'–H21'···O12' [xii] | 0.98 | 2.42 | 3.297(8) | 149 |
| | C22–H22*A*···O8' [ii] | 0.97 | 2.63 | 3.549(11) | 158 |
| | C22–H22*B*···O12 [iv] | 0.97 | 2.56 | 3.409(10) | 146 |

Symmetry codes: (i) x, y-1, z; (ii) x, y+1, z; (iii) -x+1, y+1/2, -z+1; (iv) -x, y-1/2, -z+1; (v) x,y,z; (vi) x+1, y+1, z+1; (vii) ) x-1, y-1, z-1; (viii) x, y, z+1; (ix) x, y-1, z; (x) x-1, y, z; (xi) -x, y+1/2, -z ; (xii) x-1, y-1/2, -z+1.

In the third dimension, these dimeric units are translated in Forms I, II and III crystals differently as shown in figure 6.6. Molecular layers are linked *via* C14–H14*A*···O14 along *b*-axis in Form-I [Fig. 6.6(i)] and *via* C26–H26*B*···O14 along *c*-axis in Form-II [Fig. 6.6(ii)] whereas in Form-III crystals, the translated layers bind together *via* two C–H···O interactions along *a*-axis namely, C12–H12*A*···O14' and

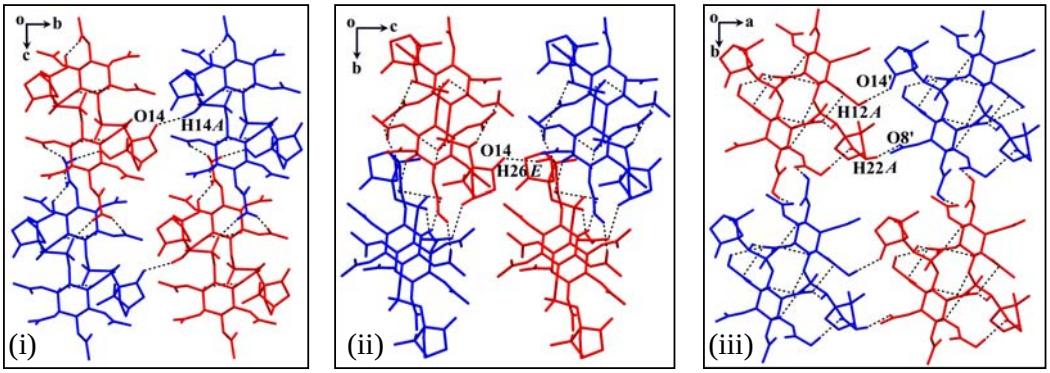


**Figure 6.6**: Molecular layer formation by diastereomers of **22** in the third dimension (i) Form-I, (ii) Form-II and (iii) Form-III crystals.

C22–H22*A*···O14 [Fig. 6.6(iii), Table 6.5]. It is interesting to note that the camphor oxygens (O14 and O14') bind the dimers in the third dimension in all the three crystal forms.

**Table 6.5**: Geometrical parameters of C–H···O interactions shown in figure 6.6.

| | D–H···A | D–H (Å) | H···A(Å) | D···A (Å) | D–H···A (°) |
|---|---|---|---|---|---|
| **22·1DCM** | C14–H14*A*···O14 [i] | 0.96 | 2.39 | 3.326(14) | 166 |
| **22·AN** | C26'–H26*E*···O14 [ii] | 0.96 | 2.61 | 3.515(4) | 158 |
| **22·NM** | C26'–H26*E*···O14 [ii] | 0.96 | 2.61 | 3.520(10) | 159 |
| **22·AC** | C12–H12*A*···O14' [iii] | 0.96 | 2.52 | 3.360(1) | 146 |
| | C22–H22*A*···O8' [iii] | 0.97 | 2.62 | 3.553(1) | 161 |
| **22·CF** | C12–H12*A*···O14' [iii] | 0.96 | 2.71 | 3.633(8) | 161 |
| | C22–H22*A*···O8' [iii] | 0.97 | 2.69 | 3.640(9) | 166 |
| **22·DCE** | C12–H12*A*···O14' [iii] | 0.96 | 2.51 | 3.386(8) | 151 |
| | C22–H22*A*···O8' [iii] | 0.97 | 2.66 | 3.615(8) | 167 |
| **22·2DCM** | C12–H12*A*···O14' [iii] | 0.96 | 2.40 | 3.347(9) | 168 |
| | C22–H22*A*···O8' [iii] | 0.97 | 2.63 | 3.549(11) | 158 |

Symmetry codes: (i) –x, y-1/2, -z+1; (ii) x, y+1, z; (iii) –x+2, y+1/2, -z+1.

Although identical molecular arrangement (translation of dimers) exists in triclinic Form-I and Form-II crystals, the intermolecular interactions between the dimers are different. Interestingly, Form-I and II crystals [Fig. 6.7(i) and 6.7(ii)] are isostructural in two-dimensions, but the difference is in the third dimension due to staggering of these layers differently [Fig. 6.8(i) and 6.8(ii)]. However, the dimeric units are more closely packed in Form-I [Fig. 6.8(i)] than in Form-II [Fig. 6.8(ii)]. As a result, Form-I crystals have shorter cell dimensions than that of Form-II crystals (~ 1 Å along *a*- and *c*-axis and ~ 0.7 Å along *b*-axis). The adjacent molecular chains in Form-II crystals create larger voids which are occupied by two guest molecules as compared to Form-I crystals where voids are occupied by only one guest molecule [Fig. 6.8(ii)].

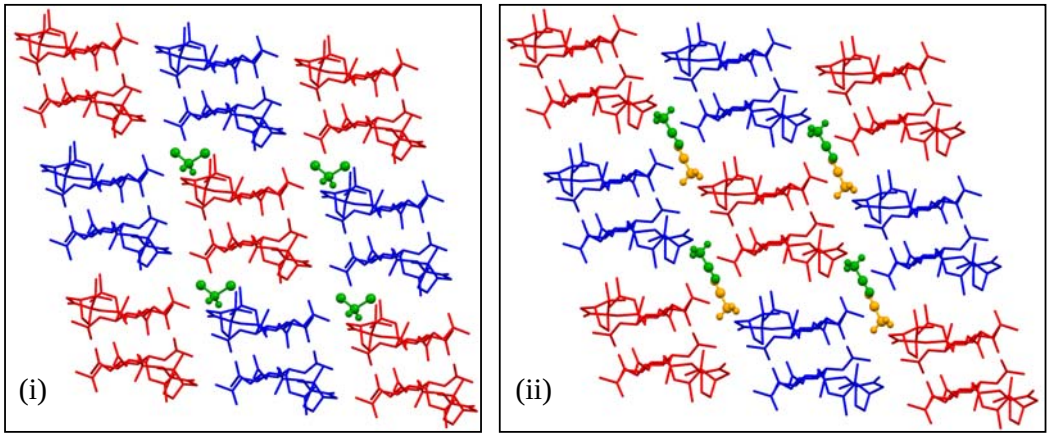


**Figure 6.7**: Isostructural molecular layers of (i) Form-I [**22·1DCM**] and (ii) Form-II [**22.AN**] crystals.

### *6.3.5. Host-Guest Interactions in Solvatomorphs of 22*

Crystallization experiments showed crystals of **22** were always obtained with the inclusion of solvents; indicating the necessity of guest solvent for the crystal lattice formation. The guest solvents included in the solvatomorphs of **22** have an electron count ranging 22-60, whereas in pseudopolymorph of **8** (*Chapter 2*) the included solvents had a narrower range of electron count 40-60 and also imposing *C2* symmetry restriction on the guests included.

In Form-I, host molecules contain one guest site [*A* in Fig. 6.8(i)] per asymmetric unit, whereas in Forms II and III, there are two guest sites per asymmetric unit [*A* and *B* in Fig. 6.8(ii) and 6.8(iii)]. All the guest solvents make weak non-covalent interactions with the host molecules as given below.

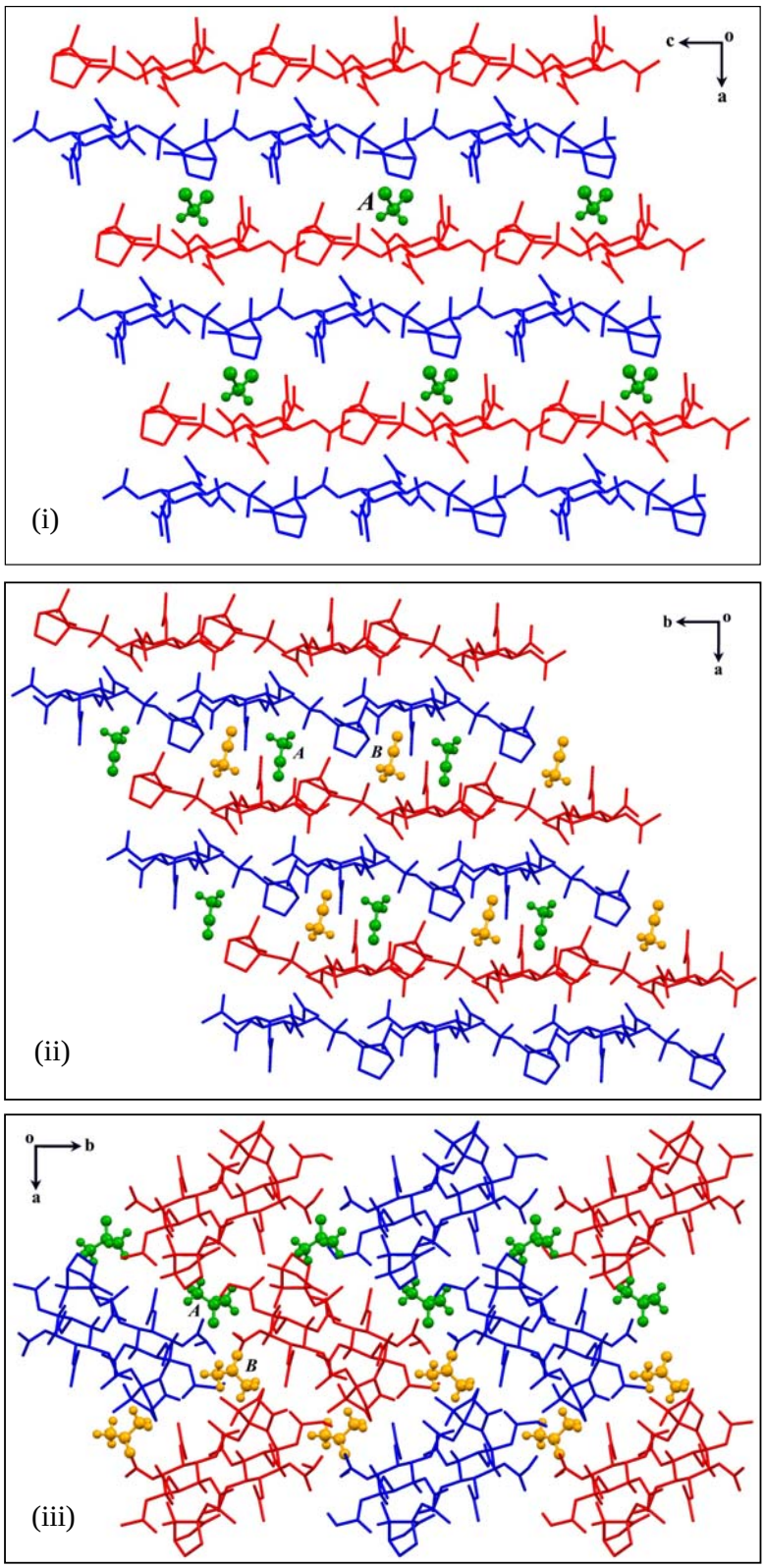


**Figure 6.8**: Molecular layer formation in (i) Form-I (**22·1DCM**), (ii) Form-II (**22·AN**) and (iii) Form-III (**22·AC**) crystals of **22**.

*6.3.5.1. Inclusion of Dichloromethane in Form-I crystals* (**22·1DCM**)

In case of Form-I crystals, the DCM molecule occupied only a single site [*A* in Fig. 6.8(i)] and is held in the lattice by various weak interactions with the host molecules. For example, H27*A* atom of the DCM makes weak C–H···O interaction with carbonyl oxygen O14. Also, the chlorine atom (Cl1) is involved in C–H···Cl as well as C–Cl···O (halogen bonding) interactions with the host, whereas the Cl2-atom binds to the host by trifurcated hydrogen bonds with H10*C*, H16*C* and H22*D* [Fig. 6.9(i), Table 6.6]. Short halogen bonding contacts (C27–Cl1···O12') were observed in this solvate with almost linear geometry [3.14 Å and 158°] indicating its significant role in the stabilization of DCM inclusion in crystals, as has been observed earlier in our laboratory.[49]

*6.3.5.2. Inclusion of Acetonitrile, Form-II crystals* (**22·AN**)

In this crystal (Form-II), there are two guest sites [*A* and *B* shown in figure 6.8(ii)] for inclusion of acetonitrile molecule. In site *A*, the guest molecule is linked to the host *via* three weak hydrogen bonding interactions, namely C27–H27*A*···O8, C27–H27*B*···O7' and C16'–H16*D*···N1 whereas in site *B*, the guest binds *via* C30–H30*B*···O11 and C14–H14*C*···N2 interactions [Fig. 6.9(ii), Table 6.6]. As mentioned earlier, two water molecules in both the sites are bound to the host molecules *via* C10–H10*C*···O15, C17–H17*A*···O15 and O16···O11 interactions.

*6.3.5.3. Inclusion of Nitromethane, Form-II crystals* (**22·NM**)

The O18 and O16 atoms of the two guests in site *A* and *B* bind to the host *via* bifurcated C–H···O interactions with H10*D*, H14*C* and H8*A*, H16*A* respectively. The H27*A* and H28*A* atoms of both nitromethane guests were additionally linked to the host carbonyl oxygens O8 and O11 respectively [Fig. 6.9(iii), Table 6.6]. A water

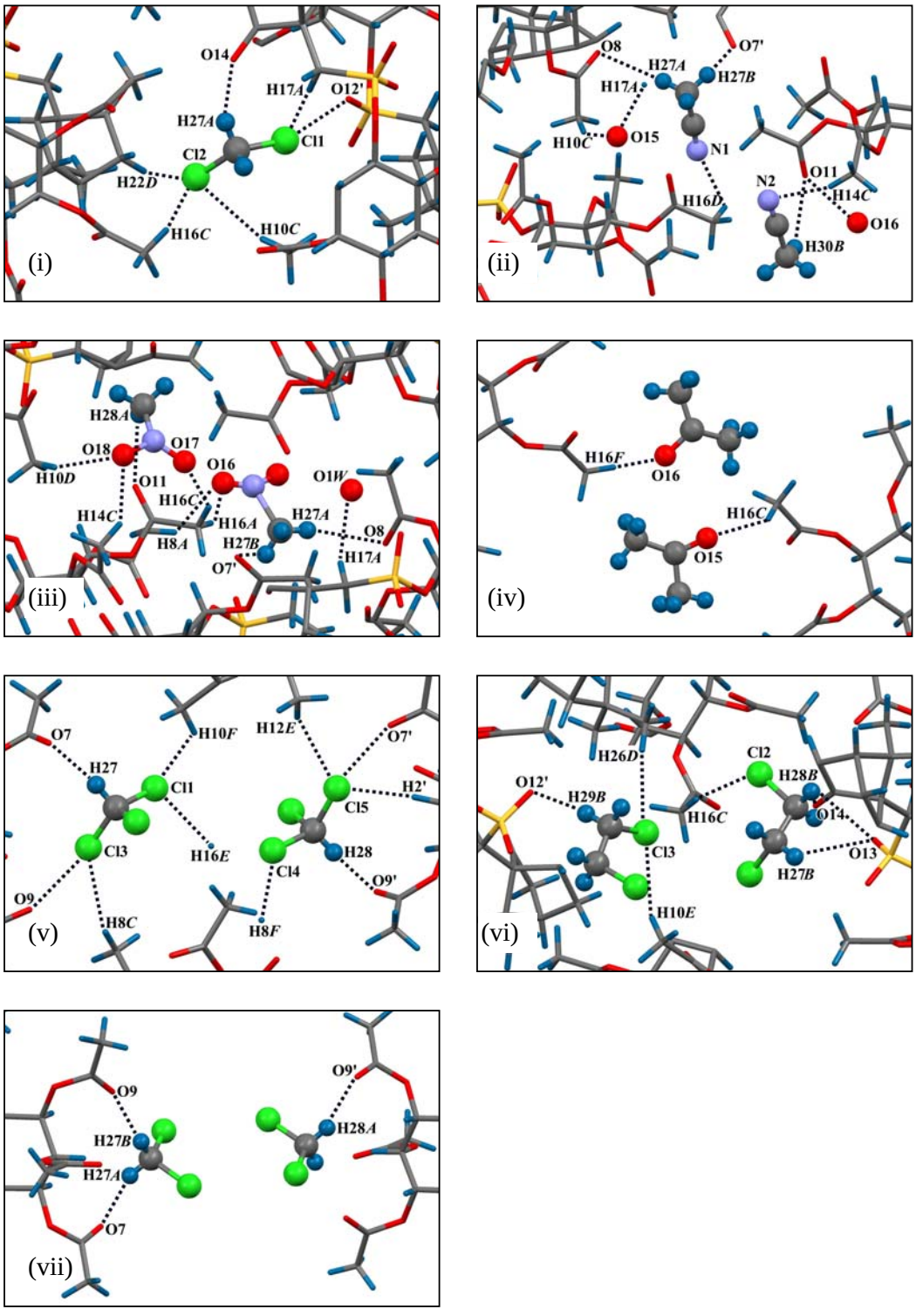


**Figure 6.9**: Significant host-guest interactions in solvatomorphs of **22**; (i) **22·1DCM**; (ii) **22·AN**; (iii) **22·NM**; (iv) **22·AC**; (v) **22·CF**; (vi) **22·DCE**; (vii) **22·2DCM**.

molecule (bound to the host *via* C17–H17*A*···O1*W* interactions) is also included along with nitromethane guest in site *B*.

*6.3.5.4. Inclusion of Acetone, Form-III crystals* (**22·AC**)

In case of inclusion crystals obtained from acetone, the guests at sites *A* and *B* make C–H···O interactions involving guest carbonyl oxygen O15 and O16 with the methyl H16*C* and H16*F* atoms of the host respectively [Fig. 6.9(iv), Table 6.6].

*6.3.5.5. Inclusion of Chloroform, Form-III crystals* (**22·CF**)

In these crystals guest chloroform molecules occupy two different sites [*A* and *B* in Fig. 6.8(v)] and bind to the host molecules *via* C–H···O, C–H···Cl and C–Cl···O (halogen bonding) interactions. In site *A*, the guest binds to the host *via* C28–H28···O9', C8'–H8*F*···Cl4 and bifurcated C–H···Cl interactions of Cl5 with H2' and H12*E* atoms [Table 6.6]. The chlorine atom (Cl1) of the guest in site *B* also makes bifurcated C–H···Cl interactions with H10*F* and H16*E* of the host molecule and the guest is additionally linked to the host *via* C27–H27···O7 and C8–H8*C*···Cl3 interactions. Interestingly, chlorine atoms (Cl3 in site *B* and Cl5 in site *A*) of both the guests make geometrically good halogen bonding contacts [2.85 Å and 2.69 Å] with the host oxygen atoms (O9 and O7') respectively [Table 6.6, Fig. 6.9(v)].

*6.3.5.6. Inclusion of 1,2-Dichloroethane, Form-III crystals* (**22·DCE**)

The 1,2-dichloroethane guests make hydrogen-bonding interactions such as C–H···O and C–H···Cl with the host molecules as shown in Fig. 6.9(vi). Hydrogen atoms H27*B* and H28*B* of the guest in site *A* bind to the host sulfonyl oxygen O13 *via* bifurcated C–H···O interactions and also by C16–H16*C*···Cl2 interactions. The other guest molecule (site *B*) is linked to the host molecules *via* bifurcated C–H···Cl

interactions (Cl3 with H10*E* and H26*D*) and C29–H29*B*···O12' interactions [Fig. 6.9(vi), Table 6.6].

*6.3.5.7. Inclusion of Dichloromethane in Form-III crystals* (**22·2DCM**)

Interestingly in this crystal (Form-III, monoclinic), the dichloromethane guests occupy two guest sites [*A* and *B* in figure 6.8(iii)], whereas the same guest occupied only one site [*A* in Fig. 6.8(i)] in Form-I, triclinic crystals (**22·1DCM**) The guest in site *A* is linked to the host *via* C27–H27*A*···O7 and C27–H27*B*···O9 interactions, whereas the guest in site *B* binds only with C28–H28*A*···O9' interactions to the host [Fig. 6.9(vii), Table 6.6]. It is noteworthy that the guest molecules in this crystal make only C–H···O interactions but in Form-I, the same guest molecule was bound more closely to the host by various non-covalent interactions as described earlier [section 6.3.5.1].

**Table 6.6**: Geometrical parameters for host-guest interactions shown in figure 6.9.

| | D–H···A | D–H (Å) | H···A (Å) | D···A (Å) | D–H···A (°) |
|---|---|---|---|---|---|
| **22·1DCM** | C10–H 10*C*···Cl2 $^{i}$ | 0.96 | 2.81 | 3.718(18) | 157 |
| | C16–H16*C*···Cl2 $^{ii}$ | 0.96 | 2.95 | 3.520(18) | 119 |
| | C17–H17*A*···Cl1 $^{i}$ | 0.97 | 2.85 | 3.815(12) | 173 |
| | C22'–H22*D*···Cl2 $^{ii}$ | 0.97 | 2.84 | 3.698(22) | 149 |
| | C27–H27*A*···O14 $^{i}$ | 0.97 | 2.23 | 3.109(31) | 151 |
| | C27–Cl1···O12' $^{iii}$ | - | 3.136(12) | - | 158.4(6) |
| **22·AN** | C10–H10*C*···O15 $^{ii}$ | 0.96 | 2.58 | 3.439(10) | 149 |
| | C14–H14*C*···N2 $^{iv}$ | 0.96 | 2.66 | 3.563(9) | 157 |
| | C16'–H16*D*···N1 $^{v}$ | 0.96 | 2.73 | 3.460(8) | 132 |
| | C17–H17*A*···O15 $^{ii}$ | 0.97 | 2.55 | 3.453(10) | 156 |
| | C27–H27*A*···O8 $^{vi}$ | 0.96 | 2.54 | 3.451(4) | 158 |
| | C27–H27*B*···O7' $^{vi}$ | 0.96 | 2.63 | 3.314(6) | 128 |
| | C30–H30*B*···O11 $^{vii}$ | 0.96 | 2.70 | 3.385(7) | 129 |

| | | | | | |
|---|---|---|---|---|---|
| **22·NM** | C8–H8*A*···O16 [viii] | 0.96 | 2.68 | 3.292(45) | 122 |
| | C10'–H10*D*···O18 [ii] | 0.96 | 2.65 | 3.552(18) | 157 |
| | C14–H14*C*···O18 [ii] | 0.96 | 2.52 | 3.301(28) | 139 |
| | C16–H16*A*···O16 [viii] | 0.96 | 2.60 | 3.503(60) | 156 |
| | C16–H16*C*···O17 [ii] | 0.97 | 2.63 | 3.433(27) | 142 |
| | C17–H17*A*···O1*W* [ii] | 0.97 | 2.59 | 3.484(31) | 154 |
| | C27–H27*A*···O8 [ix] | 0.96 | 2.60 | 3.494(17) | 156 |
| | C27–H27*B*···O7' [ii] | 0.96 | 2.67 | 3.258(26) | 120 |
| | C28–H28*A*···O11 [ii] | 0.96 | 2.59 | 3.282(15) | 129 |
| **22·AC** | C16–H16*C*···O15 [x] | 0.96 | 2.73 | 3.448(1) | 132 |
| | C16'–H16*F*···O16 [xi] | 0.96 | 2.61 | 3.354(1) | 135 |
| **22·CF** | C2'–H2'···Cl5 [xii] | 0.98 | 2.89 | 3.656(6) | 136 |
| | C8–H8*C*···Cl3 [i] | 0.96 | 2.95 | 3.821(7) | 152 |
| | C8'–H8*F*···Cl4 [iii] | 0.96 | 2.72 | 3.673(11) | 170 |
| | C10'–H10*F*···Cl1 [ii] | 0.96 | 2.75 | 3.415(22) | 128 |
| | C12'–H 12*E*···Cl5 [ii] | 0.96 | 2.66 | 3.373(9) | 131 |
| | C16'–H16*E*···Cl1 [x] | 0.96 | 2.85 | 3.791(7) | 167 |
| | C27–H27···O7 [xiii] | 0.98 | 2.34 | 3.159(9) | 140 |
| | C28–H28···O9' [xi] | 0.98 | 2.42 | 3.132(15) | 129 |
| | C27–Cl3···O9 [xii] | - | 2.845(5) | - | 166.6(3) |
| | C28–Cl5···O7' [xi] | - | 2.688(6) | - | 157.8(4) |
| **22·DCE** | C10'–H10*E*···Cl3 [xi] | 0.96 | 2.95 | 3.638(9) | 130 |
| | C16–H 16*C*···Cl2 [x] | 0.96 | 2.78 | 3.711(7) | 163 |
| | C26–H 26*D*···Cl3 [x] | 0.96 | 2.91 | 3.860(9) | 169 |
| | C27–H 27*B*···O13 [xii] | 0.97 | 2.67 | 3.311(9) | 124 |
| | C28–H 28*B*···O13 [xii] | 0.97 | 2.67 | 3.054(8) | 104 |
| | C28–H 28*B*···O14 [xii] | 0.97 | 2.65 | 3.317(9) | 126 |
| | C29–H29*B*···O12' [xiii] | 0.97 | 2.62 | 3.550(9) | 160 |
| **22·2DCM** | C27–H 27*A*···O7 [ii] | 0.97 | 2.65 | 3.267(13) | 121 |
| | C27–H 27*B*···O9 [ii] | 0.97 | 2.71 | 3.680(11) | 176 |
| | C28–H 28*A*···O9' [ix] | 0.97 | 2.67 | 3.316(13) | 125 |

Symmetry codes: (i) x-1, y+1, z; (ii) x, y, z; (iii) x, 1+y, z; (iv) x, y+1, z+1; (v) x-1, y, z-1; (vi) x+1, y, z; (vii) x, y-1, z-1; (viii) x+1, y+1, z; (ix) x, y, z+1; (x) x-1, y, z; (xi) -x+1, y-1/2, -z+1; (xii) -x+1, y+1/2, -z+1; (xiii) -x+1, y-1/2, -z.

### *6.3.2.4. Solvatopolymorphism in 22*

It is interesting to note that the host molecules are organized in two different crystalline forms, triclinic (Form-I) as well as monoclinic (Form-III) with the same guest inclusion of dichloromethane (DCM). The host molecules in Form-I (**22·1DCM**) crystals accommodate a single guest molecule but with different organization of the same host include two DCM guests in Form-III (**22·2DCM**) crystals. These solvated crystals are termed as *solvatopolymorphs*,[32] where the same solvent included (DCM, with different stoichiometric ratio) in the crystal lattice creates different arrangements of host molecules, **22** [Fig. 6.8(i) and 6.8(iii)]. The packing of host molecules can be viewed as dimeric units translated to form chains along *c*-axis in **22·1DCM** and further translated to a 2D layers along *a*-axis created single site for DCM molecule [Fig. 6.10(i)]. Whereas in **22·2DCM**, molecular strings are formed with twisted dimeric units along *b*-axis and these strings, which are related by $2_1$-screw axis are extended to form 2D layer having two sites for DCM guests [Fig. 6.10(ii)].

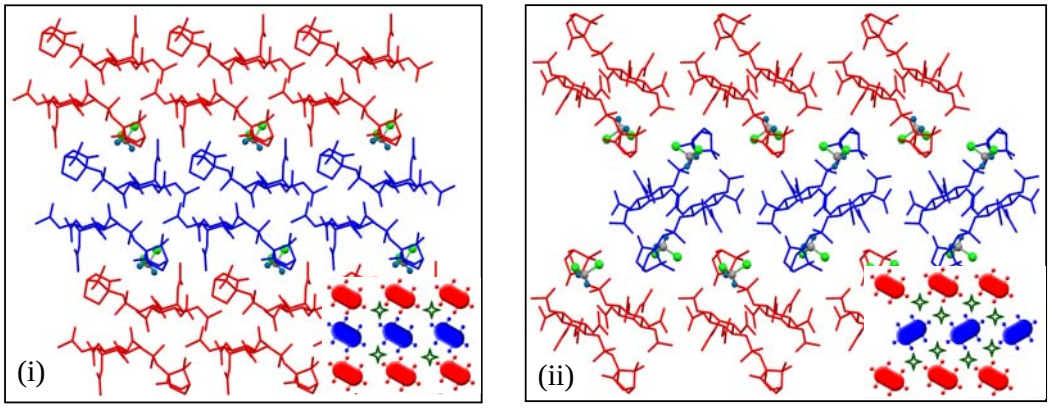


**Figure 6.10**: Solvatopolymorphs showing different molecular packing with the inclusion of dichloromethane in (i) Form-I (**22·1DCM**, down *b*-axis) and (ii) Form-III (**22·2DCM**, down *a*-axis) crystals. Inset shows the schematic representation of molecular organization in **22.1DCM** and **22.2DCM** crystals.

### 6.3.3. Molecular Organization in 23

The replacement of camphorsulfonate group in **22** with a tosyl group (resulting in **23**) results in close packing of molecules in crystals without leaving any voids for solvent inclusion. As expected association of molecules of **23** occur *via* weak hydrogen bonding interactions. In crystals of **23**, the *C1*-carbonyl oxygen O7 makes bifurcated C–H···O interactions with inositol protons *H4* and *H6* and translated along *b*-axis to form 1D-chain [Fig. 6.11(i)]; whereas in solvatomorphs of **22**, the diastereomeric association of dimmers occurred *via* trifurcated C–H···O interactions involving sulfonyl oxygen (O13 and O13') with the inositol ring protons [Fig. 6.4, page no. 165]. The 1 D-molecular string of **23** are additionally linked by three more interactions namely C3–H3···O10, C14–H14*A*···O9 and C21–H21···O12 [Table 6.7]. The strings that are mirror related further bind to each other to form a bilayer *via* C12–H12*A*···O8 and C12–H12*B*···O10 interactions as shown in Fig. 6.11(ii).

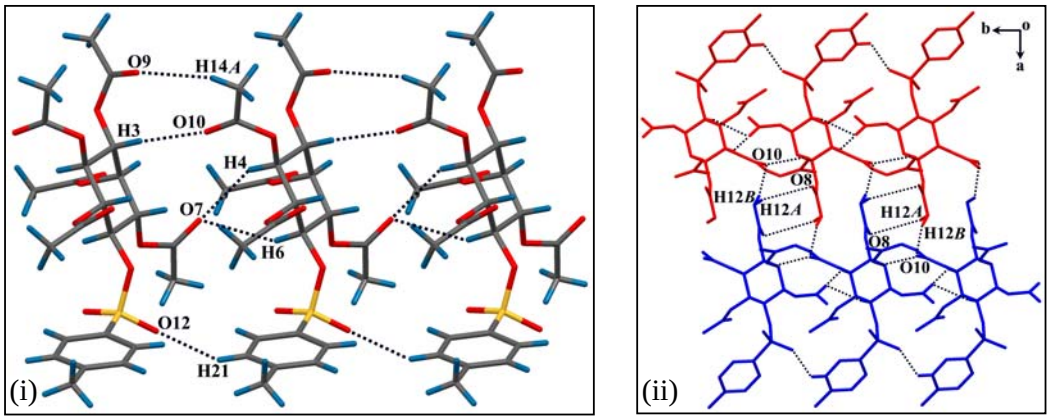


**Figure 6.11**: (i) Molecular chain formation viewed along *b*-axis *via* C–H···O interactions; (ii) bilayer formation of molecular strings along *a*-axis in the crystals of **23**.

**Table 6.7**: Geometrical parameters of trifurcated C–H···O interactions (Fig. 6.11).

| | D–H···A | D–H (Å) | H···A (Å) | D···A (Å) | D–H···A (°) |
|---|---|---|---|---|---|
| **23** | C3–H3···O10 [i] | 0.98 | 2.55 | 3.225(5) | 126 |
| | C4–H4···O7 [ii] | 0.98 | 2.43 | 3.282(5) | 145 |
| | C6–H6···O7 [ii] | 0.98 | 2.67 | 3.461(5) | 138 |
| | C14–H14*A*···O9 [ii] | 0.96 | 2.54 | 3.444(6) | 158 |
| | C21–H21···O12 [ii] | 0.93 | 2.56 | 3.246(6) | 131 |
| | C12–H12*A*···O8 [iii] | 0.96 | 2.64 | 3.576(7) | 164 |
| | C12–H12*B*···O10 [iv] | 0.96 | 2.62 | 3.367(7) | 135 |

Symmetry codes: (i) x, y-1, z; (ii) x, y+1, z; (iii) -x+1, -y, -z+2; (iv) -x+1, -y+1, -z+2.

These bilayers that are $2_1$-screw related linked each other *via* longer C23–H23*A*···O12 interaction along *a*-axis [Fig. 6.12(i), Table 6.8]. The 2D-molecular layers extended to the third dimension *via* C8–H8*A*···O13, C16–H16*B*···O11 and C23–H23*B*···O9 interactions [Fig. 6.12(ii), Table 6.8].

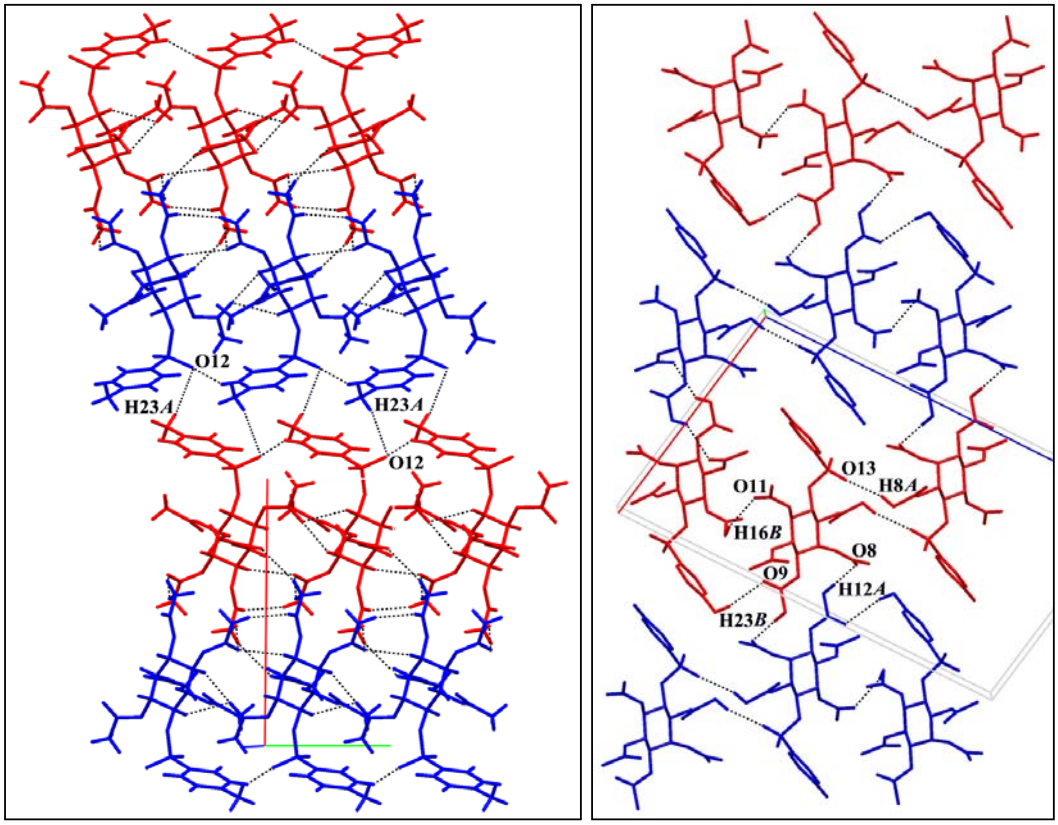


**Figure 6.12**: Molecular layers viewed down (i) *c*-axis (ii) *b*-axis in **23** crystals.

**Table 6.8**: Geometrical parameters of C–H···O interactions shown in figure 6.12.

| | D–H···A | D–H (Å) | H···A (Å) | D···A (Å) | D–H···A (°) |
|---|---|---|---|---|---|
| **23** | C23–H23*A*···O12 [i] | 0.96 | 2.93 | 3.621(7) | 130 |
| | C8–H8*A*···O13 [ii] | 0.96 | 2.62 | 3.470(5) | 148 |
| | C12–H12*A*···O8 [iii] | 0.96 | 2.64 | 3.576(7) | 164 |
| | C16–H16*B*···O11 [iv] | 0.96 | 2.53 | 3.348(6) | 143 |
| | C23–H23*B*···O9 [iv] | 0.96 | 2.71 | 3.577(6) | 151 |

Symmetry codes: (i) -x-1/2, y+1/2, -z+3/2; (ii) -x, -y, -z+2; (iii) -x+1, -y, -z+2; (iv) -x+1/2, y+1/2, -z+3/2.

## 6.4. Conclusions

In open *myo*-inositol derivatives, only camphorsulfonyl substitution yielded inclusion crystals whereas the tosyl substitution produced always close packed solvent free crystals. Interesting case of solvatopolymorphs with dichloromethane represent the diversity of molecular aggregation, keeping conserved association intact. The dipolar contacts were not observed in crystal structures of **22** and **23**.

# Chapter 7

## Strength from Weak Dipolar S=O···C=O Interactions: Statistical Analysis and Structural Consequences in Molecular Crystals

# Chapter 7

## 7.1. Introduction

Inspired by remarkable specific molecular recognitions in biological systems,[56] non-covalent interactions continue to be an area of intensive research that has applications in crystal engineering,[100] host-guest chemistry[101] and structure based drug design.[57,79] Addition of any new (weak) interaction in the list of 'non-covalent' bonding awaits its acceptance till it is substantiated by a significant number of experimental observations, theoretical calculations and possibly a gratification from the Crystallographic Database. In the absence of relatively stronger interactions such as conventional hydrogen bonds in crystals, weaker intermolecular interactions become prominent during the aggregation of molecules. Although there could be many weak interactions that exist in a crystal structure, it is necessary to analyze these interactions on a statistical basis from a large number of crystal structures using database for its preponderance.[73] Amongst bond dipole-dipole interactions in organic crystals, analysis of carbonyl, nitrile and C–F contacts have been reported in the literature.[88] However, the S=O···C=O intermolecular contacts have not been systematically analyzed so far, although intramolecular S=O···C=O contacts were noted in the crystal structures of sulfones.[98] This chapter gives an insight into the geometrical aspects of dipolar S=O···C=O interactions based on a systematic CSD analysis and the structural observation of various *myo*-inositols derivatives.

## 7.2. Methodology for Statistical Analysis of S=O···C=O Interactions

Version *5.29* of the CSD was used for the survey of dipolar S=O···C=O contacts. The searches of S=O···C=O non-covalent contacts [Chart 7.1] were carried

out using the programme *CONQUEST 1.10* and data visualizations were performed with programme *VISTA 2.1*. All the searches were restricted to those CSD entries that satisfied the following secondary search criteria: (i) organic compounds according to CSD chemical class definitions; (ii) error free co-ordinates after CSD evaluation procedure; (iii) no reported structural disorder; (iv) excluded structures that are elucidated from powder X-ray diffractions technique; (v) no ionic or polymeric compounds according to CSD classification and (vi) R≤ 0.10. A non-covalent interaction distance (*D*) cut-off value of 3.6 Å (twice the van der Waals radius of carbon with a tolerance of 0.2 Å), angles *A1* [∠O···C=O] and *A2* [∠ S=O···C] of range 0-180º were used for the search [Chart 7.1].

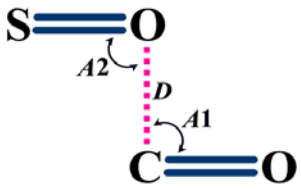


***D* = < 3.6 Å**
***A1* = 0-180º**
***A2* = 0-180º**

**Chart 7.1**: Search fragment and geometrical parameters used in the analysis.

The survey of dipolar S=O···C=O contacts in Protein Data Bank (RSCB PDB) was carried out to recognize their occurrence in macromolecular complex crystals. The key words 'sulfonyl' and 'tosyl' were used to search the protein structures with the screen applied to select structures that are determined at high resolution (≤ 2.0 Å).

### 7.3. CSD Analysis of Crystal Structures containing S=O···C=O Interactions

Out of 2590 structures containing S=O and C=O groups, a sizable number 1052 (36 %) contained non-covalent S=O···C=O interactions within the search criteria as mentioned above. This statistical survey clearly signifies the existence of bond dipolar S=O···C=O interactions in the organization of molecular crystals. The scatter plot of angle, *A1 versus* intermolecular distance, *D* showed the geometrical preference for the orientation of S=O towards the C$sp^2$ atom of the C=O group [Fig. 7.1(i)],

whereas the scatter plot of *A2 vs D* showed rather wide distribution [Fig. 7.1(iii)]. Histogram of O···C distance (*D*) did not show any trailing off value even 5 Å. Histogram of ∠ O···C=O (*A1*) also indicated remarkable preference with an average value 95.81° [Fig. 7.1(ii)], but the histogram of ∠S=O···C (*A2*) showed the distribution spread over the range 60-180 with mean value of 126.78° [Fig. 7.1(iv)]. Therefore, we have categorized S=O···C=O interactions on the basis of the preferred perpendicular approach of angle *A1* and the varying angle *A2* as given below.

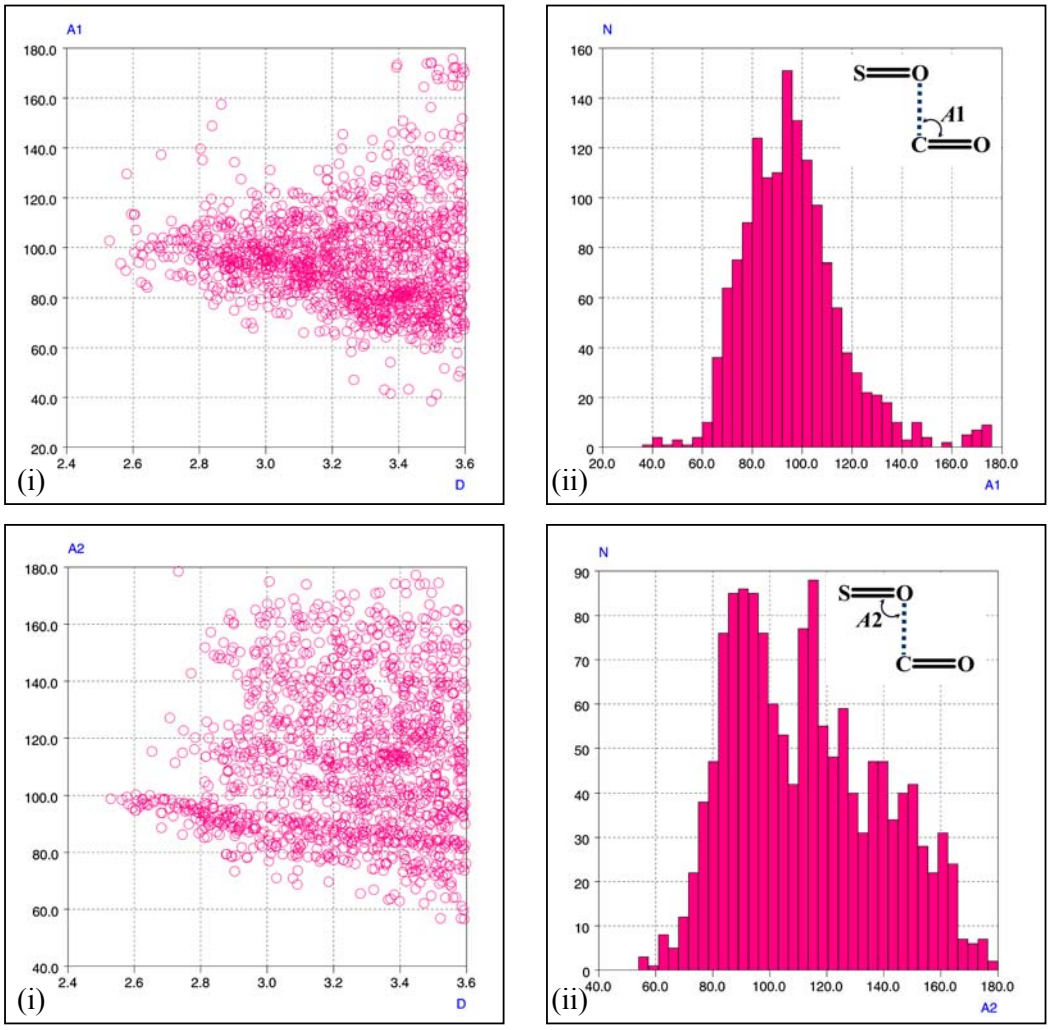


**Figure 7.1**: (i) Scatter plot of angle, *A1 versus* inter-atomic distance *D*; (ii) Histogram of angle, *A1* [∠O···C=O]; (iii) Scatter plot of angle, *A2 vs* inter-atomic distance *D*; (iv) Histogram of angle, *A2* [∠S=O···C].

The S=O···C=O dipolar contacts can be classified as perpendicular motif (Type-I), anti-parallel motif (Type-II) and sheared parallel motif (Type-III) [Fig. 7.2], as in the case of carbonyl-carbonyl interactions.[96] The angle criteria for the three interaction motifs are:

| | | |
|---|---|---|
| Type-I (perpendicular motif) | *A1* = 90±20º | *A2* = 160±20º |
| Type-II (anti-parallel motif) | *A1* = 90±20º | *A2* = 90±20º |
| Type-III (sheared parallel motif) | *A1* = 90±20º | *A2* = 120±20º |

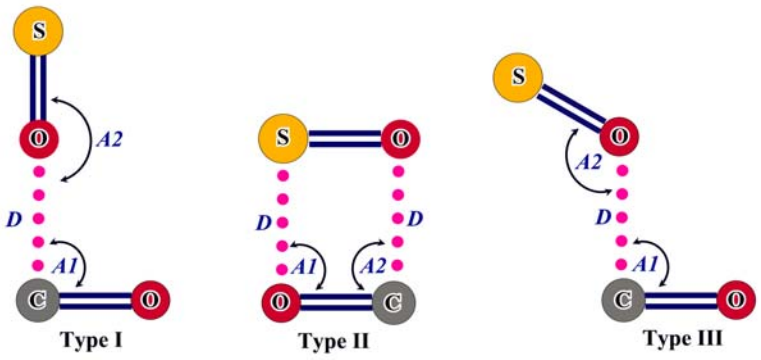


**Figure 7.2**: Different interaction motifs of dipolar S=O···C=O interactions.

The maximum number of hits (446) was found for Type-III, followed by Type-I contacts (179 hits) and the least hits (132) were found for Type-II. In case of C=O···C=O contacts, the frequency of occurrence of motifs are in the order Type-II > Type-III > Type-I. The preferred Type-III motif (and also not preferred Type II) in S=O···C=O contacts may be due to the hetero dipoles having different van der Waals radii for sulfur and carbon atoms.

### 7.4. Dipolar S=O···C=O Interactions in *myo*-Inositol Derivative Crystals

This thesis explored the involvement of S═O···C═O interactions in molecular association of crystals, results obtained clearly indicated the significant role of these dipolar interactions in the molecular aggregation. Five out of sixteen compounds (31%) studied showed S═O···C═O interactions for their conformational modifications

or molecular organization. This is also in accordance with the trend observed in the statistics from CSD. Approximately, only one third systems showing those dipolar interactions suggests that they are not the overriding predominant interactions that decide the molecular assembly hierarchy in crystal formation. Even then, we noted that this weak attractive force played its role in molecular association. The intermolecular S═O···C═O dipolar contact of Type-I (perpendicular interaction) motif was observed for the solvates of **8** [Fig. 7.2(i)] and solvent free form of **21** [Fig. 7.2(ii)]. The strength of these dipolar contacts were found be shorter in **8** compared to **21**, could be resulted in the formation of pseudopolymorphs in the former. Intermolecular S═O···C═O contacts were also exhibited in the diastereomeric association of **9** but with Type-III interaction motif *i.e.* sheared parallel motif [Fig. 7.2(iii)]. Conformational dimorphs of **14** and **16** adopt two significantly different orientations for the tosyl group in their crystals and the interesting feature is the intramolecular S═O···C═O dipolar interactions [Fig. 7.2(iv)-(v)]. The different molecular conformation in Form-II of **14** and Form-II of **16** crystals could be due to this intramolecular S═O···C═O dipolar interaction, which is Type-III motif.

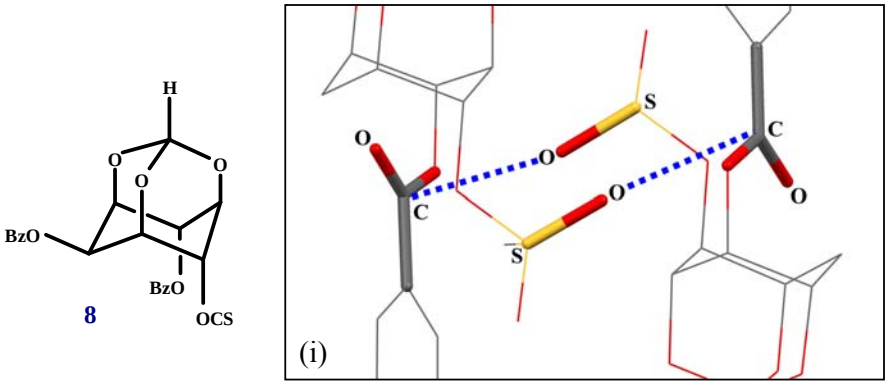


**Figure 7.2**: Different dipolar S═O···C═O interaction motifs of (i) Type-I in solvated crystals of **8**, (ii) Type-I in solvent free crystals of **21**, (iii) Type-III in solvent free crystals of **9**, (iv) Type-III in Form-II crystals of **14**, (v) Type-III in Form-II crystals of **16**.

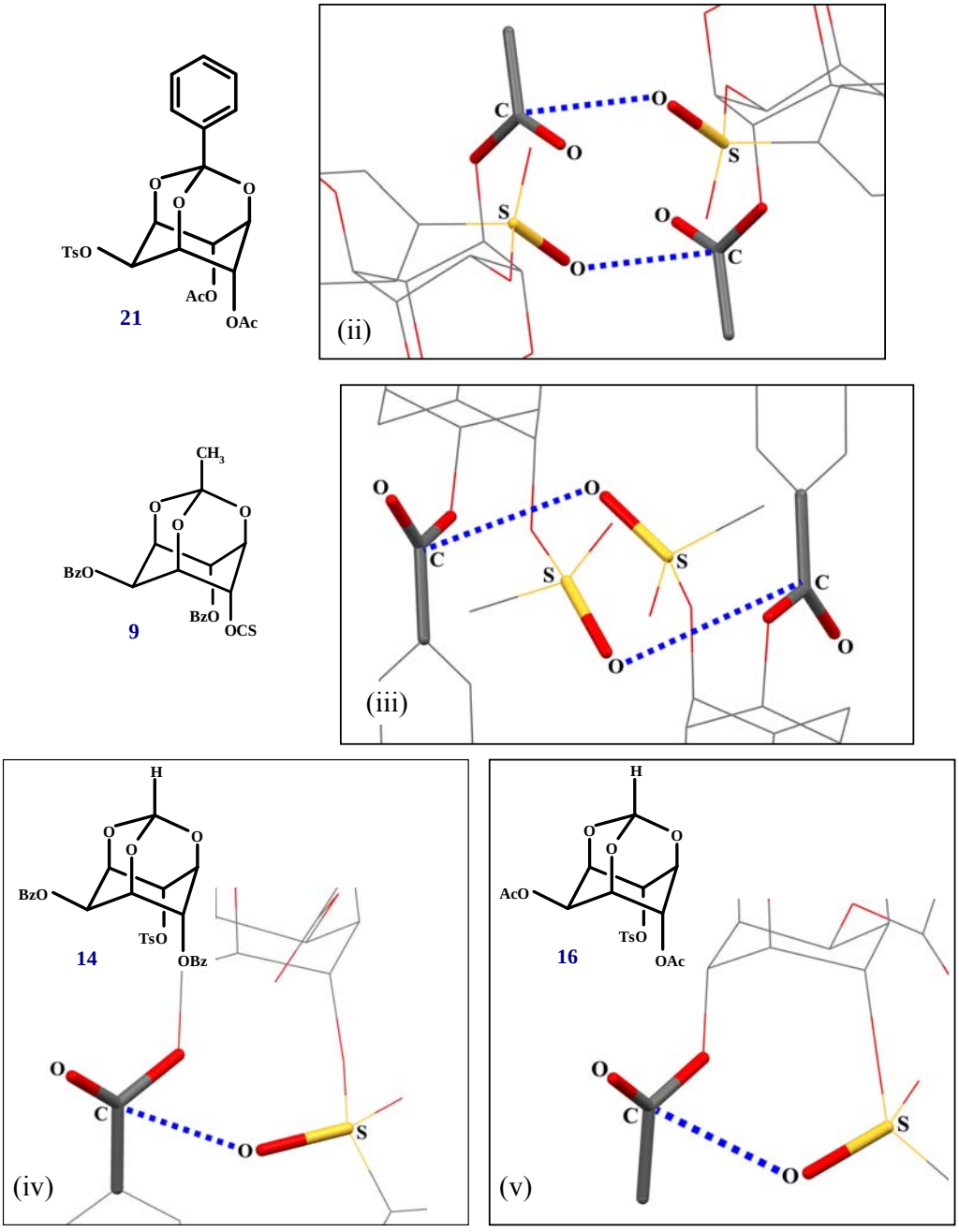


**Figure 7.2**: Continued.

All these observations seem to suggest that the sulfonyl group plays a decisive role in the formation of polymorphs or solvates *via* S═O···C═O or C–H···O interactions. This ability of the sulfonyl group to decisively adopt different

conformations could have implications in molecular recognition processes and hence the biological activity of compounds containing sulfonyl groups.

### 7.5. Analysis of S=O···C=O Interactions in PDB

Out of 196 protein structures containing 'sulfonyl' and 'tosyl' groups in the PDB only 107 were analyzed (resolution less than 2.0 Å) for the dipolar S═O···C═O contacts. The S═O···C═O contacts were observed for 13 hits. Many ligands (9 out of 13 hits) used these bond dipolar interactions to bind their counterpart along with other weak interactions. For e.g. S=O···C=O contacts were observed [Fig.7.3] in the binding of *N*-tosyl-D-proline (ligand) to thymidylate synthase (an essential enzyme in pyrimidine metabolism with therapeutic applications in cancer and infectious diseases).[125] [Geometrical parameters of S=O···C=O contacts is *D* = 3.185 Å, *A1*= 87°, *A2* = 128°].

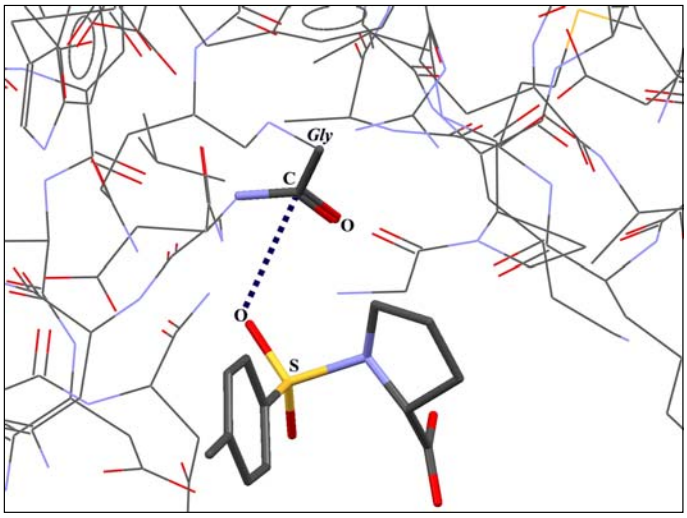


**Figure 7.3**: Crystal structure of *N*-tosyl-D-proline-thymidylate synthase complex indicating inter- and intramolecular S=O···C=O dipolar contacts [PDB code no.1F4E].

### 7.6. Conclusions

The present statistical survey of S═O···C═O interactions using CSD and PDB reveals the existence of these non-covalent interactions in molecular aggregation. The

experimentally observed polymorphic modification of *myo*-inositol derivatives endorses that the S═O···C═O contacts could be competitive with other weak interactions in the molecular recognition process during crystal growth. Like other dipolar interactions (C═O···C═O and C–F···C═O), the studies of S═O···C═O interactions in crystal structures of small molecules can be extended to stabilization of protein structures or improved binding of sulfa drugs to their receptors.

## 7.7. Scope of Future Work

As discussed so far, the synthetic and structural work pursued and presented in this dissertation had the underlying theme of observing the interplay of weak intermolecular interactions, particularly the bond dipolar interactions S=O···C=O. Having observed these short contacts in several of the structures, what should be the next action to follow? In our opinion, this weak attractive force is worth studying in more depth because of the presence of this group in biologically active molecules and drugs. The work in future is proposed on three of the main topics as described below:

### *7.7.1. Estimation of dipolar sulfonyl-carbonyl (S=O···C=O) interaction energies*

Since the bond dipolar S=O···C=O short contacts played a vital role in the formation of inclusion crystals and polymorphic behavior, we have planned to estimate their interaction energies. The energies of C=O···C=O were estimated to range from ~ 5 to 20 kJ/mol,[96] it is to be seen how the interactions under considerations stand in comparison with other dipolar contacts. Valuable results of intermolecular interaction energies can be obtained from intermolecular perturbation theory (IMPT) using high level basis sets (6-31G**). Therefore, we have planned to carry out *ab initio* molecular orbital calculation of dipolar S=O···C=O interactions to quantify the interaction energies of three types of S=O···C=O motifs.

### *7.7.2. Experimental charge density studies on model compounds*

Evaluation of weak interactions using charge density analysis allows us to observe and quantify the intermolecular interactions beyond distance-angle geometry criteria. This can be studied by the accurate measurement of charge densities in molecular crystals using high resolution (~ 0.5 Å) single crystal X-ray diffraction measurements. The *myo*-inositol derivatives reported in this thesis are rather large molecules for charge density studies. Therefore smaller model compound, thioxanthone-10,10-dioxide[126] is chosen for the charge density analysis, which exhibited short dipolar S=O···C=O contacts (Type-I motif) in its crystals [Fig. 7.9].

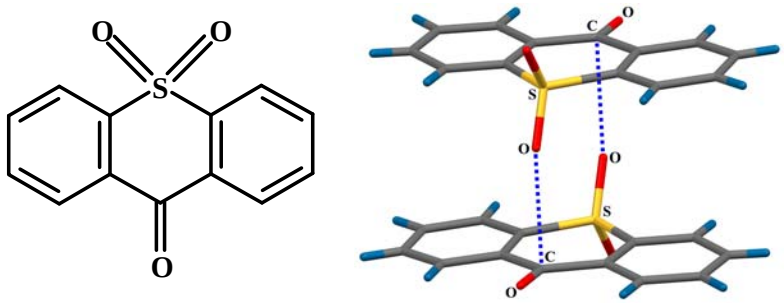


**Figure 7.9**: Structure thioxanthone-10,10-dioxide and dipolar S=O···C=O interactions in their crystals.

### *7.7.3. Protein-ligand binding studies of sulfa drugs*

Analysis of dipolar S=O···C=O interactions in the PDB reveals the existence of these contacts involved in the binding of ligand to their receptors. Sulfa drug compounds are planned to complex with proteins to explore their binding characteristics in the active sites. An insight into the interaction of these sulfa drugs can be exploited for the designing of lead compound that will have better affinity and/or specificity towards the targeted proteins. Like C═O···C═O, C–F···C═O and now S═O···C═O, there can be several combinations of bond dipolar interactions that can exist in the crystal structures. This dissertation has given attention to only one of them, but it could be worthwhile to investigate others.

## References


1. Hilfiker, R.; *Polymorphism in the Pharmaecutical Industry*; Wiley-VCH: Weinheim, Germany, **2006**.
2. Bernstein, J.; *Polymorphism in Molecular Crystals*; Oxford University Press: Oxford, Great Britain, **2002**.
3. Brittain, H. G.; *Polymorphism in Pharmaceutical Solids, Drugs and the Pharmaceutical Sciences*, Vol. 95, Ed.: Marcel Dekker, Inc.: New York, **1999**.
4. McCrone, W. C.; *Polymorphism in Physics and Chemistry of the Organic Solid State*, Eds: D. Fox, M. M. Labes, Weissberger, Wiley Interscience, New York, **1965**, Vol. II, p. 726.
5. Special issues: (a) 'Facets of Polymorphism in Crystals' in *Cryst. Growth Des*. **2008**, *8*, 3. (b) 'Polymorphism in Crystals: Fundamentals, Prediction and Industrial Practice' in *Cryst*. *Growth Des*. **2003**, *3*, 867. (c) 'Polymorphism and Crystallization' in *Org*. *Process res*. *& Dev*. **2000**, *4,* 371.
6. Day, G. M.; Motherwell, W. D. S.; Ammon, H. L.; Boerrigter, S. X. M.; Della Valle, R. G.; Venuti, E.; Dzyabchenko, A.; Dunitz, J. D.; Schweizer, B.; van Eijck, B. P.; Erk, P.; Facelli, J. C.; Bazterra, V. E.; Ferraro, M. B.; Hofmann, D. W. M.; Leusen, F. J. J.; Liang, C.; Pantelides, C. C.; Karamertzanis, P. G.; Price, S. L.; Lewis, T. C.; Nowell, H.; Torrisi, A.; Scheraga, H. A.; Arnautova, Y. A.; Schmidt, M. U.; Verwer, P.; *Acta Cryst.* **2005**, *B61*, 511.
7. Haleblian, J.; McCrone, W.; *J*. *Pharm*. *Sci*. **1969**, *58*, 911.
8. (a) Raw, A. S.; Yu, L. X.; *Adv*. *Drug Delivery Rev*. **2004**, *56*, 235. (b) Yu, L. X.; Furness, M. S.; Raw, A.; Woodland Outlaw, K. P.; Nashed, N. E.; Ramos, E.; Miller, S. P. F.; Adams, R. D.; Fang, F.; Patel, R. M.; Holcombe Jr., F. O.; Chiu, Y.; Hussain, A. S.; *Pharmceutical Res*. **2003**, *20*, 531.

9. (a) Ho, D. D.; Neumann, A. U.; Perelson, A. S.; Chen, W.; Leonard, J. M.; Markowitz, M.; *Nature* **1995**, *373*, 123. (b) Kempf, D. J.; Marsh, K. C.; Denissen, J. F.; McDonald, E.; Vasavanonda, S.; Flentge, C. A.; Green, B. E.; Fino, L.; Park, C. H.; Kong, X.; *Proc. Natl. Acad. Sci. USA* **1995**, *92*, 2484.

10. Bauer, J.; Spanton, S.; Henry, R.; Quick, J.; Dziki, W.; Porter, W.; Morris, J.; *Pharmaceutical Res.* **2001**, *18*, 859.

11. Morissette, S. L.; Soukasene, S.; Levinson, D.; Cima, M. J.; Almarsson, Ö.; *Proc. Natl. Acad. Sci. USA* **2003**, *100*, 2180.

12. (a) Zakrzewski, A.; Zakrzewski, M.; *Solid-State Characterization of Pharmaceuticals*; Assa International Inc.: Danbury, CT, USA, **2006**. (b) Morissette, S. L.; Almarsson, Ö.; Peterson, M. L.; Remenar, J. F., Read, M. J.; Lemomo, A. V.; Ellis, S; Cima, M. J.; Gardner, C. R.; *Adv. Drug Del. Rev.* **2004**, *56*, 275.

13. Datta, S; Grant, D. J. W.; *Nat. Rev., Drug Discovery*. **2004**, *3*, 42.

14. Grunenberg, A.; Henck, J. O.; Siesler, H. W.; *Int. J Pharm*. **1996**, *129*, 147.

15. Threlfall, T. L.; *Analyst* **1995**, *120*, 2435.

16. *Cambridge Structural Database* (CSD) version **5.29**, November **2007** release with **4,23,752** entries; Cambridge Crystallographic Data Centre, 12 Union Road, Cambridge, CB2 1EZ, UK.

17. (a) Vishweshwar, P.; McMahon, J. A.; Oliveira, M.; Peterson, M. L.; Zaworotko, M. J.; *J. Am. Chem. Soc.* **2005**, 127, 16802. (b) Bond, A. D.; Boese, R.; Desiraju, G. R.; *Angew. Chem., Int. Ed.* **2007**, *46*, 615. (c) Bond, A. D.; Boese, R.; Desiraju, G. R.; *Angew. Chem., Int. Ed.* **2007**, *46*, 618.

18. (a) Vujovic, D; Nassimbeni, L. R.; *Cryst. Growth Des.* **2006**, *6*, 1595. (b) Threlfall, T. L.; *Cryst. Growth Des.* **2007**, *7*, 2297.

19. Gavezzotti, A.; *J. Pharm. Sc.* **2007**, *96*, 2232.

20. (a) Jetti, R. K. R.; Boese, R.; Sarma, J. A. R. P.; Reddy, L. S.; Vishweshwar, P.; Desiraju, G. R.; *Angew. Chem. Int. Ed. Engl.* **2003**, *42*, 1963. (b) Threlfall, T.; *Org. Process Res. Dev.* **2000**, *4*, 384.

21. (a) Ostwald, W.; *Z. Physick. Chem.* **1897**, *22*, 289. (b) Ostwald, W.; *Lehrbuch der Allgemeinen, Chemie* 2, W. Engelmann, Leipzig, Germany, **1896**, p.444.

22. (a) Mullin, J. W.; *Crystallization*, 3rd Ed. Butterworth Heinemann, London, UK, **1993**, pp.172. (b) Verma, A. R.; Krishna, P.; *Polymorphism and Polytypism in Crystals*, John Wiley, New York, **1966**, p.15.

23. (a) Vrcelj, R. M.; Gallagher, G. H.; Sherwood, J. N.; *J. Am. Chem. Soc.* **2001**, 123, 2291. (b) Davey, R. J.; Blagden, N.; Righini, S.; Alison, H.; Quayle, M. J.; Fuller, S.; *Cryst. Growth Des.* **2001**, *1*, 59 and references therein.

24. (a) Guo, C.; Hickey, M. B.; Guggenheim, E. R.; Enkelmann V.; Foxman, B. M.; *Chem. Commun.* **2005**, 2220. (b) Munshi, P.; Venugopala, K. N.; Jayashree, B. S.; Guru Row, T. N.; *Cryst. Growth Des.* **2004**, *4*, 1105. (c) Bernstein, J.; Davey, R. J.; Henck, J-O. *Angew. Chem. Int. Ed. Engl.* **1999**, *38*, 3440.

25. Reed, S. M.; Weakley, T. J. R.; Hutchison, J. E.; *Cryst. Eng.* **2000**, *3*, 85.

26. (a) Nangia, A.; *Cryst. Growth Des.* **2006**, *6*, 2. (b) Bernstein, J.; *Cryst. Growth Des.* **2005**, *5*, 661. (c) Desiraju, G. R.; *Cryst. Growth Des.* **2004**, *4*, 1089. (d) Seddon, K. R.; *Cryst. Growth Des.* **2004**, *4*, 1087.

27. (a) Rafilovich, M.; Bernstein, J.; *J. Am. Chem. Soc.* **2006**, *128*, 12185. (b) Munshi, P.; Guru Row, T. N.; *Cryst. Growth Des.* **2006**, *6*, 708. (c) Chopra, D.; Mohan, T. P.; Sundaraja Rao, K.; Guru Row, T. N.; *CrystEngComm.* **2005**, *7*, 374. (d) Moorthy, J. N.; Natarajan, R.; Mala, P.; Venugopalan, P.; *New J. Chem.* **2004**, *28*, 1416.

28. Boldyreva, E. V.; Shakhtshneider, T. P.; Vasilchenko, M. A.; Ahsbahs, H.; Uchtmann, H.; *Acta Crystallogr.* **2000**, *B56*, 299.

29. (a) Chandran, S. K.; Nath, N. K.; Roy, S.; Nangia, A.; *Cryst. Growth Des*. **2008**, *8*, 140. (b) Roy, S.; Banerjee, R.; Nangia, A.; Kruger, G. J.; *Chem. Eur. J*. **2006**, 12, 3777. (c) Bis, J. A.; Vishweshwar, P.; Middleton, R. A.; Zaworotko, M. J.; *Cryst. Growth Des*. **2006**, *6*, 1048. (d) Guo, C.; Hickey, M. B.; Guggenheim, E. R.; Enkelmann, V.; Foxman, B. M.; *Chem. Commun*. **2005**, 2220.

30. Bar, I.; Bernstein, J.; *J. Pharm. Sci*. **1985**, *74*, 255.

31. (a) Brittain, H. G.; *J. Pharm. Sci*. **2007**, *96*, 705. (b) Chopra, D.; Guru Row, T. N.; *Cryst. Growth Des*. **2006**, *6*, 1267.

32. Ibragimov, B T; *CrystEngComm*. **2007**, *9*, 111.

33. Liang, C.; Ewig, C. S.; Stouch, T. R.; Hagler, A. T.; *J. Am. Chem. Soc*. **1994**, *116*, 3904.

34. Parthasarathy, R.; Eisenberg, F.; *Biochem. J*. **1986**, *235*, 313.

35. Nomenclature Committee-IUB, *Biochem. J*. **1989**, *258*, 1.

36. Potter, B. V. L.; Lampe, D.; *Angew. Chem. Int. Ed. Engl*. **1995**, *34*, 1933.

37. Thomas, J. R.; Dwek, R. A.; Rademacher, T. W.; *Biochemistry* **1990**, *29*, 5413.

38. (a) Xu, Y.; Sculimbrene, B. R.; Miller, S. J.; *J. Org. Chem*. **2006**, *71*, 4919. (b) Morgan, A.J.; Komiya, S.; Xu, Y.; Miller, S.J.; *J. Org. Chem*. **2006**, *71*, 6923.

39. Sureshan, K. M.; Shashidhar, M. S.; Praveen, T.; Das, T.; *Chem. Rev*. **2003**, *103*, 4477.

40. (a) Dixit, S. S.; Shashidhar, M.S.; *Tetrahedron*. **2008**, *64*, 2160. (b) Dixit, S. S.; Shashidhar, M.S.; Devaraj, S.; *Tetrahedron*. **2006**, *62*, 4360.

41. Rabinowitz, I. N.; Kraut, J.; *Acta Cryst*. **1964**, *17*, 159.

42. Khan, U.; Qureshi, R. A.; Saeed, S.; Bond, A. D.; *Acta Cryst*. **2007**, *E63*, o530.

43. Steiner, T.; Hinrichs, W.; Saenger, W.; *Acta Cryst*. **1993**, *B49*, 708.

44. Praveen, T.; Samanta, U.; Das, T; Shashidhar, M. S.; Chakrabarti, P; *J. Am. Chem. Soc*. **1998**, *120*, 3842.

45. Sarmah, M. P.; Shashidhar, M. S.; Gonnade, R. G.; Bhadbhade, M. M.; *Chem. Eur J*. **2005**, *11*, 2103.

46. Murali, C.; Shashidhar, M. S.; Gonnade, R. G.; Bhadbhade, M. M.; *Chem*. *Eur J*. **2007**, *7*, 1153.

47. Simperler, A.; Watt, S. W.; Bonnet, P. A.; Jones, W.; Motherwell, W. D. S.; *CrystEngComm*. **2006**, *8*, 589.

48. Day, G. M.; Streek, J.; Bonnet, A.; Burley, J.C Jones, W.; Motherwell, W. D. S.; *Cryst. Growth Des*. **2006**, *6*, 2301.

49. Sureshan, K. M.; Gonnade, R. G.; Puranik, V. G.; Shashidhar, M. S.; Bhadbhade, M. M; *Chem*. *Commun*. **2001**, 881.

50. Gonnade, R. G.; Shashidhar, M. S.; Bhadbhade, M. M; *Chem*. *Commun*. **2004**, 2530.

51. Gonnade, R. G.; Bhadbhade, M. M.; Shashidhar, M. S.; *CrystEngComm*. **2008**, *10*, 288.

52. Gonnade, R. G.; Bhadbhade, M. M.; Shashidhar, M. S.; Sanki, A. K.; *Chem*. *Commun*. **2005**, 5870.

53. Bhosekar, G.; Murali, C.; Gonnade, R. G.; Bhadbhade, M. M.; Shashidhar, M S.; *Cryst*. *Growth Des*. **2005**, *5*, 1977.

54. (a) Manoj, K.; Gonnade, R.G.; Bhadbhade, M.M.; Shashidhar, M.S.; *Cryst. Growth Des*. **2006**, *6*, 1485. (b) Manoj, K.; Sureshan, K. M.; Gonnade, R.G.; Bhadbhade, M.M.; Shashidhar, M.S.; *Cryst. Growth Des*. **2005**, *5*, 833.

55. (a) Dunitz, J. D.; Gavezzotti, A.; *Angew. Chem. Int. Ed. Engl.* **2005**, *44*, 1766. (b) Kitaigorodskii, A. I.; *Organic Chemical Crystallography*, Consultants Bureau: New York, **1961**.

56. Desiraju, G. R.; Steiner, T.; *The Weak Hydrogen Bonds*: *In Structural Chemistry and Biology*, Oxford University Press: Oxford, New York, **1999**.

57. Pascard, C.; *Acta Cryst*. **1995**, *D51*, 407.

58. (a) Stone, A. J.; *The Theory of Intermolecular Forces*, International Series of Monographs on Chemistry 32, Oxford University Press: Oxford, **1996**. (b) Kaplan, I. G.; *Theory of Intermolecular Interactions, Studies in Physical and Theoretical Chemistry*, Elsevier: Amsterdam, Vol. 42, **1986**.

59. Williams, D. H.; Westwell, M. S.; *Chem. Soc. Rev.* **1998**, *27*, 57.

60. A. Gavezzotti, *Acc. Chem. Res.* **1994**, *27*, 309.

61. (a) Motherwell, W. D. S.; Ammon, H. L.; Dunitz, J. D.; Dzyabchenko, A.; Erk, P.; Gavezzotti, A.; Hofmann, D. W. M.; Leusen, F. J. J.; Lommerse, J. P. M.; Mooij, W. T. M.; Price, S. L.; Scheraga, H.; Schweizer, B.; Schmidt, M. U.; van Eijck, B. P.; Verwer, P.; Williams, D. E.; *Acta Crystallogr.* **2002**, *B58*, 647.

62. Koritsanszky, T. S.; Coppens, P.; *Chem. Rev.* **2001**, *101,* 1583.

63. Munshi, P.; Guru Row, T. N.; *Crystallogr. Rev.* **2005**, *11*, 199.

64. Glusker, J. P.; *Topics in Current Chemistry*, Springer Verlag Berlin Heidelberg, **1998**, Vol.198, 1-56.

65. (a) Zaworotko, M. J.; *Nature*, **2008**, *451*, 410. (b) Desiraju, G. R.; In *Crystal Engineering: From Molecules and Crystals to Materials*; Braga, D.; GO, Ed; International Union of Crystallography, Erice, Italy, **1999**, Vol. I, p.95.

66. Taylor, R.; Kennard, O.; *J. Am. Chem. Soc.* **1982**, *104*, 5063.

67. (a) Choudhury, A. R.; Guru Row, T. N.; *Cryst. Growth Des.* **2004**, *4*, 47. (b) Shimoni, L.; Carrell, H. L.; Glusker, J. P.; Coombs, M. M.; *J. Am. Chem. Soc.* **1994**, *116*, 816

68. Nishio, M.; Hirota, M.; Umezawa, Y.; *The CH/$\pi$ Interaction: Evidence, Nature and Consequences,* Wiley-VCH, **1998**.

69. (a) Nishio, M.; *CrystEnggComm*. **2004**, *6*, 130. (b) Yamakawa, M.; Yamada, I.; Noyori, R.; *Angew. Chem. Int. Ed. Engl.* **2001**, *40*, 2818.

70. (a) Saha, B. K.; Jetti, R. K. R.; Reddy, L. S.; Nangia, A.; *Cryst. Growth Des.* **2005**, *5*, 887. (b) Aitipamula, S.; Nangia, A.; *Chem. Eur. J.* **2005**, 6742.

71. Hunter, C. A.; Sanders, J. K. M.; *J. Am. Chem. Soc.* **1990**, *112*, 5525.

72. Pedireddi, V. R.; Reddy, D. S.; Goud, B. S.; Craig, D. C.; Rae, A. D.; Desiraju, G. R.; *J. Chem. Soc. Perkin Trans. 2* **1994**, 2353.

73. Glusker, J. P.; *Topics in Current Chemistry*, Springer Verlag Berlin Heidelberg, **1998**, Vol.198, p.1.

74. Allen, F. H.; Motherwell, W. D. S.; *Acta Crystallogr.* **2002**, *B58*, 407.

75. *Inorganic Crystal Structure Database* (ICSD): by FIZ Karlsruhe, Max –Plank Society and National Institute of Standards and Technology (NIST).

76. *Protein Data Bank* (PDB): Research Collaboratory for Structural Bioinformatics (RCSB), USA.

77. Rosenfield, R E. Jr; Parthasarathy, R; Dunitz, J. D.; *J. Am. Chem. Soc.* **1977**, *99*, 4860.

78. Allen, F. H.; *Acta Crystallogr.* **2002**, *B58*, 380.

79. Glusker, J. P.; *Acta Cryst.* **1995**, *D51*, 418.

80. Battacharya, R.; Chakrabarti, P.; *J. Mol.Biol.* **2003**, *331*, 925.

81. Tintelnot, M; Andrews, P; *J. Comput. Aided Mol. Design*, **1989**, 67.

82. Klebe, G.; *J. Mol. Biol.* **1994**, *237*, 212.

83. *SYBYL*, *Molecular Modelling System*, *version 5.40*, 1992, Tripose Associates Inc., St.Louis, M O, 63944, USA.

84. Böhm, H. J.; *J. Comput. Aided Mol. Design*, **1992**, 61 and 593.

85. Taylor, R.; Mullaley, A.; Mullier, G. W.; *Pestic. Sci.* **1990**, 29, 197.

86. (a) Keegstra, E. M. D.; van der Mieden, V.; Zwikker, J. W.; Jenneskens, L. W.; Schouten, A.; Kooijman, H.; Veldman, N.; Spek, A. L.; *Chem. Mater.* **1996**, *8*, 1092. (b) Lockhart, D. J.; Kim, P. S.; *Science* **1993**, *260*, 198.

87. (a) Dunitz, J. D.; Filippini, G.; Gavezzotti, A. *Helv. Chim. Acta* **2000**, *83*, 2317. (b) Brock, C. P.; Dunitz, J. D.; *Chem. Mater.* **1994**, *6*, 1118.

88. Lee, S.; Mallik, A. B.; Fredrickson, D. C.; *Cryst. Growth Des.* **2004**, *4*, 279.

89. (a) Williams, D. E.; *J. Comput. Chem*. **1988**, *9*, 745. (b) Stout, J. M.; Dykstra, C. E.; *J. Phys. Chem. A* **1998**, *102*,1576.

90. (a) Bolton, W.; *Acta Cryst.* **1965**, *18*, 5. (b) Bolton, W.; *Acta Cryst.* **1963**, *16*, 166.

91. Davies, D. R.; Blum, J. J.; *Acta Cryst.* **1955**, *8*, 129.

92. Bolton, W.; *Acta Cryst*. **1964**, *17*, 147.

93. Bernstein, J.; Cohen, M. D.; Leiserowitz, L.; *The Chemistry of Quinonoid Compounds,* Ed: S. Patai, Wiley: London, **1974**, p.83.

94. Burgi, H.B.; Dunitz, J. D.; Shefter, E.; *Acta Cryst*. **1974**, *B30*, 1517.

95. Gavezzotti, A.; *J. Phys. Chem*. **1990**, *94*, 4319.

96. Allen, F. H.; Baalham, C. A.; Lommerse, J. P. M..; Raithby, P. R.; *Acta Cryst.* **1998**, *B54*, 320.

97. (a) Olsen, J. A.; Banner, D. W.; Seiler, P.; Sander, U. O.; D'Arcy, A.; Stihle, M.; Műller, K.; Diedrich, F.; *Angew Chem. Int. Ed*. **2003**, *42*, 2507. (b) Olsen, J. A.; Banner, D. W.; Seiler, P.; Wagner, B.; Tchopp, T.; Sander, U. O.; Kansy, M.; Műller, K.; Diedrich, F.; *ChemBioChem*. **2004**, *5*, 666.

98. Wolf, W. M.; *Acta Cryst.* **2001**, *B57*, 806.

99. Wolf, W. M.; *Acta Cryst.* **2001**, *B57*, 54.

100. (a) Braga, D.; Grepioni, F.; *Acc. Chem. Res*. **2000**, *33*, 601. (b) Braga, D.; Grepioni, F.; Desiraju, G. R. *Chem. Rev*. **1998**, 98, 1375. (c) Desiraju, G. R.; Crystal Engineering: *The Design of Organic Solids*, Amsterdam: Elsevier, **1989**.

101. (a) Wang, Z.; Ch. Kravtsov, V.; Walsh, R. B.; Zaworotko, M. J.; *Cryst. Growth Des*. **2007**, *7*, 1154. (b) Rebec, J. Jr.; *Acc. Chem. Res*. **1999**, *32*, 278. (c) Caira, M. R.; Nassimbeni, L. R.; *Comprehensive Supramolecular Chemistry*; Eds: Atwood, J. L.; Davies, J. E. D.; MacNicol, D. D.; Vogtle, F.; Elsevier: Oxford, **1996**; *6*, 825. (d) Lehn, J. M.; *Supramolecular Chemistry*: *Concepts and Perspectives*; VCH Verlag: Weinheim, Germany, **1995**.

102. (a) Paulus, E. F.; Leusen, F. J. J.; Schmidt, M. U.; *CrystEngComm*. **2007**, *9*, 131. (b) Schmidt, M. U.; Hofmann, D. W. M.; Buchsbaum, C.; Metz, H. J.; *Angew. Chem. Int. Ed*. **2006**, *45*,1313.

103. Evers, J.; Klapötke, T. M.; Mayer, P.; Oehlinger, G.; Welch, J.; *Inorg. Chem*. **2006**, *45*, 4996.

104. (a) Parmar, M. M.; Khan, O.; Seton, L.; Ford, J. L.; *Cryst. Growth Des.*, **2007**, *7*, 1635. (b) Reddy, C. M.; Padmanabhan, K. A.; Desiraju, G. R.; *Cryst. Growth Des.*, **2006**, *6*, 2720. (c) Chen, S.; Guzei, I. A.; Yu, L.; *J. Am. Chem. Soc.* **2005**, *127*, 9881. (d) Csikos, E; Ferenczy, G. G; Angyan, J. G.; Böcskei, Z.; Simon, K.; Gönczi, C.; Hermecz, I.; *Eur. J. Org. Chem*. **1999**, 2119.

105. (a) Hellingsworth, D.; Brown, M. E.; Hillier, A. C.; Santarsiero, B. D.; Chaney, J. D. *Science* **1996**, *273*, 1355. (b) Yaghi, O. M.; Li, G.; Li, H.; *Nature* **1996**, *378*, 703. (c) Bernstein, J.; Etter, M. C.; Leiserowitz, L. *Structure Correlation*, edited by Burgi H.B. and Dunitz, J. D.; Vol.2, p.431-507, Weinheim: VCH. **1994**.

106. Allan, D.R.; Clark, S J.; Ibberson, R.M.; Parsons, S; Pulham, C.R.; Sawyer, L; *Chem. Commun*. **1999**, 751.

107. Maccallum, P. H.; Poet, R.; Milner-White, E.J; *J. Mol.Biol*. **1995**, 248.

108. Hughes, D. H.; Sieker, L. C.; Bieth, J.; Dimicoli, J.L.; *J. Mol. Biol*. **1982**, *162*, 645.

109. Weissbuch, I.; Torbeev, Y. V.; Leiserowitz, L.; Lahav, M.; *Angew. Chem. Int. Ed.* **2006**, *44*, 3226.

110. (a) Pole, D. L.; *J. Pharm. Sci*. **2008**, *97*, 1071 and references therein. (b) Braga, D.; Giaffreda, S. L.; Grepioni, F.; Chierotti, M. R.; Gobetto, R.; Palladino, G.; Polito, M.; *CrystEngComm*. **2007**, *9*, 879.

111. Praveen, T.; Das, T.; Sureshan, K. M.; Shashidhar, M. S.; Samanta, U.; Pal, D.; Chakrabarti, P.; *J. Chem. Soc. Perkin Trans. 2*, **2002**, 358.

112. Manoj, K.; Gonnade, R. G.; Bhadbhade, M. M.; Shashidhar, M. S.; *Acta Crystallogr*. **2007**, *C63*, o555.

113. Bruker, *SMART*, *SAINT*, *SADABS*, *XPREP*. **1998**, Bruker AXS Inc., Madison, WI, USA.

114. G.M. Sheldrick, SHELXS 97 and SHELXL 97, Programs for the Solution and Refinement of Crystal Structures, University of Göttingen, Germany.1997.

115. Sureshan, K. M.; Shashidhar, M. S.; Das, T.; Gonnade, R. G.; Bhadbhade, M. M. *Eur. J. Org. Chem.* **2003**, 1035.

116. (a) Kálmán, A.; *Acta Cryst.* **2005**, *B61*, 536. (b) Kálmán, A.; Fábián, L.; Argay, G.; Bernáth, G.; Gyarmati, Z.; *J. Am. Chem. Soc.* **2003**, *125*, 34.

117. (a) Kálmán, A.; Fábián, L.; *Acta Cryst*. **2004**, *B60*, 547. (b) Fábián, L.; Kálmán, A.; Argay, G.; Bernáth, G.; Gyarmati, Z.; *Chem. Commun*. **2004**, 2114.

118. (a) Murali, C.; Shashidhar, M. S.; Gonnade, R. G.; Bhadbhade, M. M.; *Eur. J. Org. Chem.* **2007**, *7*, 1153. (b) Sarmah, M. P.; Shashidhar, M. S.; Gonnade, R. G.; Bhadbhade, M. M.; *Chem*. *Eur J*. **2005**, *7*, 2103.

119. Brant, D. A.; Flory, P. J.; *J. Am. Chem. Soc.* **1965**, *87*, 663.

120. Blagden, N; Davey, R. J.; *Cryst*. *Growth Des*. **2003**, *3*, 873.

121. Yu, L.; *J*. *Am*. *Chem*. *Soc*. **2003**, *125*, 6380.

122. Frisch, M. J.; Trucks, G. W.; Schlegel, H. B.; Scuseria, G. E.; Robb, M. A.; Cheeseman, J. R.; Montgomery, Jr., J. A.; Vreven, T.; Kudin, K. N.; Burant, J. C.; Millam, J. M.; Iyengar, S. S.; Tomasi, J.; Barone, V.; Mennucci, B.; Cossi, M.; Scalmani, G.; Rega, N.; Petersson, G. A.; Nakatsuji, H.; Hada, M.; Ehara, M.; Toyota, K.; Fukuda, R.; Hasegawa, J.; Ishida, M.; Nakajima, T.; Honda, Y.; Kitao, O.; Nakai, H.; Klene, M.; Li, X.; Knox, J. E.; Hratchian, H. P.; Cross, J. B.; Bakken, V.; Adamo, C.; Jaramillo, J.; Gomperts, R.; Stratmann, R. E.; Yazyev, O.; Austin, A. J.; Cammi, R.; Pomelli, C.; Ochterski, J. W.; Ayala, P. Y.; Morokuma, K.; Voth, G. A.; Salvador, P.; Dannenberg, J. J.; Zakrzewski, V.

G.; Dapprich, S.; Daniels, A. D.; Strain, M. C.; Farkas, O.; Malick, D. K.; Rabuck, A. D.; Raghavachari, K.; Foresman, J. B.; Ortiz, J. V.; Cui, Q.; Baboul, A. G.; Clifford, S.; Cioslowski, J.; Stefanov, B. B.; Liu, G.; Liashenko, A.; Piskorz, P.; Komaromi, I.; Martin, R. L.; Fox, D. J.; Keith, T.; Al-Laham, M. A.; Peng, C. Y.; Nanayakkara, A.; Challacombe, M.; Gill, P. M. W.; Johnson, B.; Chen, W.; Wong, M. W.; Gonzalez, C.; Pople, J. A.; *Gaussian 03*, Revision C.02; Gaussian, Inc., Wallingford, CT, **2004**.

123. Bűrgi, H.; Dunitz, J. D.; Shefter, E.; *Acta Crystallogr*. **1974**, *B30*, 1517.

124. Jacques, J.; Collet, A.; Wilen, S. H.; *Enantiomers, Racemates and Resolutions*, Wiley: New York, **1981**, p. 4.

125. Erlanson, D. A.; Braisted, A. C.; Raphael, D. R.; Randal, M.; Stroud, R. M.; Gordon, E. M.; Wells, J. A.; *Proc. Natl Acad. Sci. USA* **2000**, *97*, 9367.

126. Brock, J. W.; Bott, S. G.; *J. Chem. Crytallogra*. **1995**, *25*, 321.

# Appendix

There are eight compounds in the CSD containing tosyl group that exhibits polymorphic behavior, as listed below.

| No. | CSD Ref Code | Polymorph | Torsion angle X-X-S-C (°) | Difference (°) |
|---|---|---|---|---|
| 1.1 | BILCOO10 | Dimorphs | 69.98 | ~ 3 |
| 1.2 | BILCOO11 | | 73.05 | |
| 2.1 | CUMTAF | Dimorphs | 64.91 | ~ 5 |
| 2.2 | CUMTAF01 | | 69.42 | |
| 3.1 | DETZUX01 | Trimorphs | 70.73 | ~ 3 |
| 3.2 | DETZUX01 | | 71.63 | |
| 3.3 | DETZUX01 | | 68.49 | |
| 4.1 | JAKKUB | Dimorphs | 71.11 | ~ 1 |
| 4.2 | JAKKUB01 | | 71.67 | |
| 5.1 | JAWXEK | Dimorphs | 58.97 | ~ 3 |
| 5.2 | JAWXEK01 | | 61.40 | |
| 6.1 | NAQRIG | Dimorphs | 64.49 | ~ 9 |
| 6.2 | NAQRIG01 | | 55.86 | |
| 7.1 | WENVER | Dimorphs | 85.32 | ~ 12 |
| 7.2 | WENVER01 | | 97.72 | |
| 8.1 | ZZZPUS01 | Dimorphs | 71.73 | ~ 6 |
| 8.2 | ZZZPUS01 | | 77.46 | |

## List of Publications

1. Short S=O···C=O contacts associates diastereomers of 2,4(6)-di-*O*-benzoyl-6(4)-*O*-[(1S)-10-camphorsulfonyl]–*myo*-inositol 1,3,5-orthoformate in their inclusion. *Cryst. Growth Des*. **2005**, *5*, 833-836.

   **K. Manoj**, K. M. Sureshan, R. G. Gonnade, M. M. Bhadbhade and M. S. Shashidhar.

2. O-H···O Bridged Dimers link *via* C-H···O and C-H···π Interactions in the Crystal Structure of 4,6-di–*O*-benzyl *myo*-inositol 1,3,5-orthoformate. *Acta Cryst*. **2005**, *C61*, o628-630.

   **K. Manoj**, S. Devaraj, R. G. Gonnade, M. M. Bhadbhade and M. S. Shashidhar

3. Subtle cross over from C-H···O to S=O···C=O short contacts in the association of diastereomers of 2,4(6)-di-*O*-benzoyl-6(4)-*O*-[(1S)-10-camphorsulfonyl]–*myo*-inositol 1,3,5-orthoformate upon formation of pseudopolymorphs. *Cryst.Growth Des*. **2006**, *6*, 1485-1492.

   **K. Manoj**, R. G. Gonnade, M. M. Bhadbhade and M. S. Shashidhar.

4. Different interaction motifs of dipolar S=O···C=O contacts that associate diastereomers of 2,4(6)-di-*O*-benzoyl-6(4)-*O*-{[(1S)-7,7-dimethyl-2-oxo-bicyclo[2.2.1]heptan-1-ylmethyl]-sulfonyl}-myo-inositol-1,3,5-orthoacetate.

   *Acta Cryst.* **2007**, *C63*, o555-558.

   **K. Manoj**, R. G. Gonnade, M. M. Bhadbhade and M. S. Shashidhar.

5. Concomitant dimorphism in 2,4-di-*O*-benzoyl-6-*O*-tosyl-myo-inositol-1,3,5-orthoacetate (manuscript under preparation).

   **K. Manoj**, R. G. Gonnade, M. M. Bhadbhade and M. S. Shashidhar.

6. Identical molecular string associated *via* O···C=O in conformational dimorphs of 2,4-di-*O*-acetyl-6-*O*-tosyl-myo-inositol-1,3,5-orthoesters (manuscript under preparation).

**K. Manoj**, R. G. Gonnade, M. M. Bhadbhade and M. S. Shashidhar.

7. Effect of conformational modification for solvent inclusion in 2-*O*-tosyl-4,6-di-*O*-acetyl-myo-inositol-1,3,5-orthoesters (manuscript under preparation).

   **K. Manoj**, R. G. Gonnade, M. M. Bhadbhade and M. S. Shashidhar.

8. Solvatopolymorphism in diastereomeric mixture of 1,2,3,4(6),5-penta-*O*-acetyl-6(4)-*O*-[(1S)-10-camphorsulfonyl]–*myo*-inositol (manuscript under preparation).

   **K. Manoj**, R. G. Gonnade, M. M. Bhadbhade and M. S. Shashidhar.

## Contribution to National/International Symposia/Conferences

1. Pseudopolymorphic behavior of diastereomeric mixture of 2,4(6)-di-*O*-benzoyl-6(4)-*O*-[(1S)-10-camphorsulfonyl]–*myo*-inositol 1,3,5-orthoformate. **K. Manoj**, K. M. Sureshan, R. G. Gonnade, M. M. Bhadbhade and M. S. Shashidhar.

   *33rd National Seminar on Crystallography*, held at National Chemical Laboratory, Pune, Maharashtra, India on *8-10th January 2004*.

2. Studies in chlathration bevaior and guest selectivities in diastereomeric mixture of 2,4(6)-di-*O*-benzoyl-6(4)-*O*-camphorsulfonyl-*myo*-inositol 1,3,5-orthoformate. **K. Manoj**, K. M. Sureshan, R. G. Gonnade, M. M. Bhadbhade and M. S. Shashidhar.

   *6th National Symposium on Chemistry* held at Indian Institute of Technology, Kanpur, Uttarpradesh, India on *6-8th February 2004*.

3. Guest induced polymorphism in 4(6)-*O*-camphorsulfonyl-1,2,3,5,6(4)-penta-*O*-benzoyl-*myo*-inositol. **K. Manoj**, R. G. Gonnade, M. M. Bhadbhade and M. S. Shashidhar.

   *34th National Seminar on Crystallography*, held at Guwahati University, Guwahati, Assam, India on *9-12th January 2005*.

4. Conformational polymorphs of racemic 2,4-di-*O*-benzoyl-6-*O*-tosyl-*myo*-inositol 1,3,5-orthoacetate. **K. Manoj**, R. G. Gonnade, M. M. Bhadbhade and M. S. Shashidhar.

   *International Symposium on Advances in Organic Chemistry*, held at Mahatma Gandhi University, Kottayam, Kerala, India on *9-12$^{th}$ January 2006*.

5. Identical One Dimensional Molecular Assembly in Conformational Polymorphs of Racemic 2,4-di–*O*-acetyl 6-*O*-tosyl *myo*-inositol 1,3,5-orthoformate. **K. Manoj**, R. G. Gonnade, M. M. Bhadbhade and M. S. Shashidhar.

   *Joint Conference of the Asian Crystallographic Association and the Crystallographic Association of Japan*, held at Epochal, Tsukuba, Japan on *20-23$^{rd}$ November 2006*.